Understanding the role of Merkel cell polyomavirus oncoproteins in the cellular transformation of mammalian Merkel cells

Laura Mattie Knight

BSc (Hons)

Submitted in accordance with the requirements for the degree of Doctor of Philosophy

University of Leeds

Faculty of Biological Sciences

School of Molecular and Cellular Biology

September 2014

The candidate confirms that the work submitted is her own, except where work which has formed part of a jointly authored publication has been included. The contribution of the candidate and the other authors to this work has been explicitly indicated within the text. The candidate confirms that appropriate credit has been given within the thesis where reference has been made to the work of others.

Chapter 3, 4 and 5 contain material in a jointly authored publication:- Knight, L.M., Stakaityte, G., Grifiths, D.A., Howell, G.J., Abdul-Sada, H., Wheat, R., Blair, G.E., Macdonald, A., Blackbourn, D.J., & Whitehouse, A. Merkel cell polyomavirus small T antigen mediates microtubule destabilisation to promote cell motility and migration. Journal of Virology, 89:1 35-47. All figures within these Chapters are directly attributable to L. M. Knight, except Chapter 3 Figure 3.7 (performed by Rachel Wheat and David Blackbourn) and Chapter 5 Figure 5.11 (performed by Hussein Abdul-Sada). Credit for these two Figures has been explicity stated within the text.

Acknowledgements

I would like to say a special thank you to my supervisor, Professor Adrian Whitehouse for his unwavering support, encouragement and guidance through the four years of my PhD. I would also like to thank him for the many hours (too many to count) that he has aided me in writing grant and Fellowship applications and publications. I would like to thank all the members of the Whitehouse laboratory, past and present, which have supported me and created a lovely friendly environment to work in. A big thank you to Rosie Doble, now Dr Rosie Brakefield, whom I began my PhD with for all her support and friendship, and the extended coffee breaks.

I am grateful to the British Skin Foundation and the Rosetrees Trust whom funded the three years of my PhD and the final fourth year of additional research, respectively. I would also like to thank all of the collaborators who have kindly provided reagents and expertise during the last four years. In particular I would like to thank Dr Andrew Macdonald and his laboratory for reagents and a productive collaboration. In addition, a thank you to the Virology group, whose support and regular meetings have aided me in many presentations in both national and international meetings.

A heartfelt thank you to my parents for their unwavering support thoughtout my entire education, for always encouraging and inspiring me, even when experiments were not working. To my best friend and twin sister, Charlotte Knight, for all the times I've needed you and all the times you are always there. A heartfelt thank you as well to Mike Grethe, for all the continual encouragement and support and for always giving me a sense of perspective.

Abstract

Merkel cell carcinoma (MCC) is a highly aggressive skin cancer of neuroendocrine origin with a high propensity for metastasis through the dermal lymphatic system. In 2008, Merkel cell polyomavirus (MCPyV) was discovered monoclonally integrated within the host genome of more than 80% of MCC tumours. MCPyV is known to contribute to the transformation and maintenance of MCC tumour cells through the expression of the Large and Small Tumour (LT and ST) antigens. To date, a number of mechanisms by which MCPyV T antigen expression promotes cell transformation and viral replication have been elucidated. Although, no studies have addressed the molecular mechanisms associated with MCPyV T antigen expression and the highly aggressive, metastatic nature of MCC.

Herein, a quantitative proteomic approach has been used to identify cellular proteins and gene ontology pathways that are differentially expressed upon MCPyV ST expression. This highlighted that MCPyV ST expression promotes the upregulation of cellular proteins involved in microtubule-associated cytoskeletal organisation and dynamics.

Further analysis, has demonstrated that MCPyV ST promotes cell motility, migration and invasion and that MCPyV ST-induced microtubule destabilisation is fundamental for this phenotype. Bioinformatical analysis highlighted the upregulation of stathmin, a microtubule destabilising protein, which is required for MCPyV ST-induced cell motility. Furthermore, through protein interaction studies and cell motility assays, the cellular phosphatase catalytic subunit PP4C has been implicated in the regulation of this process.

Herein, these findings present the first study into the metastatic nature of MCC and the underlying mechanisms by which MCPyV T antigen expression can promote cell migration. This in turn should allow for enhanced therapeutic studies and chemotherapy regimes, in order to improve current treatments of MCC.

Table of Contents

Chapter 1

Chapter 1 1

Introduction 1

1.1 Viruses and Cancer 2

1.2 Polyomaviruses 3

1.2.1 Human polyomaviruses 4

1.2.1.1 JCPyV and BKPyV 4

1.2.1.2 Other human polyomaviruses 5

1.2.2 SV40 – The polyomavirus model 6

1.2.2.1 Genetic Organisation 7

1.2.2.2 Viral life Cycle 8

1.2.2.3 Genome integration 10

1.2.2.4 Polyomavirus early proteins 11

1.2.2.4.1 Small T antigen 12

1.2.2.4.1.1 Structure and domains 12

1.2.2.4.1.2 ST interacts with PP2A 13

1.2.2.4.1.3 The role of ST in the viral life cycle 15

1.2.2.4.1.4 The Role of ST in transformation 16

1.2.2.4.2 Large T antigen 18

1.2.2.4.2.1 Structure and domains 18

1.2.2.4.2.2 The Role of LT in the viral life cycle 18

1.2.2.4.2.2.1 DNA binding capabilities 19

1.2.2.4.2.2.2 Recruitment of cellular proteins 19

1.2.2.4.2.3 The Role of LT in transformation 20

1.2.2.4.2.3.1 Binding pRB 20

1.2.2.4.2.3.2 Binding p53 21

1.2.2.4.2.3.3 Binding Cullin 7 21

1.2.2.4.2.3.4 IRS I 22

1.2.2.4.2.3.5 Binding β-catenin 22

1.2.2.4.2.3.6 Other transcription factors 22

1.2.2.4.3 Middle T antigen 23

1.2.2.4.3.1 Structure and domains 23
1.2.2.4.3.2 The Role of MT in the viral life cycle 24
1.2.2.4.3.3 The Role of MT in transformation 25
1.2.2.4.3.3.1 Binding PP2A 25
1.2.2.4.3.3.2 Src family sequestration 25
1.2.2.4.4 Other alternative early proteins 26
1.3 Merkel cell carcinoma 26
1.3.1 Merkel cells 26
1.3.2 Merkel cell carcinoma 28
1.3.3 MCC histology and presentation 29
1.3.4 Epidemiology 30
1.3.5 Clinical Staging 31
1.3.6 Prognosis and treatment 31
1.3.7 Infectious origin of MCC 32
1.4 Merkel cell polyomavirus 32
1.4.1 MCPyV discovery 32
1.4.2 Seroprevalence 33
1.4.3 MCPyV present in non-MCC samples 34
1.4.4 Phylogeny 34
1.4.5 Genetic Organisation 36
1.4.5.1 MCPyV Genome 36
1.4.5.1.1 MCPyV Origin of Replication 37
1.4.5.1.2 MCPyV T antigen locus 38
1.4.5.1.2.1 Large T antigen 38
1.4.5.1.2.2 Small T antigen 39
1.4.5.1.2.3 57 kiloDalton T antigen 40
1.4.5.1.2.4 Alternative T antigen open reading frame 40
1.4.5.1.3 MCPyV Late Proteins 41
1.4.5.1.4 MCPyV microRNA 42
1.4.6 Viral Life Cycle 43
1.4.6.1 Attachment and Entry 44
1.4.6.2 Replication 45
1.4.6.2.1 The role of LT 45
1.4.6.2.2 The role of ST 47

1.4.6.3 Assembly and egress 47
1.4.7 MCPyV and the immune response 48
1.4.8 MCPyV in the pathogenesis of MCC 51
1.4.8.1 The role of ST in transformation 53
1.4.8.1.1 A role for 4E-BP1 53
1.4.8.1.2 The LSD domain 55
1.4.8.1.3 MCPyV ST, a dichotomy of functions 56
1.4.8.2 The role of LT in transformation 57
1.4.8.2.1 DNA damage response 57
1.4.8.2.2 Survivin 57
1.5 Cancer and Metastasis 58
1.5.1 Steps to achieve metastasis 59
1.5.1.1 Loss of cell adhesion 59
1.5.1.2 Acquisition of motility 62
1.5.1.3 ECM degradation and entry into the vasculature 64
1.5.1.4 Integrin expression and motility 65
1.5.1.5 Colonisation of remote sites 66
1.5.2 Cell cytoskeleton and motility 67
1.5.2.1 Actin cytoskeletal network 67
1.5.2.2 Microtubule cytoskeletal network 69
1.5.2.2.1 Stathmin, a MT-associated protein 71
1.5.3 DNA tumour viruses and cell motility 75
Thesis Aims 77
Chapter 2 79
Materials and Methods 79
2.1 Materials 80
2.1.1 MCC tumour samples 80
2.1.2 Chemicals 80
2.1.3 Enzymes 80
2.1.4 Antibodies 81
2.1.5 Mammalian cell culture reagents 83
2.1.6 Oligonucleotides 83
2.1.7 Plasmid constructs 84
2.2 Methods 85

2.2.1 Extraction of DNA from MCC tumour sections 85
2.2.2 Molecular Cloning 85
2.2.2.1 Construction of recombinant vectors 86
2.2.2.2 Polymerase chain reaction (PCR) 87
2.2.2.2.1 Overlap extension PCR (OE-PCR) 88
2.2.2.3 Agarose gel electrophoresis 88
2.2.2.4 Gel purification of DNA 89
2.2.2.5 DNA ligation 89
2.2.2.6 Restriction enzyme digestion 90
2.2.2.7 Preparation of chemically competent DH5α 90
2.2.2.8 Transformation of chemically competent bacteria 91
2.2.2.9 Plasmid purification 91
2.2.2.9.1 Mini prep (small scale) plasmid purification 91
2.2.2.9.2 Maxi prep (large scale) plasmid purification 92
2.2.2.10 Sequencing of DNA 93
2.2.3 Mammalian cell culture 93
2.2.3.1 Cell lines 93
2.2.3.2 Cell line maintenance 94
2.2.3.3 Maintaining cells in SILAC media 95
2.2.3.4 Generating inducible cell lines 95
2.2.3.5 Mammalian cell culture based protocols 96
2.2.3.5.1 Mammalian cell transfection 96
2.2.3.5.2 Induction of inducible cell lines 96
2.2.3.5.3 Stabilisation of microtubules 97
2.2.3.5.4 Analysis of protein stability 97
2.2.3.5.5 Analysis of translational inhibition 97
2.2.3.5.6 siRNA based knockdown of protein expression 98
2.2.4 Immunofluorescence microscopy 98
2.2.4.1 Analysis of the actin cytoskeletal network 99
2.2.5 Electrophoretic analysis of proteins 100
2.2.5.1 Preparation of mammalian cell lysates 100
2.2.5.2 Determination of protein concentration 100
2.2.5.3 Tris-glycine SDS-Polyacrylamide gel electrophoresis (PAGE) 101
2.2.5.4 Western blot analysis 102

2.2.5.5 Coomassie stain analysis 103
2.2.6 Analysis of mammalian cell motility 103
2.2.6.1 Invasion and migration transwell assays 103
2.2.6.2 Live cell imaging 104
2.2.6.3 Scratch wound-healing assay 105
2.2.7 SILAC-based quantitative proteomics 105
2.2.7.1 Cell fractionation assay 105
2.2.7.2 Sample preparation and proteomics analysis 106
2.2.8 Analysis of cellular proliferation 106
2.2.8.1 Standard cell proliferation assay 106
2.2.9 Multicolour immunohistochemistry 107
2.2.10 Gene expression analysis by qRT-PCR 108
2.2.10.1 RNA extraction 108
2.2.10.2 DNase I treatment 109
2.2.10.3 Reverse transcription 109
2.2.10.4 Ethanol precipitation 109
2.2.10.5 qRT-PCR reaction 110
2.2.11 Co-immunoprecipitation assay 110
Chapter 3 111
Quantitative proteomics identifies that MCPyV ST promotes host cell cytoskeletal alterations 111
3.1 Introduction 112
3.2 Using the 293 FlpIn™ system to generate a cell line capable of inducible expression of MCPyV ST 113
3.3 Quantitative proteomic analysis identifies that cytoskeletal regulatory proteins are affected by MCPyV ST expression 119
3.4 Stathmin is overexpressed in primary MCC tumour tissue 122
3.5 MCPyV ST promotes redistribution of stathmin 123
3.6 MCPyV ST promotes microtubule destabilisation 125
3.7 MCPyV ST affects stathmin phosphorylation levels and microtubule stability 128
3.8 MCPyV ST affects the distribution of the actin cytoskeletal network 134
3.9 Discussion 136
Chapter 4 139
MCPyV ST promotes cell motility, migration and invasion by facilitating microtubule destabilisation 139

4.1 Introduction 140
4.2 MCPyV ST promotes cell motility, migration and invasion in i293-ST cells 141
4.3 MCPyV ST promotes cell motility, migration and invasion in MCC13 cells 145
4.4 Taxane compounds inhibit MCPyV ST-mediated microtubule destabilisation.... 147
4.5 Microtubule destabilisation is crucial for MCPyV ST-mediated cell motility and migration 149
4.6 Stathmin depletion inhibits MCPyV ST-mediated cell motility, migration and invasion 154
4.7 Discussion 158
Chapter 5 160
Cellular phosphatases are required for MCPyV ST-enhanced cell motility and migration.. 160
5.1 Introduction 161
5.2 ST binding mutants identify specific cellular phosphatases required for MCPyV ST-mediated microtubule destabilisation 162
5.3 ST binding mutants identify specific cellular phosphatases required for MCPyV ST-enhanced cell motility 166
5.4 PP4C is important for microtubule organisation and dynamics 168
5.5 MCPyV ST interacts with stathmin 175
5.6 MCPyV ST may enhance stathmin translation 176
5.7 Discussion 180
Chapter 6 182
Final discussion and future perspectives 182
Chapter 7 194
Appendix 194
References 196

List of Figures

Chapter 1

Figure 1.1. Polyomavirus life cycle. 10
Figure 1.2. Diagrammatic representation of the polyomavirus ST antigen 12
Figure 1.3. Polyomavirus ST antigen binds and affects the inherent functions of PP2A 14
Figure 1.4 Diagrammatic representation of the polyomavirus LT antigen 18
Figure 1.5. Diagrammatic representation of the polyomavirus MT antigen 24
Figure 1.6. Diagrammatic representation of the location of Merkel cells within the skin 28
Figure 1.7. MCC appearance and histology 30
Figure 1.8. Phylogenetic study of the relationships of human polyomaviruses 36
Figure 1.9. Genome organisation of MCPyV 37
Figure 1.10. MCPyV T antigen structure and domains 38
Figure 1.11. A schematic to represent the de novo gene birth of ALTO by overprinting 41
Figure 1.12. Attachment and entry receptors for MCPyV 44
Figure 1.13. NF-κB mediated gene transcription 50
Figure 1.14. The molecular mechanism associated with MCPyV-induced tumour formation 52
Figure 1.15. MCPyV ST promotes cell proliferation downstream of the Akt pathway 55
Figure 1.16. Steps required for escape from the primary tumour site 61
Figure 1.17. The process of mesenchymal, directional cell motility 63
Figure 1.18. Actin cytoskeletal dynamics in cell motility 69
Figure 1.19. Microtubule dynamics and the action of stathmin 73

Chapter 3

Figure 3.1. Schematic representation for the generation of a stably inducible cell line 115

Figure 3.2. Screening of i293-ST clones for the expression of MCPyV ST.....116
Figure 3.3. A schematic representation of the SILAC-based quantitative proteomic analysis approach.....117
Figure 3.4. Expression of MCPyV ST in SILAC samples.....118
Figure 3.5. Subcellular fraction analysis of SILAC lysates.....119
Figure 3.6. MCPyV ST expression promotes upregulation of proteins involved in microtubule cytoskeletal organisation and dynamics 122
Figure 3.7. Primary MCC tumours upregulate the microtubule-associated protein, stathmin 123
Figure 3.8. Cytoplasmic visualisation is imapired in 293 FlpIn cells. 124
Figure 3.9. MCPyV ST promotes redistribution of endogenous stathmin.....125
Figure 3.10. MCPyV ST promotes microtubule destabilisation and stathmin redistribution 126
Figure 3.11. MCPyV-positive MCC cells (MKL-1) demonstrate microtubule destabilisation and stathmin redistribution 128
Figure 3.12. MCPyV ST expression affects the cellular levels of phosphorylated stathmin and acetylated tubulin.....130
Figure 3.13. Doxycyline hylcate induction does not affect protein levels.....131
Figure 3.14. MCPyV-positive MKL-1 MCC cells shows microtubule destabilisation and altered phosphorylated stathmin levels 132
Figure 3.15. MCPyV ST expression promotes microtubule destabilisation in MCC13 cells.....133
Figure 3.16. An EGFP tag does not affect MCPyV ST function.....134
Figure 3.17. MCPyV ST promotes a rearrangement of the actin cytoskeletal network..... 129

Chapter 4

Figure 4.1. MCPyV ST expression promotes cell motility in HEK 293 FlpIn™ cells ..142
Figure 4.2. Scratch-wound healing analysis indicates that MCPyV ST expression promotes cell motility and migration in i293-ST 143
Figure 4.3. MCPyV ST expression promotes cell motility, migration and invasion 144

Figure 4.4. MCPyV ST does not promote cell proliferation expression in i293-ST and HEK 293 FlpIn™ cells.....145
Figure 4.5. MCPyV ST expression promotes cell motility in MCC13 cells.....146
Figure 4.6. MCPyV ST expression promotes cell motility, migration and invasion in MCC13 cells.....147
Figure 4.7. Paclitaxel treatment inhibits MCPyV ST-mediated microtubule destabilisation.....149
Figure 4.8. Paclitaxel treatment inhibits MCPyV ST-mediated cell motility and migration.....151
Figure 4.9. Paclitaxel inhibits MCPyV ST ability to promote microtubule destabilisation and stathmin dephosphorylation.....152
Figure 4.10. MCPyV ST is required for microtubule destabilisation in MKL-1 cells 153
Figure 4.11. MCPyV ST is required cell motility and migration in MKL-1 cells 154
Figure 4.12. Stathmin is required for MCPyV ST-mediated cell motility and migration.....156
Figure 4.13. Stathmin is required for MCPyV ST-mediated cell migration in transwell assays 157

Chapter 5

Figure 5.1. Cellular phosphatases are required for MCPyV ST-mediated microtubule destabilisation in MCC13 cells 163
Figure 5.2. Cellular phosphatases are required for MCPyV ST-mediated microtubule destabilisation and affect microtubule stability 165
Figure 5.3. Cellular phosphatases are required for MCPyV ST-mediated cell motility in HEK 293 FlpIn™ cells.....166
Figure 5.4. Cellular phosphatases are required for MCPyV ST-mediated cell motility in MCC13 cells.....167
Figure 5.5. Live cell tracking shows that cellular phosphatases are required for MCPyV ST-mediated cell motility in MCC13 cells 168
Figure 5.6. PP2A Aα is important for microtubule stability in control cells 169

Figure 5.7. Expression of a transdominant PP4C mutant inhibits MCPyV ST-mediated microtubule destabilisation 171
Figure 5.8. Expression of a transdominant PP4C mutant promotes microtubule destabilisation 172
Figure 5.9. Expression of a transdominant PP4C mutant inhibits MCPyV ST-mediated cell motility in i293-ST cells 173
Figure 5.10. Expression of a transdominant PP4C mutant inhibits MCPyV ST-mediated cell motility in MCC13 cells 174
Figure 5.11. Stathmin interacts with both MCPyV and PP4C 176
Figure 5.12. MCPyV ST does not promote enhanced transcription of stathmin 177
Figure 5.13. MCPyV ST does not enhance stathmin protein stability 178
Figure 5.14. MCPyV ST dysregulation of cap-dependent translation is required for enhanced stathmin expression 179

List of Tables

Chapter 1

Table 1.1. Human tumour viruses 3

Chapter 2

Table 2.1. List of enzymes and the corresponding suppliers 81

Table 2.2. List of primary antibodies, the corresponding suppliers and the working dilutions for either western blotting or immunofluorescence microscopy. 78-83

Table 2.3. List of primers used for various applications such as cloning or qRT-PCR including the sequences for both the forward and reverse primer pair. 84

Table 2.4. List of constructs purchased from suppliers for provided by collaborators 85

Table 2.5. List of recombinant constructs, the primer sequences used for cloning, restriction enzymes and the original parental vectors. 87

Table 2.6. Reagents and corresponding volumes required to prepare 6%, 8%, 10% and 12% SDS-PAGE gels 102

Chapter 3

Table 3.1. Gene ontology groupings and pathways hits based on SILAC analysis of i293-ST cells 120

Table 3.2. MCPyV ST promotes the differential expression of proteins involved in microtubule-associated cytoskeletal organisation and dynamics 121

Chapter 7

Table 7.1. Bioinformatical analysis highlighting gene ontology groupings differentially expression upon MCPyV ST expression 195

Abbreviations

α	alpha
β	beta
κ	kappa
γ	gamma
°c	degrees celcius
%	percentage
4E-BP1	eukaryotic translation initiation factor 4E-binding protein 1
aa	amino acid
ADP	adenosine diphosphate
Amp	ampicillin
ATP	adenosine triphosphate
BKPyV	BK virus
bp	base pair
BSA	bovine serum albumin
$CaCl_2$	calcium chloride
Cdk	cyclin dependent kinase
cDNA	complimentary DNA
CK	cytokeratin
CMV	cytomegalovirus
CNS	central nervous system
CRE	cyclic AMP response element
CREB	cyclic AMP response element binding

C-terminus	carboxyl-terminus
DAPI	4’, 6-Diamidino-2-Phenylindole
DDR	DNA damage response
dH_2O	distilled water
DMEM	dulbecco’s modified Eagle’s medium
DMSO	dimethyl sulphoxide
DNA	deoxyribonucleic acid
DNase	deoxyribonuclease
dNTP	deoxyribonucleoside (5’-) triphosphate
dox	doxycycline hyclate
ds	double stranded
DTT	dithiothreitol
EB-1	end binding protein - 1
EBV	Epstein-Barr virus
E.Coli	*Escherichia coli*
ECL	enhanced chemiluminescence
ECM	extra cellular matrix
EDTA	ethylenediaminetetraacetic acid disodium salt
EGFP	enhanced green fluorescent protein
EMT	epithelial to mesenchymal trasition
ERK	extracellular signal-regulated kinases
EtBr	ethidium bromide
FCS	foetal calf serum
FGFR	fibroblast growth factor recpetor
FRT	FLP recombination target
GAG	glycosaminoglycan

GAPDH	glyceraldehyde 3-phosphate dehydrogenase
GFP	green fluorescent protein
GOI	gene of interest
H_2O	water
HAT	histone acetyltransferase
HBV	Hepatitis B virus
HCl	hydrochloric acid
HCV	Hepatitis C virus
HEK	human embryonic kidney
HIF	hypoxia inducible factor
His	histidine
HPV	human papilloma virus
HPyV	human polyomavirus
HRP	horseradish peroxidase
hTERT	human telomerase reverse transcriptase
HTLV	Human T-cell leukaemia virus
IκB	Inhibitor of kappa B
IF	immunofluorescence
IgG	immunoglobulin G
IKK	IκB kinase enzyme complex
IL	interleukin
IP	immunoprecipitation
IPTG	isopropyl-β-D-thio-galactoside
IRS I	insulin receptor substrate I
JCV	JC virus
Kan	kanamycin

kb	kilobase
kbp	kilobase pair
kDa	kilodalton
KIPyV	KI virus
KOAc	potassium acetate
KOH	potassium hydroxide
KS	Kaposi's sarcoma
KSHV	Kaposi's sarcoma-associated herpesvirus
LB	luria broth
LPyV	B-lymphotropic polyomavirus
LSD	LT stabilisation domain
LT	large T antigen
M	molar
MAP	microtubule associated protein
MCC	Merkel cell carcinoma
MCPyV	Merkel cell polyomavirus
MEK	mitogen activated protein kinase
$MgCl_2$	magnesium chloride
MHC	major histocompatibility complex
MAPK	mitogen activated protein kinase
MEK	MAP and ERK kinase
$MgCl_2$	magnesium chloride
MgSO4	magnesium sulphate
mg	milligram
miRNA	micro RNA
ml	millilitre

mm	millimetre
mM	millimolar
MMP	matrix metalloproteinase
$MnCl_2$	magnesium chloride
MOPS	3-(N-morpholino)propanesulfonic acid
MPyV	Murine polyomavirus
mRNA	messenger RNA
MT	middle T antigen
MT	microtubule
mTOR	mammalian target of rapamycin
MUR	Merkel cell polyomavirus unique region
MWPyV	Malawi polyomavirus
NaCl	sodium chloride
Na_2CO_3	sodium carbonate
NaOH	sodium hydroxide
NCCR	non coding control region
NDEL1	nuclear distribution protein nudE-like 1
NEMO	NF-κB essential modulator
NF-κB	nuclear factor κB
ng	nanogram
NLS	nuclear localisation signal
nm	nanometre
nM	nanomolar
NP40	tergitol-type NP-40
NPC	nuclear pore complex
N-terminus	amino terminus

OBD	origin binding domain
OD	optical density
OE-PCR	Overlap extension polymerase chain reaction
ORF	open reading frame
PAGE	polyacrylamide gel electrophoresis
PAMPs	pathogen associated molecular patters
PBS	phosphate buffered saline
PCR	polymerase chain reaction
PET	polyethylene terephthalate
PI	Propridium Iodide
PI3K	phosphatidylinositol 3-kinase
PML	progressive multifocal leukoencephalopathy
pmol	picamole
PP2A	protein phosphatase 2A
PP4	protein phosphatase 4
PP4C	protein phosphatase 4 catalytic subunit
psi	pounds per square inch
PRRs	pattern recognitions recpetors
qRT-PCR	quantitative reverse transcriptase PCR
RACE	rapid amplification of cDNA ends
Rb	retinoblastoma protein
RbCl	rubidium chloride
RCA	rolling circle amplification
rcf	relative centrifugal force
RNA	ribonucleic acid
RNA pol II	RNA polymerase II

RNase	ribonuclease
rpm	revolutions per minute
RPMI	Roswell Park Memorial Institute medium
RSV	Rous sarcoma virus
RT	reverse transcriptase
RTK	receptor tyrosine kinase
SDS	sodium dodecyl sulphate
SILAC	stable isotope labelling with amino acids in cell culture
siRNA	small interfering RNA
ST	small T antigen
STLPyV	Saint Louis polyomavirus
SV40	simian virus 40
TANK	TRAF family member-associated NF-kappa-B activator
TBE	tris-borate-EDTA buffer
TBS	tris buffered-saline
TE	tris-EDTA buffer
TEMED	N-N-N'-N'-tetramethylethylenediamine
TGFβ	transforming growth factor beta
+TIP	plus end tracking protein
TK	tyrosine kinase
TLR	toll-like receptor
TNF	tumour necrosis factor
TRAF	TNF receptor associated factor
Tris	tris (hydroxymethyl)-aminoethane
TSPyV	trichodysplasia spinulosa-associated polyomavirus
U	unit

Ub	ubiquitin
UV	ultra-violet
µg	microgram
µl	microlitre
µm	micrometer
µM	micromolar
V	volt
VEGF	vascular endothelial growth factor
VP	viral protein
v/v	volume per volume
w/v	weight per volume
WCL	whole cell lysate
WHIM	warts, hypogammaglobulinema, infections and myelokathexis
WUPyV	WU virus
XRCC4	X-ray defective repair in Chinese hamster cells 4

Bases

A	adenine
T	Thymine
C	cytosine
G	guanine

Amino acids

Glycine	Gly	G
Alanine	Ala	A
Valine	Val	V

Leucine	Leu	L
Isoleucine	Ile	I
Serine	Ser	S
Threonine	Thr	T
Cysteine	Cys	C
Methionine	Met	M
Tyrosine	Tyr	Y
Proline	Pro	P
Aspartate	Asp	D
Glutamate	Glu	E
Asparagine	Asn	N
Glutamine	Gln	Q
Lysine	Lys	K
Arginine	Arg	R
Histidine	Hs	H
Phenylalanine	Phe	F
Tryptophan	Trp	W

Chapter 1

Introduction

1.1 Viruses and Cancer

Worldwide cancer deaths account for 13% of deaths worldwide[1,2] and is a major public health concern, both in terms of logistics and medical treatment. More people die from cancer each year than AIDs, tuberculosis and malaria combined and it is likely the death toll will remain high, due to inadequate diagnosis and treatment in developing countries. In the developed world cancer accounts for 20% of all deaths and is the highest cause of death after cardiovascular disease. In the United Kingdom alone, 2 million people live with cancer and this number is set to increase by 3.2% each year[2].

In the second half of the 20th century it became increasingly apparent that viral infection played a significant role in cancer formation and maintenance. In 1911, Peyton Rous discovered the first tumour virus, Rous sarcoma virus (RSV) which causes tumours in chickens[3]. From here intensive research began and in the subsequent years multiple mammalian tumour viruses were identified, including murine polyomavirus (MPyV) and simian vacuolating virus 40 (SV40)[4-6]. Through intensive research it has been shown that most cancer associated viruses express specific oncoproteins which facilitate cell growth, proliferation and transformation of the host cell.

The International Agency on Cancer has estimated that 20% of cancer cases worldwide are caused by chronic infections[7]. The known human tumour associated viruses include Human papilloma virus (HPV), Hepatitis B virus (HBV), Hepatitis C virus (HCV), Human T-lymphotrophic virus (HTLV-1), Kaposi's sarcoma associated herpes virus (KSHV), Merkel cell polyomavirus (MCPyV) and Epstein-Barr virus (EBV). These are believed to account for 10-15% of human viral-associated cancers (Table 1.1).

In general, upon infection the host suffers little or no symptoms, but a percentage of those infected will later develop a cancer intrinsically linked to the initial infection. Human tumour viruses have been widely studied and represent a wide range of different virus types from RNA viruses to retroviruses (Table 1.1), thus a

variety of different infectious routes, target sites and life cycles. While the current estimate stands at 20%, other reports speculate that the percentage of cancers caused by virus involvement may be much higher at 30%[8]. With the rapid progression of deep sequencing technologies it is likely that more oncogenic viruses will be discovered. For example, these new sequencing technologies have allowed the discovery of nine new polyomaviruses in the last six years, although none have been implicated in cancer.

Virus	**Family/Genome**	**Examples of Oncoproteins**	**Associated cancers**
Merkel Cell Polyomavirus (MCPyV) - 2008	Polyomaviridae - dsDNA	T antigens - namely, LT and ST	80-95% Merkel cell carcinoma cases
Kaposi's scarcoma associated herpesvirus (KSHV) - 1994	Herpesviridae - dsDNA	LANA, vflip, vBcl-2 and others	Kaposi's sarcoma, primary effusion lymphoma and some multicentric Castleman's disease
Hepatitis C Virus (HCV) - 1989	Hepaciviridae - (+)ssRNA	NS5A	Some hepatocellular carcinomas and lymphomas
Human papillomaviruses (HPV) 16 and 17 - 1983 and 1984	Papillomaviridae - dsDNA	E5, E6, E7	Cervical cancer and most penile cancers
Human T-lymphotrophic virus-1 (HTLV-1) - 1980	Retroviridae - ssRNA	Tax	Adult T cell lymphoma
Hepatitis B Virus (HBV) - 1965	Hepadnaviridae - ssDNA and dsDNA	HBx	Some hepatocellular carcinomas
Epstein-Barr Virus (EBV) - 1964	Herpesviridae - dsDNA	LMP1	Burkitt's lymphoma, nasopharyngeal carcinoma, most lymphoproliferative disorders

Table 1.1. Human tumour viruses. A list showing the 7 known human tumour viruses, date of discovery, virus family, genome structure and the viral-associated cancer.

1.2 Polyomaviruses

The polyomaviridae family are composed of non-enveloped, small double stranded DNA viruses with icosahedral capsids capable of infecting multiple different species including humans, birds, primates and rodents[9,10]. While the number of possible species susceptible to polyomavirus infection is high, the host range for each specific polyomavirus in highly restricted and productive viral infections do not occur in non-native hosts[11].

In the late 1950s and early 1960s, the first polyomaviruses were identified. In 1958 the murine polyomavirus (MPyV) was shown to induce tumours in newborn mice[12]. A further two years later in 1960, the simian vacuolating virus 40 (SV40) was isolated as a contaminant in Salk's inactivated poliovirus vaccine, however its natural host is the rhesus macaque[13,14]. These two polyomaviruses have been excellent models to study viral-induced cancers, oncogenic processes and have highlighted fundamental cell biology processes[12].

1.2.1 Human polyomaviruses

1.2.1.1 JCPyV and BKPyV

Despite the identification of polyomaviruses in the late 1950s, human polyomaviruses were first identified in 1971. JC polyomavirus (JCPyV) was isolated in 1971 from a patients' brain tissue who was suffering from the CNS demyelinating disease, progressive multifocal leukoencephalopathy (PML)[15]. JCPyV is now established as the causative agent in PML and is thought to be a common infection contracted during childhood and early adolescence with a seroprvalence of 70-90% in the adult population[16,17]. The virus is prevalent in urban sewage systems suggesting that the virus is contracted and spread through the faecal-oral route[18]. The initial site of infection is in the tonsils, followed by spread and replication within lymphoid cells and then infection in the gastrointestinal tract and kidneys, where it establishes a latent infection[19-21]. PML mainly occurs in patients with compromised immune systems, such as AIDS and transplant patients, under these conditions virus reactivation can occur and lytic infection is established in oligodendrocytes, resulting in focus formation and demyelinated areas, symptoms of PML[22].

Besides its role in PML, JCPyV has also been shown to induce human and rodent cell transformation *in vitro* and in animal models[23]. However, this phenotype has only been demonstrated in neural cells, which are non-permissive for JCPyV infection.

Glial cell specific regulation of JCPyV large T (LT) antigen expression results in higher T antigen protein levels which facilitates transformation[23]. Similar to SV40, JCPyV DNA has been detected in paediatric medulloblastomas[24], however there is no conclusive evidence linking JCPyV infection with human tumours.

BK polyomavirus (BKPyV) was also identified in 1971 from a urine sample of a kidney allograft patient presenting with chronic pyelonephritis and advanced renal failure[25]. Both JCPyV and BKPyV share 75% sequence identity and have similar infection routes[21].

Similar to JCPyV, BKPyV is an asymptomatic ubiquitous infection among the adult population with a seroprevalence of approximately 80%, however under immune suppression BKPyV can reactivate and enter a lytic replication cycle[26]. In the case of kidney transplantations, lytic BKPyV infection can result in polyomavirus-associated nephropathy (PVAN) and is the highest cause of graft loss at 10%[27]. Similar to JCPyV, BKPyV is capable of inducing transformation *in vitro* and in animal models[28]. However, no data has indicated a causal role of BKPyV in human tumour formation[29].

1.2.1.2 Other human polyomaviruses

Since the discovery of JCPyV and BKPyV in 1971, a renaissance in human polyomavirus research began in 2007, and is a direct result of new genomic amplification technologies, such as digital transcriptome subtraction and rolling circle amplification. In the past eight years 12 further human polyomaviruses have been identified, as described below.

KIPyV and WUPyV were identified from respiratory tract samples and are present in approximately 1-10% of nasopharyngeal aspirates[30-32], however they have not been associated with any disease pathology[33]. Furthermore, neither KIPyV or WUPyV seem to follow the route of infection and viral life cycle typical of JCPyV and BKPyV, as the viruses have not been identified from either urine or blood samples[30,31].

The fifth human polyomavirus, Merkel cell polyomavirus (MCPyV), discovered in 2008 will be discussed in Section 1.4. Following this in 2010, two human polyomaviruses (HPyV) were isolated from human skin: HPyV6 and HPyV7, but show no clinical symptoms[34]. Later in 2012, trichodysplasia spinulosa-associated polyomavirus (TSPyV) was isolated from the inner root sheath cells of hair follicles[35]. Lytic reactivation in immune-compromised individuals result in a rare skin disease called Trichodysplasia Spinuloas (TS). Following this a novel human polyomavirus (HPyV9) was isolated from kidney transplant patients[36]. In 2012, the tenth HPyV was isolated from healthy stool samples and termed Malawi polyomavirus (MWPyV)[37], followed by identification of HPyV10 from a patient presenting with warts, hypogammaglobulinemia, infections and myelokathexis (WHIM) syndrome[38].

Also identified in 2012, from acute diarrheal samples of children, was the MX polyomavirus (MXPyV)[39]. This was followed by two further discoveries in 2013, starting with HPyV12 which was isolated from resected liver samples and infects between 10-20% of the population[40], and by STLPyV isolated from human faeces[41]. The role of human polyomaviruses in disease is now under intense investigation, as it is clear that they are important in human pathology, as viral reactivation under specific circumstances can be associated with pathology.

1.2.2 SV40 – The polyomavirus model

The natural host for permissive SV40 infection is the rhesus macaque and the resulting infection is generally asymptomatic. However in immune-compromised hosts a demyelinating disease can occur, similar to the human condition PML[42-44]. Furthermore, infection in non-permissive hosts, such as rodents, can cause transformation of host cells leading to tumour establishment and growth.

The ability of SV40 to replicate in human cells *in vitro* is low and both SV40 and MPyV infection can result in transformation of the host cells[12]. In the years since the discovery of SV40, its tumour antigens (T antigens) have been widely studied for

their contribution to cellular transformation which is thought to only occur in non-permissive cells[45-48]. Non-permissive cells are those that lack the correct cellular machinery required for viral-induced replication, thus expression of T antigens interferes with cellular signalling pathways resulting in increased cell proliferation and eventual transformation[45,48].

Between 1955 and 1963, the polio vaccination programme resulted in millions of people being exposed to SV40 and later on SV40 DNA has been detected in certain human cancers including mesotheliomas[49]. However, despite extensive study the role of SV40 in human tumour formation remains inconclusive and to date SV40 infection has not been conclusively associated with *in vivo* human tumour formation[50,51]. However, there are a number of other human viruses that are capable of inducing cellular transformation, including the recently identified Merkel cell polyomavirus (MCPyV).

1.2.2.1 Genetic Organisation

The polyomavirus family are composed of a small non-enveloped virus with a circular double-stranded DNA genome of approximately 5.3 kilobase pairs (kbp). There are three distinct genomic regions: a non-coding control region (NCCR), an early and late coding region[52]. The NCCR contains the viral bi-directional origin of replication and transcriptional control elements, while the early and late coding regions are encoded on opposite strands of the template DNA.

Transcription of the early and late coding regions produces one primary transcript respectively, which undergoes differential splicing to produce multiple mRNA species for production of distinct proteins. This is an evolutionary mechanism which maximises protein coding capacity due to the limited genomic size constraints. The early region is transcribed in a clockwise fashion and generally encodes three T antigens, the large T antigen (LT), the small T antigen (ST) and the middle T antigen (MT). Other splice variants have also been observed, and are discussed in Section 1.2.4.8.

The late region is transcribed in a counter-clockwise direction and encodes three structural proteins required for viral capsid formation: VP1, VP2 and VP3. Interestingly, SV40, BKPyV and JCPyV encode an additional protein, VP4, termed agnoprotein which may function as a viroporin[52-54].

1.2.2.2 Viral life Cycle

Using SV40 as a model, the life cycle of polyomaviruses has been well characterised from viral attachment and entry to viral replication and virion release. Moreover, the life cycle of JCPyV has also been fairly well characterised and provides a good human model for polyomavirus infections, as other human polyomaviruses are poorly understood. Figure 1.1 represents the main stages in the polyomavirus life cycle.

To initially infect animal cells, viruses must first attach to specific receptor molecules on the cell surface, which are commonly proteins or carbohydrates, but in some cases lipid molecules. With SV40, initial viral infection is mediated by binding to sialic acids. A crucial cell surface receptor required for initial attachment for SV40, is the ganglioside GM1, however SV40 can also infect most cell types by virion attachment to the major histocompatibility complex (MHC)[55-57]. JCPyV has also demonstrated tropism for α2-6-linked sialic acids on cell membrane glycoproteins and glycolipids[58]. The well characterised MPyV and the human polyomavirus BKPyV have also been shown to bind sialylated glycans, such as GT1B[59-61].

Endocytosis is the main mechanism by which polyomaviruses enter and are transported from the cell surface to the nucleus. However various types of endocytosis mechanisms have been identified between different polyomavirus species. SV40 virion entry is fully dependent on caveolin-mediated endocytosis, whereas JCPyV depends on a clathrin-dependent mechanism[62,63]. Following entry into the cells, the virus must be transported to the nucleus in order to replicate its DNA. Recent evidence has demonstrated that JCPyV VP1, the structural capsid

protein, contains a nuclear localisation signal (NLS), allowing binding of cellular importins and entry into the nucleus via the nuclear pore complex (NPC)[64].

Once the virion has entered the nucleus by one of these mechanisms, the viral DNA is uncoated from the capsid and viral DNA transcription begins. SV40 LT transactivates the early promoter region and LT is capable of promoting viral DNA replication by directly binding the viral origin of replication within the NCCR[65]. Viral DNA synthesis in polyomaviruses depends on the host cell machinery, enzymes and co-factors expressed during S-phase, this is crucial to the viral life cycle, hence both ST and LT modify specific signalling pathways to promote entry into S-phase. Furthermore, once LT protein levels reach a certain concentration, LT acts to inhibit early viral promoter activity and alternatively binds the late viral promoter to drive production of structural proteins required for virion assembly[66,67]. Upon synthesis of the structural proteins these are then imported back to the nucleus where virion assembly begins. Assembled virions are most commonly released from the cell through cell lysis, although other modes of escape have been documented, such as cell membrane fusion exocytosis[48].

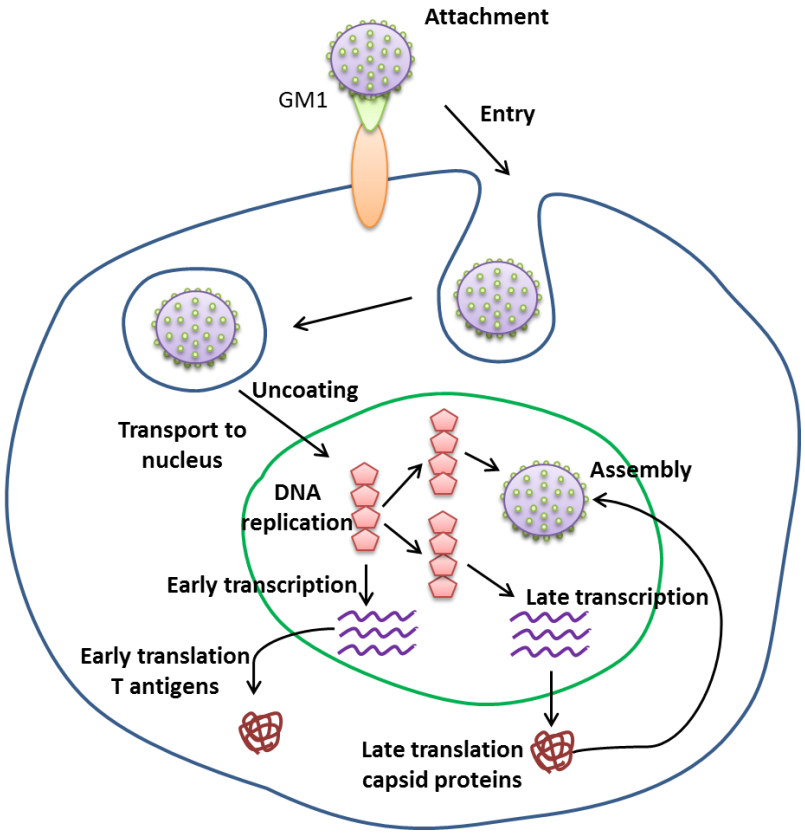

Figure 1.1. Polyomavirus life cycle. A schematic representing the major steps during lytic SV40 infection including, viral attachment, entry, transport to the nucleus, gene transcription and translation and virion assembly.

1.2.2.3 Genome integration

A fairly common phenomena during polyomavirus infection in non-permissive cell lines is the integration of the viral genome into the host chromosomal DNA. This has been demonstrated for MPyV, SV40, JCPyV and BKPyV with up to six copies of the viral genome being integrated into one host cell[68-70]. Interestingly, the pattern of integration seems to occur at random sites within the host genome, and has recently been confirmed using MCPyV as a model, where integration was seen to be random but localised in fragile sites within the host genome[71-73]. While Martel-Jantin and colleagues concluded that integration occurred at random sites in MCPyV, they also identified specific cellular genes involved in carcinogenesis, at the site of integration[72]. These included X-ray defective repair in Chinese hamster cells

4 (XRCC4) and phospholipase A2, group IVA (9PLA2G4A), indicating that these genes may play a role in MCC pathology, and warrant further study.

With regards to the viral integration junction, no specific patterns have been demonstrated however in MCPyV this seems to be located within the LT antigen, and in all samples, occurs after the pRB binding domain[72]. It is thought that integration may result in MCPyV LT tumour specific truncations, removing the helicase binding domain, thus inhibiting viral replication and in turn facilitating transformation[71,74,75]. Literature regarding the mechanism of polyomavirus integration is sparse, although it has been suggested that integration occurs by a double-crossing over event, or homologous recombination event[76].

1.2.2.4 Polyomavirus early proteins

All polyomaviruses encode the regulatory LT and ST antigens, which are transacting factors required for viral replication. It has also been demonstrated that the T antigens are oncogenic proteins with the ability to transform cells *in vitro* and in mouse models[77,78].

The central polyomavirus dogma concludes that LT is the more oncogenic, with ST playing an accessory role, however there is also an emerging role for ST in transformation. Currently, most human polyomaviruses are discussed in terms of the known functions of other better characterised polyomaviruses, such as SV40 and MPyV. Polyomavirus regulatory proteins are crucial for viral DNA replication and stimulate quiescent host cells into S phase[52,79]. This ensures the virus has all the necessary host cell machinery required to synthesise its DNA, as polyomaviruses themselves do not encode the required replicative proteins to synthesise their own DNA[12]. This is the driving force behind polyomavirus-induced cellular transformation as early gene expression in non-permissive cells results in aberrant cell cycle stimulation and interference with host cell signalling pathways[48].

There exists a high degree of sequence homology between the regulatory proteins of HPyV and other polyomaviruses (PyV). Differential splicing of the early transcript

allows for the production of both LT and ST, both of which share a common region (first 80-82 residues of the N-terminal), and a unique region at the C-terminal[52].

1.2.2.4.1 Small T antigen

1.2.2.4.1.1 Structure and domains

The coding region of ST is approximately 500 base pairs (bp) in length and codes for a 17 kDa protein of approximately 170 amino acids in length. ST localises to the nucleus and cytoplasm and is highly conserved across PyV species, with JCPyV sharing 96% sequence homology with BKPyV ST and 79% identity with SV40 ST[52].

The common region, termed the J domain is present at the N-terminus of all T antigens and is thought to have similar functions within host cells. The J domain contains a conserved Cr1 domain and a conserved DnaJ (HPDKGG) binding domain for the cellular heat shock protein, Hsc70, which acts as a chaperone protein to prevent protein aggregation during viral invasion and stress[23,80], as shown in Figure 1.2.

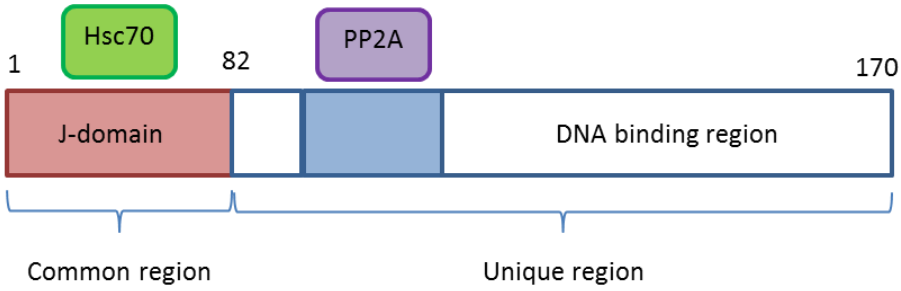

Figure 1.2. Diagrammatic representation of the polyomavirus ST antigen. The common J domain (residues 1-90) contains conserved DnaJ and Cr1 motifs. The unique region contains a binding domain for PP2A and two cysteine rich motifs for Zinc binding.

The latter portion of ST, is distinct from MT and LT and is referred to as the unique region. While the N-terminal region shows a high degree of sequence homology across the polyomavirus family, the C-terminal region is more divergent[23]. This may enable species and tissue specific tropism of each polyomavirus and may influence viral replication and tissue specific transformation.

The unique region of the SV40 ST antigen contains a conserved motif (CxxP/CxC) at 97-103 residues which is required for binding protein phosphatase 2A (PP2A), the major serine/threonine phosphatase in mammalian cells[81,82]. A consensus among polyomavirus literature maintains that the main functional roles of ST within the host cell are PP2A-dependent and through this interaction ST aids viral replication and cellular transformation.

1.2.2.4.1.2 ST interacts with PP2A

PP2A is a family of serine/threonine phosphatases that are widely expressed throughout the cell and are highly conserved among species[46]. PP2A is a heterotrimeric holoenzyme, composed of three subunits with varying functional roles. Subunit A (approximately 65 kDa) functions as a scaffold protein and its C-terminus binds Subunit C (approximately 32 kDa), which acts as the catalytically active phosphatase and together they form the core heterodimer[83].

Subunit B provides the regulatory specificity of this complex and binding results in the predominant cellular form of PP2A as a heterotrimeric complex. Binding occurs through the Subunit B N-terminus which directly binds Subunit A[84,85]. There are numerous B subunits all with variability within the N-terminal region, allowing for distinct substrate specificity[81].

Due to this diverse range of possible substrates, PP2A is an important regulator of multiple downstream signalling pathways and can affect signal transduction, apoptosis, cell cycle regulation and proteolysis pathways[86]. De-regulation of this system has been associated with multiple disorders and cancer types, and is a critical cellular regulator through which ST can interact, as shown in Figure 1.3.

The PP2A A subunit is present as two isoforms within the cell, namely alpha (α) and beta (β), however SV40 ST has only been shown to interact with the Aα subunit not Aβ[87]. Crystallisation studies have determined that the SV40 ST J domain and the unique region are important for ST binding to PP2A[87]. Both SV40 and JCPyV ST have

been shown to directly bind the A subunit and via this interaction ST is able to make contact with the C subunit[88-90].

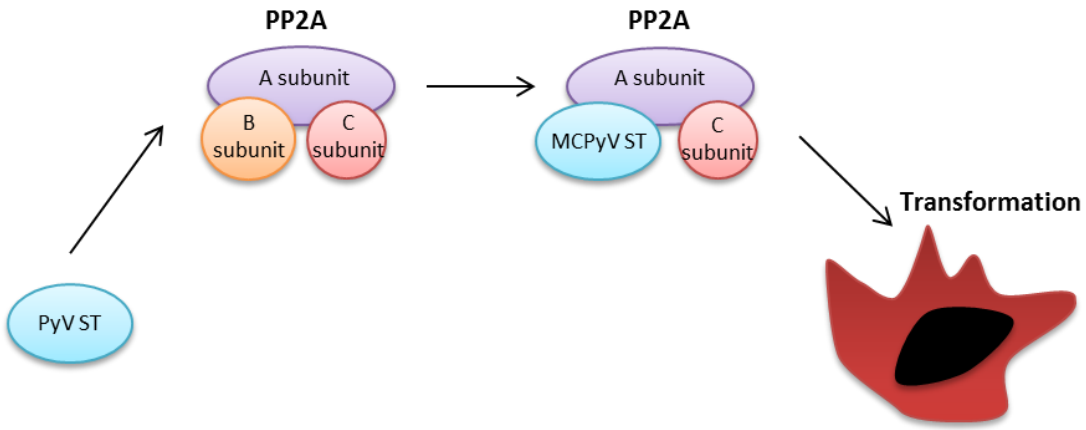

Figure 1.3. Polyomavirus ST antigen binds and affects the inherent functions of PP2A. ST acts as a competitive inhibitor for the B subunit binding site on the A subunit of PP2A. The A subunit is present as two isoforms with ST binding only the Aα subunit. The J domain of ST is required for binding PP2A A subunit and this can alter the specificity and/or inhibit PP2A activity. This can affect cell signalling pathways and promote cell proliferation and transformation.

Ruediger *et al* demonstrated that the SV40 ST-PP2A binding site responsible for binding subunit A, does so in a manner that overlaps the B subunit binding site[91]. This is important as ST can therefore act as a competitive inhibitor and compete with B subunits for A subunit binding. SV40 ST has been shown to inhibit the activity of PP2A both *in vitro* and *in vivo* and prevent binding of multiple different substrates to PP2A[78,88,92].

Using this information, there are two distinct theories to explain how downstream pathways are regulated by the PP2A complex upon subversion by the ST antigen. Firstly, ST may function as a negative inhibitor of the PP2A complex and competitively replace the B subunit, thereby inhibiting dephosphorylation of specific downstream cellular targets. Secondly, ST could act in a positive manner, whereby ST facilitates the selection of specific substrates and may redirect PP2A activity towards different cellular targets. Interestingly, ST has been shown to act by both mechanisms. SV40 ST can increase PP2A-mediated histone H1 dephosphorylation and at the same time inhibit dephosphorylation of substrates, such as relA[88]. Through this interaction, ST is capable of affecting a wide range of

cellular signalling pathways which could aid in viral replication or in non-permissive cells may induce transformation.

1.2.2.4.1.3 The role of ST in the viral life cycle

There is substantial evidence to conclude that the polyomavirus LT is important for viral DNA replication, however emerging data indicates that ST is also required for this function. Both MCPyV and SV40 ST have *trans*-acting regulatory functions *in vitro* on promoters transcribed by RNA polymerase II and III[93,94], and while ST is not essential for viral DNA replication, it is capable of enhancing LT-mediated DNA replication. This is supported by mutational studies rendering SV40 ST defective which results in diminished viral growth *in vitro* compared to wild type[95]. Moreover, expression of SV40 ST increases early viral promoter activity and enhances LT-mediated late promoter activity[65,96]. Although ST is not essential for LT-mediated viral replication, it is clear that ST plays a significant role in the viral life cycle and in the efficiency of viral DNA replication.

The J domain contains specific residues required for binding to Hsc70, which is important for the correct and timely folding and transport of cellular proteins[97]. Hsc70 acts through its inherent ATPase activity and binding of the J domain results in ST acting as a chaperone[97]. Interestingly, studies involving chimeric constructs have demonstrated that the SV40 ST J domain is crucial for ST-mediated enhancement of viral replication[98]. However, studies have not yet concluded whether this is a direct result of ST binding Hsc70 or possible uncharacterised indirect effects of the J domain within the host cell.

One of the major functional roles of ST involves the interaction with PP2A, as mentioned previously. The ST-PP2A interaction is thought to contribute to virus replication in an indirect manner through disrupting the cell cycle and driving cells into S-phase, thus allowing recruitment of the host cell machinery required for virus DNA replication[99]. Furthermore, MPyV ST has been implicated in promoting progression of the cell cycle by activating the MAP kinase cascade in a

PP2A-dependent manner[82]. Phosphorylation of serine/threonine kinases, such as ERK and MEK, within this signalling cascade result in increased binding of transcription factors, such as AP-1, which stimulate the transition from G_1 to S-phase[82].

In addition, ST has been shown to affect cell cycle progression through decreasing cellular levels of p27/kipI[23]. Cyclin dependent kinases (cdk) inhibitors are key components regulating cell cycle progression, and increased levels of one such inhibitor - p27/kipI – prevent efficient complex formation between cyclin dependent kinase 4 (CDK4) and its substrate pRB resulting in pRB-mediated cell cycle arrest[100,101]. While the mechanism by which ST mediates this decrease is unknown, it is possible that the ST-PP2A interaction could result in a decrease in dephosphorylation of cyclin E/cdk2 which regulates p27/kipI, thereby stimulating cell cycle progression. ST expression also upregulates other cell cycle progression factors including cyclin D1 and B and thymidine kinase[102], indicating other possible mechanisms of ST-mediated cell cycle progression.

1.2.2.4.1.4 The Role of ST in transformation

Several studies have demonstrated that LT and ST J domain deletions inhibit T antigen-mediated transformation[23]. Therefore, it is conceivable that the J domain, through its functions in promoting S-phase entry, may promote both replication in permissive cells and transformation in non-permissive cells. In addition, the J domain contains a conserved Cr1 domain which functions in a similar manner to that of the adenovirus E1A protein which binds p300, the cellular transcriptional co-factor[103,104], both of which have been shown to induce cellular transformation[89].

As previously discussed, the ST-PP2A interaction is essential for stimulating cell entry into S-phase, thereby promoting viral replication in permissive cells. However, in non-permissive cells, aberrant stimulation and entry into S-phase can result in cellular transformation. Both SV40 ST and LT are required for cellular transformation in rodent cells, although ST is only required when LT expression is

low[96]. However, in human cells full transformation requires expression of both SV40 T antigens in combination with oncogenic ras and hTERT, whose expression is dependent of ST[78]. Hahn *et al* also demonstrated that using SV40 ST as a model, ST is essential for cell cycle progression, anchorage independent growth and transformation.[78]

The ST-PP2A interaction has been shown to play a role in cellular transformation and can affect the levels of transcription factors within the host cell. C-myc is an important transcription factor and is activated by phosphorylation which promotes binding to more than 15% of human gene promoters and enhancer sequences[105]. The ST-PP2A interaction inhibits dephosphorylation of C-myc and promotes C-myc stabilisation[106], thereby altering cell proliferation, growth and apoptosis signalling and can directly induce cell transformation[90]. ST also activates other cellular transcription factors, such as AP-1, Sp1, CREB and NF-$_K$B, all important in cell proliferation and growth and all have been implicated in tumourigensis[52,107-109].

Furthermore, SV40 ST has been shown to induce aberrant activation of the phosphatidylinositol 3-kinase (PI3K) pathway, which is implicated in tumourigenesis in multiple human cancers and results in phosphorylation of cellular targets, such as Akt[110]. Akt is a serine/threonine kinase important in cell survival, metabolism and angiogenesis, and inhibition of PI3K activity can inhibit ST-mediated transformation[82].

Interestingly, the ST-PP2A interaction has also been implicated in promoting cell immortalisation, both *in vitro* and *in vivo*[111]. It has been demonstrated that telomerase is upregulated upon SV40 ST expression[112] and it has been suggested that inhibition of Akt desphosphorylation, at conserved Akt phosphorylation sites[113], may promote an increase in telomerase phosphorylation and activity.

Furthermore, upregulation of Bub1 (a mitotic spindle checkpoint protein) is thought to lead to aneuploidy within the host chromosomes, and this has been demonstrated in MCC tumour cells[114]. The SV40 ST-PP2A interaction has been implicated in hyperphosphorylation of Bub1 through activation of the MAP kinase

signalling pathway, and has previously shown to induce tumourigenesis and aneuploidy in transgenic mice[52,115].

1.2.2.4.2 Large T antigen

1.2.2.4.2.1 Structure and domains

Transcription and alternative splicing of the polyomavirus early gene transcript results in production of a protein of approximately 700 amino acids in length referred to as LT. LT contains the common J domain at its N-terminal and a unique C-terminal region (Figure 1.4). The J domain contains the characteristic protein binding domain for Hsc70 and the conserved Cr1 domain. However, within its unique region the LT protein contains multiple distinct protein binding domains, such as the LxCxE motif required for binding pRB[116]. Furthermore, LT contains a DNA binding domain within the mid-region of the protein (~350-450) and a C-terminal bipartite region (~530-630), which facilitates an interaction between LT and the tumour suppressor protein p53[117,118]. LT also contains a nuclear localisation signal which is required for localisation to the nucleus in mammalian cells[119].

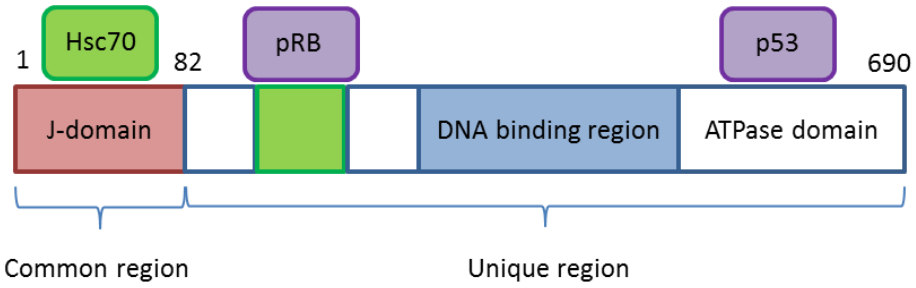

Figure 1.4 Diagrammatic representation of the polyomavirus LT antigen. Taken from [23]. The common J domains contains the DnaJ and Cr1 motifs (residues 1-90). The unique region contains binding domains for pRB, and p53.

1.2.2.4.2.2 The Role of LT in the viral life cycle

Similar to ST, the LT antigen promotes cell cycle dysregulation by driving the host cell into S-phase and is thought to be the major T antigen responsible for this function[52]. This is aided by the LT helicase and ATPase activity which promotes DNA unwinding, along with specific domains required for binding cellular replication proteins, such as DNA polymerase-α, replication protein A, topoisomerase I and nucleolin[48,120-122].

1.2.2.4.2.2.1 DNA binding capabilities

SV40 LT acts as an essential factor in early viral DNA replication and binds to the viral origin of replication, through its DNA binding domain thus promoting double helix unwinding and recruitment of DNA replication machinary[121,122]. SV40 and JCPyV LT also facilitate DNA transcription and recuit cellular component to both the early and later promoter regions. Late promoter activity requires suppressing early gene transcription through an origin binding dependent mechanism[67,123,124].

1.2.2.4.2.2.2 Recruitment of cellular proteins

As discussed previously, the ability of LT to stimulate viral DNA replication depends upon the recruitment of cellular proteins required for efficient viral replication complex formation at the viral origin (*ori*). The NCCR contains the viral *ori*, promoter and enhancer sequences and the TATA box, this facilitates recruitment of cellular proteins required for transcription, such as RNA polymerase II and various other cellular transcription proteins[122]. During lytic infection, transcription of the early and later regions is temporally regulated. Transcription of the early regions results in the production of LT and ST, which stimulate the cell to enter S phase, thus facilitating viral DNA synthesis and replication of the viral genome, required for progeny virion formation.

Initiation of viral replication occurs within the *ori*, and proceeds bidirectionally until the two replication forks terminate at approximately 180 degrees from the *ori*. Both the J domain and the ATPase domain of SV40 LT are necessary for direct

binding of LT to the catalytic subunit of DNA polymerase-α *in vitro*[125]. Furthermore, SV40 LT is capable of binding the cellular replication protein A which enables the activity of DNA polymerase and stimulates replication of the viral genome[126].

The DNA helicase activity of SV40 LT is required for efficient viral DNA replication as the circular double stranded DNA helix must first be unwound to allow replication fork formation[127]. Through this activity SV40 LT recruits nucleolin and topoisomerase I to form components of the holoenzyme required for DNA unwinding[127].

1.2.2.4.2.3 The Role of LT in transformation

LT alone is sufficient to induce transformation of rat fibroblast cells and is thought to be a result of LT binding to the tumour suppressor proteins, p53 and pRB[48,128,129]. Despite this, mutations within LT (that do not affect its ability to bind either pRB or p53) can inhibit LT-mediated transformation, demonstrating that other LT functions must contribute to tumourigenesis[130]. An alternative explanation may be due to ability of BKPyV and SV40 LT to induce mutagenic effects in the host DNA by more than 100 fold, through SV40 LT binding to Mre11, a double stranded break response component[48,52].

1.2.2.4.2.3.1 Binding pRB

All polyomaviruses studied to date contain a highly conserved LxCxE motif within LT, required for binding the cellular tumour suppressor protein pRB. Importantly, LT binding mutants defective for pRB binding are all incapable of inducing cellular transformation[48,116,131-133].

In phenotypically normal cells, binding and sequestration of E2F transcription factor proteins inhibit expression of E2F responsive genes, such as C-fos and C-myc[134,135]. Phosphorylation of pRB allows the release of E2F, thus progression from G_1 to S-phase[136,137]. SV40 LT binds and sequesters pRB and pRB family proteins, such as p130 and p107, and inhibits binding to E2F, allowing transcription of E2F responsive

genes and progression to S-phase[52,132]. In addition, SV40 and BKPyV LT can also downregulate the expression of pRB proteins by promoting proteolysis of p130 and other pRB family members in mouse fibroblast cells[138]. Furthermore, evidence suggests that the Hsc70 binding domain has *cis*-acting activities that aid in dissociation of pRB-E2F in an ATPase dependent manner[139]. This suggests that LT has a redundancy mechanism by which to subvert the pRB signalling pathways in order to promote S-phase entry.

1.2.2.4.2.3.2 Binding p53

Aberrant p53 regulation is the most common feature of human cancers, due to its crucial role as a regulator of the cell cycle, apoptosis and DNA damage repair[140]. JCPyV, BKPyV and SV40 LT all bind p53, a mechanism dependent on two ATPase domains within the C-terminal region[117,132]. Polyomavirus regulation of p53 is required as inhibition of pRB activity by LT binding results in the transcription of E2F responsive genes and activates $p14^{ARF}$, whose downstream effect results in activation of p53 and transcription of p53-regulated genes [141]. This would result in cell growth arrest and apoptosis, however LT binding renders p53 transcriptionally inactive, as p53 can no longer access promoters[142,143]. LT expression alone is sufficient to downregulate the expression of p53 responsive genes which allows viral replication to proceed in permissive cells but in non-permissive cells can lead to transformation[12,144].

1.2.2.4.2.3.3 Binding Cullin 7

More recently, studies have demonstrated that SV40 LT is able to interact with cullin7 (cul7), a core protein in the E3 ubiquitin ligase protein degradation complex[145,146]. This interaction is able to prevent cell growth arrest in low serum conditions and deficiencies in anchorage dependent growth[146]. The mechanism behind this phenotype is poorly understood but demonstrates the importance of this interaction in tumourigenesis.

1.2.2.4.2.3.4 IRS I

It has been demonstrated that polyomavirus LT expression results in inhibition of the homologous recombination-direct DNA repair (HRR) response[147]. Both JCPyV and SV40 LT have been shown to induce translocation of insulin receptor substrate I (IRS I) to the nucleus, resulting in an interaction between IRS I and Rad51 (a DNA repair component), thus inhibiting HRR[148-150]. Furthermore, the expression of a dominant negative IRS I mutant inhibits anchorage independent growth of JCPyV LT transformed cells[149]. This demonstrates that there may be multiple mechanisms by which LT mediates anchorage independent growth of transformed cells.

1.2.2.4.2.3.5 Binding β-catenin

β-catenin is a crucial component of the Wnt signalling pathway, which is able to form complexes with transcription factors in order to activate transcription of specific target genes, such as C-myc and cyclin D1[151,152]. Constitutive activation of the Wnt signalling pathway has been associated with tumour formation and progression in various cancer types[69,153]. Several studies have demonstrated that LT can directly bind β-catenin, thereby increasing its stability and thus enhancing activation of its target genes. This is another contributing mechanism by which LT can induce tumour formation[151,152].

1.2.2.4.2.3.6 Other transcription factors

Studies have demonstrated that SV40 LT can alter the mRNA transcript levels of a number of transcription factor genes, such as AP-1, C-myc, TFIIC and Sp1[52]. These transcription factors regulate a wide range of gene families involved in cell proliferation, DNA repair, angiogenesis and apoptosis, as such SV40 LT regulation of transcription factors has wide ranging downstream effects on the mRNA levels of a wide range of effector proteins involved in these processes.

Furthermore, the transcription factor thyroid embryonic factor-1 (TEF-1) has been identified as a binding partner of SV40 LT, and through this interaction LT is able to inhibit TEF-1-mediated repression of the late viral promoter, thereby stimulating DNA replication[154]. Interestingly, this may also play a role in transformation as LT mutants unable to bind TEF-1 showed reduced numbers of foci in transformation assays, implicating TEF-1 inhibition in viral induced transformation[155].

1.2.2.4.3 Middle T antigen

1.2.2.4.3.1 Structure and domains

Alternative splicing of rodent polyomavirus primary early transcript results in production of a 421 residue protein with a molecular weight of 55 kDa, known as the middle T (MT) antigen[156]. MT is very similar in structure to ST and is composed of all but the final 4 C-terminal amino acids from ST, thus sharing the J domain and PP2A binding domains (Figure 1.5). The remaining 230 amino acids at the C-terminal portion of MT are unique and contain multiple phosphorylation sites which are crucial for the ability of MT to recruit or activate specific cellular components[156].

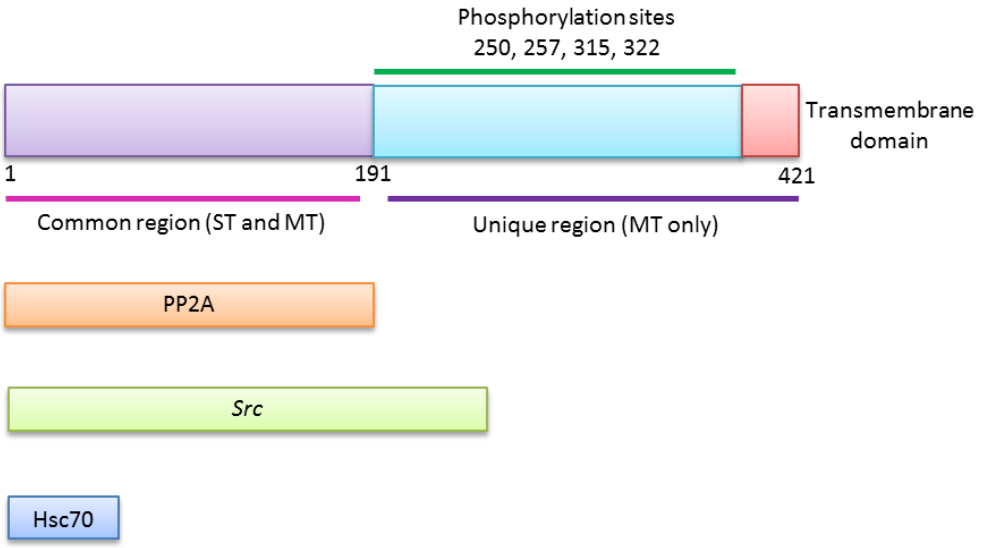

Figure 1.5. Diagrammatic representation of the polyomavirus MT antigen. MT shares the N-terminal region with ST and contains the J domain and PP2A binding site, along with a Src binding domain. The unique region contains multiple phosphorylation sites and a transmembrane binding domain.

MT is able to span the lipid bi-layer through its long hydrophobic region within its C-terminus, and the inherent functions associated with MT expression are a result of its association with the cellular membrane[157,158].

1.2.2.4.3.2 The Role of MT in the viral life cycle

Similar to ST and LT, the MPyV MT antigen can bind the viral origin of replication thereby regulating viral DNA replication. It facilitates this through activation of the AP-1 transcription factors, Ets protein families and C-jun promoters[159-163]. In addition, MT is pivotal for maturation of the viral capsid, as the absence of MT expression results in aberrant phosphorylation of VP1 which impedes viral capsid assembly[164,165].

Clearly MT is important in regulating cell cycle entry to enable efficient viral DNA replication, as such in non-permissive cells MT also contributes to tumourigenesis. It is interesting to note, that the transcripts encoding MT have not been identified in human specific polyomaviruses, such as MCPyV. Thus human polyomavirus LT and ST may compensate for or encode alternative proteins, such as ALTO, that may function in a similar manner as MT, as discussed in Section 1.4.5.3.4.

1.2.2.4.3.3 The Role of MT in transformation

In rodent polyomaviruses it has been shown that the MT is the major transforming protein and its expression alone is sufficient to induce transformation in cell culture[158]. The C-terminal hydrophobic region is pivotal for viral-mediated transformation and deletion of a six amino acid C-terminal of this region fully ablates the ability of MT to induce transformation[166-169]. It has also been demonstrated that both the N-terminal and C-terminal regions are pivotal for MT binding to cellular protein kinases, and while MT membrane binding is required for this activity it is not sufficient[167].

Interestingly, recent analysis has demonstrated that MT is important during the early stages of transformation. Initial expression of MT correlates with host cell morphological changes resulting in altered actin filament organisation[168]. Furthermore, perinuclear localisation of MT was consistent with condensation of tubular endosomes in the perinuclear region, thus this may contribute to the morphological changes seen during early transformation of host cells by SV40 T antgens[168].

1.2.2.4.3.3.1 Binding PP2A

As mentioned previously, ST and MT share a large proportion of their coding sequence including the J domain and the PP2A binding motif. To this end, MT is capable of binding PP2A in the same manner as described for ST[170]. However, in contrast to ST, MT can bind both isoforms of PP2A (Aα and Aβ), although the functional significance of this has yet to be addressed. Mutations in the PP2A Aβ isoform are associated with multiple cancers[87], hence there may be precedence for MT-mediated transformation through binding PP2A Aβ. In addition, MT has been shown to activate tyrosine kinases and C-jun, similar to ST, through binding PP2A[171].

1.2.2.4.3.3.2 Src family sequestration

MT is able to associate and sequester Src family tyrosine kinases (TKs) at the cell membrane in a PP2A dependent manner[172]. The N-terminal region (residues 185-210) is responsible for binding TKs and mutations within this site abolish the interaction[172,173]. Upon binding of MT to the TK proteins, MT is phosphorylated at specific tyrosine residues (250, 315 and 322), subsequently enhancing MT transforming capabilities[174,175].

1.2.2.4.4 Other alternative early proteins

In addition to the three previously described T antigens, SV40 also produces an additional protein by alternative splicing of the early transcript, termed 17kT, composed of 131 amino acids (from the LT N-terminus) and an addition A-L-L-T at the C-terminus[176]. The role of 17kT in the viral lifecycle is relatively unknown, however phosphorylation of 17kT can affect the inherent functions of SV40 LT[52]. In addition, 17kT is capable of immortalising rat fibroblasts (when co-expressed with H-ras)[176,177].

JCPyV encodes three addition early proteins – T_{135}, T_{136} and T_{165}. The first two are composed of the 132 amino acids at the N-terminus of LT and 3 or 4 additional amino acids at the C-terminus, respectively. T_{165} contains the same N-terminus as its predecessor, but combines the last 32 amino acids from the C-terminus of LT[177,178]. These alternative proteins are highly expressed during JCPyV lytic infection and are fundamental for viral DNA replication, as demonstrated by mutational studies which result in reduced viral replication in glial cells[178]. In terms of transformation, it has been suggested that they may act in a similar manner as MT, as co-expression of the T' proteins and H-ras can induce immortalisation of rat embryo fibroblasts[177,178].

1.3 Merkel cell carcinoma

1.3.1 Merkel cells

The Merkel-cell neurite complex, is one of the four main classes of mammalian sensory receptors and is an important complex for sensing light touch, shape, texture and curvature[179]. As seen in Figure 1.5 this receptor complex consists of Merkel cells situated at the epidermal/dermal border and the afferent somatosensory fibers that stimulate them[180]. Merkel-cell neurite complexes are located in touch sensitive regions of the skin, such as glabrous skin surfaces of the hands and feet, whisker follicles and touch domes (specialised epithelial structures in hairy skin)[181]. Merkel cells are oval shaped and approximately 10-15 µm in diameter with spinous projections on the surface of the cells[182]. The exact function and mechanism of action of Merkel cells is still undetermined, however evidence suggests that neuropeptides that accumulate near the nerve fibre junctions are required for synaptic transmission via voltage gated ion channels[183]. Moreover, the use of histochemical markers indicate that Merkel cells may also act in a paracrine fashion[183].

Since the discovery of Merkel cells in 1875, there has been debate as to whether they are derived from the skin lineage or the neural crest[180,181,184,185]. However in 2009, using neural crest and epidermal *Cre*-driver lines which specially delete *Atoh1*, it was shown that deletion of the Atoh1 protein in the skin lineage resulted in complete loss of Merkel cells from all skin regions, while deletion from the neural crest lineage had no effect[179], clearly indicating that Merkel cells arise from the skin lineage (Figure 1.6).

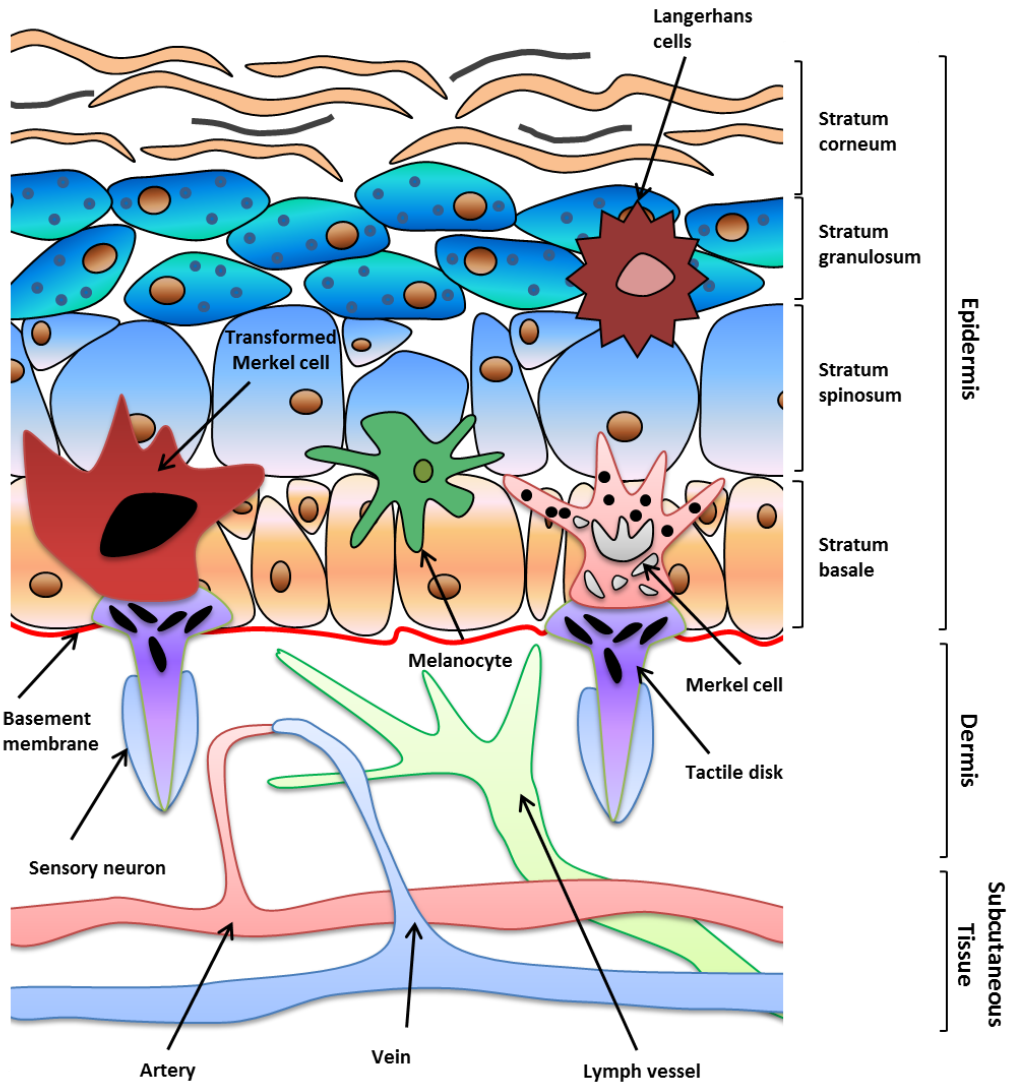

Figure 1.6. Diagrammatic representation of the location of Merkel cells within the skin. All skin layers shown, with Merkel cell neurite complex at the epidermal/dermal border with veins, arteries and lymph systems.

1.3.2 Merkel cell carcinoma

Merkel cell carcinoma (MCC) is a rare and highly metastatic neuro-endocrine tumour which originates from mammalian Merkel cells[186] and has been classed as the most aggressive form of skin cancer due to its propensity to spread through the dermal lymphatic system[187].

1.3.3 MCC histology and presentation

MCC primary tumours present as small pink nodules which are less than 2 mm in diameter or as a mass which is more than 2 mm in diameter (Figure 1.7)[188]. Primary MCC tumours can be located on any region of the body, however more than 90% appear on sun-exposed regions of the body such as the head and neck[189].

Historically, identification of MCC tumours has been particularly difficult and was often mistaken for small-cell carcinoma of the lung and Ewings sarcoma which present as visibly similar tumours[190]. MCC tumours are visualised as a lesion of nested or stranded small round cells, with an oval/round nucleus, inconspicuous nuclei, dispersed granular chromatin and scanty cytoplasm, in a bed of vascular and infiltrating cells (Figure 1.7)[191,192]. It is only recently that a robust detection system has been established; MCC cells display a specific arrangement of cytokeratin (CK) 20 filaments and is a specific and highly sensitive MCC biomarker which can clearly distinguish MCC from other tumours[193].

It has been shown that most MCC tumours are CK20 positive and CK7 negative, however a few CK20 negative and CK7 positive MCC tumours have been characterised[194]. Other MCC neuro-endocrine biomarkers include chromatogranin and somatostatin along with neuron-specific enolase[191,195]. Despite the rare differences in cytokeratin reactivity, clinical MCC diagnosis usually includes reactivity to CK20, a thyroid transcription factor and leukocyte common antigen, in addition to the presence of one of the above neuro-endocrine markers[190].

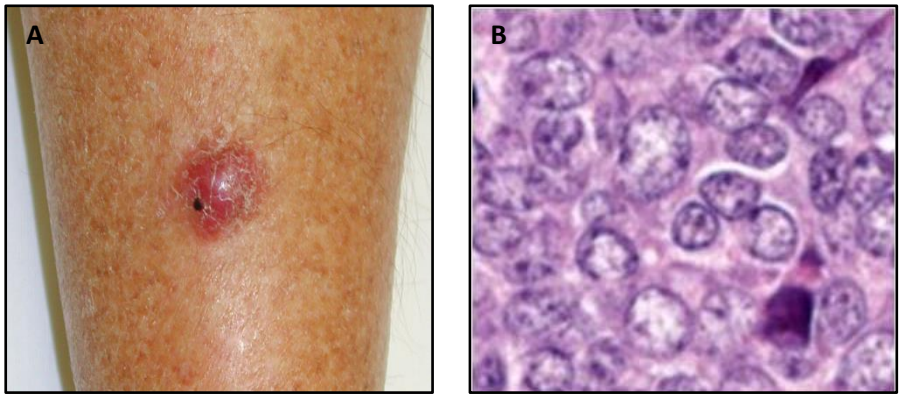

Figure 1.7. MCC appearance and histology. (A) A typical primary MCC tumour nodule present on the leg (Image kindly provided by Howard Peach, Leeds Teaching Hospital NHS Trust, UK). (B) MCC tumour cells characterised by dispersed granular chromatin, scanty cytoplasm and large nuclei[186].

1.3.4 Epidemiology

The reported cases of MCC have tripled in the past 20 years to 1500 new cases being diagnosed each year in the United States of America[8,190]. In the UK, a similar trend has been recorded, with the age standardised incidence rate of MCC at 0.9 per 100,000 population[196]. This increase in incidence is partially due to recent advances in MCC diagnostic techniques, such as CK20 staining. Melanoma and non-melanoma are the most common causes of skin cancer in the US with 76 thousand cases being diagnosed each year. While MCC is thirty times rarer than melanoma, it is twice as lethal. These numbers suggest that MCC is as prevalent as HTLV-induced cancers and is likely to affect similar numbers as those affected by KSHV-induced cancers (4,100 new KSHV cases are diagnosed in the developed world each year)[8].

Studies have highlighted that MCC incidence is highest in white-caucasians, and intermediate incidence in other ethnic groups and an extremely low incidence in dark-skinned ethnic groups[197]. Furthermore, those of European descent have a higher risk of developing MCC, due to UV light being a strong co-factor associated with MCC development. This is likely due to the degree of melanin present in the skin which confers protection against DNA damaging UV exposure and development of MCC[192,198].

Interestingly, the incidence of MCC is higher in males than females with a 2:1 ratio for white-Caucasians and 5:1 ratio in other ethnic groups[197], however the reason for this observed difference in incidence due to sex has yet to be established. Furthermore, age poses a significant co-factor in developing MCC, which is very rare in those under 50 years of age[190]. This indicates the need for accumulation of oncogenic mutations within the host genome for MCC development and suggests that the increase in MCC incidence is in part due to an ageing population.

1.3.5 Clinical Staging

Before 2010 the clinical staging system for MCC used a four tiered arrangement. Stage I disease was classified as 'localised tumour with a nodule of less than 2 mm', Stage II disease defined as 'localised tumour with a mass of more than 2 mm', Stage III disease 'regional metastasis' and Stage IV disease defined as 'distant metastasis'[192]. While this system is still in use, it has been redefined to include differences in regional metastasis for patients with inconsistencies in pathological and clinical appearances[199].

1.3.6 Prognosis and treatment

As mentioned previously MCC is highly aggressive, with 28% of patients dying within the first 2 years of diagnosis and a 5 year survival rate less than 45% due to the high rate of metastasis[197,200]. The cancer is associated by significant incidence of local recurrence (45%), early involvement of local lymph nodes (70%) and distant metastasis (50%) and of those patients with distant metastasis an 80% mortality rate[200].

The high mortality rate associated with MCC is due directly to the metastatic nature of the tumour[201,202]. As such management of MCC is presently a concerning issue and there are unfortunately no specific therapeutic regimes available for treatment. Current clinical therapeutic regimes are those used for small-cell carcinoma of the lung, however no chemotherapeutic regimes have shown an increase in survival[203].

As a result MCC is treated aggressively, with a wide surgical excision of the primary tumour with pathological verification of complete tumour removal, followed by ionising radiation therapy to decrease the incidence of local recurrence[190,204]. After metastasis of the tumour to local lymph nodes, the patients will undergo extensive surgical removal of tumours including lymphadenectomy followed by radiation therapy at the excision sites and lymph nodes[192]. While distant metastasis is treated with chemotherapy regimes such as cyclophosphamide, anthracyclines and etoposide, while half of MCC patients respond to chemotherapy, prognosis is very poor with a median survival of 21.5 months[205].

1.3.7 Infectious origin of MCC

Interestingly, it has been established that the risk of developing MCC is higher in immune compromised individuals such as AIDs patients (8 fold increase), transplant recipients (10 fold increase) and chronic lymphocytic leukaemia patients (48 fold increase)[188]. The associated incidence of immune suppression is similar to the cancer caused by Kaposi's sarcoma-associated herpesvirus (KSHV)[206], indicating that MCC may have an infectious aetiology.

1.4 Merkel cell polyomavirus

1.4.1 MCPyV discovery

In 2008, a novel human polyomavirus was discovered and first isolated from MCC tumours[71]. Digital transcriptome subtraction (DTS) was employed, whereby mRNA was extracted from primary MCC tumour cells followed by cDNA library preparation and pyrosequencing. The subsequent cDNA data was analysed and all known human transcripts were removed. This then identified foreign transcripts of unknown origin, which were compared to pathogen sequence databases, highlighting sequence similarity to other polyomaviruses[71]. 3'-RACE was then

performed followed by viral genome walking to generate a complete circularised MCPyV genome.

Identical RACE products were generated from both the primary MCC tumour and from metastatic tumours derived from the lymph nodes, indicating that clonal viral integration occurred prior to tumour formation and metastasis[71]. This suggests that MCPyV is unlikely to be a passenger virus and that MCPyV is a contributing factor for MCC development and progression. Furthermore, analysis demonstrated that 80% of MCC tumours analysed were positive for a clonally integrated MCPyV genome. This finding has been confirmed by others in the field[71,207], once again supporting the finding that MCPyV is a contributing factor for development of MCC. Furthermore, a new report using sensitive antibody staining techniques has suggested that MCPyV may be present in 97% or more MCC tumour samples[208]. This demonstrates the need for multiple MCPyV screening methods and eludes to the fact that MCPyV may be ubiquitous among the MCC tumour population.

MCPyV is the first human polyomavirus to date that has been conclusively shown to be associated with a human malignancy. Despite this, the role of MCPyV in the pathogenesis of MCC is still poorly understood highlighting the importance for studying the molecular biology and life cycle of the virus.

1.4.2 Seroprevalence

Until recently, the seroprevalence of MCPyV, was unknown. However new serological data detecting MCPyV VP1 and VP2 in patient blood has determined that the majority of the general population is seropositive, with 50% of children under 15 years infected and approximately 80% of the adult population[209]. As such this virus is thought to be a common ubiquitous childhood infection of the skin and a common skin commensal. Furthermore, there was no age-related waning of antibody titre indicating a persistent MCPyV infection possibly through latent infection[209].

1.4.3 MCPyV present in non-MCC samples

Evidence exists to suggest that MCPyV may play a role in other non-MCC related cancers, as MCPyV DNA has been isolated from Kaposi's sarcoma[210], small cell lung carcinoma[211] and various melanoma skin cancers[212]. However these findings are inconclusive and have not as of yet demonstrated MCPyV involvement in any of these malignancies.

Furthermore, replication-deficient MCPyV genomes have been isolated from a subset of patients with Chronic lymphocytic leukemic (CLL) and MCPyV-positive MCC patients have a greater risk factor of developing CLL than MCPyV-negative MCC patients[213,214]. While most CLL tumours do not show any particular pattern concerning MCPyV infection, there may be precedence for MCPyV involvement in a small subset of CLL cases.

In addition, squamous cell carcinoma (SCC) has also been highlighted as having a potential link to MCPyV infection, with studies indicating the presence of MCPyV in 40% of cutaneous SCC cases[215]. Perhaps the most important finding in this study is that nearly all MCPyV–positive SCC tumours have a mutation in exon 2 of LT, theoretically producing a truncated LT[216]. This mutation could produce a similarity truncated LT protein that is present in MCPyV-positive MCC tumours. However further characterisation is required to identify if a truncated LT protein is expressed in these cases, helping to confirm the role of MCPyV in SCC. Due to the recent discovery of the virus, detection and confirmation of MCPyV in other clinical samples is ongoing, but it is possible that MCPyV may have a causal role in other malignancies.

1.4.4 Phylogeny

MCPyV is closely related to the other known polyomaviruses and phylogenetic studies using VP1, VP2 and LT sequences from all known human polyomaviruses have been conducted (except HPyV10 and after) (Figure 1.8)[37]. Initially studies just

after the discovery of MCPyV concluded it was most closely related to the African Green Monkey lymphotrophic polyomavirus[217]. However more recent analysis has indicated that MCPyV is more closely related to MPyV and Chimpanzee polyomavirus (ChPyV), due to the high degree of sequence homology between the VP2 coding region and LT genes[37]. Furthermore MCPyV VP1 coding sequence resembles ChPyV and also shares a high degree of homology with one of the recently discovered human polyomaviruses, HPyV9[37].

Currently, MCPyV resides in the Orthopolyomavirus genus of the Polyomaviridae family[218]. Interestingly, MCPyV VP1, VP2 and LT all share a high degree of sequence homology with trichodysplasia spinulosa-assocaited polyomaviruses (TSV)[35,37]. TSV was first isolated from patients with a rare skin disorder, while the role of TSV in this disease has not yet been elucidated, it suggests that both MCPyV and TSV are common skin commensals.

Recent findings also suggest that there is distinct variability within the MCPyV genome. Phylogenetic analysis of MCPyV strains present in the GenBank database clearly indicate that the Japanese and Asian strains form a distinct dominant clade from the Caucasian clade[219]. This suggests that MCPyV genotypes are geographically related and that further characterisation of MCPyV genomes from distinct human descents will illuminate the distinct differences between clades which perhaps affect MCPyV pathogenesis and tumourigenesis.

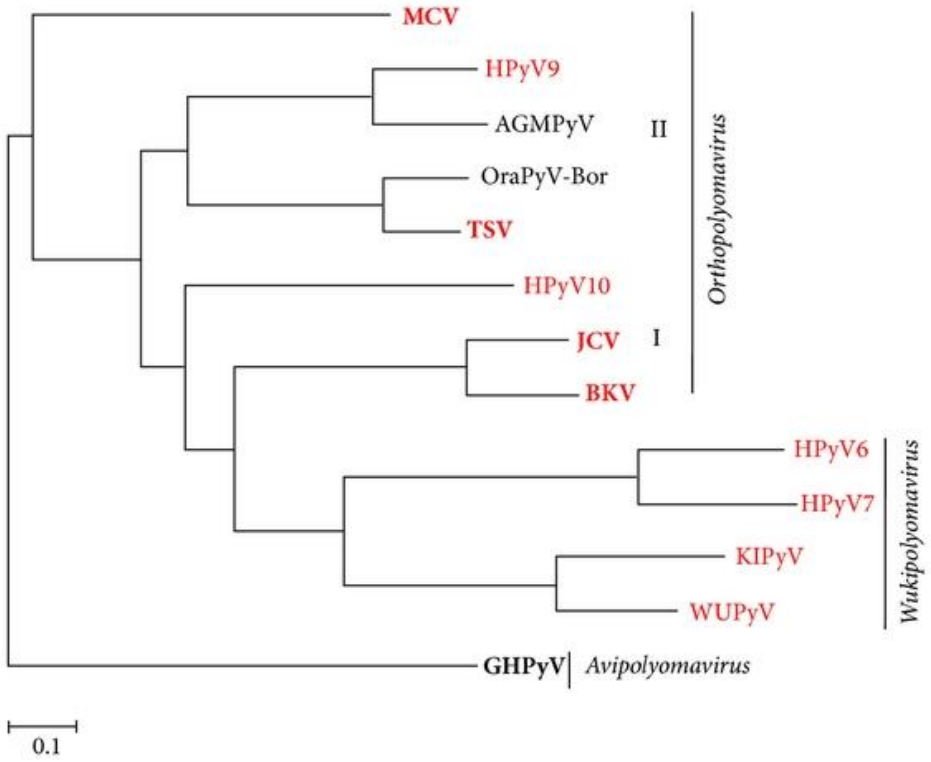

Figure 1.8. Phylogenetic study of the relationships of human polyomaviruses. Taken from[220]. Each human polyomavirus is highlighted in red and those associated with human disease in bold and genera within the polyomavirus family are indicated in italics. Whole genome nucleotide sequence analysis was performed using a maximum likelihood phylogenetic analysis. Phylogenetic analysis suggests MCPyV is most closely related to TSV, HPyV9, HPyV10 and AGMPyV. Abbreviations are as follows: AGMPyV (African Green Monkey polyomavirus; BKV (BK polyomavirus); GHPyV (goose haemorrhagic polyomavirus; HPyV6 (human polyomavirus 6); HPyV7 (human polyomavirus 7); JCV (JC polyomavirus); KIPyV (KI polyomavirus); MCV (Merkel cell polyomavirus); HPyV9 (human polyomavirus 9), MWHPyV (Malawi polyomavirus); TSV (trichodysplasia spinulosa-associated polyomavirus) and WUPyV (WU polyomavirus).

1.4.5 Genetic Organisation

1.4.5.1 MCPyV Genome

The MCPyV genome is similar to the genetic organisation of other polyomaviruses, with a genomic size comprising 5387 base pairs, split into three distinct regions; the non-coding control region (NCCR) contains viral promoters and the bi-directional origin of replication and the early and late coding regions. The latter two are

present on opposite strands of the viral genome and are transcribed in opposing directions, as shown in Figure 1.9.

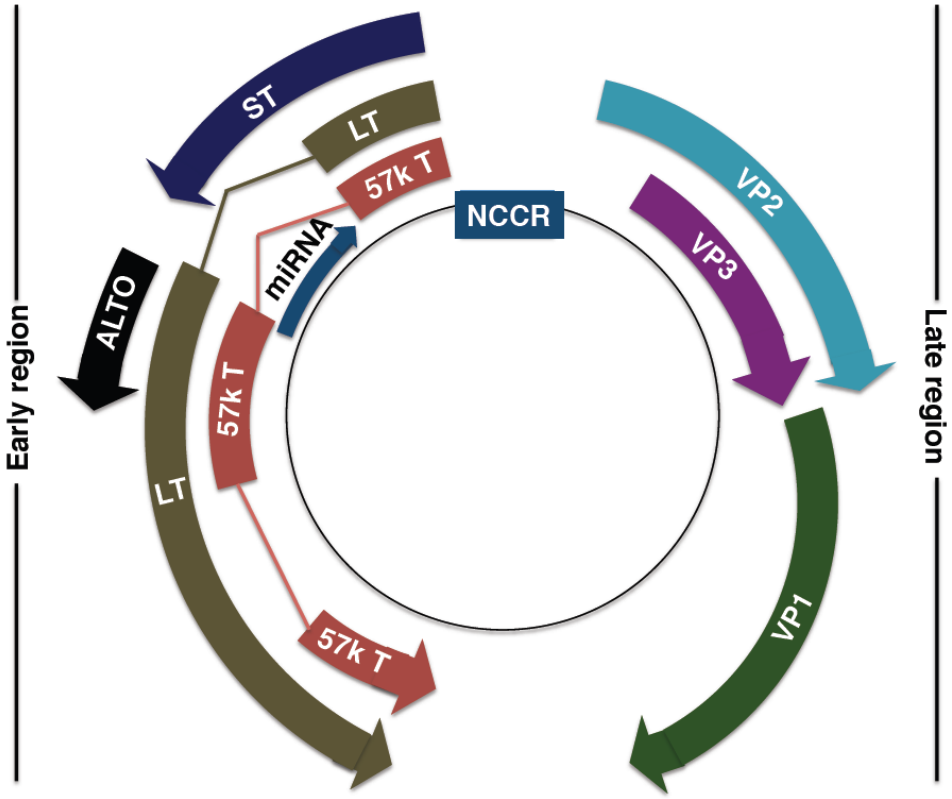

Figure 1.9. Genome organisation of MCPyV. Taken from[221]. Genetic organisation of the MCPyV genome, including three distinct regions. Non-coding control region (NCCR), containing the bipartite origin of replication. The early coding region containing the large T antigen (LT), small T antigen (ST), 57 kT antigen (57kT), alternative T antigen open reading frame (ALTO), microRNA (miRNA). The late coding region comprises structural genes, the capsid proteins, VP1, VP2 and VP3.

1.4.5.1.1 MCPyV Origin of Replication

The MCPyV non-coding control region (NCCR) contains the origin of replication which is 71 base pairs in length. Similar to other well characterised polyomaviruses the NCCR contains an AT rich region, a LT binding domain (to initiate viral replication) and an early enhancer domain. This binding site is comprised of eight repeating guanine-rich pentanucleotide sequences, very similar to the polyomavirus consensus sequence: 5'-GAGGG-3'. However, the other two

pentanucleotide sequences are distinct from other polyomaviruses (5'-GAGCC-3' and 5'-GGGGC-3'), and the proximity of these sequences and the number are also clearly distinct[222].

1.4.5.1.2 MCPyV T antigen locus

Similar to other PyV, MCPyV T antigens (ST, LT an 57kT) are *trans*-acting factors required for viral genome replication and tumourigensis[52,71,79] and their structure and protein binding domains are depicted in Figure 1.10.

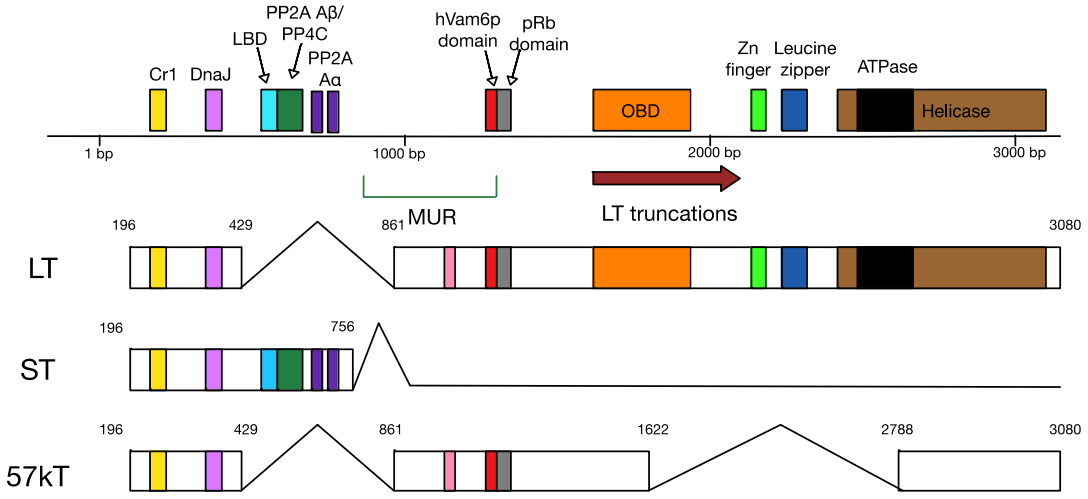

Figure 1.10. MCPyV T antigen structure and domains. Taken from[221]. The schematic shows the relative locations of each gene that encode specific protein binding domains and splicing patterns associated with differential splicing of the primary early transcript. The ST binding domains for PP2A Aα are at R7 and L142 and for a PP2A Aβ/PP4C at 97-11.

1.4.5.1.2.1 Large T antigen

The MCPyV LT protein comprises 816 amino acids and is transcribed across two exons. As mentioned previously, the J domain comprises the first 80-82 residues; however the remaining C-terminal region is unique, with distinct protein binding domains required for its interaction with the host cell (Figure 1.10). The MCPyV LT comprises all the major functional domains associated with other polyomaviruses, such as a highly conserved pRB binding domain (LXCXE), an origin binding domain

(OBD) and a nuclear localisation signal (NLS)[74]. The NLS encoded by MCPyV LT is responsible for nuclear localisation of LT when expressed in mammalian cells[119]. However truncation of the LT, as seen in tumour samples, may result in loss of this signal and hence some cytoplasmic localisation (general consensus from several abstracts at the DNA Tumour Virus Meeting 2013, Birmingham).

MCPyV LT is a highly multifunctional protein and is involved in viral genome replication as well as manipulation of host pathways through numerous protein-protein interactions and described in Section 1.2.4.6.

Similar to SV40, MCPyV LT has DNA binding and helicase features within its C-terminus and can also interact with p53[223]. The inherent helicase activity of PyV T antigens is important for viral DNA unwinding, facilitating the loading of cellular complexes required for transcription[117,118]. Despite MCPyV sharing many similar protein binding domains inherent in SV40 LT, they share only 30% sequence identity[224], clearly indicating novel regions may be present within MCPyV LT. One such unique region has recently been identified – MCPyV unique region (MUR) – and is a 200 amino acid sequence located between the OBD and the first exon[119]. In addition, MCPyV LT has also been shown to encode a viral miRNA important in regulating early gene expression[119,225].

1.4.5.1.2.2 Small T antigen

Similar to LT, the ST antigen (186 amino acids) has roles in both viral DNA replication and cellular transformation. MCPyV ST shares a common J domain, however the unique C-terminal is produced by transcriptional read-through of the exon splice site used by both 57kT and LT and has been shown to localise to both the nucleus and the cytoplasm[52]. Similar to other polyomaviruses, MCPyV ST contains a protein binding domain for PP2A[71] (Figure 1.8). In addition, the MCPy ST protein encodes a binding site for another cellular phosphatase, PP4C[226], as shown in Figure 1.10. Moreover, the novel LBD (LT-binding domain) has been identified and prevents LT proteolysis[227].

1.4.5.1.2.3 57 kiloDalton T antigen

While 432 residues of the 57kT protein shares the J domain of LT and ST, with similar protein binding domains (Hsc70, Cr1 epitope, MUR and pRB domain) very little is known regarding the role of MCPyV 57kT in the viral life cycle. SV40 17kT has been shown to be homologous with 57kT, thus it could play a role in promoting host cell proliferation[176,228].

1.4.5.1.2.4 Alternative T antigen open reading frame

The MCPyV early region encodes the three previously discussed T antigens, however recently an overprinting gene within the T antigen locus was discovered[229]. Overprinting results in production of two unrelated proteins which are encoded as overlapping ORFs within the same stretch of DNA and is an interesting mechanism by which viruses can maximise protein coding capacity under genome size constraints[230]. The alternative T antigen open reading frame (ALTO) is located within the 200 amino acid MUR region encoded by LT[229]. Phylogenetic analysis has demonstrated that while ALTO is evolutionarily related to murine polyomavirus MT they share next to no sequence similarity[229] (Figure 1.11).

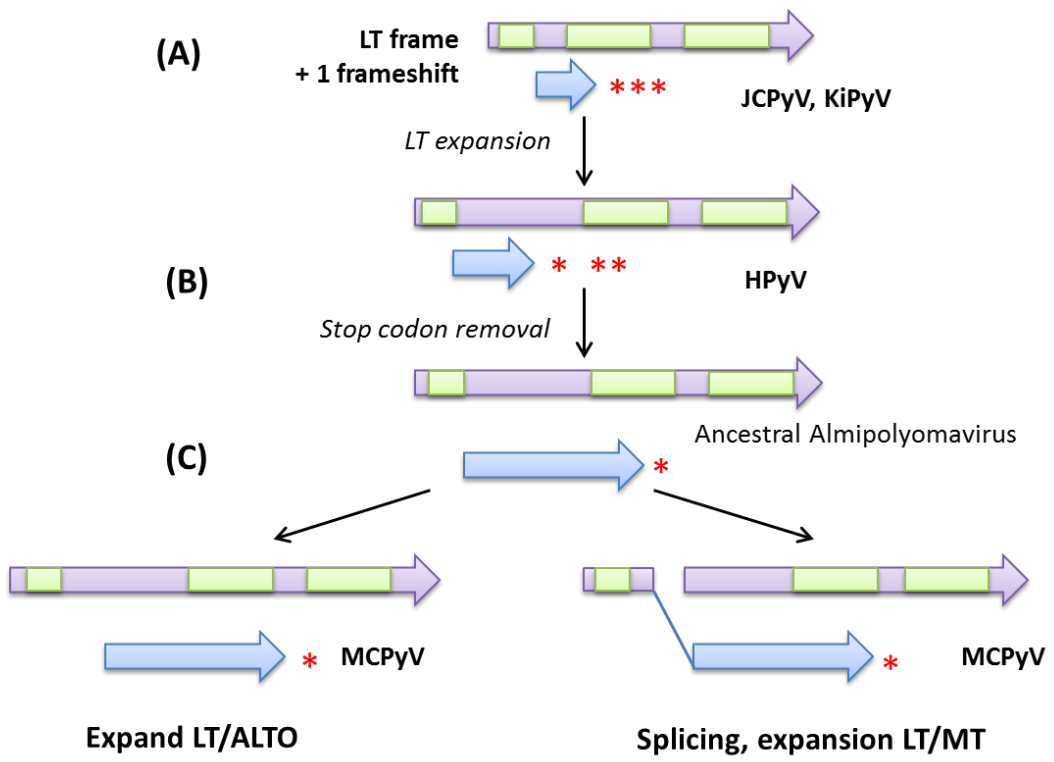

Figure 1.11. A schematic to represent the de novo gene birth of ALTO by overprinting. ORFs corresponding to the LT and ALTO/MT alternative frame and blue shows ALTO/MT region. Stop codons are denoted by asterisks.

Carter and colleagues have demonstrated that the start codon of ALTO overlaps exactly with the YGS/T motif of LT located near the pRB binding domain, while the function of the YGS/T motif is unknown, it may be required for the correct and timely folding of the DnaJ domain[229]. Furthermore, ALTO has a hydrophobic C-terminus (similar to MT) which is required for the subcellular localisation of ALTO when expressed in mammalian cells[229]. While the functional significance of ALTO, in terms of MCPyV biology, has yet to be determined, this data suggests that ALTO may be the twin protein of other PyV MT antigens.

1.4.5.1.3 MCPyV Late Proteins

MCPyV, like other PyV encodes three structural proteins, VP1, VP2 and VP3. Both the major capsid protein (VP1) and the minor capsid protein (VP2) have been shown to self-assemble into virus-like particles *in vitro*[231,232]. However, while there

is an open reading frame for VP3 it does not form part of the native MCPyV capsid and actually may not be expressed at all[233]. The capsid structure of MCPyV forms an unenveloped, icosahedral capsid composed of 72 pentamers of VP1. The overall capsid size is similar to other polyomavirus capsids at approximately 40-55 nm, with a VP1:VP2 ratio of 5:2[233]. Using crystallography techniques the VP1 monomer structure has been shown to be composed of two antiparallel β sheets, forming a β-sandwich structure with a jelly-roll topology[234]. The overall shape of the VP1 monomer is classed as a symmetrical, ring-shaped homopentamer arranged around a central axis, and variable loops have been shown to create unique interaction surfaces possibly involved in viral attachment[234].

Interestingly, the current function of VP2 in the MCPyV lifecycle is unknown as the protein is not required for entry mechanisms in most cell lines currently studied, nor does it affect viral DNA packaging into the capsid, trafficking of viral proteins nor is it responsible for binding cellular receptors[233]. One possible role of VP2 is through VP2 myristoylation, which may enable cellular membrane disruption, however this has yet to be characterised[233]. Co-expression of both VP1 and VP2 result in redistribution of VP2 from the cytoplasm to the nucleus, as VP2 does not encode a NLS signal[233], therefore it would seem that VP1 is crucial for the function of VP2.

1.4.5.1.4 MCPyV microRNA

SV40, BKPyV and JCPyV have all been shown to encode microRNAs (miRNAs) which function to regulate early gene transcription[235,236]. Similarly, MCPyV encodes a miRNA within the late region, MCPyV-miR-M1-5p, and is transcribed from the antisense DNA strand encoding the LT gene sequence[225]. Recent evidence suggest that this miRNA is required to regulate early gene transcript levels and expression of the MCPyV miRNA acts in a negative feedback loop, whereby expression results in a decrease in T antigen expression, thus facilitating the switch from early to late gene transcription[225].

1.4.6 Viral Life Cycle

The cellular tropism for MCPyV infection has yet to be identified, however MCPyV virions are shed from the skin of healthy adult patients[34], indicating that the natural host cell may reside within the epidermis. Only a few human skin-derived primary keratinocytes and transformed melanocytes have been shown to be susceptible to infection, while more than sixty others demonstrated no MCPyV cell tropism[237]. Recently, several groups have established a MCPyV genome capable of productive viral infection[233,238]. Schowalter *et al* were able to isolate full-length wild-type MCPyV genomic DNA from surface skin swabs taken from healthy adult volunteers. The DNA extracted from these skin forehead swabs underwent random hexamer-primed rolling circle amplification (RCA)[233]. While Neumann *et al* generated a synthetic MCPyV genomic clone using sequence data of MCPyV genomes from MCC tumour samples, accessible from the NCBI database[238]. Both of these systems have resulted in the production of plasmids, such as pR17b, which contain the full recircularised MCPyV genome.

Presently, the most successful way to recapitulate efficient replication of the MCPyV viral genome, both early and late gene expression and viral particle formation, is by transfection of the pR17b plasmid in HEK-293 cells that overexpress the MCPyV LT and ST *in trans*[239], also known as 293-4T cells. Five days after transfection, 293-4T cells are lysed to release pseudovirions, and these are subsequently allowed to mature overnight at 37 ^{o}C prior to purification. Samples are then clarified and layered over an Optiprep gradient, followed by centrifugation and fraction collection. These fractions can then be analysed for the presence of infectious virus particles by Quant-iT Picogreen dsRNA Reagent and/or by western blot analysis for viral capsid proteins such as VP1, VP2 and VP3. This viral replication system is key in the pursuit of understanding MCPyV biology and the specific viral-host interactions that contribute to MCC pathology.

1.4.6.1 Attachment and Entry

SV40, BKPyV and MPyV are well characterised in terms of host cell attachment mechanisms and use either ganglisosides or sialic acid-containing glycolipids to initially attach to the host cell membrane[240,241]. Unlike most other PyV, MCPyV displays a preference for glycosaminoglycans (GAGs) (Figure 1.12), in particular heparan sulphate and chondroitin sulphate as initial attachment receptors[239]. Interestingly, MCPyV is capable of initial attachment to cells deficient in sialylated glycans, however this results in impairment in MCPyV transduction of genes using reporter vectors[239]. This demonstrates that while the siaylated glycans are not strictly necessary for initial attachment, lack of them severely restricts MCPyV downstream entry processes.

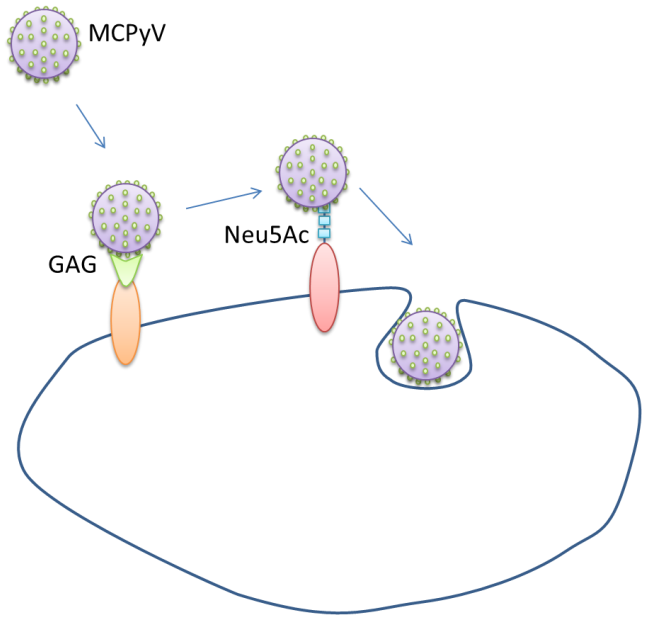

Figure 1.12. Attachment and entry receptors for MCPyV. A two-step attachment and entry mechanism, MCPyV binds glycosaminoglycan (GAG), specifically heparan sulphate as the initial mode of attachment. MCPyV the binds a ganglioside with a Neu5Ac-α2,3-Gal motif to facilitate viral entry.

MCPyV can also bind gangliosides, specifically the GT1b receptor, which contains three different sialic acids and is important for entry of the virus after initial attachment[242]. More recently, X-ray crystallography has confirmed that the MCPyV VP1 protein structure contains a binding site that is consistent with binding to host glycans which specifically contain sialic acid with a Neu5Ac motif[234]. Furthermore,

MCPyV shows specificity for binding carbohydrates with a Neu5Ac-α2,3 motif, however mutational studies rendering the binding site defective has no discernable effect on virus attachment[234]. Taken together, these results suggest that MCPyV is capable of binding two distinct cell membrane receptors with a separate mechanism for both initial virus attachment and post-attachment entry into the host cell.

1.4.6.2 Replication

MCPyV is a ubiquitous infection of the skin and can complete a full replication cycle in permissive cells without inducing transformation. As with other small viruses, MCPyV relies upon multiple host cell factors to successfully replicate its genome and expression of viral T antigens is essential for this function. Feng *et al* demonstrated that upon transfection of the MCPyV full circularised genome an ordered gene expression profile occurs, with LT and 57kT being the first proteins to be transcribed, followed by ST then VP1, 3 days after transfection[243].

Similar to other PyV, the early genes are required to promote G_1-S phase progression to allow viral replication to occur. It is thought that after sufficient levels of the T antigens have been expressed, transcription of a MCPyV encoded miRNA results in a negative feedback loop to inhibit further T antigen expression[225]. This is an important switch between early and late viral gene transcription and allows the late encoded capsid genes to be transcribed for viral capsid assembly.

1.4.6.2.1 The role of LT

The LT antigen is highly conserved among the polyomaviruses, as such is thought to act in a similar manner and initiate viral genome replication. However, there are several unique features of the MCPyV LT protein that affect viral replication which have recently been characterised. Liu *et al* characterised a novel virus-host interaction between MCPyV LT and the cellular cytoplasmic vacuolar sorting protein

hVam6p[119]. Mutation studies demonstrated that MCPyV LT binds to hVam6p via its unique MUR region adjacent to the pRB binding domain[119]. hVam6p is part of the HOPS (homotrohpic fusion and protein sorting) complex, and MCPyV LT expression results in a redistribution of hVam6p from the cytoplasm to the nucleus, disrupting lysosome clustering. Interestingly, overexpression analysis of hVam6p suggests an inhibitory role, as overexpression leads to a reduction in MCPyV virus formation by more than 90%[243]. Furthermore, mutation studies abrogating the LT-hVam6p binding domain significantly increases infectious virion production between 4-6 fold[119,243]. This clearly demonstrates that hVam6p, not only inhibits viral replication and particle formation, but highlights the possible role of hVam6p as a novel MCPyV anti-viral cellular response factor.

Another critical factor in MCPyV LT-mediated viral replication is the chromatin-associated bromodomain containing protein 4 (Brd4). Brd4 is part of the BET protein family and plays a role in recruitment of cellular replication factors required for viral replication. The LT-Brd4 interaction facilitates recruitment of cellular replication factor C (RFC) to MCPyV replication complexes[244]. RFC facilitates loading of PCNA clamp and DNA polymerase δ, both of which are required for elongation of MCPyV DNA[243]. In line with this notion, viral DNA replication can be inhibited by expression of a dominant negative Brd4 inhibitor[244], highlighting the important role of the LT-Brd4 interaction in facilitating successful viral DNA replication.

DNA damage response (DDR) factors also play a role in MCPyV LT-mediated DNA replication[245]. The two DNA damage response pathways, ATM and ATR are both involved in LT-mediated replication. MCPyV LT expression redistributes such factors to the nucleus, specifically replication foci where they co-localise with LT activity[245]. HPV has also been shown to induce DDR activation and recruitment of these factors to sites of viral replication[246]. This indicates the importance of the DDR pathways across multiple viral families, however the implication of DDR activation and redistribution in MCPyV DNA replication have yet to be fully determined.

1.4.6.2.2 The role of ST

The mechanism by which MCPyV ST enhances viral replication does not rely upon binding to either PP2A or Hsc70, as specific mutations within these domains do not affect viral genome replication[247]. This is in stark contrast to other polyomavirus ST proteins, as SV40 ST co-expression has minimal effect on SV40 LT-mediated viral genome replication and despite SV40 ST having conserved PP2A and Hsc domains is unable to cross-enhance MCPyV LT-mediated viral replication[247]. This suggests that MCPyV ST acts through novel mechanisms, distinct from the well characterised ST-PP2A interaction.

Furthermore, MCPyV ST is able to prevent proteasomal degradation of LT by specifically targeting the cellular SCF ubiquitin E3 ligase complex, of which Fbw7 serves as the recognition component[227,248]. Fbw7 is deregulated in multiple cancers and loss of Fbw7 can result in tumourigenesis and genetic instability[249-252]. SV40 LT is a pseudosubstrate for Fbw7 and recognition by Fbw7 results in phospho-dependent degradation of many cellular proto-oncogenes, including c-Myc, mTOR and Notch[248,252,253].

Both ST and LT readily bind Fbw7 and through the use of chimeric proteins composed of various SV40 and MCPyV ST domains and mutation analysis, an important region was identified (aa 91-95), termed the LT stabilisation domain (LSD)[227]. The ST LSD region is crucial for binding Fbw7 and this interaction inhibits Fbw7 targeting of LT, thereby increasing LT stability and half-life (by approximately 18 hours), enabling efficient viral replication[227].

1.4.6.3 Assembly and egress

Little is known regarding the mechanisms MCPyV employs during virion assembly and egress from the host cell. A permissive host cell line has yet to be established, adding to the complexity of studying the MCPyV life cycle, especially at the latter

stages. Though the recent advances in recapitulation of virus replication using engineered MCPyV genomes will aid in this endeavour.

Polyomavirus infection studies demonstrated that endosomal and lysosomal trafficking are important for viral transit from the cell membrane to the nucleus. Furthermore, the SV40, BKPyV and JCPyV agnoprotein is important in polyomavirus virion assembly and SV40 VP4 is required to trigger lytic virion release[254,255]. MCPyV encodes neither of these proteins, therefore it must utilise other mechanisms to facilitate virus capsid assembly, maturation and egress and it has been suggested that MCPyV may utilise hVam6p for egress, via lysosomal processing pathways[119].

Interestingly, cell lysis and shedding have also been shown to be important for polyomavirus escape and this may be a plausible mechanism as MCPyV infection resides in the skin[256]. The natural human skin cycle requires keratinocyte desquamation and this may facilitate MCPyV virion release. This area of MCPyV biology is poorly understood and will benefit from the generation of MCPyV genomic clones capable of recapitulating virus particle formation.

1.4.7 MCPyV and the immune response

Innate immunity is an obstacle that viruses must overcome in order to establish a persistent infection, and microorganisms have developed multiple mechanisms by which to subvert or evade the host immune response. Griffiths *et al* demonstrated that the MCPyV ST is able to disrupt the NF-κB pathway, thus downregulating the host innate immune response[226]. Activation of NF-κB is stimulated by recognition of pathogen associated molecular patterns (PAMPs), recognised by pattern recognitions receptors (PPRs). PAMPS include foreign proteins and nucleic acids and recognition results in the production of antimicrobial peptides, cytokines and chemokines capable of clearing microbial infections[257].

Recognition also results in a coordinated signalling cascade leading to the activation of the IKK complex[257,258]. Activation results in phosphorylation of IκB and thus its degradation, allowing for the release of NF-κB from the IKK complex (Figure 1.13).

Upon release, NF-κB is free to translocate to the nucleus where it can stimulate gene transcription of proinflammatory cytokines and type 1 interferons[257,258]. An important component of the IKK complex is the NF-κB essential modulator (NEMO), which is a non-catalytic regulatory subunit and acts as an essential molecular scaffold to allow the recruitment of upstream signalling components[258].

Recent evidence suggests that through an interaction with NEMO, MCPyV ST is able to inhibit IKKα/IKKβ phosphorylation, thus rendering NF-κB incapable of translocating to the nucleus due to its association with the IKK complex[226]. This function is dependent on ST binding the cellular phosphatases, PP2A Aβ and/or PP4C, which promote the dephosphorylation of the IKK complex[226]. This is the first characterised mechanism by which MCPyV can interact with the NF-$_{K}$B complex and provides insights into possible immune evasion strategies employed by MCPyV.

Other viruses have also demonstrated the ability to prevent NF-κB-mediated signalling[259]. HPV E7 and HCV core protein both inhibit IκB degradation thus rendering NF-κB unable to translocate to the nucleus, while cytomegalovirus (CMV) disrupts NF-κB activation through a direct interaction with NEMO[260-263]. Interestingly, SV40 has been shown to act in the opposite manner and promotes NF-κB activation in a PP2A dependent manner[102].

Furthermore, MCPyV ST has also been shown to downregulate the expression involved in the innate immune response such as CCL20, IL-8, TANK and CXCL-9e[102]. This suggests that MCPyV is capable of mediating the immune response to allow the virus to establish a persistent and lifelong viral infection.

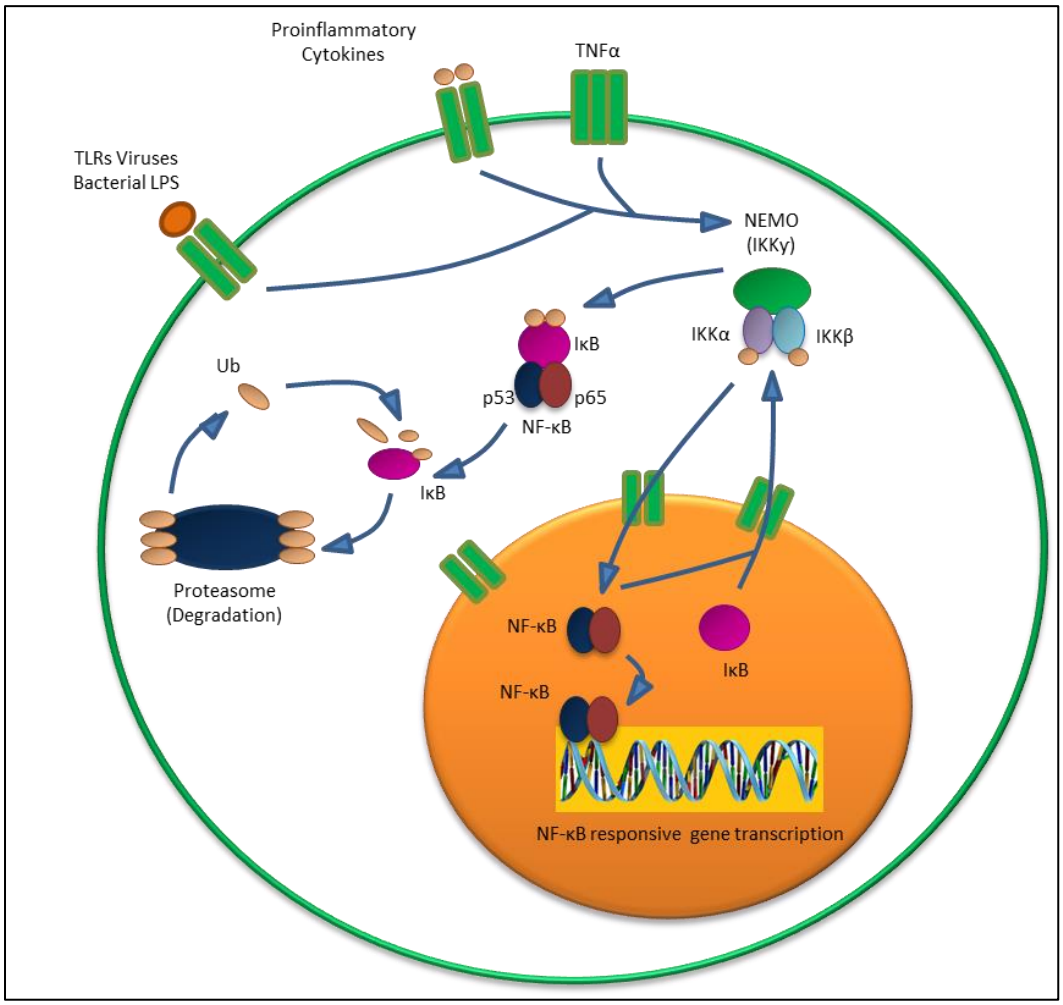

Figure 1.13. NF-κB mediated gene transcription. Taken from[221]. Recognition of PAMPS by PRRs facilitates activation of the IKK complex and subsequent degradation of IκB. NF-κB is thereby free to translocate to the nucleus and stimulate transcription of genes involved in mounting an innate immune response.

MCPyV LT also facilitates immune evasion strategies by inhibiting Toll-like receptor 9 (TLR9) in both MCC and epithelial cell lines[264]. Inhibition of TLR9 is an important factor in immune evasion, as TLRs are subset of PRRs that specifically detect viral/bacterial dsDNA and can activate the IKK complex and production of inflammatory molecules[265]. This feature is not uncommon among viruses, as EBV and HPV have been shown to act in a similar manner[266,267]. MCPyV LT reduces the mRNA levels of C/EBPβ, a positive regulator of the TLR9 promoter, thus decreasing TLR9 transcription[264]. Interestingly, ST may also play a role, as MCPyV ST expression alone is able to inhibit TLR9 production[264], however the underlying mechanisms have not yet been addressed.

Recently, a study has implicated the role of prokineticins, particularly prokineticin 2 (PROK2) in MCPyV infection[268]. Prokineticins are chemokine-like factors that mediate inflammatory reactions and are mainly present on innate immune cells, such as macrophages, monocytes and neutrophils. The results indicate that MCPyV infection can alter the expression profiles of prokineticins and may contribute to MCPyV immune evasion strategies[268], however the specific pathways utilised and the mechanism by which MCPyV contributes to this phenotype are unknown and is an area currently under investigation.

Altogether, these results indicate that MCPyV T antigens affect various innate immune response pathways in a multifaceted manner, preventing host clearance of MCPyV infection, thus allowing persistent and lifelong MCPyV infection.

1.4.8 MCPyV in the pathogenesis of MCC

MCPyV is a common childhood infection however development of MCC is rare, as such it is important to understand the predisposing factors which contribute to the tumourigenic potential of MCPyV. An acronym has been used to clearly address the predisposing factors of MCC – AEIOU – Asymptomatic, Expanding rapidly, Immune suppression, Older than 50 years, Ultraviolet light[188].

Broadly speaking, infectious agents that contribute to tumour formation have been divided into two categories. Direct carcinogens that express viral oncoproteins that directly cause transformation or indirect carcinogens which cause tumour formation through infection and inflammation, resulting in accumulation of mutations that lead to tumour formation[29]. MCPyV can be considered a direct carcinogen as the expression of tumour antigens directly contribute to transformation of the host cell.

There are several key stages to MCPyV-induced carcinogenesis as seen in Figure 1.14. The first step is rare and involves integration of the MCPyV genome into a host chromosome in a monoclonal integration pattern[71,208]. Integration results in

activation of the MCPyV T antigens, facilitating DNA replication. This is detrimental to the host cells as DNA strand breaks occur, leading to replication fork collisions and cell death[74,210]. Therefore a second truncating mutation has to occur, only in neoplastic cells, leading to premature truncations of the T antigen, eliminating its OBD and helicase activity; thereby preventing MCPyV viral replication[212]. This feature is essential for cell survival and is a strong selective pressure for elimination of MCPyV viral replication activities.

The truncating mutation removes the helicase and p53 binding activity but the pRB protein binding domain remains intact, thus retaining the transforming ability associated with pRB[74].

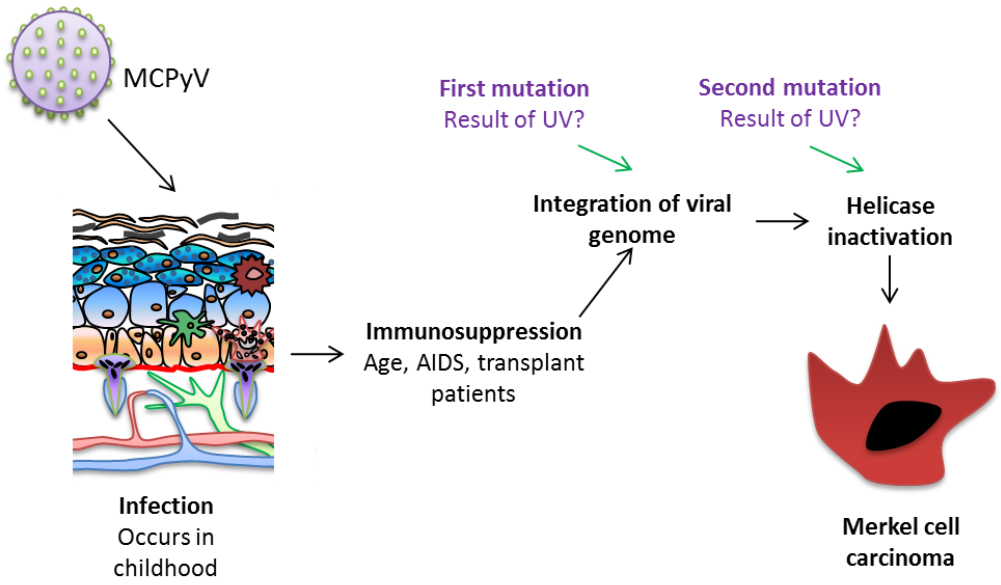

Figure 1.14. The molecular mechanism associated with MCPyV-induced tumour formation. Taken from[4]. Illustrates the common evolutionary features required for MCPyV ability to induce transformation through integration, truncating mutations and loss of immune surveillance through aging, AIDs and immune suppression drugs.

Interestingly, a deletion mutation within the promoter region of integrated VP1 has also been identified and is linked with decreased viral replication efficiency and virion assembly[222,238,243], suggesting another process that may contribute to MCPyV-mediated transformation.

To support the role of MCPyV as a direct carcinogen, MCPyV positive MCC cells lines (MKL-1 among others) demonstrated growth arrest and cell death upon

knockdown of both the LT and ST proteins[75]. This demonstrates the importance of these proteins in MCPyV-mediated tumour formation and maintenance of the tumour state.

1.4.8.1 The role of ST in transformation

Initially, the tumourigenic potential of MCPyV T antigens was compared to the well established role of other polyomavirus T antigens, however in the last few years novel mechanisms of MCPyV action have been identified. Most literature concludes that the polyomavirus LT, rather than ST, is more oncogenic, with ST providing a supporting role[78,96]. However, it has been demonstrated that MCPyV ST is more commonly expressed in MCC tumour samples than LT, indicating the importance of ST in MCC pathology[247]. Shuda *et al* demonstrated 92% of MCPyV-positive MCC tumours stained positive for MCPyV ST expression whereas only 75% stained positive for LT[247]. Furthermore, lentiviral knockdown of ST induced growth arrest of MCPyV-positive MKL-1 cell lines[247]. Moreover, only MCPyV ST, not LT, is sufficient to induce rodent fibroblast transformation, loss of contact inhibition, anchorage-independent and serum independent growth[247]. These are key hallmarks of an oncogenic viral protein and there is a substantial body of evidence to suggest that MCPyV ST is more oncogenic, which is in stark contrast to other polyomaviruses.

1.4.8.1.1 A role for 4E-BP1

SV40 ST is capable of activating the Akt pathway by preventing PP2A-mediated dephosphorylation of Akt[82,269]. However evidence suggests that MCPyV ST acts downstream of the Akt-mTOR pathway[247]. Interestingly, recent studies have highlighted a role of the PI3K-AkT-mTOR signalling pathway in the regulation of cap-dependent translation in MCPyV tumourigenesis[270,271]. A key stage in cap-dependent translation involves binding of the eukaryotic translation initiation

factor 4E (eIF4E) to specific mRNA molecules[272]. Loading of the multisubunit eIF4E complex at the cap of mRNA molecules allows for initiation of ribosome recruitment and translation.

The chief regulator of this process is the eukaryotic translation initiation factor 4E-binding protein 1 (4E-BP1), which can inhibit eIF4E complex formation by binding and sequestering eIF4E[273]. Aberrations within this pathway are significant, as eIF4E overexpression induces rodent cell transformation[274,275]. 4E-BP1 is phosphorylated by mammalian target of rapamycin (mTOR), realising eIF4E from 4E-BP1, thus stimulating cap assembly and cap-dependent translation[276], as shown in Figure 1.15.

In 2011, a novel interaction between MCPyV ST and 4E-BP1 was identified which is both PP2A and Hsc70 independent[247]. MCPyV ST has been shown to reduce hyperphosphorylated 4E-BP1 turnover, which in turn promotes eIF4E activity and cap-dependent translation. To support this, a constitutively active 4E-BP1 mutant was able to both inhibit and reverse ST-mediated transformation[247]. In contrast, SV40 ST has been shown to diminish 4E-BP1 phosphorylation in a PP2A dependent manner[92]. These findings demonstrate the significance of MCPyV ST in regulating cap-dependent translation and the importance of this mechanism in tumour development.

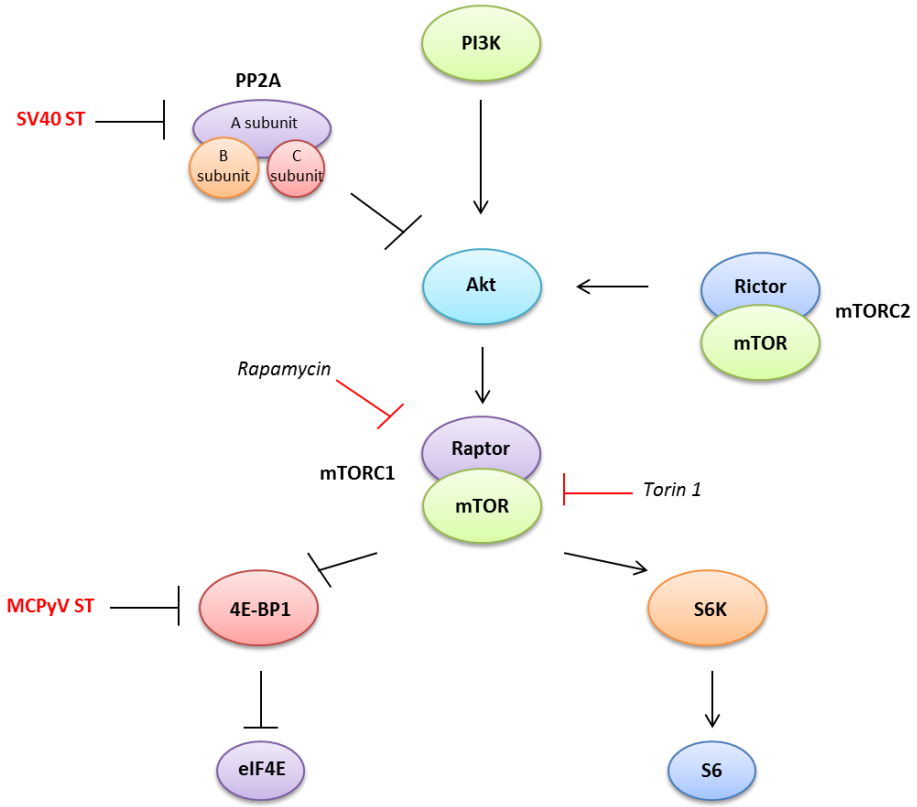

Figure 1.15. MCPyV ST promotes cell proliferation downstream of the Akt pathway. MCPyV ST targets the translational regulator 4E-BP1, and reduces hyperphosphorylated 4E-BP1 turnover. This promote eIF4E activity and cap-dependent translation. Alternatively, SV40 ST promotes Akt activity by preventing PP2A-mediated Akt dephosphorylation.

1.4.8.1.2 The LSD domain

The MCPyV ST LSD domain is important for inhibition of LT proteolysis and is crucial in promoting viral DNA replication[227]. However, recent evidence indicates that the LSD domain is also important for rodent cell transformation. Mutations within the LSD domain inhibit MCPyV ST-mediated transformation in both focus formation and soft agar colony growth assays, and is PP2A independent[227]. However, targeting of Fbw7 by ST is not sufficient to induce transformation, demonstrating that MCPyV ST utilises multiple mechanisms to induce transformation in a PP2A independent manner. This, once again confirms that MCPyV is distinct from other polyomaviruses.

1.4.8.1.3 MCPyV ST, a dichotomy of functions

Although MCPyV is closely related to SV40 and shares similar gene structure, it is increasingly apparent that they differ drastically in terms of their dependency on PP2A binding to facilitate viral replication and transformation. The SV40 ST-PP2A interaction is critical for SV40-mediated transformation and cell proliferation[78,170]. However, mutations within the MCPyV ST-PP2A binding domain which ablate this interaction, are still capable of inducing both rodent cell transformation and anchorage-independent colony formation[247]. Clearly indicating that while these viruses may contain similar protein structures and binding domains their mode of action is distinct.

On the contrary, a recent study has concluded that MCPyV LT is more oncogenic than ST and is crucial to proliferation and maintenance of established MCC cell lines. Houben *et al* demonstrated that knockdown of MCPyV ST by lentiviral shRNA expression inhibited the growth of three MCPyV-positive cell lines and one MCPyV-negative cell line[75]. Furthermore, T antigen knockdown induced growth inhibition is completely rescued by expression of a LT insensitive to T antigen shRNA[277]. This data indicates that MCPyV ST is not essential for proliferation and survival of MCC MCPyV-positive cell lines, however this data also suggests possible off-target effects of these shRNA as a MCPyV-negative cell line also exhibited growth inhibition. Houben and colleagues suggest that LT shows true oncogenic addiction[75,277], however multiple studies have demonstrated that only MCPyV ST can induce rodent fibroblast transformation[247,277].

Consequently, this may suggest that while MCPyV ST is essential for initial transformation it may no longer be required once transformation has taken place and that MCPyV LT becomes necessary for tumour cell maintenance. Despite this, there is a large robust body of evidence that indicates MCPyV ST is crucial for tumourigenesis and maintenance of the tumour state. This remains a controversial topic and requires further investigation to determine the role of ST and LT in terms of oncogenic potential and tumour cell survival. However, what is clear is that

MCPyV is the only known human tumour-associated polyomavirus suggesting that there are novel functions of MCPyV that set it apart from its counterparts.

1.4.8.2 The role of LT in transformation

Despite this controversy, neither full-length or truncated MCPyV LT has been shown to be capable of initiating cellular transformation[247]. However, LT is highly expressed in 75% of MCPyV-positive MCC tumour samples[278], clearly indicating a role for this protein in the tumour environment. One possible explanation for this diminished transforming ability, when compared to the SV40 homologue is that truncated MCPyV LT does not interact with p53[279]. Although, the LT truncated form is more effective at inducing cellular proliferation compared to its full length counterpart. This is due to the C-terminal 100 amino acids which possesses growth inhibitory effects[279].

1.4.8.2.1 DNA damage response

Recent evidence has highlighted that MCPyV infection results in activation of the cellular DNA damage response (DDR) pathway in a LT-dependent manner, requiring the C-terminal interaction with p53 [223]. Similarly, SV40 infection has also been shown to activate the DDR pathway, specifically the ATM DNA damage response[280]. However, while SV40 LT inhibits downstream activities of p53 to promote tumourigenesis, cell proliferation is not affected. Therefore, it is likely that MCPyV LT tumour specific truncations removing the C-terminal region are required to prevent activation of the host DDR in the absence of p53 activation, in order to prevent apoptosis.

1.4.8.2.2 Survivin

The SV40 and MCPyV LT-pRB interaction interferences with pRB-E2F binding and promotes cell proliferation[281]. Survivin is a member of the inhibitor-of-apoptosis protein family and its proteins levels are elevated in lymphoma and metastatic melanoma and contributes to chemotherapy resistance[282]. Interestingly, survivin mRNA levels are elevated more than seven-fold in MCPyV-positive MCC cell lines compared to MCPyV-negative lines, and MCPyV LT alone is sufficient to induce an upregulation of survivin in human fibroblasts[281]. Arora *et al* also demonstrated that knockdown of MCPyV T antigens in MCPyV-positive MCC cell lines results in a decrease in both mRNA and protein levels of survivin and results in cell death[281-282,283]. This demonstrates that MCPyV LT-mediated upregulation of survivin is critical for the survival of MCPyV-positive MCC cell lines.

Therefore, this may present a unique avenue for therapeutic intervention and chemotherapy. The small molecular inhibitor of survivin, YM155, was identified and can initiate selective and irreversible non-apoptotic cell death of MCPyV-positive MCC cells[281]. Furthermore, this inhibitor has been shown to stop the growth of MCPyV-positive xenograft tumours. Other compounds tested, such as bortezomib (Velcade), were just as potent however non-selective in killing MCPyV-positive cells[281]. Despite this, YM155 has been shown to be cytostatic rather than cytotoxic *in vivo*, with xenograft tumour resuming growth after YM155 treatment was halted[281]. Survivin presents an exciting avenue by which to treat MCC patients, however the underlying molecular mechanisms involved in inhibition of survivin require further identification in order to design drug candidates capable of cytotoxic effects.

1.5 Cancer and Metastasis

The spread of malignant cells from a primary solid tumour to remote sites within the body is one of the biggest problems facing cancer treatment, resulting in more than 90% of cancer associated-deaths[284]. Despite the clinical importance of metastasis, the molecular mechanisms by which this phenotype is acquired have yet to be fully elucidated[285]. This poses a significant problem in real terms, for

cancer prognosis and treatment of patients and is an area of cancer biology that needs much research.

Concurrent with this, MCC is regarded as the most aggressive form of skin cancer and is associated with a poor patient prognosis with quick progression to distant metastases[201]. Recently, novel interactions have been identified that implicate MCPyV in the transformation of Merkel cells, however to date no studies regarding the mechanisms by which MCC tumour cells acquire a metastatic phenotype have been addressed.

1.5.1 Steps to achieve metastasis

The genetic diversity of the tumour cell population and the tumour microenvironment results in environmental selective pressures that dictate cell behaviour. This explains, why despite millions of tumour cells being released from the primary tumour into the vasculature daily, only a small percentage of those cells are capable of surviving and colonising distant organs. There are several discrete steps in the metastatic cascade that are required for metastases to form and include loss of cellular adhesion, acquisition of cell motility, entry and survival in the vasculature and colonization of distant sites[286]. At each discrete step the process of metastasis encounters numerous physiological barriers and in order to achieve metastasis tumour cells must overcome all of them[286,287].

1.5.1.1 Loss of cell adhesion

Most solid tumours originate from epithelial tissue, which is composed of rigid cell sheets that are separated from the basement membrane by stroma forming highly organised structures, requiring cell-cell adhesion complexes and cell-matrix components. In order for epithelial cells to detach, deregulation of the cell adhesion complexes must occur, as such carcinoma cells show distinct loss of intracellular adhesive properties[288]. An important feature of malignant epithelial

cells that allows for an invasive phenotype is the loss of E-cadherin[289]. The cadherin family is composed of multiple members each showing specific tissue specificity and are required to maintain tissue integrity[290,291]. Cadherins are transmembrane glycoproteins which localise to specialised cell junctions, termed zonula adherens and are responsible for calcium-dependent cell adhesion and cell signalling[290,291].

'Cadherin switching' – a loss of E-cadherin and increased expression of N-cadherin (mesenchymal tissue specificity) correlates with increased invasiveness of multiple carcinomas, reviewed in[289], invasiveness of tumour cells in mouse models[292] and can be represented under a broader program known as the epithelial-to-mesenchymal transition (EMT). EMT is characterised by a loss of cell polarity and epithelial proteins such as E-cadherin, occludins, claudins, catenins and cytokeratin among others, which are responsible for maintaining cell-cell junctions[292]. Thus cells acquire a more mesenchymal phenotype allowing invasion into neighbouring tissues[292], as shown in Figure 1.16.

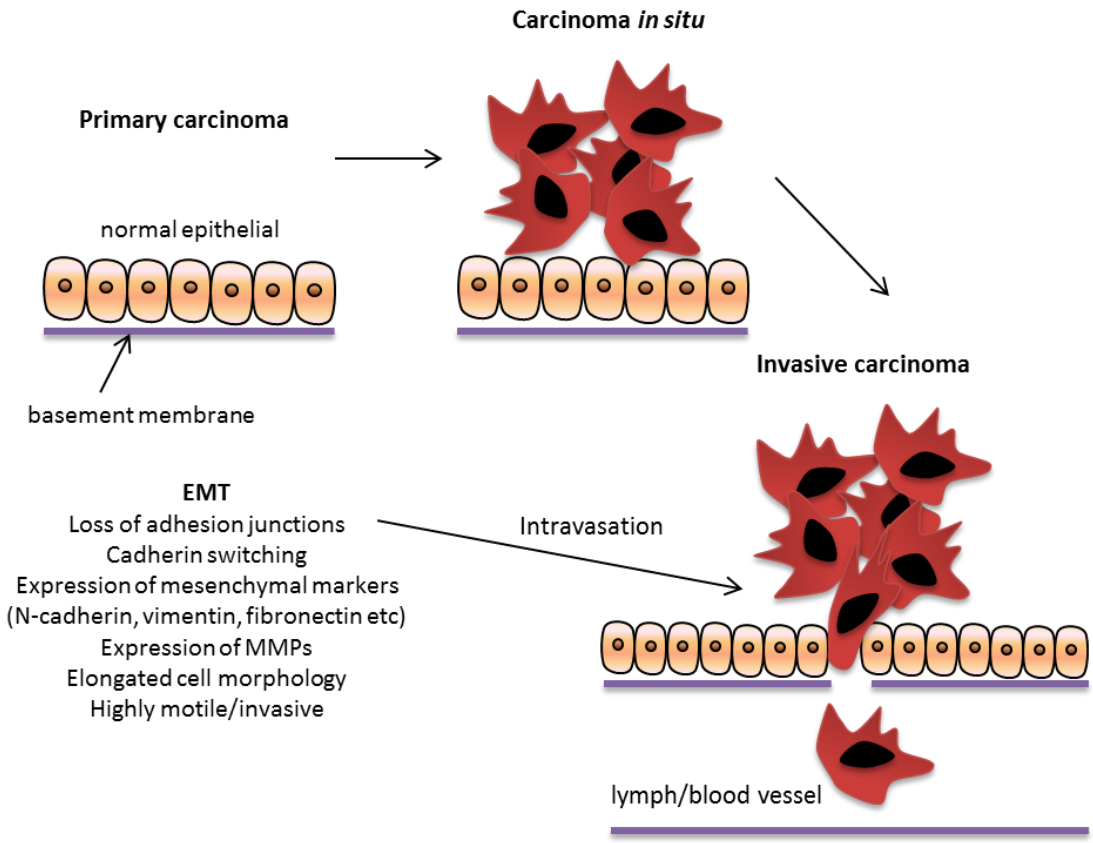

Figure 1.16. Steps required for escape from the primary tumour site. Upon transformation, some primary carcinoma cells will acquire the capabilities to escape from the primary tumour site into the vasculature. This process involves epithelial-to-mesenchymal transition (EMT) where cells become more motile and express specific integrins and MMPs required to invade local tissue and escape through the basement membrane into blood and/or lymph vessels.

There are multiple cellular signalling pathways that control E-cadherin loss/EMT and include Receptor Tyrosine Kinases (RTKs), the transforming growth factor β (TGFβ) family, Notch, WNT and hedgehog[292]. Many of these signalling pathways are deregulated in tumour cells with a metastatic phenotype, through transcriptional repression (promoter methylation), proteolytic degradation or cleavage of the extracellular domain[288,289]. Increased expression of N-cadherin also functions towards promoting tumour invasion as it can bind and activate fibroblast growth factor receptor (FGFR), stimulating cell survival, migration and invasion[293].

Interestingly, DNA tumour viruses have also been shown to be actively involved in promoting loss of cell adhesions. HPV E6 expression promotes degradation of epithelial cell tight junctions through an interaction with E6AP (a ubiquitin-protein ligase) allowing for proteosomal degradation of cell adhesion molecules in a

manner similar to EMT[294,295]. More specifically, HBV HBx protein downregulates E-cadherin expression (frequently found in HCC), which results in morphological alterations that render cells incapable of forming aggregates in cell culture, reflecting the loss of intracellular adhesion molecules[296-298].

In addition, the SV40 ST antigen has the ability to promote redistribution and downregulation of proteins involved in tight junction complexes such as E-cadherin, Zo-1, claudin-1 and occludin, in a PP2A dependent manner[299]. Moreover, analysis of MCC tumours demonstrate a pronounced redistribution of E-cadherin from the cell membrane adhesion complexes to the nucleus[300]. This suggests that MCC cells possess mesenchymal-like qualities which may promote an invasive phenotype seen in MCC.

1.5.1.2 Acquisition of motility

A critical parameter in tumour cell metastasis is the ability for cells to acquire a motile phenotype to allow dissemination[286,301]. Extensive studies have been carried out to visualise cell motility *in vitro* using 2D and 3D matrices and advanced *in vitro* imaging techniques[292]. Motility analysis demonstrated that there are three broad categories of cell migration: mesenchymal, amoeboid and collective motility. The best categorised of these is mesenchymal motility, as 10-40% of carcinomas undergoing EMT use this mechanism[302]. It is characterised by a polarised, elongated cell body and requires degradation of extra cellular matrix components (ECM) and is generally initiated by activation of RTKs, such as c-Met (ECM), reviewed in[302]. Together these changes result in directional movement with extended protrusions at the leading edge and retraction at the rear[302], as seen in Figure 1.17.

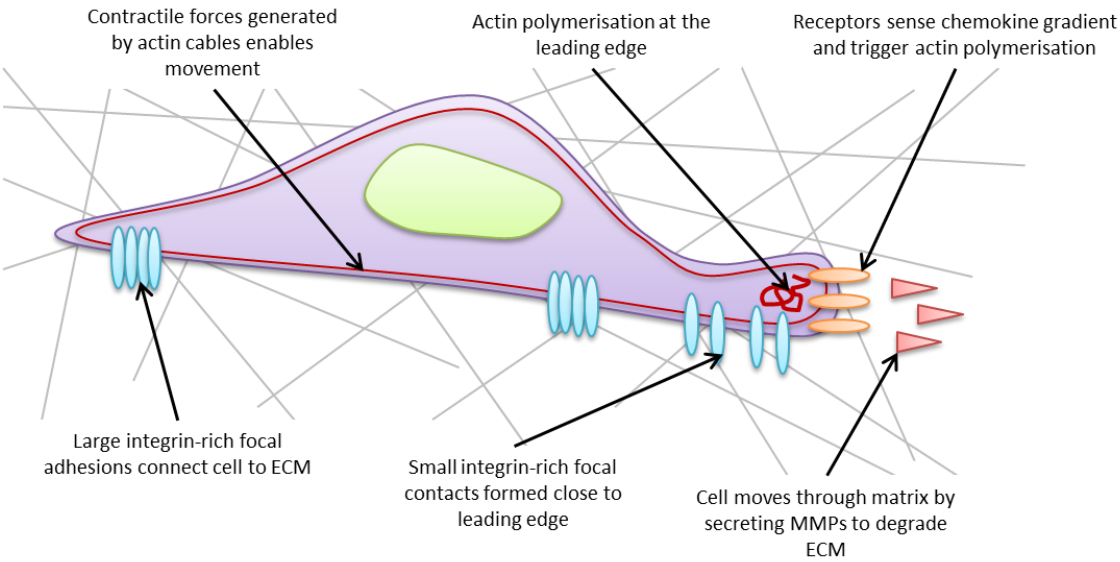

Figure 1.17. The process of mesenchymal, directional cell motility. Key components of directional, polarised cell motility using the actin cytoskeleton to form protrusions and extracellular matrix degradation to invade local tissue.

Amoeboid motility is similar to leukocyte movement and is generally a feature of malignant cells that do not undergo EMT[302]. Receptors on the cell surface sense chemokine gradients which can stimulate the Rho-ROCK signalling pathway, which promotes rapid actin remodelling and cortical actin contraction allowing the invading cells to 'squeeze' between other cells and change direction rapidly[292]. In contrast to mesenchymal motility, amoeboid movement does not require degradation of the ECM due to the ability of cells to 'squeeze' through gaps, thus no formation of large actin-based protrusions are observed, characteristic of mesenchymal motility[302].

The final form of motility relies on similar mechanisms to mesenchymal motility and is termed as collective migration which involves whole sheets of cells moving as one and has been demonstrated in breast, colon and ovarian carcinomas[302]. This requires the cells at the leading edge of movement to generate proteases that degrade the ECM thereby creating a path for lagging cells to follow[303]. The main difference between these two forms of motility is that collective motility requires active adhesion complexes, whereas mesenchymal motility requires the loss of these complexes[304]. This method is less widely understood due to the lack of *in vitro* techniques capable of modelling this movement.

1.5.1.3 ECM degradation and entry into the vasculature

The epithelial basement membrane is important for epithelial structure and integrity and is composed of a dense network of glycoproteins and proteoglycans, including laminin and type IV collagen. The basement membrane poses a barrier to invading tumour cells, as they must first degrade the ECM and invade through the basement membrane in order to circulate within the body.

Extracellular matrix proteases are under strict regulatory control through localisation, tissue secreted inhibitors and autoinhibition[289,305]. Malignant cancer cells utilise multiple mechanisms to activate these proteases and degrade the ECM, and is a key feature of mesenchymal motility. Furthermore, proteolysis of ECM components can result in production of bioactive cleaved peptides which can further mediate migration, proliferation, angiogenesis and survival of tumour cells, reviewed in[302].

Another important family in mediating invasiveness and signalling in tumour cells are the ADAM (A disintegrin and metalloproteinase) protein family[306-308]. ADAMs are membrane-anchored glycoproteins and regulatory enzymes associated with cell adhesion and shedding/cleavage of extracellular bound proteins, such as integrins[307,309]. ADAM proteins themselves are catalytically inactive until autocatalysis, however upon activation are capable of cleaving the ectodomain of membrane proteins[307]. ADAM proteins are important for sensing external stimuli and provide an important regulatory component of numerous cell signalling pathways, such as anchorage dependent growth and cell adhesion complex formation[306-308]. Deregulation of ADAMs has been associated with progression of multiple cancers and ADAM10 has been shown to activate the HER2 receptor by cleaving the extracellular portion in breast cancer and is associated with poor patient prognosis[310].

Multiple DNA tumour viruses have demonstrated the ability to promote matrix degradation and a subsequent increase in the invasive potential of tumour cells.

Both HPV E7 and HBV HBx induce the expression of matrix transmembrane metalloprotease 1 (MT1-MMP), a transmembrane protein crucial for degradation of the ECM and facilitates activation of pro-MMP2 (matrix metalloprotease 2)[311,312]. MT1-MMP expression promotes tumour growth and angiogenesis through an up-regulation of vascular endothelial growth factor (VEGF) which correlates with invasiveness and poor prognosis in cervical cancer, reviewed in[313]. This demonstrates that there is precedence for human tumour viruses to promote invasive properties through ECM degradation which allows escape through the basement membrane into the vasculature.

1.5.1.4 Integrin expression and motility

During the last 20 years there have been dramatic changes in our understanding of integrin-mediated cell migration. Integrins are the most widely characterised transmembrane receptors and are composed of αβ heterodimers that facilitate interactions between the ECM and the actin cytoskeletal network during cell motility. Integrins bind to specific motifs and can recognise a large repertoire of ECM components such as fibronectin, collagen, and laminin amongst others. Importantly, nine different integrins are capable of mediating interactions with fibronectin through an RGD motif (Arg-Gly-Asp). Through this interaction, integrins can mediate matrix-induced adhesions which affect cell motility and migration and have been associated with tumour invasiveness, reviewed in[314,315]. It is therefore important to note that changes in cell signalling pathways that affect the integrin profile can facilitate changes in cell motility and thus migratory potential.

In line with this, human tumour viruses have demonstrated the ability to induce changes in the integrin profile to those that favour increased cell motility. For example, EBV LMP1, LMP2 and EBNA2 have been shown to promote expression of αv integrins, which are predominantly expressed on highly migratory cells and metastatic melanomas and have been shown to promote invasion[316-318].

1.5.1.5 Colonisation of remote sites

One of the inherent steps in tumour growth is the ability to induce the outgrowth of the vasculature, a process known as 'angiogenesis', this prevents hypoxia and necrosis within the growing tumour from lack of oxygen and other nutrients, reviewed in[302,305]. In order for tumour cells to successfully gain access to remote sites within the body they must infiltrate the vasculature as a form of transportation. Specific tumour-associated virus antigens, such as EBV LMP1 have demonstrated the ability to induce expression of vascular endothelial growth factor (VEGF) and hypoxia-inducible factor 1 alpha (HIF-1α), reviewed in Morris[313]. Both these proteins are pivotal in promoting neo-vascularisation and sensing hypoxic conditions in tumour cells. Not only is this important in tumour cell survival and growth but it also facilitates metastasis to distant sites.

The process of intravasation – entry into the vasculature – begins with tumour cells orientating themselves towards the vasculature vessels, followed by directional cell motility[292]. Some studies concluded that the majority of tumour cells are 'trapped' in the capillary bed due to their size, while others suggest the vast majority of tumour cells rapidly die upon entry into the circulatory system[292]. Despite this, only a minority of tumour cells that manage to travel within the body will have the capabilities to exit the vasculature and even less have the ability to establish metastases.

Extravasation – escape from the vasculature – largely depends on the same principles involved in intravasation, with integrin profiles playing a pivotal role along with platelets and selectin proteins, reviewed in[292]. Establishment of tumour cells in niche sites and eventual macrometastasis formation is not a random process as has been demonstrated by breast cancer preferentially spreading to the liver but not the spleen and bone cancer targeting breast tissue. This has led to the ''seed and soil hypothesis' that concludes that the microenvironment (organ) must be compatible with the specific migrating tumour cell[292,319].

Another layer of complexity has been added to this model and was revealed by an eloquent mouse study demonstrating that bone-marrow derived cells are mobilised and colonize a small section within the lung to establish a microenvironment suitable for secondary tumour formation, before the migrating tumour cells reach the site[320]. The timing associated with the establishment of the pre-metastatic niche is unknown but represents an intriguing mechanism that not only facilitates metastasis but may also directly promote cell motility and migration.

The findings demonstrate that DNA tumour viruses have a range of mechanisms that can promote metastasis of viral-induced tumour cells at all stages of the metastatic cascade and presents viable therapeutic targets in order to prevent this occurrence in a clinical setting.

1.5.2 Cell cytoskeleton and motility

Despite the clinical importance of metastasis, the exact molecular mechanisms by which tumour cells acquire the ability to move and migrate from the solid tumour have yet to be fully elucidated. What is known is that the actin cytoskeletal network is important for this process[321] and recent evidence highlights the emerging role of the microtubule network in regulating and facilitating cell motility[322].

1.5.2.1 Actin cytoskeletal network

Directional or polarised cell motility is a fundamental cell biology process and is pivotal for wound healing, immune responses, embryonic and tissue development. Furthermore, several studies have implicated the actin network in facilitating cell motility in metastasis[323]. The key molecular components of the actin cytoskeleton, including the regulatory components have been conserved across the species and date back approximately 1 billion years. Directional movement, as seen with mesenchymal motility involves protrusion of the leading edge, adhesion to the substratum, retraction at the rear and then de-adhesion from the ECM.

The actin network is the main component of cellular protrusions, of which there are several types; lamellipodia (flat), pseudopods (cylindrical/round) and filopodia (spike-like)[305]. Other protrusions such as invadepodia, have been named however there are difficulties in clearly distinguishing these protrusions from others. After formation of these protrusions, integrin-mediated focal adhesion complexes attach the new protrusion to the ECM components, to facilitate movement through the ECM[305].

Receptors are activated upon extracellular signals which result in activation of downstream signalling cascades, leading to active Rho-family GTPases and an increase in PIP2 (phosphatidylinositol 4,5-bisphosphate), which are crucial for actin filament formation. Through the activity of Rho-GTPases activation of WASp and Scar proteins occurs, recruiting the Arp2/3 complex and initiating new filament branch forming from existing filaments. Actin polymerisation and depolymerisation is controlled by profilin which catalyses the exchange of ADP to ATP, thereby facilitating depolymerisation and returning the actin monomers to the free pool of ATP-actin bound to profilin[305,321], as shown in Figure 1.18.

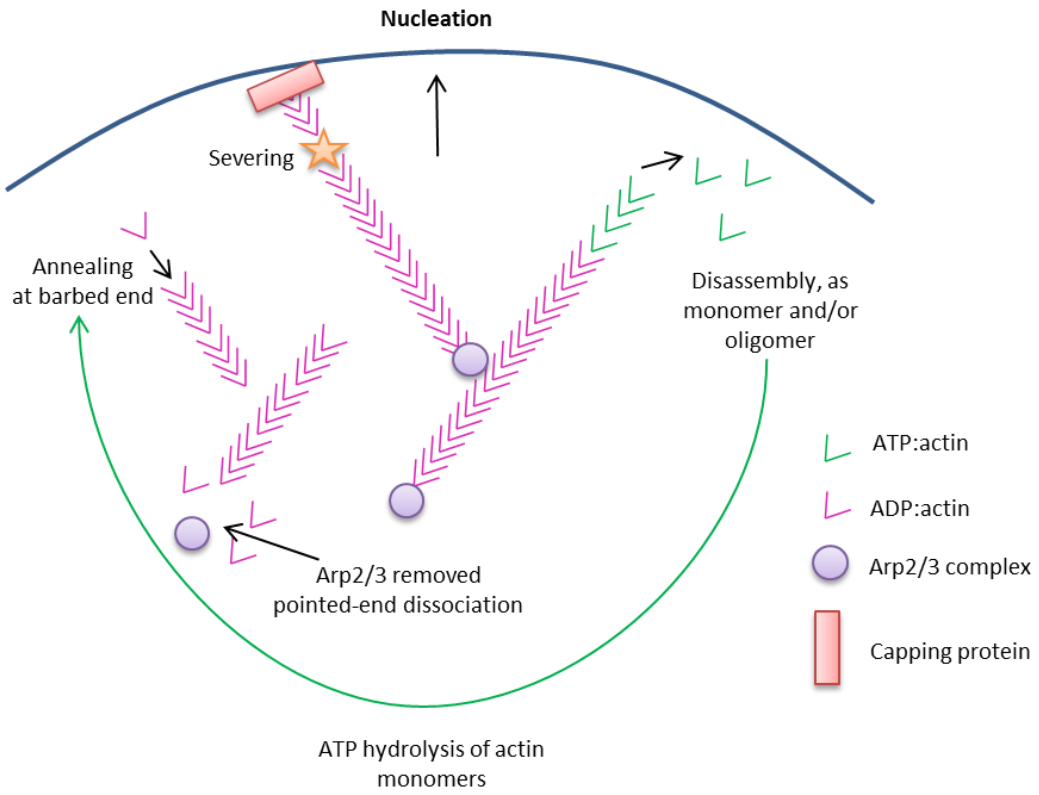

Figure 1.18. Actin cytoskeletal dynamics in cell motility. Arp2/3 facilitates building of actin structures by binding to the sides of existing actin filaments, thereby nucleating growth of further filaments. Actin polymerisation and depolymerisation is controlled by profilin, which catalyses the exchange of ADP to ATP, thus facilitating depolymerisation. Free actin monomers can then be hydrolysed and used for further filament formation. This process if controlled by internal and external stimuli. During cell motility, actin polymerisation occurs at the leading edge and actin filaments are built in such a ways as to extend the cell membrane in the direction of movement.

Cell directionality is coordinated by Cdc42, which facilitates actin polymerisation at the leading edge along with MT filaments[302]. Through formation of these protrusions, cells are able to move by actin-mediated physical forces as the filaments grow beneath the plasma membrane[321].

1.5.2.2 Microtubule cytoskeletal network

The microtubule (MT) cytoskeletal network is pivotal for cell maintenance and also plays an important part in cell functions such as, intracellular vesicle transport, organelle positioning and mitotic spindle formation for segregation of chromosomes during mitosis[324-327]. In recent years it has also been established that MTs play an important role in the control of cell shape and polarised cell

motility[322,328]. All these functions require specific MT arrays with different MT densities and geometry and is a tightly regulated process.

Microtubules form a dense cytoplasmic network and are dynamic structures composed of hollow tubes composed of αβ-tubulin heterodimers. The tubulin heterodimer is polarised, thus the MT structure is also polarised and orients with β-tubulin exposed at the plus end and α-tubulin exposed at the minus end. Formation of the MT requires nucleation at organising centres, known as the MTOC (microtubule organising centre)[329,330]. Tubulin heterodimers can self-assemble and disassemble, a process known as dynamic instability[329]. Dynamic instability results in slow plus end growth of the main MT structure and rapid depolymerisation, also known as shrinkage or 'catastrophe', followed by subsequent rescue[329,330]. The minus end of the main MT structure is usually capped and does not generally participate in MT dynamics as it is anchored at the MTOC.

New MT structures can be formed by two main types of mechanisms, either by *de novo* MT nucleation or by mechanical/enzymatic disruption of pre-existing MT structures[331]. The overall MT state is largely determined by four specific parameters, the speed of MT growth, speed of MT shrinkage, catastrophe frequency and the rescue frequency. Maintaining a balance between periods of growth (stable) and shrinkage (unstable) is highly regulated by proteins capable of binding either tubulin dimers or the assembled MT structures. These are generally divided into two classes of MT-associated proteins (MAPs) known as either MT stabilising or MT destabilising proteins[324,329].

Recent research into the properties of MAPs have identified multiple different mechanisms by which they can stabilise or destabilise MT structures. MAPs such as the tau protein, MAP2 and DCX are able to bind and stabilise the MT lattice, thereby strongly suppressing catastrophe and also promoting growth[332-334]. Similarly, the end-binding 1 (EB1) can prevent catastrophe by directly binding growing MT tips and facilitating growth[335]. Whereas the MT plus-end tracking proteins (+TIPs) form a large group of evolutionary unrelated MAPs that specifically bind to growing MT plus ends and are able to stabilise MT structures, promoting

MT rescue. Such proteins include CLASPs (cytoplasmic linker protein-associated proteins), which act as stabilising factors at the cell cortex and APC (adenomatous polyposis coli) which reduces the MT catastrophe rate of MTs present in cell protrusions[336-338].

Other proteins that induce MT catastrophe/disassembly and inhibit MT polymerisation include non-motile kinesins from the kinesin-13 family. These are one of the most widely characterised subset of MT destabilising proteins and have both ATP-dependent catastrophe-promoting activity and ATP-independent tubulin-sequestering abilities[339]. One such kinesin, MCAK (mitotic centromere-associated kinesin), is thought to act through binding the MT ends and accelerating catastrophe by destabilising the lateral interactions which exist between MT protofilaments[339]. In terms of regulation, both tubulin heterodimers and MAPs undergo post translational modification including phosphorylation, acetylation, polyglutamylation and poly-glycylation, all of which can affect the binding of MAPs to MT structures, thus altering the structure of MTs.

1.5.2.2.1 Stathmin, a MT-associated protein

Stathmin, also known as oncoprotein-18, is the original member of a conserved family of proteins that play an important role in microtubule dynamics and is a key regulator of the mitotic spindle during cell progression[340-342].

Stathmin is a 17kDa, soluble cytosolic protein whose function relies on its ability to bind tubulin dimers[340]. Characterisation of the amino acid structure of stathmin reveals that stathmin has a strong bias towards small polar residues (more than 66% of stathmin's sequence composition) and a low preference for bulky hydrophobic amino acids[343]. As a result, stathmin itself lacks a stable tertiary structure in isolation and its conformational behaviour marks stathmin as an intrinsically disordered protein[343].

In recent years the action of stathmin in MT destabilisation has been hotly debated and controversy exists regarding the exact molecular mechanism by which stathmin

can promote microtubule catastrophe; either through direct or indirect mechanisms. The indirect sequestrating ability of stathmin has long since been established and has been demonstrated by electron micrograph analysis[344], a schematic of stathmin function ca be seen in Figure 1.19. Stathmin possess two binding sites of equal affinity for tubulin heterodimers, and one stathmin molecular (S) is capable of sequestering two α/β-heterodimers (T), giving rise to a stable, microtubule assembly incompetent T_2S complex[346]. Sequestration of tubulin heterodimers reduces the substrate required for growing MT polymers, thereby promoting MT destabilisation and catastrophe[346]. Analysis of the binding equilibrium between tubulin heterodimers and stathmin by nucleotide dissociation studies and sequestration assays has demonstrated that the dissociation constants can vary by three orders of magnitude[345]. Further analysis is required to determine the nature of this difference and its relevance to the biological function of stathmin.

More recently, several studies have demonstrated that stathmin can directly promote MT catastrophe, involving other functions that do not rely on its tubulin sequestering abilities[343]. It has been demonstrated that the T_2S binding interface may be able to directly bind the MT plus ends and the lattice wall[344]. This activity results in stathmin specifically binding protofilaments present at the growing MT tips, thus abolishing the interaction to maintain its structure and function[346,347]. While more work is required to understand the thermodynamics involved in stathmin ability to bind growing MT structures, it is becoming clear that stathmin promotes MT destabilisation and catastrophe through indirect and direct methods.

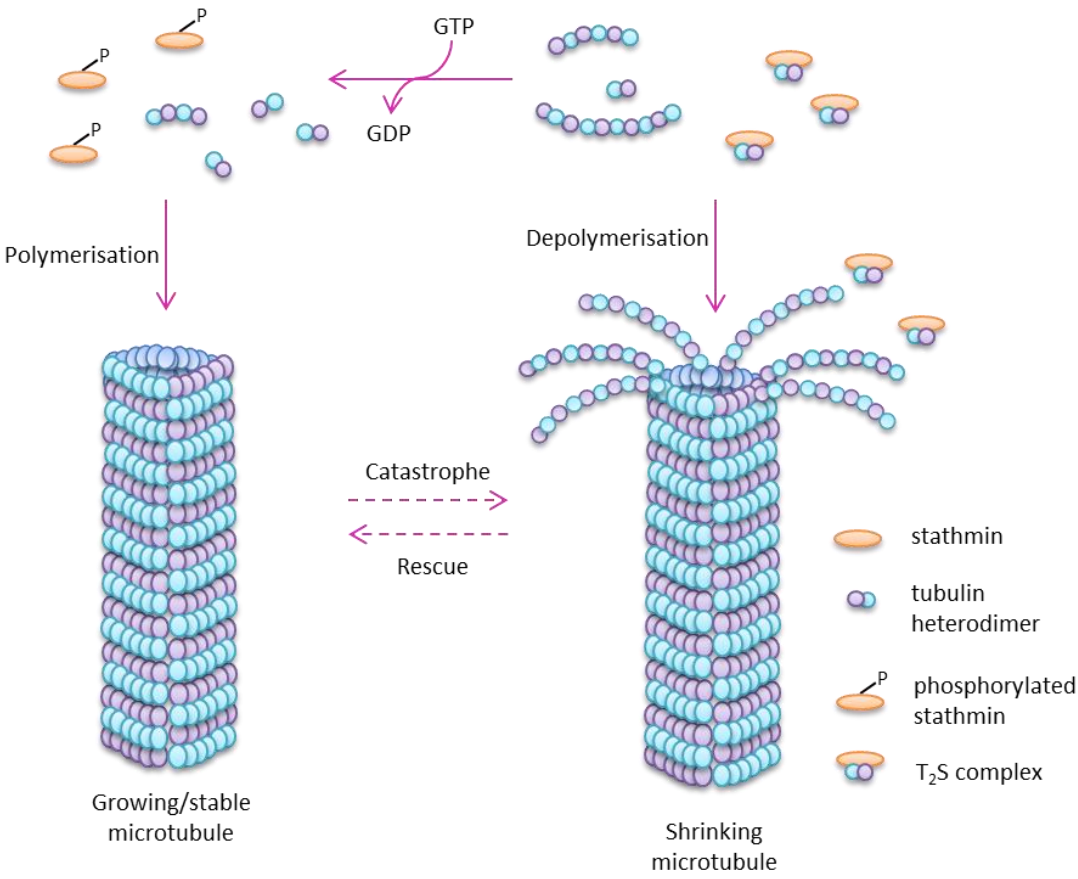

Figure 1.19. Microtubule dynamics and the action of stathmin. Stathmin, when unphosphorylated, binds αβ-tubulin heterodimers to form a T_2S complex. This decreases the pool of free heterodimers required for microtubule polymerisation and destabilises the microtubule structures, resulting in catastrophe. Upon stathmin phosphorylation, stathmin can no longer bind the tubulin heterodimers, thereby promoting microtubule stability and growth. Furthermore, the exchange of GTP to GDP in the tubulin heterodimer promotes dissociation of the microtubule filaments, thereby increasing the pool of free tubulin heterodimers, required for microtubule growth.

Stathmin is a phosphoprotein and it is well established that the ability of stathmin to sequester tubulin heterodimers relies upon multisite phosphorylation at four specific serine residues (Ser16, Ser25, Ser38, Ser63)[343,347]. Phosphorylation of stathmin at one or more of these serine residues weakens stathmin's tubulin binding ability, thereby increasing the free pool of tubulin heterodimers required for MT polymerisation[343]. While stathmin dephosphorylation promotes stathmins tubulin binding ability, resulting in MT destabilisation and catastrophe[343].

Interestingly, these four serine residues display differing degrees of effect on stathmins tubulin binding ability. It has been demonstrated that isoforms of stathmin, phosphorylated at either Ser16 or Ser63 show a significant decrease in the tubulin binding ability of stathmin[345,348]. However, phosphorylation of either Ser25 or Ser38 results only in a slight but non-significant decrease in tubulin binding affinities[345]. Furthermore *in vivo* data indicates that stathmin phosphorylation is sequential and that phosphorylation of Ser25 and Ser38 facilitate the phospshorylation of Ser16 and Ser63[348].

This data suggests that Ser16 and Ser63 are the dominate phosphorylation residues within stathmin and explains the reduce activity/inactivation of stathmin *in vivo*, upon phosphorylation of these residues. Furthermore, dephosphorylation at either Ser16 or Ser63 have been shown to be important in tumour formation and progression[346]. This can be explained by recent evidence indicating the position of these residues within the tertiary structure of stathmin. Circular dichroism spectroscopy has demonstrated that Ser63 phosphorylation significantly reduces the helical content and the thermal stability of stathmin[346]. While Ser16 is located within the T_2S tight turn of the β-hairpin turn, which has been shown disrupt the intramolecular interactions within the backbone[349]. This demonstrated that phosphorylation of theses serine residues compromises the formation and integrity of the tubulin-interacting β-hairpin and a helical segment, resulting in significant differences in the tertiary structure of stathmin which affect its tubulin binding capabilities.

One of the major documented functions of stathmin is its important role in cell cycle progression and its effects on mitotic spindle formation[350]. It was observed that the phosphorylation levels of stathmin significantly increased upon entry to erythroleukemia cells into the mitotic cycle[350], and this has been further demonstrated in HeLa cells and Jurkat T cells[351]. The exact molecular mechanism by which stathmin controls cell cycle progression has yet to be fully elucidated but it is known that its ability to promote MT depolymerisation is essential[352].

Upon entry into mitosis, stathmin is inactivated by phosphorylation, thus allowing MT to polymerise and assemble into MT lattices that form the mitotic spindle[353]. To further support this, Marklund and colleagues demonstrated that overexpression of wild-type stathmin and phosphorylation deficient stathmin mutants promoted depolymerisation of interphase MTs. This resulted in randomly arranged chromosome (rather than those arranged at the metaphase plate), no chromosome segregation and cell cycle arrest in the early stages of mitosis[353]. In contrast, stathmin inhibition at later mitotic stages prevents the timely exit from mitosis, such as spindle disassembly which requires MT depolymerisation facilitated by statmin dephosphorylation[341].

Importantly, stathmin overexpression is a feature of multiple cancer types and has been shown to correlate with tumour growth, poor patient prognosis and a high metastatic/invasive potential[340,354]. Furthermore, RNA interference studies have demonstrated that reducing stathmin levels can drastically reduce the motility potential of various tumour cells[355-358]. This is supported by studies addressing the role of phosphorylation on stathmin MT destabilising activity and transforming potential[359]. Taken together this suggests that stathmin deregulation in various cancers can facilitate alterations in the microtubule network that contribute to cell motility and increased cell migration. Thus stathmin may play a crucial role in cancer cell metastasis.

1.5.3 DNA tumour viruses and cell motility

Interestingly in 2006, Grossmann and colleagues demonstrated that the KSHV vFLIP protein can promote remodelling of the actin cytoskeletal network through activation of the NF-$_{K}$B signalling pathway[360]. Similarly SV40 ST, through an interaction with PP2A, can promote alterations in the cytoskeletal network[299]. Moreover, there is increasing evidence to suggest that PP2A suppression alone can promote cell motility and invasiveness of multiple cancers[361]. SV40 ST has been shown to induce F-actin remodelling resulting in membrane ruffling, lamellipodia and filopodia formation[299]. Furthermore, actin remodelling is associated with loss

of cell polarity and increased tumour invasion thus contributing to ST-mediated actin disorganisation and thus cell transformation and invasiveness[299].

In terms of MT-destabilising proteins, transgenic expression of the PyV MT (under the control of the mouse mammary tumour virus (MMTV) promoter) in mouse prostate cells, results in an increase in stathmin mRNA levels, this was conducted as part of a large screening process which identified 360 differentially expressed genes and has yet to be further studied[362,363].

This clearly demonstrates a precedence of DNA tumour virus promoting alterations in the host cell cytoskeleton that facilitate and promote motile phenotypes. In the viral-induced cancer context these interactions could aid in cells establishing migratory patterns and facilitate metastasis to remote sites. Thus this could identify exciting new therapeutic targets for clinical treatment of viral-associated cancers in the endeavour to reduce the metastatic potential of these tumours.

Thesis Aims

Upon commencing this study, very few MCPyV-related reagents were available, due to its recent discovery in 2008. Therefore, in Chapter 3 it was necessary to produce a range of MCPyV ST expression vectors and a stable cell line capable of inducible expression of MCPyV ST. Furthermore, an initial aim of this project was to generate a library of proteins that were differentially expressed upon MCPyV ST expression, in an endeavour to identify specific cellular signalling pathways and virus-host interactions affected by MCPyV ST expression. Therefore, a high throughput quantitative proteomics approach was utilised to identify multiple gene ontology pathways.

One of the key overall aims of this study was to determine if MCPyV ST expression plays a role in the highly metastatic phenotype of MCC tumour cells. Thus, quantitative proteomic analysis revealed that MCPyV ST expression affects the expression of numerous proteins important for microtubule organisation and dynamics. Importantly, it has previously been shown that the microtubule cytoskeletal network plays an important role in cell shape and polarised cell motility[322,328].

Therefore, through proteomic analysis and motility assays, described in Chapter 3 and 4, it was shown that MCPyV ST expression promotes cell motility, migration and invasion in multiple motility assays. Furthermore, analysis revealed that MCPyV ST expression promotes microtubule destabilisation and is essential for MCPyV ST-induced cell motility.

Data presented in Chapter 4, demonstrates that stathmin, a key microtubule-associated protein, is upregulated upon MCPyV ST expression. Interestingly, previously studies have shown that stathmin overexpression correlates with tumour formation, enhanced metastasis and poor patient prognosis[340,354]. Therefore in order to study stathmin in greater detail and the effects of stathmin upregulation on MCPyV ST-induced cell motility, siRNA studies demonstrated that

upregulation of stathmin by MCPyV ST is a requirement for MCPyV ST-induced cell motility and migration.

Following this, a further aim was to address how upregulation of stathmin by MCPyV ST is able to promote enhanced cell motility. Stathmins' inherent activity is regulated through phosphorylation and data presented in Chapter 3, 4 and 5 indicates that MCPyV ST expression promotes an increase in the cellular pool of unphosphorylated stathmin. This finding is consistent with stathmins' microtubule destabilising activity[364,365], thereby suggesting that MCPyV ST expression promotes microtubule destabilisation by enhancing stathmin microtubule destabilising activity through dephosphorylation.

It has long since been established that polyomavirus ST antigens contain binding sites required for interactions with cellular phosphatases, such as PP2A Aα and PP2A Aβ[247]. Moreover, Griffiths and colleagues recently demonstrated that MCPyV ST interacts with the cellular phosphatase catalytic subunit PP4C[226]. As stathmin activity is regulated by dephosphorylation by specific cellular phosphatases, it was necessary to determine if any known MCPyV ST interactions with these cellular phosphatases played a role in stathmin dephosphorylation. Herein, data presented indicates that PP4C plays an important role in facilitating MCPyV ST-induced microtubule destabilisation and cell motility, through promoting the dephosphorylation of stathmin.

In summary Chapters 3, 4 and 5 present a novel molecular mechanism by which MCPyV ST expression promotes cell motility, migration and invasion and is the first study to demonstrate this link. Data here also eludes to the possibility of specific chemotherapy drugs which could aid in inhibiting this phenotype, thereby decreasing or preventing metastasis of MCC tumour cells.

Chapter 2

Materials and Methods

2 Materials and Methods

2.1 Materials

2.1.1 MCC tumour samples

Fresh MCC tumour samples were supplied by Professor Julia Newton-Bishop at St James' Hospital, Leeds. Upon removal of samples from two patients undergoing surgery, these samples were immediately frozen on dry ice and stored at -80 °C. Tumour samples for immunohistochemistry tissue staining were kindly provided by Dr Neil Steven (University of Birmingham).

2.1.2 Chemicals

All chemicals and solvents (analytical grade) were provided by Sigma-Aldrich®, Melford Laboratories Ltd. and Life Technologies™, unless stated otherwise. Solutions were sterilised using 0.22 µm filters (Millex), or by autoclaving (121 °C, 30 minutes, 15 psi). All water used throughout, unless mentioned otherwise, was deionised water sterilised through an ELGA PURELAB ultra machine (ELGA).

2.1.3 Enzymes

All restriction enzymes were supplied by either Life Technologies™ or New England BioLabs Inc. Other enzymes and their suppliers are listed in Table 2.1.

Enzyme	Supplier
Platinum® *Pfx* DNA polymerase	Life Technologies™
Taq DNA polymerase	
Superscript® II reverse transcriptase	
Proteinase K	
RNase out	
T4 DNA ligase	New England BioLabs Inc.
DNA-free™ DNase I treatment kit	Ambion®
DNase I Amplification Grade	Sigma-Aldrich®
2x SensiMix™ SYBR No-ROX kit	Quantace Ltd.

Table 2.1. List of enzymes and the corresponding suppliers.

2.1.4 Antibodies

Primary antibodies were obtained from a variety of suppliers, detailed in Table 2.2. Horseradish peroxidase (HRP) conjugated anti-mouse and anti-rabbit secondary antibodies were supplied by Dako™ and used for western blotting at concentration of 1:5000. Alexa-fluor conjugated anti-mouse and anti-rabbit Immunoglobulin G (IgG) antibodies used for immunofluorescence microscopy were supplied by Life Technologies™. An actin stain, Phalloidin was supplied by Life Technologies™ and used at a working concentration of 1:5000. The 2T2 antibody (kindly provided by Dr Christopher Buck, National Cancer Institute, Bethesda, MD), which recognises the J-domain leader peptides present in both MCPyV ST and MCPyV LT was used at a dilution of 1:5 for western blot analysis.

Antibody (supplier catalogue number)	Origin	Working dilution		Supplier
		WB	IF	
Anti-FLAG (F7425)	Rabbit	1:1000	1:250	Sigma
Anti-β-actin (A2228)	Mouse	1:5000	-	
Anti-GST (G1160)	Mouse	1:3000	-	
Anti-HA (H9658)	Mouse	1:3000	1:250	
Anti-Myc (M4439)	Mouse	1:5000	1:250	
Anti-His (H1029)	Mouse	1:1000	-	
Anti-GAPDH (ab8245)	Mouse	1:10,000	-	
Anti-Glu-Glu (ab24627)	Mouse	1:1000	-	
Anti-β-tubulin (2146)	Rabbit	-	1:200	
Anti-acetylated-tubulin	Mouse	1:5000	-	
Anti-GFP (632569)	Mouse	1:5000	-	Living Colors
Anti-Lamin B (101-B7)	Mouse	1:5000	-	Calbiochem
Anti-Statmin 1	Rabbit	1:1000	1:200	Abcam
Anti-Stathmin 1 (phospho S16)	Rabbit	1:500	-	Abcam
Anti-Arp3	Rabbit	1:1000	-	GeneTex
Anti-Cortactin	Rabbit	1:1000	-	
Anti-STRAP	Rabbit	1:1000	-	
Anti-KIF14	Rabbit	1:1000	1:200	

Anti-PKM2	Rabbit	1:1000	-	GeneTex
Anti-PSPH	Rabbit	1:1000	-	
Anti-PSAT1	Rabbit	1:1000	-	
Anti-PHGDH	Rabbit	1:1000	-	
Anti-HK1	Rabbit	1:1000	-	
Anti-c-Myc	Rabbit	1:1000	-	
Anti-AMPK	Rabbit	1:1000	1:200	
Anti-Pirin	Rabbit	1:1000	-	
Anti-ADAMTS1	Rabbit	1:1000	1:200	
Anti-TBCC	Rabbit	1:1000	-	
Anti-JAM-B	Rabbit	1:1000	-	
Anti-ZO-1	Rabbit	1:1000	1:200	
Anti-2T2	Mouse	1:5	-	Dr C Buck

Table 2.2. List of primary antibodies, the corresponding suppliers and the working dilutions for either western blotting or immunofluorescence microscopy.

2.1.5 Mammalian cell culture reagents

All tissue culture media and culture supplements were supplied by either Life Technologies™, Lonza™, Sigma-Aldrich™ or Dundee Cell Products (SILAC media only). Selection antibiotics were provided by either InVivoGen™ or Life Technologies™ and Lipofectamine™ 2000 was supplied from Life Technologies™.

2.1.6 Oligonucleotides

Oligonucleotide primers for DNA sequencing and polymerase chain reaction (PCR) were supplied by Sigma-Aldrich®. A full list of primers used are shown in Table 2.3. Oligo(dT)$_{12-8}$ was supplied by Promega, in order to perform reverse transcription.

Primer	Use	Sequence (5'-3') and restriction site
Primer 1	PCR, cloning	GGGGGTACCATGGATTTAGTC (*Kpn*I)
Primer 4	PCR, cloning	GCTGGATTCTCTTCTTGAA (-)
Primer 3	PCR, cloning	GATATACCTCCCGAACACCATGAG (-)
3' STOP REV	PCR, cloning	GGGCCCGGGACTTGCTGAACTAGCAGAGCTTG (*Sma*I)
pcDNA/FRT/TO-LT Forward	PCR, cloning	GGGGGTACCACCATGGATTTAGTCCTAAATAGGAAAG (*Kpn*I)
pcDNA/FRT/TO-LT Reverse	PCR, cloning	CGAGCGGCCGCTCACTTATCGTCGTCATCCTTGTAATCATGATCGA ATGGAGGAGGGGTCTTCGGGGTG (*Not*I)
pEGFP-C1-LT Forward	PCR, cloning	GGGCTCGAGATACCATGGATTTAGTCCTAAATAGGAAAG (*Xho*I)
pEGFP-C1-LT Reverse	PCR, cloning	CGAGGTACCTCAGAATGGAGGAGGGGTCTTCGGGGTG
Stathmin1 Forward	qRT-PCR	GAGTGTGGTCAGGCGGCTCG
Stathmin1 Reverse	qRT-PCR	GAGAATCAGCTCAAAAGCCTGGC
GAPDH Forward	qRT-PCR	GTGGTCGTTGAGGGCAATG
GAPDH Reverse	qRT-PCR	TGTCAGTGGTGGACCTGAC

Table 2.3. List of primers used for various applications such as cloning or qRT-PCR including the sequences for both the forward and reverse primer pair.

2.1.7 Plasmid constructs

Plasmid constructs were either purchased or supplied by other laboratories and are listed in Table 2.4.

Construct	Source
pcDNA5-FRT-TO	Life Technologies™
pOG44 (pPGK/Flip/ObpA)	Life Technologies™
pEGFP-C1	Clonetech Laboratories, Ic
pcDNA3.1-FLAG-PP4C	Marilyn Goudrealt, University of Toronto, Canada
RL-PP4C-HA (transdomiant mutant)	Tse-Hua Tan, National Health Research Institute, Taiwan
pcDNA3.1-HA-PP2A Cα	Peter Cron, University of Basel, Switzerland
PcDNA5-EE-PP2A Aα	Stefan Strack, University of Iowa, USA

Table 2.4. List of constructs purchased from suppliers for provided by collaborators

2.2 Methods

2.2.1 Extraction of DNA from MCC tumour sections

Fresh tumour sections were lysed for 1 hour using digestion buffer [100 mM NaCl, 10 mM Tris-HCl (pH 8.8), 2.5 mM EDTA, 0.5% SDS (pH 8), 0.1 mg/ml fresh Proteinase K]. DNA was extracted by carefully mixing the lysate with Phenol/Chloroform isoamyl alcohol (25:24:21) and precipitated by incubation for 1 hour in cold Ethanol (66.6%) and 0.3 M Sodium Acetate (pH 5.2) at -80 °C, before pelleting in a microcentrifuge at 13,000 x g for 30 minutes. Absolute ethanol was collected and the DNA pellet resuspended in 70% Ethanol. DNA was pelleted and air dryed at room temperature, followed by resuspension in autoclaved, distilled H_2O (dH_2O) and storage at -20 °C.

2.2.2 Molecular Cloning

2.2.2.1 Construction of recombinant vectors

DNA was PCR amplified (Section 2.2.2.2) and separated by agarose gel electrophoresis (Section 2.2.2.3), then gel purified and ligated into the appropriate linearised double stranded DNA vector (Section 2.2.2.5 and Section 2.2.2.6). This was done via a cloning vector, pCR Blunt (Life Technologies™). Table 2.4 and Table 2.5 display a list of recombinant vectors and the corresponding primers used for PCR amplification of their inserted fragments. After amplification in chemically competent bacteria (Section 2.2.2.8) and purification of plasmid DNA (Section 2.2.2.9), these constructs and inserts were verified by restriction digest analysis (Section 2.2.2.6). All constructs were sequenced to validate the identity of the inserted fragments (Section 2.2.2.10).

Recombinant vector	Parent vector	Primer Sequence (5'-3')	Restriction Enzyme	Primer name
pEGFP-ST	pEGFP-c1	(F)GGGGGTACCATGGATTTAGTC	*Kpn*I	Small T F
		(R)GGGCCCGGGCTAGAAA	*Sma*I	Small T R
pi293-ST	pcDNA 5/ frt/To/ His	(F)GGGGGTACCATGGATTTAGTC	*Bam*HI	Small T F
		(R)CGAGCGGCGCCTCACTTATCGTCGTCATCCTTGTAATCATGATGGAAAAGGTGCAGATGCAGTAAGC	*Not*I	FLAG-Small T R
		(R)GGGCCCGGGCTAGAAA	*Eco*RI	Small T R
pEGFP-T antigen	pEGFP-c1	(F)GGGCTCGAGATACCATGGATTTAGTCCTAAATAGGAAAG	*Xho*I	EGFP-T F
		(R)CGAGGTACCTCAGAATGGAGGAGGGGTCTTCGGGGTG	*Kpn*I	EGFP-T R
pi293-T antigen	pcDNA 5-FRT-TO	(F)GGGGGTACCACCATGGATTTAGTCCTAAATAGGAAAG	*Kpn*I	Tantigen F
		(R)CGAGCGGCCGCTCACTTATCGTCGTCATCCTTGTAATCATGATCGAATGGAGGAGGGGTCTTCGGGGTG	*Not*I	Tantigen R
pi293-LTcDNA		(F)GGGGGTACCATGGATTTAGTCCTAAATAGGAAAG	*Kpn*I	LTcDNA F
		(R)CGAGCGGCCGCTCACTTATCGTCGTCATCCTTGTAATCATGATCGAAGGAGGAGGGGTCTTCGGGGTG	*Not*I	LTcDNA R
pEGFP-LTcDNA	pEGFP-c1	(F)GGGCTCGAGATACCATGGATTTAGTCCTAAATAGGAAAG	*Xho*I	EGFP-LTcDNA F
		(R)CGAGGTACCTCAGAATGGAGGAGGGGTCTTCGGGGTG	*Kpn*I	EGFP-LTcDNA R

Table 2.5. List of recombinant constructs, the primer sequences used for cloning, restriction enzymes and the original parental vectors.

2.2.2.2 Polymerase chain reaction (PCR)

PCRs were performed using a Mastercycler, epgradient (Eppendorf™) in thin-walled 0.2 ml PCR tubes (Greiner™). For cloning purposes Platinum® *Pfx* DNA polymerase was used due to the need for proofreading ability, otherwise *Taq* DNA polymerase was used. Reactions were performed in a total volume of 50 µl, containing the following components: 0.2mM of each primer, 1 x polymerase amplification buffer, 1.5 mM $MgSO_4/MgCl_2$, 1-10 ng template DNA and 1 µl DNA polymerase. The remaining volume consisted of deionised water. Typical PCR amplifications were performed using an initial denaturing temperature of 95 °C for 5 minutes, followed by 35 cycles of; 95 °C for 1 minute, annealing temperatures in the range of 50-60 °C for 1 minute and an extension temperature of 68 or 72 °C, for 2 minutes. Following the final thermal cycling step, a period of 10 minutes at 68 or 72 °C respectively was performed to ensure that all polymerising templates were complete. All reactions were performed with the heated lid setting on, to prevent sample evaporation. After PCR amplification, products were analysed by agarose gel electrophoresis (Section 2.2.2.3).

2.2.2.2.1 Overlap extension PCR (OE-PCR)

To generate the MCPyV T antigen region the N-terminal/C-terminal fragments of the T antigen were gel purified (Section 2.2.2.4) and used in an overlap extension-polymerase chain reaction (OE-PCR). The 2 purified T antigen fragments were used as the template DNA in a single PCR reaction (Section 2.2.2.2) using only the outermost forward (Primer 1) and outermost reverse (3'STOP REV) primers. The same PCR protocol was performed as in Section 2.2.2.2 however an annealing temperature of 51.2 ^{o}C was used.

2.2.2.3 Agarose gel electrophoresis

Double stranded DNA fragments were separated by agarose gel electrophoresis, using 0.8-1.2% agarose gels, depending on the size of the DNA product. Agarose was dissolved in 1 x TBE buffer [90 mM Tris-base, 2mM EDTA, 80mM boric acid] with 0.5µg/ml ethidium bromide. A 10x solution of gel loading buffer [0.25% (w/v) Orange G dye, 30% (v/v) glycerol] was added to DNA samples at 1 x final concentration. An appropriately sized DNA ladder (either 100 bp or 1 kb (Life Technologies™)), depending on DNA product size, was loaded alongside samples to indicate the size of the DNA product. Electrophoresis was performed at 90-120V in 1 x TBE buffer using a HE 99X Max horizontal electrophoresis tank (Hoefer™). DNA bands were visualised under ultra-violet light using a transilluminator and images taken using the GeneGenius bio-imaging system (Syngene™).

2.2.2.4 Gel purification of DNA

DNA fragments were excised using a sterile scalpel following agarose gel electrophoresis and purified using the QIAquick gel extraction kit (Qiagen), according to the manufacturers instructions. The weight of the DNA gel slice was recorded and then followed by incubation at 50 ^{o}C with 3 gel volumes of buffer QG, to melt the agarose. Upon melting, one gel volume of isopropanol was added to the sample and mixed. This mixture was then applied to a QIAuick column and centrifuged for 1 minute at 13,000 x g, room temperature. DNA bound to the membrane was washed using 750 µl PE buffer and centrifuged at 13,000 x g for 1 minute, room temperature. DNA was eluted into a sterile eppendorf tube using 30-50 µl TE buffer, followed by centrifugation at 13,00 x g for 1-2 minutes at room temperature. Pure DNA was stored at -20 ^{o}C until further use.

2.2.2.5 DNA ligation

A standard ligation reaction was performed in a total volume of 20 µl, using 1 x T4 DNA ligase buffer, 1 U of T4 DNA ligase (both Life Technologies^{TM}), 10-100 ng of

linearised vector and varied molecular proportions of insert DNA. Ligation reactions were performed at 16 ^{o}C for 1-2 hour. Control reactions lacking either DNA insert or DNA ligase were also used for each reaction to determine the efficiency of the digest.

2.2.2.6 Restriction enzyme digestion

All DNA restriction digests were carried out according to the manufacturers protocol (New England Biolabs^{TM}). All reactions were prepared in a volume of 20 µl in the appropriate buffer for each restriction digest enzyme, with 1 U of restriction digest enzyme used per 1 µg of DNA to be digested. Double digests, using two restriction digest enzymes were performed in a compatible buffer, to minimise DNA loss as a result of purification of DNA from sequential digests. All digest reactions were performed at 37 ^{o}C for 2-4 hours or overnight at room temperature. Resulting digests were terminated by heat inactivation at 65 ^{o}C for a minimum of 20 minutes. Resulting fragments were analysed by agarose gel electrophoresis (Section 2.2.2.3) and gel purified (Section 2.2.2.4).

2.2.2.7 Preparation of chemically competent DH5α

All cloning was carried out using *Escherichia coli* (*E.coli*) strain DH5α (Genotype: F^{-}, Ψ80d*lac*ZΔM15, Δ(*lacZYA-argF*)U169, *deoR*, *recA*1, *endA*1, *hsdR*17(rk^{-}, mk^{+}), *phoA*, *supE*44, λ^{-}, *thi*-1, *gyrA*19, *relA*1).

Chemically competent *E.coli* was prepared using a rubidium chloride-based method and liquid cultures were grown in autoclaved Luria broth (LB) [1% (w/v) tryptone, 0.5%(w/v) NaCl, 0.5% (w/v) yeast extract, pH 7.5] and incubated at 37°C with shaking (200 rpm). *DH5α* cells were streak plated on LB agar plates (1% NaCl, 1% Tryptone, 0.5% Yeast Extract and 1.5% Agar) followed by incubation at 37 ^{o}C. One colony was used to inoculate 2 ml of LB media and incubated for 5-7 hours at 37°C with shaking. Following this 0.5 ml of the culture was used to inoculate 50 ml of LB

media and the cells were grown at 37 ^{o}C with shaking, until an OD_{600} of 0.3-0.6 was reached. The cells were subsequently pelleted by centrifugation at 5,000 x g for 5 minutes at 4 ^{o}C. The pellet was resuspended in 40 ml ice-cold filter-sterilised TFB1 buffer [30 mM KOAc, 10 mM CaCl2, 50mM MnCl2,100 mM RbCl, 15% (v/v) glycerol, adjusted to pH 5.8 with acetic acid] and incubated for 5 minutes at 4 ^{o}C. The cells were centrifuged at 5,000 x g for 5 minutes at 4°C followed by gentle resuspension of cells in 2 ml ice-cold filter-sterilised TFB2 buffer [10 mM MOPS, 75mM CaCl2, 10 mM RbCl, 15% (v/v) glycerol, adjusted to pH 6.4 with KOH]. This was followed by incubation at 4°C for 15-60 minutes and subsequently cells were aliquoted and quick frozen on dry ice, followed by storage at -80°C.

2.2.2.8 Transformation of chemically competent bacteria

100 ng of a pre-chilled DNA expression construct was mixed with a 50 µl aliquot of chemically competent cells (either DH5α or BL21 Gold Cells (Stratagene)), and incubated for 5-30 minutes at 4 ^{o}C. Mixtures were then incubated for precisely 30 seconds at 42 ^{o}C then subjected to a rapid cool down for 2 minutes at 4 ^{o}C. Followed by addition of 250 µl LB media and incubation with shaking at 37 ^{o}C for 1 hour. Samples were then spread plated onto LB agar containing the appropriate selective antibiotic (either ampicillin or kanamycin) at a concentration of 50 µg/ml. These plates were then incubated overnight for approximately 16 hours at 37 ^{o}C.

2.2.2.9 Plasmid purification

2.2.2.9.1 Mini prep (small scale) plasmid purification

A single transformed (Section 2.2.2.8) *E.coli* colony was used to inoculate 2 ml LB media, containing either ampicillin or kanamycin at 50 µg/ml, followed by shaking incubation at 37 ^{o}C overnight for 16 hours. *E.coli* cells were centrifuged for 5

minutes at 5,000 x g and were resuspended in 100 µl autoclaved Solution I [25 mM Tris-HCL (pH 8.0), 10mM EDTA, 50mM glucose]. This was followed by addition of 200 µl Solution II [200mM NaOH, 1% (w/v) SDS] and incubated for 5 minutes at room temperature to allow for cell lysis. Followed by precipitation of DNA, proteins and SDS by addition of 150 µl Solution III [5 M potassium acetate, 30% (v/v) glacial acetic acid]. Samples were gently inverted and incubated for 20 minutes at 4 ^{o}C, followed by centrifugation at 4 ^{o}C for 10 minutes at 13,200 x g, to separate out precipitate and lysate. Lysates containing plasmid DNA was extracted by addition of equal volumes of phenol:chloroform:isoamyl alcohol (25:24:21) solution, followed by centrifugation at 4 ^{o}C for 5 minutes at 13,200 x g. The aqueous containing DNA layer was removed and 2 volumes of pre-chilled ethanol (4 ^{o}C) was added, followed by incubation for a minimum of 20 minutes at -20 ^{o}C, to allow precipitate of the DNA. Following centrifugation at 13,200 x g the DNA pellet was washed using 70% (v/v) ethanol, air-dried and resuspended in 20 µl deionised water containing 10 µg/ml RNase A.

2.2.2.9.2 Maxi prep (large scale) plasmid purification

For large scale plasmid purification QIAGEN maxi prep kits and column were used according to the manufacturers protocol. A single transformed (Section 2.2.2.8) *E.coli* colony was used to inoculate 2 ml LB media, containing either ampicillin or kanamycin at 50 µg/ml, followed by shaking incubation at 37 ^{o}C overnight for 16 hours. This 2 ml culture was then mixed with 200 ml LB media and incubated with shaking at 37 ^{o}C for 16 hours. The culture was then centrifuged at 4,500 x g for 20 minutes at 4 ^{o}C. The cell pellet was then resuspended in 10 ml Buffer P1 [10mM EDTA, 50Mm Tris-HCl (pH 8.0), 100 µg/ml RNase A] and 10 ml Buffer P2 [1% SDS, 200nM NaOH], this mixture was then inverted 10 times and incubated at room temperature for 5 minutes. Following this 10 ml of pre-chilled (4 ^{o}C) Buffer P3 [3 M potassium acetate, pH 5.5] was added, followed by immediate mixing (inverted 10 times) and incubation at 4 ^{o}C. Mixtures were centrifuged at 4 ^{o}C for 20 minutes at 13,000 x g and the solution was added to a pre-equilibrated QIAGEN-tip 500 column

and allowed to drain by gravity, to allow binding of DNA. The column was equilibrated with Buffer QBT [50 mM MOPS (pH 7.0), 750 mM NaCl, 0.15% (v/v) Triton X-100]. The column resin was subsequently washed twice with 30 ml Buffer QC [50mM MOPS (pH 7.0), 1 M NaCl, 15% (v/v) isopropanol], followed by DNA elution by addition of 15 ml Buffer QF [15% (v/v) isopropanol, 1.25 M NaCl, 50 mM Tris-HCl]. To precipitate the DNA, 10.5 ml isopropanol was added to the eluted solution and centrifuged at 4,500 x g for 30 minutes at 4 ^{o}C. The DNA pellet was then subsequently air-dried and resuspended in 200 µl deionised water. To determine the concentration and purity of the DNA recovered, 1 µl samples were analysed using a NanoDrop ND-1000 spectrophotometer (NanoDrop Technologies) at 260 nm wavelengths.

2.2.2.10 Sequencing of DNA

All DNA sequencing was conducted by GATC, London. Plasmid DNA was sent at a concentration of 30 ng/ml in a total volume of 50 µl and corresponding primers at a 10 pmol/µl in 30 µl. Sequencing data was analysed using BioEdit sequence alignment editor and ClustalW (EBI, UK) against corresponding reference sequences obtained from the NCBI database.

2.2.3 Mammalian cell culture

2.2.3.1 Cell lines

Human embryonic kidney (HEK) 293 FlpIn^{TM} (Life Technologies^{TM}), were kindly supplied by Stuart Wilson (University of Sheffield, UK), the parental cell line for generation of the i293-ST. The hepatocellular carcinoma cell line (HuH-7) and fibrosarcoma cell line (HT-1080) were provided by Professor Eric Blair (University of Leeds, UK) and used for immunofluorescence microscopy and invasion assays,

respectively. Merkel cell carcinoma, MCPyV negative cell lines (MCC13) and a Merkel cell carcinoma, MCPyV positive cell lines (MKL-1) were obtained from the European Collection of Cell Cultures (ECACC).

2.2.3.2 Cell line maintenance

HEK 293 FlpIn™, i293-ST, i293-T antigen, iEGFP, iEGFP-ST, HuH-7 and HT-1080 cell lines were maintained in Dulbecco modified eagle medium (DMEM) (Lonza™), supplemented with 5 U/ml penicillin and streptomycin and 10% (v/v) foetal calf serum (FCS), herein referred to as ''10% DMEM''. HEK 293 FlpIn™ cells were maintained in 10% DMEM supplemented with 100 µg/ml zeocin (Life Technologies™). i293-ST, iEGFP and iEGFP-ST cells lines were maintained in 10% DMEM supplemented with 100 µg/ml Hygromycin B (Life Technologies™). These cell lines were passaged every 3-4 days, whereby confluent cells layers were removed by kinetic force from the surface of a 75 cm^3 tissue culture vessel (Sigma-Aldrich®) and split in a 1:10 to 1:20 ratio into new flasks made up to a total volume of 20 ml using 10% DMEM and supplemented with the corresponding selective antibiotic.

HuH-7 and HT-1080 cells were maintained in 10% DMEM and passaged every 3-4 days, whereby the confluent cell layer was removed by trypsinisation and the cells were subsequently split 1:20 into new flask containing 10% DMEM. MCC13 and MKL-1 cells were maintained in Roswell Park Memorial Institute (RPMI) media, supplemented with 5 U/ml penicillin and streptomycin and either 15% FCS or 10% FCS, respectively. Herein referred to either ''15% RPMI'' or ''10% RPMI'' MCC13 cells were passaged in the same fashion as HuH-7 cells but using 15% RPMI. MKL-1 cells are a non-adherent cell line, hence cells were first centrifuged at 1,500 x g for 3 minutes and resuspended in 10% RPMI, and split at a 1:4 ratio every 4 days into new tissue culture flasks.

Long term storage of cell lines, required cells to be aliquoted into 1.8 ml Cryotubes™ (NUNC™) at 1 x 10^6 cells/ml. Cells were resuspended in freezing media [90% (v/v) FCS, 10% (v/v) DMSO], Cryotubes were then stored at -80 ^oC for 24 hours in an isopropanol containing freeze flask and then transferred to liquid nitrogen for long term storage. All cell lines were incubated in an InCu saFe Copper-Enriched Stainless Steel CO_2 incubator (Panasonic), with 5% CO_2 concentration, unless otherwise stated.

2.2.3.3 Maintaining cells in SILAC media

Media used to label i293-ST cells prior to SILAC based quantitative proteomic analysis was supplied by Dundee Cell Products and supplemented with 10% dialysed foetal calf serum (Dundee Cell Products). i293-ST and i293-T antigen cells were passaged 7 times in both R_0K_0 DMEM (containing ^{12}C L-Arginine and ^{12}C L-Lysine), and R_6K_4 DMEM (containing ^{12}C L-Arginine and ^{12}C L-Lysine), herein referred to as ''light DMEM'' and ''heavy DMEM'', respectively. Upon each passage both light media and heavy media was supplemented with Hygromycin B (Life Technologies™) (as described in Section 2.2.3.5.2).

2.2.3.4 Generating inducible cell lines

To generate cell lines capable of inducible expression of either MCPyV ST, HEK 293 FlpIn™ cells were co-transfected (Section 2.2.3.5.1) with iST-FLAG or iT-FLAG (respectively) and pPGK/Flip/ObpA (kindly supplied by M.Walsh, University of Sheffield, UK) at a 1:3 ratio, respectively using 0.5 µg of iST-FLAG and 1.5 µg pPGK/Flip/ObpA. The cell line was selected and maintained by Hygromycin B resistance at concentration of 100 µg/ml. Cells were monoclonally selected to ensure the resulting cell line was derived from a single cell/colony.

2.2.3.5 Mammalian cell culture based protocols

2.2.3.5.1 Mammalian cell transfection

A standard transfection protocol was followed for all assays unless stated otherwise. Approximately 5 x 10^5 were seeded into each 6-well (35mm diameter) plate the day before transfection, to allow cells to grow to 70% confluency upon transfection. All transfections used Lipofectamine™2000, according to the manufacturers protocol. Per reaction (1 x 6-well), 3 µl Lipofectamine™ 2000 was diluted in 100 µl media (either DMEM or RPMI depending on the cell line) and mixed with 2 µg total plasmid DNA diluted in 100 µl media. This mixture was incubated for 10 minutes at room temperature, during this time the media on the seeded cells was replaced with either 2 ml DMEM or RPMI (6-8 hour transfection) or 2.5% FCS containing DMEM or 2.5% FCS containing RPMI (overnight, 16 hour transfection). Herein referred to as ''2.5% DMEM'' or ''2.5% RPMI''. Following incubation the transfection mixture was then added to the cells in a drop-wise manner and cells were incubated at 37 ^{o}C for either 6-8 hours or 16 hours, depending upon the experiment. Following this allotted time allowance the transfection containing media was replaced with the corresponding media for that cell line (either 10% DMEM, 10% RPMI, 15% RPMI, respectively) and allowed to express for 24, 48 or 72 hours depending upon experiment.

2.2.3.5.2 Induction of inducible cell lines

3 x 10^5 cells were seeded per 6-well dish (35mm diameter) in 2 ml 10% DMEM, cells seeded were either i293-ST, iEGFP or iEGFP-ST, depending upon experiment. Upon adherence of cells to the culture dish surface (~6 hours), 4 µl doxyclycline hyclate (Life Technologies™) was added to 2 ml 10% DMEM and mixed, resulting in a final concentration of 2 µg/ml per well. This induction media replaced the 10% DMEM on the seeded cells, cells were then allowed to grow to confluence over the course

of 48 hours in the presence of the induction media. SILAC analysis required a large scale up of cells resulting in 5 x 175 cm^3 tissue culture vessels (Sigma-Aldrich™) (Section 2.2.7). Concurrent with this approximately 1 x 10^7 cells per flask were induced with 2 µg/ml doxycycline hyclate in a volume of 30 ml light DMEM (Section 2.2.3.5.2), as explained previously.

2.2.3.5.3 Stabilisation of microtubules

Either i293-ST or MCC13 cells were seeded into 6 well plates at either 4 x 10^5, for western blot analysis (Section 2.2.5.4) or scratch assay analysis (Section 2.2.6.3) or 2 x 10^5 on coverslips for immunofluorescence analysis (Section 2.2.4.1). Following transfection (Section 2.2.3.5.1) or induction (Section 2.2.3.5.2) or both, cells were incubated with 2 ml media (10% DMEM, 10% RPMI or 15% RPMI, depending upon the cells line) containing 10 µM Paclitaxel™ (Sigma-Aldrich™) for 4 hours prior to harvest, scratch wound or fixation.

2.2.3.5.4 Analysis of protein stability

i293-ST cells were seeded at a density of 3 x 10^5 in duplicate for each condition (uninduced and induced) and time points for both control and cyclohexamide treated cells. Cells were incubated with doxycycline hyclate for 48 hours prior (as described in Section 2.2.3.5.2) prior to treatment with 50 µg/ml cyclohexamide (Sigma™) or 50 µg/ml DMSO (Sigma™) for control cells (as cyclohexamide was resuspended in DMSO). Cells were harvested at the corresponding time points (0, 2, 4, 6, 8 hours), as described in Section 2.2.5.1 and protein samples analysed via western blot analysis (Section 2.2.5.4).

2.2.3.5.5 Analysis of translational inhibition

i293-ST cells were seeded at a density of 3 x 10^5 in duplicate for each condition (uninduced and induced) and time points for both control and rapamycin treated cells. Cells were incubated with doxycycline hyclate for 48 hours prior (as described in Section 2.2.3.5.2) prior to treatment with 500 µM Rapamycin (Sigma™) for 5 hours at 37 ^{o}C. Control cells were treated with 500 µM DMSO (Sigma™). Cells were harvested after incubation as described in Section 2.2.5.1 and protein samples analysed via western blot analysis (Section 2.2.5.4).

2.2.3.5.6 siRNA based knockdown of protein expression

i293-ST cells were seeded at a density of 3 x 10^5 and incubated overnight at 37 ^{o}C followed by induction for 24 hours with doxycycline hyclate (Section 2.2.3.5.2). Media was then replaced with DMEM and cells incubated for 6-8 hours with either a control scrambled siRNA or stathmin specific siRNA using 10 nM concentrations of each Flexi-Tube siRNA premix. Transfection media was replaced with fresh 10% DMEM and left overnight. The following day the same procedure was repeated, so cells were transfected two days in a row with siRNA for 6-8 hours. In the context of scratch assays cells were transfected at 0 hours scratch and at 24 after scratch. MKL-1 cells were centrifuged at 1,200 x g for 3 minutes and resuspended in 10 ml RMPI. 5 X 10^5 cells were seeded into 6-well tissue culture dishes and left overnight and immediately incubated with scrambled siRNA and stathmin specific siRNA for 6-8 hours. Cells were centrifuged at 1,200 x g for 3 minutes and resuspended in 10% RPMI and incubated overnight at 37 ^{o}C. The following day the same procedure was followed, so that cells were incubated with Flexi-Tube siRNA on two consecutive days for 6-8 hours. For invasion and migration transwell assays this was performed in triplicate and after both days of transfection cells were seed into the transwells.

2.2.4 Immunofluorescence microscopy

Glass coverslips were sterilised in 100% ethanol and allowed to air-dry before placing in individual wells in a 6 well tissue culture plate. Coverlips were treated with 0.01% poly-L-lysine solution (Life Technologies™) for 3-5 minutes at room temperature, followed by 3 washes with 2 ml phosphate buffered saline (PBS) (Lonza™). Coverlsip were air-dried for a minimum of 3 hours before cell seeding. For all cell lines ~2 x 10^5 cells were seeded onto the coverslips in their respective media and incubated for ~16 hours at 37 ^{o}C. Cells were either transfected (Section 2.2.3.5.1) or induced (Section 2.2.3.5.2) or both. Following the appropriate incubation depending upon the experiment, the media was removed and the cell monolayer washed 3 times in 2 ml PBS, followed by fixation in 2 ml PBS containing 4% (v/v) paraformaldehyde for 15 minutes at room temperature, followed by 3 washes with 2 ml PBS. This was followed by cell permeabilisation in 2ml PBS containing 1% (v/v) Tritin X-100 for a further 15 minutes and washed a further 3 times in 2 ml PBS. Cells then underwent blocking for 1 hour at 37 ^{o}C in 2 ml blocking solution [PBS, 1% (w/v) bovine serum albumin (BSA)]. After blocking coverlsips were transferred to a humidity chamber to prevent cells drying out and incubated for 1 hour at 37 ^{o}C or overnight at 4 ^{o}C with an appropriate primary antibody (See Table 2.6 for dilutions) diluted in blocking solution. Following incubation, cells were washed gently with PBS and incubated with the appropriate AlexaFluor conjugated secondary antibody for 1 hour at 37 ^{o}C. Subsequently cells were washed gently 5 times with PBS and mounted on coverslides using VECTORSHIELD® with DAPI mounting media (Vector Laboratories) to stain the nucleus. Cells were then visualised using the LSM510 META laser scanning inverted confocal microscope and the ZEN 2009 or ZEN 2011 image analysis software (Zeiss).

2.2.4.1 Analysis of the actin cytoskeletal network

The immunofluorescence microscopy protocol was followed as in Section 2.2.4. An actin stain, Phalloidin (Life Technologies™) was used at a 1:5000 dilution in 1% BSA at room temperature for 30-60 minutes. This stain was either used after cells had been washed following permeabilisation with 1% (v/v) Triton X-100, if primary or

secondary stains were not required. Otherwise cells were exposed to Phalloidin after PBS washes following secondary antibody exposure. Cells were then gently washed 5 times with PBS and mounted using VECTORSHIELD® with DAPI (Section 2.2.4).

2.2.5 Electrophoretic analysis of proteins

2.2.5.1 Preparation of mammalian cell lysates

Upon completion of cell culture based protocols, for experiments that required analysis of cellular protein composition, mammalian cells were removed from the tissue culture plates (usually a 6 well) by pipetting with 1 ml PBS. Adherent cells such as MCC13, HuH-7 or HT-1080 were removed from the surface of the culture plate by scraping in 1 ml PBS. The cells suspension was then centrifuged at 3,500 x g at room temperature, followed by washing, 3 times in 1 ml PBS and further centrifugation, as per the previous step. After which, the cell pellet was resuspended and lysed in 100 µl, 4 ^{o}C pre-chilled, 100 µl RIPA lysis buffer [150nM Tris-HCl, 50mM Tris base ultrapure, 1% NP40, pH 7.6, with 1 x protease inhibitor EDTA (Roche)]. This was immediately mixed and incubated on ice for 30 minutes, with mixing every 10 minutes. Followed by centrifugation of the cell lysates in a pre-chilled centrifuge at 4 ^{o}C, 13,200 x g for 10 minutes. The supernatant was then transferred to a clean Eppendorf and stored at -20 ^{o}C until further use.

2.2.5.2 Determination of protein concentration

All protein concentrations were determined using the DC Protein Assay Kit (BIO-RAD), according to the manufacturers protocol. Briefly, using a microplate (96-well plate), 5 dilutions of a protein standard (BSA) was prepared with concentrations ranging from 0.2 mg/ml to 1.5 mg/ml. This was used to prepare a

standard curve for each plate measurement. The standard was prepared in the same buffer that the test protein samples were prepared in to ensure accuracy of the standard curve. 5 µl of each standard were pipetted into the micro plate in triplicate, as were the test samples in triplicate. Following this 20 µl of Reagent S was mixed thoroughly with 1 ml Reagent A. 25 µl of the mixed solution was then added to each individual well, followed by 200 µl Solution B. This was then mixed for at least 15 minutes and the absorbance read at 750 nm. Protein concentrations of the test samples were determined by plotting a standard curve using the standard dilution series.

2.2.5.3 Tris-glycine SDS-Polyacrylamide gel electrophoresis (PAGE)

Polyacrylamide Tris-glycine gels (Table 2.6) were overlaid with a stacking gel [per 2 ml: 300 µl acrylamide/bis acrylamide solution 37.5:1 (Severn Biotech Ltd), 1 ml 0.25 M Tris-HCL (pH 6.8), 40 µl 10% (v/v) SDS, 600 µl dH_2O, 10 µl ammonium persulfate, 2 µl TEMED]. Polymerisation of the gels was initiated by the addition of ammonium persulfate and TEMED.

Protein lysates (Section 2.2.5.1) for analysis, were mixed with 2 x protein solubilising buffer [50 mM Tris-HCl (pH 6.8), 2% (w/v) SDS, 20% (v/v) glycerol, 50 µg/ml Bromophenol Blue and 10 mM DTT] and denatured by heating at 95 ^{o}C for 3-5 minutes. Heated samples were loaded onto polyacrylamide Tris-glycine gels of the appropriate percentage (see Table 2.6 for volumes). Samples were loaded next to the appropriate pre-stained protein ladder (Life Technologies™), as an indicator of molecular (kDa). Prior to ladder or sample loading gels and the SDS-PAGE apparatus were immersed in Tris-glycine running buffer [0.25 M Tris-base, 192 mM glycine, 0.1% (w/v) SDS]. Gels were run at 180 V for ~45 minutes or until the solubilising buffer reached the bottom to the gel. All SDS-PAGE was carried out using a Bio-Rad™ Mini-PROTEAN 3 cell, set up according to the manufacturer's

instructions. Proteins were then analysed by western blot or coomassie stain (Section 2.2.5.4 and Section 2.2.5.5, respectively).

	6%	**8%**	**10%**	**12%**
dh_2O	2.6 ml	2.3 ml	1.9 ml	1.6 ml
Acrylamide/bisacrylamide 37.5:1	1.0 ml	1.3 ml	1.7 ml	2.0 ml
1 M Tris-HCl (pH 8.8)	1.3 ml	1.3 ml	1.3 ml	1.3 ml
10% (w/v) SDS	0.05 ml	0.05 ml	0.05 ml	0.05 ml
10% (w/v) ammonium persulfate	0.05 ml	0.05 ml	0.05 ml	0.05 ml
TEMED	0.004 ml	0.003 ml	0.002 ml	0.002 ml

Table 2.6. Reagents and corresponding volumes required to prepare 6%, 8%, 10% and 12% SDS-PAGE gels.

2.2.5.4 Western blot analysis

Proteins from SDS-PAGE gels (Section 2.2.5.3) were transferred onto Hybond C extra (nitrocellulose membrane) (Amerhsam Biosciences™, UK), using the Bio-Rad Mini Trans-Blot Electrophoretic Transfer Cell (wet blotting system), according to the manufacturers protocol. Briefly, 4 pieces of Whatman 3 mm filter paper, 1 SDS-PAGE gels and one Hybond C extra membrane were soaked in transfer buffer [25mM Tris-base, 190 mM glycine, 20% (v/v) methanol] and placed in a cassette in a specific order. Proteins were transferred from the gel to the membrane at 100 V for 1-2 hours (depending upon protein size), followed by incubation of the membrane in 5% blocking buffer [500 mM NaCl, 20 mM Tris, 0.1% (v/v) Tween-20, 5% non-fat dried milk (Marvel)] at room temperature for 1 hour. Subsequently, the membrane was incubated in the corresponding primary antibody (See table 2.2 for concentrations) diluted in 1 % blocking buffer [500 mM NaCl, 20 mM Tris, 0.1%

(v/v) Tween-20, 1% non-fat dried milk (Marvel)] overnight (~16 hours) at 4 ^{o}C. This was followed by three washes for 10 minutes in 1 x TBS-tween solution (20 mM Tris, 0.1% Tween-20, 500 mM NaCl). The membrane was then incubated in the appropriate secondary antibody (Section 2.1.4 and Table 2.2) diluted 1:5000 in 1% blocking buffer and incubated for 1 hour at room temperature. Followed by three washes for 10 minutes each in 1 x TBS-tween solution. Protein bands were then visualised by enhanced chemiluminescence using EZ-ECL enhancer solutions A and B kit (Geneflow™) (A:B in a ratio of 1:1) and exposed to ECL™ hyperfilm (Amersham™). Films were developed using a Konica SRX-101A developer. All incubations were carried out using a roller mixer and washing steps on a washing platform.

2.2.5.5 Coomassie stain analysis

Proteins were visualised by soaking SDS-PAGE gels (Section 2.2.5.3) in coomassie stain [0.1% (w/v) Coomassie Blue R-250, 50% (v/v) methanol, 10% (v/v) acetic acid] for 1 hours at room temperature. Followed by incubation with coomassie de-stain [25% (v/v) methanol, 10% (v/v)acetic acid] for 30 minutes, subsequently used de-stain was replace with fresh de-stain and incubated for a further 30 minutes at room temperature.

2.2.6 Analysis of mammalian cell motility

2.2.6.1 Invasion and migration transwell assays

Inducible cell lines, MCC13 and MKL-1 cells were seeded in duplicate (per condition) at a density of 3 x 10^5 cells per 6-well tissue culture plate. Cells were incubated at 37 ^{o}C overnight before transfection (Section 2.2.3.5.4) or Induction (Section 2.2.3.5.2); all conditions had corresponding control wells also (e.g. uninduced/induced or pEGFP-C1/pEGFP-ST transfected). The MKL-1 cell line was

transfected with siRNA to Stathmin on 2 consecutive days. HT-1080 cells were also used as a positive control. After 48 hours post induction/transfection, cells were counted using a haemocytometer and seeded in triplicate (per condition) at a density of 1 x 10^5 cell per well, on to pre-coated BD BioCoat™ Angiogenesis System: Endothelial Cell Migration or Endothelial Cell Invasion (BD Bioscience) tissue culture plates for the appropriate time allowance per experiment. This was also replicated for an uncoated control plate. The cells were then analysed for migration and invasion in triplicate, according to the manufacturers protocol. 750 µl FCS containing media was added as a chemoattractant in the bottom wells via the sample ports and the plates incubated for 22 hours at 37 ^{o}C. After incubations, the culture medium was removed from the upper chambers and the insert plates were transferred to 24 well culture plates containing 4 µg/ml Calcein AM™ (BD Biosceince) in 500 µl PBS (per well). The cells were incubated for a further 90 minutes at 37 ^{o}C, 5% Co_2. The fluorescence of invaded and migrated cells was determined using a fluorescence plate reader at excitation wavelengths of between 494-517 nM. Each condition was measured in triplicate and from this the percentage of invasion/migration compared to the control plate could be calculated, as per the manufacturers instructions.

2.2.6.2 Live cell imaging

Inducible cells or MCC13 cells were seed at a density of 3000 cells per 96-well plate, and were incubated overnight (~16 hours), followed by either induction with doxycycline hyclate at 2 µg/ml (as described in Section 2.2.3.5.2) or transfected using 250 ng of plasmid DNA per well, at 37 ^{o}C . Cells were incubated for 24 hours at 37 ^{o}C. Subsequently, the induction/transfection media was removed and replaced with Ham's F-12 media (Gibco™) supplemented with 10% FCS. Cells were then analysed using an IncuCyte™ Live-Cell Imaging System (Essen BioScience), as per the manufacturers protocol. Imaging was performed every 30 minutes over the course of 24 hours and cell motility was then tracked using Image J software.

2.2.6.3 Scratch wound-healing assay

6-well tissue culture plates were incubated with 2 ml poly-L-lysine (Life Technologies™) for 5 minutes, followed by three washes with 2 ml PBS. Treated tissue culture plates were then air-dried for a minimum of 3 hours prior to cell seeding. Cells were seeded at 3 x 10^5 per 6-well (35mmm diameter) and incubated overnight at 37 ^oC. Cells were then either induced (Section 2.2.3.5.2) or transfected (Section 2.2.3.5.1), or both. In this case, cells were induced for 24 hours, then transfected for 6-8 hours, the transfection media was replaced with induction media. After the corresponding time allowance cells were subjected to a manual straight line scratch with a p1000 pipette tip in a continuous straight line through the centre of the well. The cell monolayer was gently washed twice in 2 ml PBS to remove floating/loose cells dislodged by the scratch, to ensure an even line and that cells did not re-adhere in the wound. Images were taken under using a Zeiss light microscope (Zeiss) at 4 X magnification at 0, 24, 48 and 72 hours post-scratch for i293-ST cells and 0 and 24 hours post scratch for MCC13 cells. Paclitaxel™ based scratch assays were incubated for 4 hours prior to a scratch with 10 µM Pacliatxel™, and controls incubated with 10 µM DMSO. siRNA knockdown studies for stathmin were transfected at 0 and 24 hours post scratch.

2.2.7 SILAC-based quantitative proteomics

2.2.7.1 Cell fractionation assay

Inducible cell lines (i293-ST and i293-Tantigen, in two separate experiments) were seeded and passaged until there was 15 x 75 cm^2 tissue culture flask per condition (R_0K_0/induced and R_6K_4/uninduced). For each condition cells were harvested and washed twice in 10 ml PBS, with centrifugation after each wash at 1,200 x g for 4 minutes at 4 ^oC. The cell pellet was resuspended in 5 ml ice cold Buffer A [10mM Hepes, pH 7.9, 10 mM KCl, 1.5 mM $MgCl_2$, 0.5 mM DTT] and incubated at 4 ^oC for 15

minutes. Upon cytoplasmic swelling, the cytoplasm was ruptured using a pre-chilled dounce-homogeniser (25 strokes), and the suspension was centrifuged at for 5 minutes at 228 x g at 4 ^{o}C. Following this the supernatant was removed and stored at -80 ^{o}C as the cytoplasmic fraction. The nuclear pellet was resuspended in 3 ml Solution 1 [0.25 M sucrose, 10 mM $MgCl_2$] and layered over a sucrose cushion of 3 ml Solution 2 [0.35 M sucrose, 0.5 mM $MgCl_2$] and centrifuged for 10 minutes at 2,800 x g. The sucrose cushion wash step was repeated three times, after which the nuclear pellet was resuspended in 3 ml Solution 2 and stored at -80 ^{o}C until further use. All solutions contained 1 protease inhibitor tablet (Roche™).

2.2.7.2 Sample preparation and proteomics analysis

Following cellular fractionation (Section 2.2.7.1) the R_0K_0 and R_6K_4 samples were mixed for each cellular compartment in a 1:1 ratio (total protein concentration). The proteins were then separated by SDS-PAGE and ten gel slices per fraction were extracted and trypsin digested (in-gel digestion). Extracted and purified proteins were analysed and identified using a LTQ-Orbitrap Velos mass spectrometer (University of Bristol Proteomics Facility). Peptides were quantified and identified using MaxQuant[366] based on 2-D centroid isotope clusters within each SILAC pair. The peak list was subsequently searched with the Mascot search engine (version 2.1.04, Matrix Science, London) against the International Protein Index human protein database (version 3.6, forward and reverse database) of 80,412 proteins. For analysis and quantification of proteins levels a 2.0 fold cut-off was chosen and a 2 peptide cut-off. Pathway analysis was performed using the Database for Annotation, Visualisation and Integrated Discover (DAVID, version 6.7)[367].

2.2.8 Analysis of cellular proliferation

2.2.8.1 Standard cell proliferation assay

i293-ST cells were seeded into 6-well plates in triplicate for each condition (uninduced and induced) and time point. HEK 293 FlpIn™ cells were also seed in triplicate as a control. Cells were induced with doxycycline hyclate at 2 µg/ml and incubated at 37 ^{o}C. At the chosen time point (24, 48, 72 hours), cells were detached from the tissue culture plate surface via trypsinisation [0.25% (v/v) trypsin, in PBS], washed in 1 ml PBS and centrifuged at 1,200 x g for 3 minutes at room temperature. The cell pellet was then resuspended in 1 ml HBSS (Hank's Balanced Salts) (Sigma™). Using a dilution of 5:0.2 ml cell suspension was added to 0.3 ml HBSS and 0.5 ml Trypan Blue solution [(0.4% (w/v) (Sigma™)], mixed thoroughly and incubated at room temperature for 10 minutes. Cells were then counted on a 0.1 mm depth haemocytometer (Nebauer Improved).

2.2.9 Multicolour immunohistochemistry

Tumour samples were provided by Dr Neil Steven (University of Birmingham) and immunohistochemistry analysis performed by Rachel Wheat (University of Birmingham) and Professor David Blackbourn (University of Surrey). Primary MCC tumour samples and isotype control samples (tissue adjacent to the tumour) were Formalin-fixed, paraffin-embedded (FFPE), each 4 µm section was mounted onto charged microscope slides by drying overnight at 37 ^{o}C. Followed by incubation at 60 ^{o}C for 30 minutes and deparaffinised in Histo-Clear (National Diagnostics HS-200), cleared in 100% ethanol and washed briefly in water. Antigen retrieval treatment was conducted by heating the slides for 40 minutes at 99 ^{o}C in Wax Capture (W-Cap) TEC Buffer pH 8.0 (BioOptica 15-6315/F). Samples were then blocked (for non-specific antibody binding) in blocking reagent [with 20% normal goat serum, 20% donkey serum, 0.1% BSA in PBS, (all serum was heat inactivated)] for 4 hours. Samples were incubated with appropriate primary antibodies overnight in a humidified chamber at 40 ^{o}C, using anti-CK20 at 1:50 dilution (Dako) and anti-stathmin 1 at 1:250 dilution (Abcam). Sections were first washed three times with PBS for 5 minutes each followed by sample incubation for 1 hour in mouse monocolonal isotype control antibody Dako X-0943 (Dako) for CK20 and a

rabbit polyclonal isotype control antibody (Abcom) for stathmin. Subsequently sections were washed a further three times for 5 minutes each in PBS and incubated with the appropriate secondary antibody, labelled with fluorochromes. These were AlexaFluor 488 IgG2B and AlexaFluor 633 IgG2A (Life Technologies™) and Igg (H+L)-TRITC (Jackson ImmunoResearch). The nucleus was counter-stained using bis-benzimide (Life Technologies™), and slides were then mounted with Immu-Mount (Thermo Scientific™). Sections were analysed using a Zeiss LSM 510 confocal microscope (Zeiss)[368].

2.2.10 Gene expression analysis by qRT-PCR

2.2.10.1 RNA extraction

i293-ST cells were seeded at a density of 4 x 10^5 in triplicate per condition (uninduced and induced) and induced for 48 hours at 37 ^oC with 2 µg/ml doxycycline hyclate. Following incubation cells were directly lysed by addition of 1 ml TRIzol reagent (Life Technologies™) per well, and mixed by pipetting in an RNase-free eppendorf , followed by incubation at room temperature for 5 minutes. Subsequently, 200 µl chloroform was added to each sample with vigorous mixing for 15 seconds and incubated at room temperature for 2-3 minutes. Samples were centrifuged at 12,000 x g for 15 minutes at 4 ^oC and the upper RNA containing aqueous/colourless phase (~500 µl) was transferred to a fresh RNase-free eppendorf. RNA was then precipitated by addition of 500 µl isopropanol and incubation at room temperature for 10 minutes before being centrifuged at 12,0000 x g at 4 ^oC for 10 minutes. The supernatant was carefully aspirated and the pellet washed in 1 ml 75% ethanol and briefly vortexed, followed by centrifugation at 7,500 x g for 5 minutes at 4 ^oC. Supernatant was once again aspirated and the pellet air-dried for 5 minutes. The pellet was resuspended in 49 µl DEPC-treated water and 1 µl RNaseOUT™ (Life Technologies™) and incubated at 57 ^oC for 10 minutes. The RNA was immediately DNase I treated (Section 2.2.10.2) and reverse transcribed (2.2.10.3). Any remaining RNA was stored at -80 ^oC until further use.

2.2.10.2 DNase I treatment

A DNase I kit supplied by Ambion™ was used to remove contaminating DNA from RNA samples (Section 2.2.10.1) as per the manufacturers protocol. 0.1 volume of DNase reaction buffer and 0.5 µl Amplification Grade DNase I were added to each sample, gently mixed and incubated for 30 minutes. The was followed by addition of 0.1 volume Stop solution, mixed thoroughly and heated at 70 ^{o}C for 10 minutes. Samples were then briefly chilled on ice and then long term storage at -80 ^{o}C. The RNA concentration was measured on a NanoDrop and all samples diluted in RNase-free water to a final concentration of 50 ng/µl.

2.2.10.3 Reverse transcription

Superscript™ II Reverse Transcriptase (Life Technologies™) was used to synthesise cDNA from the total extracted cellular RNA, according to the manufacturers protocol. The initial sample mixture contained 1 µg DNase I treated RNA , 1 µl dNTP mix, 10 mM total or 0.25mM per dNTP, 1 µl Oligo$(dT)_{12\text{-}18}$ primer and made up to a total volume of 12 µl. Samples were then mixed and incubated at 65 ^{o}C for 5 minutes and then quick-chilled on ice. Following this, 4 µl 5X First-Strand buffer, 2 µl 0.1 M DTT, 1 µl RNaseOUT™ and 1 µl Superscript™ II Reverse Transcriptase were added to each sample. Samples were mixed gently and incubated at 42 ^{o}C for 50 minutes, followed by enzyme inactivation at 70 ^{o}C for 15 minutes. This was then followed by ethanol precipitation to remove dNTPs.

2.2.10.4 Ethanol precipitation

2 µl 3 M sodium acetate, pH 5.6 and 60 µl ice cold 100% ethanol was added to each cDNA sample (Section 2.2.10.3) and mixed gently, followed by incubation at 4 ^{o}C for 10 minutes. Samples were then centrifuged at 12,000 x g for 10 minutes at 4 ^{o}C and the supernatant discarded. The pellet was then washed in 1 ml ice cold 100%

ethanol and further centrifuged at 12,000 x g for 10 minutes at 4 ^{o}C. The supernatant was removed and the pellet air-dried briefly, followed by resuspension of the cDNA pellet n 20 µl nuclease-free water (Sigma™). The cDNA concentration was determined by NanoDrop and subsequently diluted to 2 ng/ml in nuclease-free water.

2.2.10.5 qRT-PCR reaction

PCR reactions were set up Corbett tubes and a pre-chilled Corbett tube rack (both Corbett Life Sciences). Each reaction PCR reaction was performed in duplicate using different primers (GAPDH as a reference and test primers, in this case stathmin). The PCR master mix contained the following for each reaction: 12.5 µl SensiMix*Plus* SYBR™ No-ROX (Quantace™), 2 µl primer mix (5 µM of both forward and reverse primers), 5.5 µl nuclease-free water and 5 µl cDNA (10 ng final amount). The PCR reactions were performed using a Rotor-Gene™ Q 5plex MRM Platform (Qiagen™) using a 3 Step with Melt program. A typical PCR cycle parameter consisted of 95 ^{o}C for 10 minutes and then 40 cycles of: 95 ^{o}C for 15 seconds, 60 ^{o}C for 30 seconds and 72 ^{o}C for 20 seconds. Quantitative analysis was then performed using the comparative C_T method as previously described[369].

2.2.11 Co-immunoprecipitation assay

All co-immunoprecipitation assays were performed by Dr Andrew Macdonald and Hussein Abdul-Sada (both University of Leeds), as previously described[370]. Briefly, HEK 293 FlpIn™ cells were transfected with the appropriate vectors and cellular lysates harvested after 48 hours. Cell lysates were then incubated with either GFP-TRAP A beads (Chromotek) or Anti-FLAG M1 affinity gel (Sigma-Aldrich™) for 2 hours at 4 ^{o}C, followed by washes with PBS. Beads were then resuspended and analysed by immunoblotting (Section 2.2.5.4) with appropriate antibodies.

Chapter 3

Quantitative proteomics identifies that MCPyV ST promotes host cell cytoskeletal alterations

3. SILAC analysis identifies that MCPyV ST promotes host cell cytoskeletal alterations

3.1 Introduction

MCC is a highly aggressive form of skin cancer of neuroendocrine origin, with a propensity to spread through the dermal lymphatic system and a poor 5 year survival rate[190,197]. It is now established that MCPyV is a causative factor in the formation of MCC and tumour pathology[71]. The MCPyV genome is monoclonally integrated within the host genome in both primary and metastatic cancer forms, and has been observed for all MCC tumours positive for MCPyV. Furthermore, all MCPyV LT sequences derived from MCC tumour cells contain a tumour specific deletion, rendering the virus replication defective upon integration[71]. Due to the monoclonal integration pattern and acquisition of tumour specific mutations within the virus genome the notion that MCPyV may be a passenger virus has been dismissed.

Recent evidence has demonstrated that expression of both MCPyV ST and LT are required for MCC tumour cell survival and cell proliferation, as depletion of the T antigens in MCPyV-positive MCC cells results in cell cycle arrest and cell death[75]. In contrast to SV40, MCPyV ST expression alone can facilitate transformation and anchorage independent growth of rodent cells[247]. This is currently a highly debated topic, as several studies involving MCPyV ST depletion and have shown contradictory results with regard to the requirement of MCPyV ST for cell proliferation[277,371].

Therefore it is essential to understand the mechanisms by which MCPyV ST can interact with the host cell and facilitate tumour formation and maintenance. MCPyV ST is thought to be a multifunctional protein with multiple cellular interactions. Briefly, MCPyV ST has been shown to target the cellular ubiquitin ligase SCF^{Fbw7}, through an internal LSD domain and acts to stabilise the MCPyV LT antigen[227], its expression also inhibits NF-κB-mediated transcription and the host

immune response[226] and acts downstream of mTOR, deregulating cap-dependent translation, through hyperphosphorylation of 4E-BP1[247].

Despite the recent identification of these novel virus-host interactions, all have been attributed to transformation of MCC tumour cells though T antigen expression. To date, no studies have investigated the role MCPyV T antigens may play in the highly aggressive and metastatic nature of MCC tumour cells. The importance of this should not be underestimated, as metastasis of MCC tumour cells directly correlates with poor prognosis and patient survival rates[284]. Therefore the initial aims of this project were to begin analysing and identifying possible cellular targets of MCPyV ST that may contribute to cellular transformation and metastasis. Initially MCPyV ST expression constructs and inducible cell lines had to be generated, which could then be used to conduct high-throughput quantitative proteomic analysis. Stable isotope labelling by amino acids in cell culture (SILAC) coupled with LC-MS/MS and bioinformatial analysis was the used to identify important proteins that were differentially expressed upon MCPyV ST expression. This chapter discusses the initial experiments conducted to identify cellular proteins and pathways that are differentially expressed upon MCPyV ST expression.

3.2 Using the 293 FlpIn™ system to generate a cell line capable of inducible expression of MCPyV ST

Two samples of fresh MCC tumours were supplied by Professor Julia Newton-Bishop at St James' University Hospital, Leeds. The first objective was to isolate cellular genomic DNA from these tumour sections using a standard protocol[372]. Polymerase chain reaction (PCR) could then be applied to amplify the MCPyV ST antigen coding sequence (579 base pairs) with incorporated *Kpn*I and *Sma*I restriction sites, followed by cloning into the respective vectors (pEGFP-C1 or pCDNA5-FRT-TO).

While expression of EGFP-ST in mammalian cells is valuable for subcellular localisation and co-localisation studies the nature of a transient transfection poses

several problems. Firstly, some human cell lines react poorly when subjected to serum starvation which may affect the inherent function of MCPyV ST. Furthermore, transfection does not result in 100% MCPyV ST expression in the cell population, thus posing problems when examining the fold change of protein levels on a global scale i.e. SILAC analysis. Therefore, to address these problems, a cell line capable of inducible expression of MCPyV ST was developed. Induction of this cell line is capable of achieving between 95-100% cell induction of the gene of interest, substantially higher than transfection.

PCR was used to amplify the MCPyV ST coding region from MCC genomic DNA with incorporation of a C-terminal FLAG tag, for localisation and co-immunoprecipitation studies. This produced a fragment containing a FLAG tag, and C-terminal and N-terminal restriction sites (*Bam*I and *Not*I), resulting in a fragment of 624 base pairs.

This MCPyV ST fragment was then sub-cloned into the mammalian expression construct, pCDNA5-FRT-TO, and termed iST-FLAG. This expression construct contains a FLP Recombination Site (FRT) and facilitates Flp recombinase-mediated integration of the gene of interest into the host genome (HEK 293 FlpIn™ cell line). Figure 3.1 shows a schematic for the integration and expression of a gene of interest in the HEK 293 FlpIn™ system.

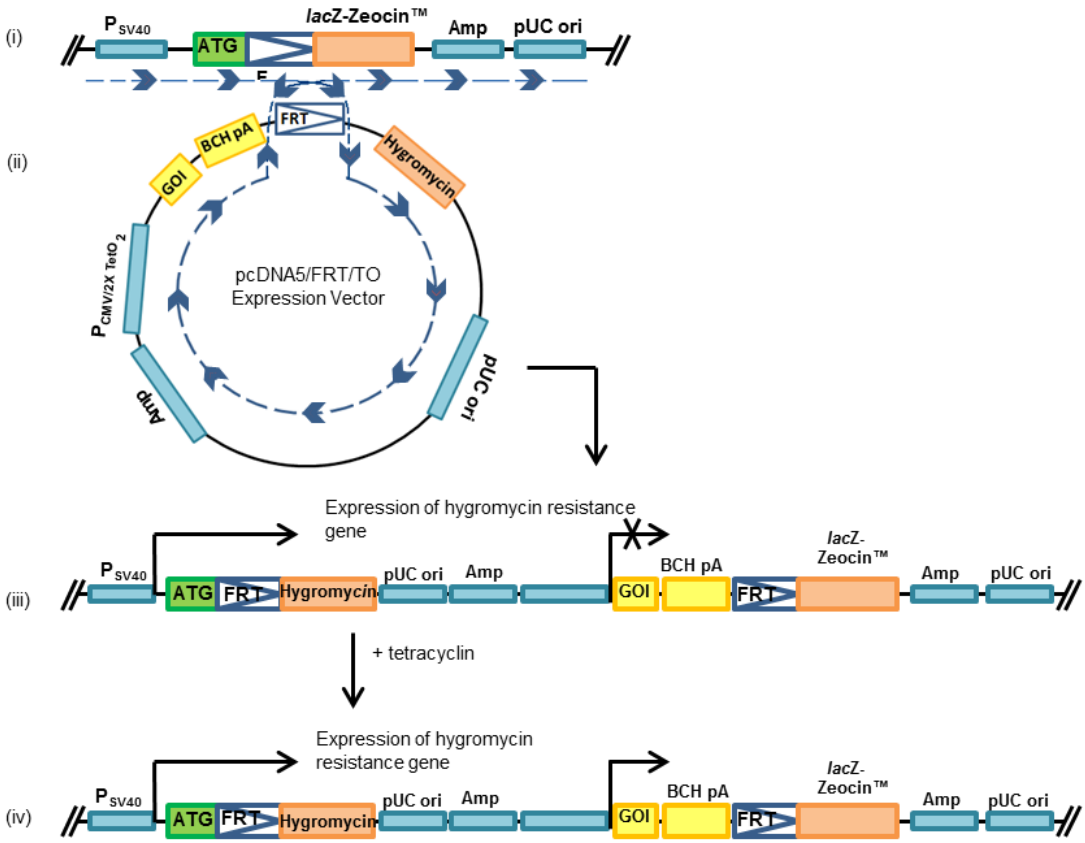

Figure 3.1. Schematic representation for the generation of a stably inducible cell line. (i) and (ii) The pcDNA5/FRT/TO™ mammalian expression vector containing a gene of interest (GOI) in this case MCPyV-ST, is co-transfected with pPGK/Flip/ObpA into the HEK 293 FlpIn™. The Flp recombinase expressed from the pPGK/Flip/ObpA vector facilitates a homologous recombination event between the FRT site in the pcDNA5/FRT/TO™ expression vector and the FRT site in the HEK 293 Flp-In™ cell genome. (iii) Integration of the pcDNA5/FRT/TO™ expression vector confers antibiotic resistance to hygromycin. The Tet repressor (TetR) represses expression of the GOI (MCPyV ST). Addition of tetracycline (Doxcycline hyclate at 2 µg/ml) results in induction of gene expression.

iST-FLAG was then used to produce a stable inducible cell using the HEK 293 FlpIn™ system. Briefly, transfection of iST-FLAG and a plasmid encoding a flip recombinase enzyme (pPGK/Flip/ObpA), resulted in a site specific recombination of MCPyV ST into the HEK 293 FlpIn™ genome. This cell line was generated in a monoclonal fashion using Hygromycin B selection and was termed i293-ST.

Multiple i293-ST clones were screened in order to establish the expression levels of MCPyV ST within each clone. To induce the expression of MCPyV ST, cells were incubated with 2 µg/ml Doxycycline hyclate (Dox) for 24 and 48 hours. It was also necessary to assess if clones that were left uninduced demonstrated expression of MCPyV ST. This is an important point, as a control should show no 'leaky' expression of MCPyV ST in order to establish a reliable cell line for further

investigation. Figure 3.2 (i) shows screening of multiple i293-ST clones for expression of MCPyV ST via immunoblotting at 48 hours post induction with Dox. All clones demonstrated expression of MCPyV ST, with clone 2 (herein referred to as i293-ST) subsequently being used for further analysis, after verification by DNA sequencing.

It was also important to establish that the expression levels of MCPyV ST in the i293-ST were similar to the expression of MCPyV ST in the tumour setting, in order to draw the appropriate conclusions regarding MCPyV ST functions. Using a MCPyV ST-specific antibody (2T2), capable of recognising the J-domain leader peptides in MCPyV T antigens, Figure 3.2 (ii) demonstrates that MCPyV ST protein levels in both i293-ST and MCPyV-positive MCC cells lines (MKL-1) are fairly consistent. The minor discrepancy between the molecular weight of MCPyV ST in Figure 3.2 (ii) can be attributed the C-terminal FLAG tag fused to MCPyV ST in the i293-ST cells, whereas MKL-1 cells express wild type MCPyV ST.

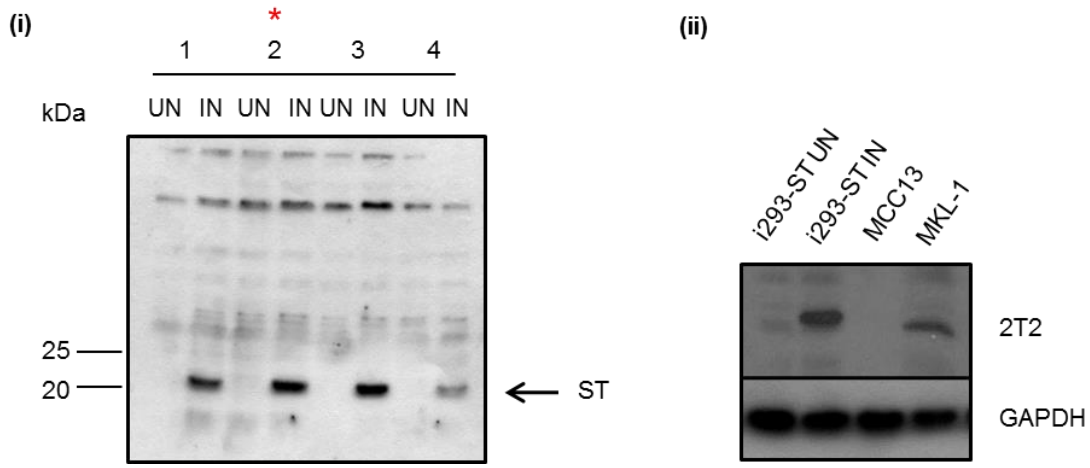

Figure 3.2. Screening of i293-ST clones for the expression of MCPyV ST. (i) i293-ST clones were induced with Doxycyline hyclate for 48 hours and the cellular lysates (both uninduced and induced) were analysed by immunoblotting using an anti-FLAG polyclonal antibody to detect the presence of MCPyV ST. Clone 2 as denoted by *, was taken forward for all future i293-ST experiments, unless stated otherwise. (ii) i293-ST cells were induced and cellular lysates collected at 0 and 48 hours post induction. MCPyV-negative and MCPyV-positive MCC cell lines (MCC13 and MKL-1, respectively) were lysed and analysed by immunoblotting using the 2T2-specifc antibody.

In order to analyse the effect of MCPyV ST on the host proteome, SILAC-based quantitative proteomics was performed using the i293-ST inducible cell line. This is a robust method to analyse protein levels on a global scale under various conditions

and in specific sub-cellular compartments. Figure 3.3 shows a schematic representation of the experimental procedure required to conduct such analysis.

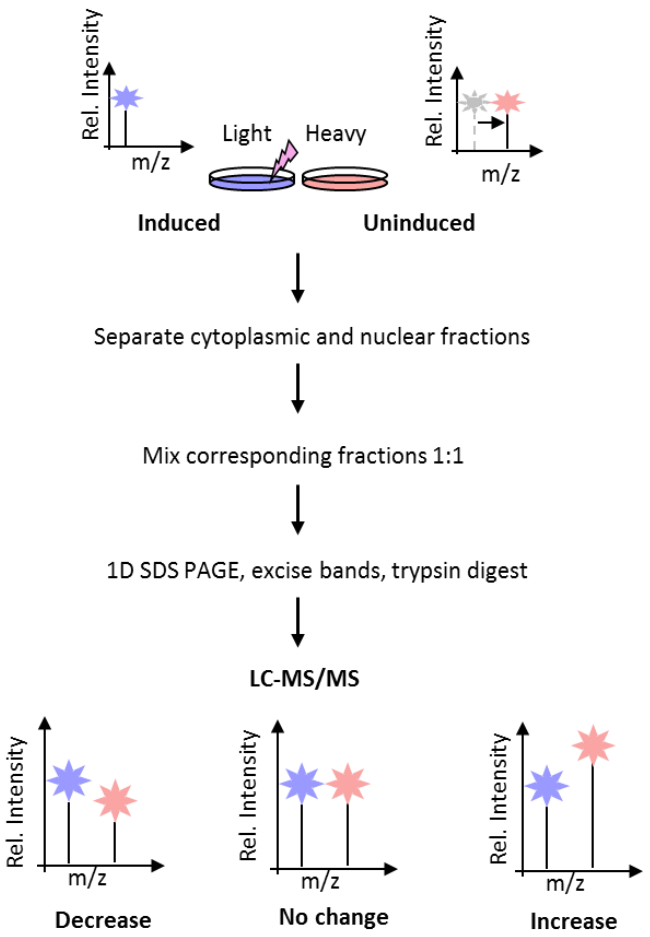

Figure 3.3. A schematic representation of the SILAC-based quantitative proteomic analysis approach. Heavy and light labelled i293-ST cells remained uninduced or induced for 48 hours, respectively. Cells were subjected to fractionation into nuclear and cytoplasmic fractions, with confirmation of fraction purity by immunoblotting. Corresponding fractions were mixed in a 1:1 ratio before being separated by SDS-PAGE. 10 gel slices per lane were excised and trypsin digested, followed by sample analysis by LC-MS/MS to determine to relative abundance of proteins in light isotope containing cells compared to heavy labelled cells.

Briefly, heavy and light labelled i293-ST cells were left uninduced or induced for 48 hours, respectively. Figure 3.4 shows immunoblotting analysis demonstrating that MCPyV ST is only expressed in light-labelled cells which were induced with Dox.

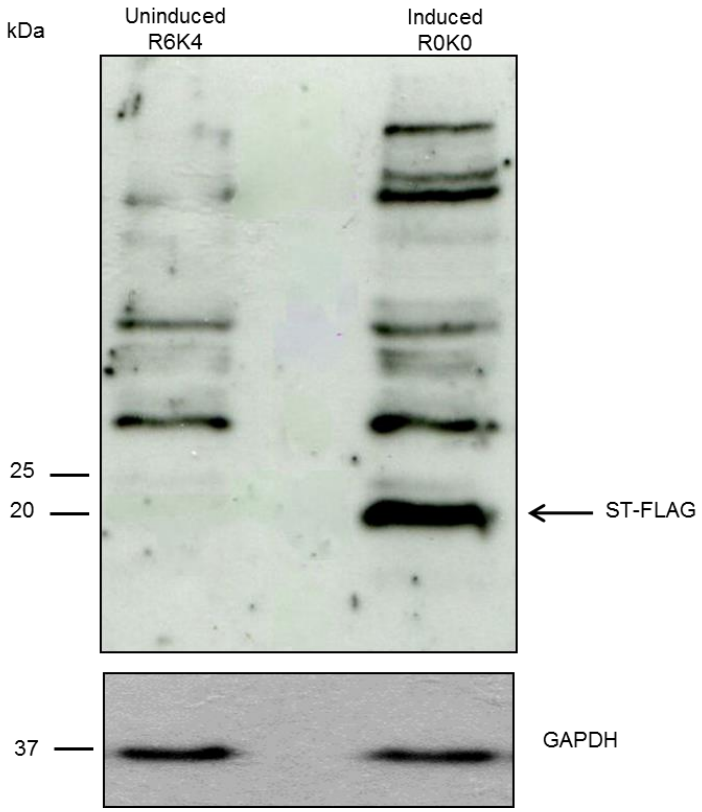

Figure 3.4. Expression of MCPyV ST in SILAC samples. i293-ST heavy and light labelled cells were left uninduced or induced for 48 hours, respectively. A 1 ml sample of cell suspension was collected from each prior to cell fractionation. Each sample was lysed and analysed by immunoblotting with a FLAG-specific antibody.

Following this, cells underwent nuclear and cytoplasmic fractions in order to reduce the complexity of the samples and these samples were analysed by immunoblotting to ensure sample purity. Figure 3.5 demonstrates that the cytoplasmic marker GAPDH in only present in the cytoplasmic fraction of both uninduced and induced samples. Actin is also highly enriched in the cytoplasmic fraction, with a nuclear presence of actin accounted for by the presence of actin in the nuclear matrix[373]. While the nuclear marker Lamin B is present only in the nuclear fractions.

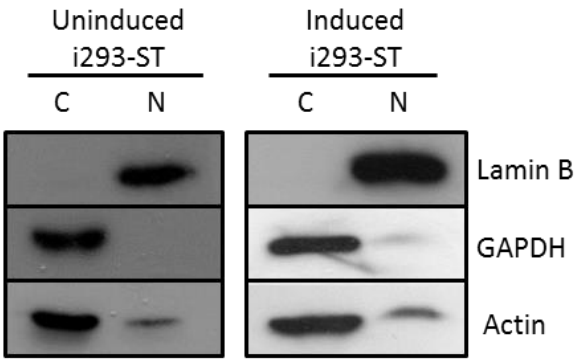

Figure 3.5. Subcellular fraction analysis of SILAC lysates. i293-ST heavy and light labelled cells were left uninduced or induced for 48 hours, respectively. Cells were collected and subjected to cytoplasmic and nuclear fractions using an adapted protocol from the Lamond Laboratory. A sample of each fraction for both uninduced and induced was analysed by immunoblotting using the cytoplasmic markers, GAPDH- and Actin-specific antibodies and a nuclear marker Lamin B-specific antibody.

Corresponding fractions were mixed in a 1:1 ratio and separated by SDS-PAGE, with each lane divided into 10 gel fragments. These fragments were then trypsin digested and submitted for LC-MS/MS analysis.

3.3 Quantitative proteomic analysis identifies that cytoskeletal regulatory proteins are affected by MCPyV ST expression

Following LC-MS/MS analysis, peptides were identified and quantified using MaxQuant[366], with each peptide from the induced cells being expressed as a fold change in comparison to the endogenous proteins expressed in the uninduced cells. A large library of proteins were identified within both the cytoplasmic and nuclear data sets. The cytoplasmic data set consisted of 2454 identified proteins, of which 1626 demonstrated a 1.5 fold increase in MCPyV ST expressing cells, and of these 273 showed more than a 2 fold increase. The nuclear fraction identified 1908 proteins, with 1307 showing a 1.5 fold increase upon MCPyV ST expression and of these 861 demonstrated more than a 2 fold increase.

Interestingly, LC-MS/MS on both the cytoplasmic and nuclear fractions only identified a handful of proteins that were downregulated. This feature has been demonstrated within the laboratory on numerous SILAC based LC-MS/MS analyses

and could be a result of the downregulation itself, resulting in few peptides and hence less likely to be identified during the process of LC-MS/MS.

Due to the large number of proteins identified bioinformatical analysis of the data sets was conducted using the Database for Annotation, Visualization and Integrated Discovery (DAVID) v6.7 software[367]. This analysis indicated that a significant number of highly differentially expressed proteins were those involved in gene ontology classes concerning cytoskeletal dynamics and regulation. Table 3.1 highlights the seven most prominent gene ontology groupings, many of which are cytoskeletal dominated. In order to reduce the complexity to begin validating potentially crucial changes within the proteome, following identification of these specific gene ontology groupings, all peptide hits below 2 were dismissed as unreliable (as theye were only identified once), and could be an artefact the the experiment. Furthermore, a 2.0 fold cut-off in protein fold change was chosen as a basis to begin investigating any potential changes in the proteome.

Gene Ontology headers
1. Cytoskeletal regulation, organisation and dynamics
2. Microtubule cytoskeletal organisation
3. Microtubule based movement and motility
4. Microtubule motor activity
5. Head and neck cancer
6. Regulation of Microtubule depolymerisation and polymerisation
7. Establishment and maintenance of cell polarity

Table 3.1. Gene ontology groupings and pathways hits based on SILAC analysis of i293-ST cells. SILAC samples were analysed by LC-MS/MS. Peptides were identified and quantified using MaxQuant, with peptide hits below 2 being discarded and a 2.0 fold cut-off for protein fold change between conditions being employed. Bioinformatical analysis was conducted using the DAVID v6.7 software and highlighted a number of highly differentially expressed proteins upon MCPyV ST expression and the respective gene ontology grouping that these featured.

Further analysis of the specific proteins within these gene ontology groupings highlighted that a significant proportion were involved in microtubule-associated cytoskeletal organisation, dynamics and regulation as shown in Table 3.2. In addition, the Appendices highlight other differentially expressed proteins in gene ontology groupings ranging from cancer cell metabolism, DNA replication and post-translation modifications. This further demonstrates the wide ranging effects of MCPyV ST expression on cellular pathways and the host proteome.

Protein	IPI Accession no.	Function	Fold increase	Peptide hits
Tubulin-specific chaperone A	IPI00217236	Tubulin-folding protein	7.23	10
Microtubule-associated protein, RP/EB family member 1	IPI00017596	Regulates the microtubule dynamics by promoting nucleation and elongation	2.92	13
Microtubule-associated protein 1B (MAP1B)	IPI00008868	Involved in cell polarisation, required for efficient cross talk between microtubules and actin cytoskeleton	2.4	59
Dystonin (DST)	IPI00645369	Cytoskeletal linker protein, regulates keratinocyte polarity and motility	2.0	155
Stathmin 1	IPI00479997	Involved in the regulation of the microtubule cytoskeletal network	8.33	11
Microtubule-associated protein 4	IPI00396171	Promotes microtubule assembly and disassembly	3.72	32
Kinesin-like protein 14 (KIF14)	IPI00299554	A microtubule motor protein essential for cell cytokinesis	11.39	2

Table 3.2. MCPyV ST promotes the differential expression of proteins involved in microtubule-associated cytoskeletal organisation and dynamics. Microtubule-associated regulatory proteins identified during i293-ST SILAC-based quantitative analysis. Details include protein names, IPI accession number, functions, fold increase in MCPyV ST expressing cells compared to uninduced cells and peptide hits.

This analysis represented a novel finding and in order to independently demonstrate that expression of MCPyV ST promotes upregulation of proteins involved in microtubule dynamics, immunoblotting was conducted. Figure 3.6 demonstrates that cells expressing MCPyV ST show an increase in microtubule associated proteins 48 hours post induction. Proteins upregulated include stathmin, TBCC (tubulin folding cofactor C) and STRAP (serine/threonine receptor associated protein) and further supports the quantitative proteomic analysis.

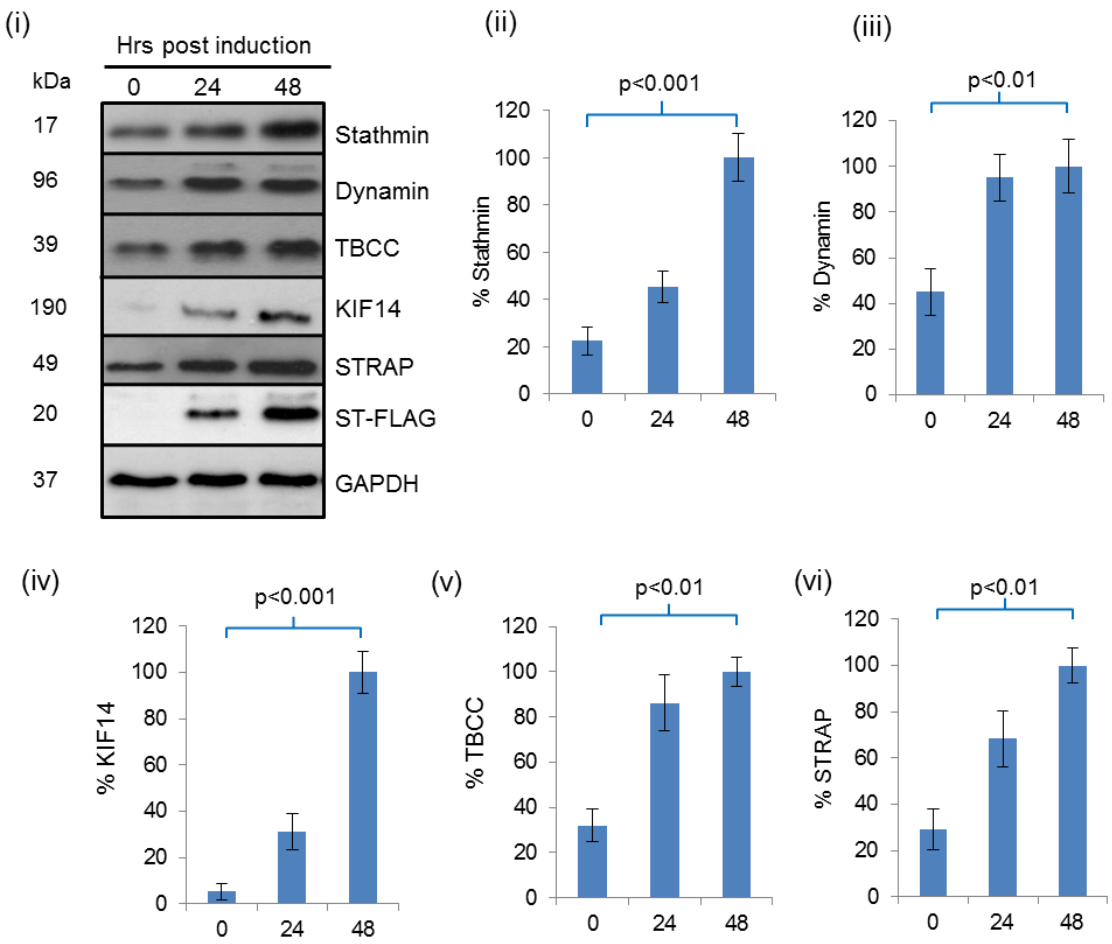

Figure 3.6. MCPyV ST expression promotes upregulation of proteins involved in microtubule cytoskeletal organisation and dynamics. (i) i293-ST cells were uninduced or induced for either 24 or 48 hours with Doxycycline hyclate. Following induction, cells were lysed and analysed by immunoblotting using a range of microtubule associated- and FLAG-specific antibodies. A GAPDH-specific antibody was used as a measure of equal loading. (ii) (iii) (iv) (v) and (vi) GAPDH was used as a measure of equal loading and densitometry analysis using Image J software enabled calculation of the percentage of relative densitometry of stathmin, dynamin, TBCC, KIF14 and STRAP, normalised to the loading control. Data analysed using three biological replicates per experiment, n=3. Statistical analysis employed was a two-tailed T-test with unequal variance.

3.4 Stathmin is overexpressed in primary MCC tumour tissue

One of the most highly upregulated microtubule-proteins upon MCPyV ST expression is stathmin, with an 8.33 fold increase in the cytoplasm. Stathmin is an important regulatory protein in microtubule dynamics and has been associated with multiple human cancers, particularly those with a metastatic phenotype[354,364,374]. Due to the highly aggressive nature of MCC tumours, the ability of MCPyV ST to promote upregulation of stathmin became of interest.

To further investigate stathmin in the context of MCC tumours, Rachel Wheat (University of Birmingham) and Professor David Blackbourn (University of Surrey) conducted multicolour immunohistochemistry analysis using formalin-fixed, paraffin-embedded (FFPE) sections of primary MCC tumours. Tumour sections and isotyped-matched negative controls were incubated with the MCC tumour marker, cytokeratin 20 (CK20) and stathmin-specific antibodies. Figure 3.7 demonstrated that higher levels of stathmin expression were coincident with CK20 staining regions of the tumour. This provides initial *in vivo* evidence that stathmin levels are increased in MCC tumour cells and supports the *in vitro* quantitative proteomic analysis conducted using i293-ST cells.

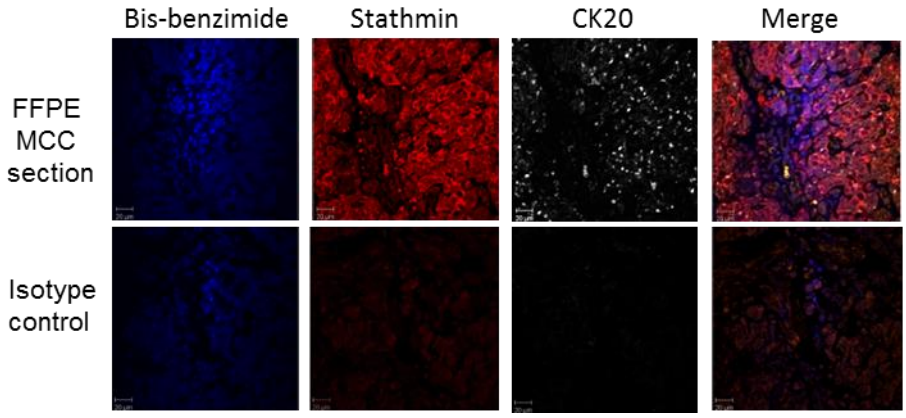

Figure 3.7. Primary MCC tumours upregulate the microtubule-associated protein, stathmin. Experiment performed by Rachel Wheat and Professor David Blackbourn. Formalin-fixed, paraffin-embedded (FFPE) sections of primary MCC tumours and an isotype negative control were stained with stathmin- and CK20-specific antibodies. After washing, sections were incubated with Alexa Fluor labelled secondary antibodies and a nuclear stain, bis-benzimide. Sections were analysed using a Zeiss LSM 510 confocal laser scanning microscope.

3.5 MCPyV ST promotes redistribution of stathmin

To further investigate the potential role of stathmin in MCPyV-induced transformation and metastasis of MCC tumour cells, immunofluorescence studies were conducted. A MCPyV-negative MCC cell line (MCC13) was transfected with mammalian expression constructs, expressing either EGFP or EGFP-ST. Cells were fixed and permeablised and the subcellular distribution of endogenous stathmin was analysed using a stathmin-specific antibody and GFP fluorescence was analysed by direct visualisation.

Initially, 293 FlpIn cells were transfected with either EGFP or EGFP-ST and the localisation of endogenous stathmin and β-tubulin (a marker for microtubule structures) determined. However, as demonstrated in Figure 3.8, 293 FlpIn cells posses a distinct nucleus but there is very little cyctoplasm to visualise. Therefore, any changes in the cyctoplasmic localisation of stathmin or the distribution of the MT structure would be underterminable.

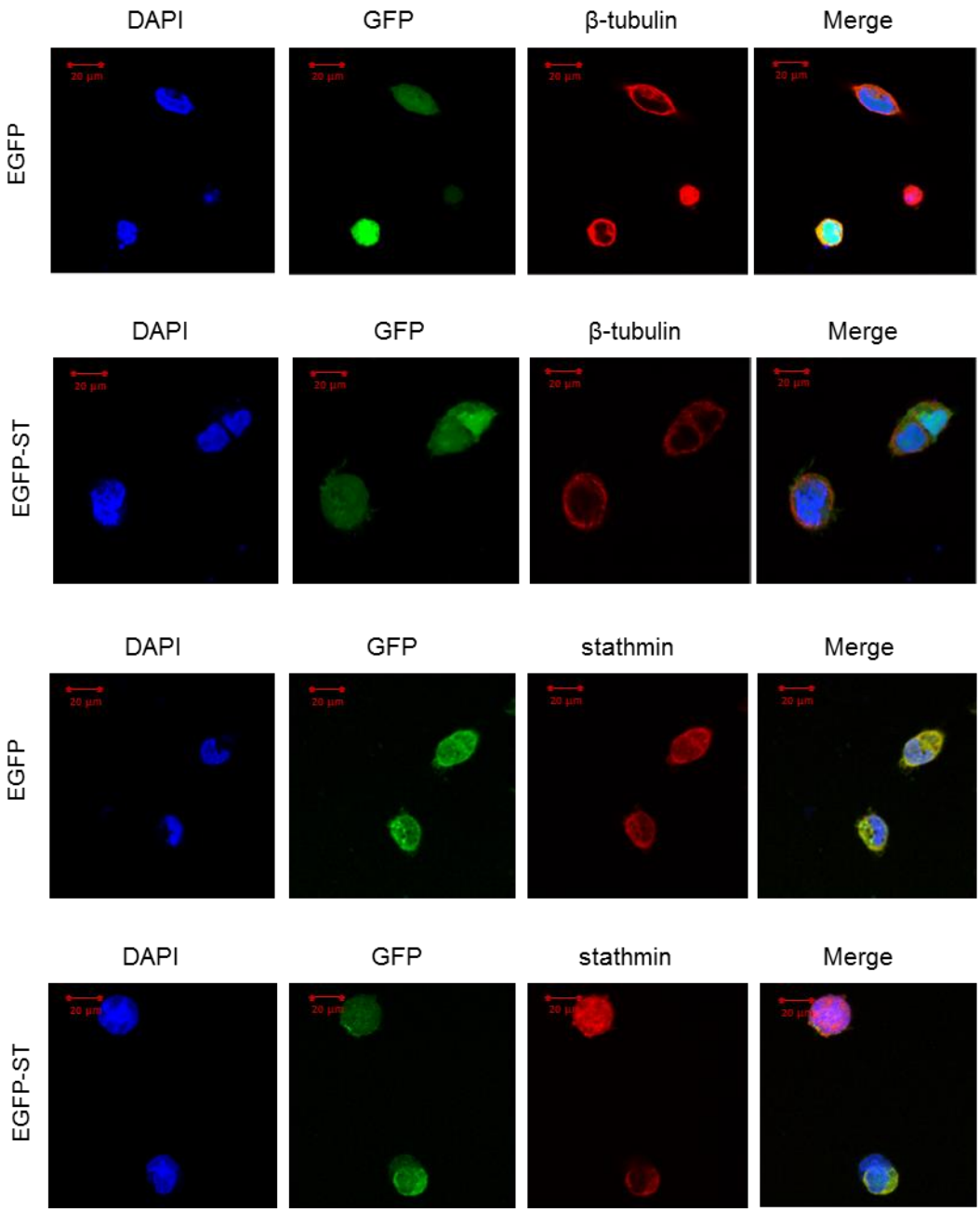

Figure 3.8. Cystoplasmic visualisation is impaired in 293 FlpIn cells. 293 FlpIn cells were transfected with either EGFP or EGFP-ST mammalian expression vectors. Cells were fixed and permeabilised 24 hours after transfection. DAPI-containing mounting medium was used to visualise

the nucleus. GFP fluorescence was analysed by direct visualisation whereas endogenous stathmin and β-tubulin was analysed by indirect immunofluorescence using a stathmin- and β-tubulin-specific antibody. Images were taken using a Z-stack protocol, where 10 slices evenly spaced throughout the cell were imaged and then combined by maximum intensity fluorescence to generate a single image per channel.

As such, MCC13 cells were transfected as they posses a great nuclear to cyctoplasmic ratio, thus visualisation of any redristrubition occurring within the cyctoplasm would be distinguishable. Figure 3.9 demosntrates that MCC13 cells expressing EGFP, show that endogenous stathmin has a diffuse cytoplasmic staining. However, in MCC13 cells expressing EGFP-ST, stathmin in redistributed in a halo-like pattern, colocalising with a small proportion of MCPyV ST, indicating a possible interaction. Interestingly, this cytoplasmic halo-like staining pattern is indicative of microtubule destabilisation[341,359,375]. Interestingly, MCPyV ST staining is not present in the nucleus, as seen in Figure 3.9. This could be a result of MCPyV ST binding to stathmin at increasing stathmin concentrations, resulting in its relocalisation.

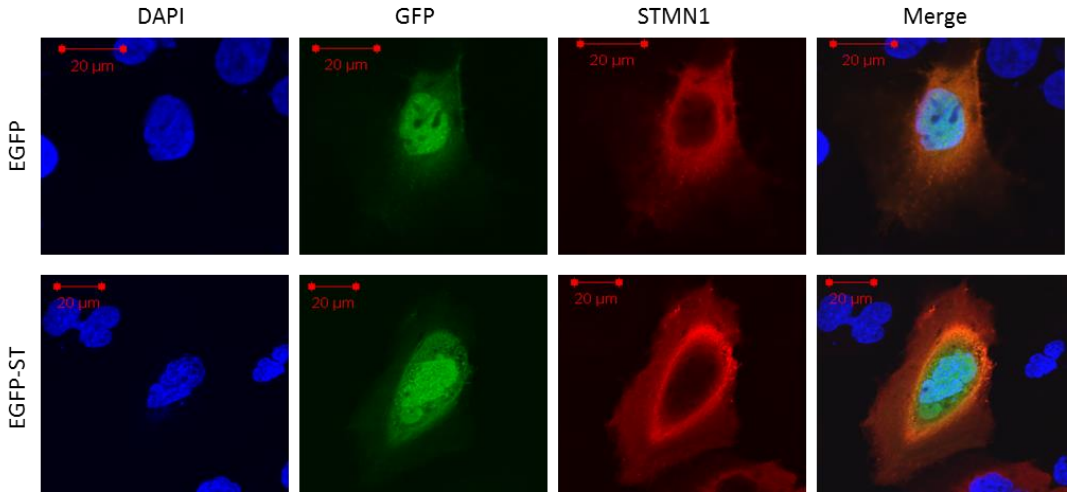

Figure 3.9. MCPyV ST promotes redistribution of endogenous stathmin. MCC13 cells were transfected with either EGFP or EGFP-ST mammalian expression vectors. Cells were fixed and permeabilised 24 hours after transfection. DAPI-containing mounting medium was used to visualise the nucleus. GFP fluorescence was analysed by direct visualisation whereas endogenous stathmin was analysed by indirect immunofluorescence using a stathmin-specific antibody. Images were taken using a Z-stack protocol, where 10 slices evenly spaced throughout the cell were imaged and then combined by maximum intensity fluorescence to generate a single image per channel.

3.6 MCPyV ST promotes microtubule destabilisation

Stathmin is a known microtubule-associated protein, whose activity regulates microtubule dynamics[365]. Therefore, to investigate the effect of MCPyV ST expression on the microtubule network, immunofluorescence analysis was conducted. MCC13 cells were transfected either EGFP or EGFP-ST expression constructs, followed by fixation and permeabilisation after 24 hours. Cells were then incubated with a β-tubulin-specific antibody, a marker for the microtubule network. Cells were imaged using a Z-stack protocol, with 10 image slices through the cell taken. These images were then combined through 'Maximum intensity fluorescence' allowing a clear and concise view of the microtubule network throughout the cell to be observed. Figure 3.10 demonstrates that cells expressing EGFP show a dense, stable network of microtubule filaments throughout the cell. However, cells expressing EGFP-ST demonstrate a destabilised microtubule network, congregated around the nucleus, in a similar manner as stathmin expression in MCPyV ST expressing cells.

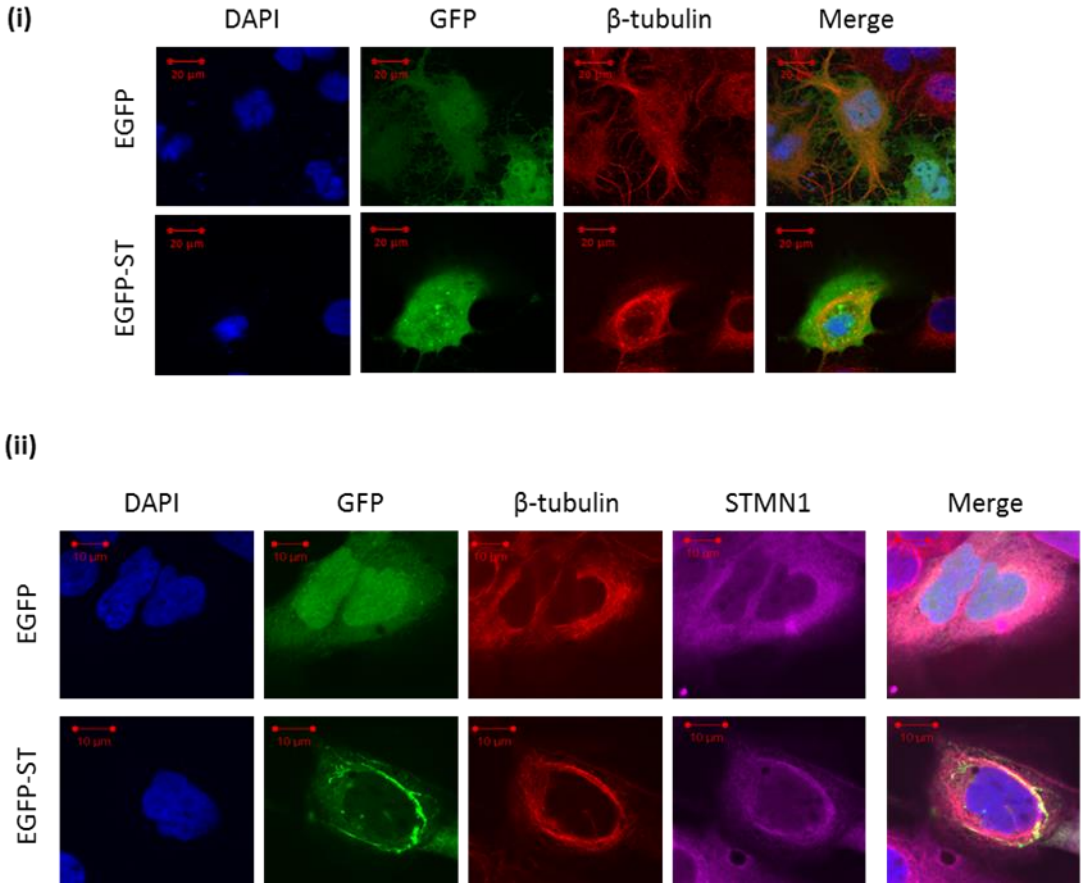

Figure 3.10. MCPyV ST promotes microtubule destabilisation and stathmin redistribution. MCC13 cells were transfected with EGFP or EGFP-ST expression constructs. 24 hours after transfection cells

were fixed and permeablised, followed by staining with (endogenous β-tubulin- (i)) and (endogenous stathmin- (ii)) specific antibodies. The nucleus was stained with DAPI-containing mounting medium and GFP fluorescence analysed by direct visualisation.

To further confirm that MCPyV ST promotes redistribution of stathmin and results in microtubule destabilisation, immunofluorescence analysis was conducted using MCPyV-negative MCC cells and MCPyV-positive MCC cells (MCC13 and MKL-1, respectively).

Figure 3.11 (i) demonstrates that stathmin is redistributed in a halo-like manner in MCPyV-positive MKL-1 cells, while the MCPyV-negative MCC13 cells show a diffuse cytoplasmic stathmin localisation. The results in Figure 3.11 (ii) also show a destabilised microtubule network in MKL-1 cells, as depicted by the localisation of β-tubulin around the nucleus. In comparison the MCC13 cells show a dense and stable microtubule network. This highlights that the presence of MCPyV in MCC tumour cells, concurrent with MCPyV ST expression, results in a redistribution of stathmin promoting destabilisation of the microtubule network.

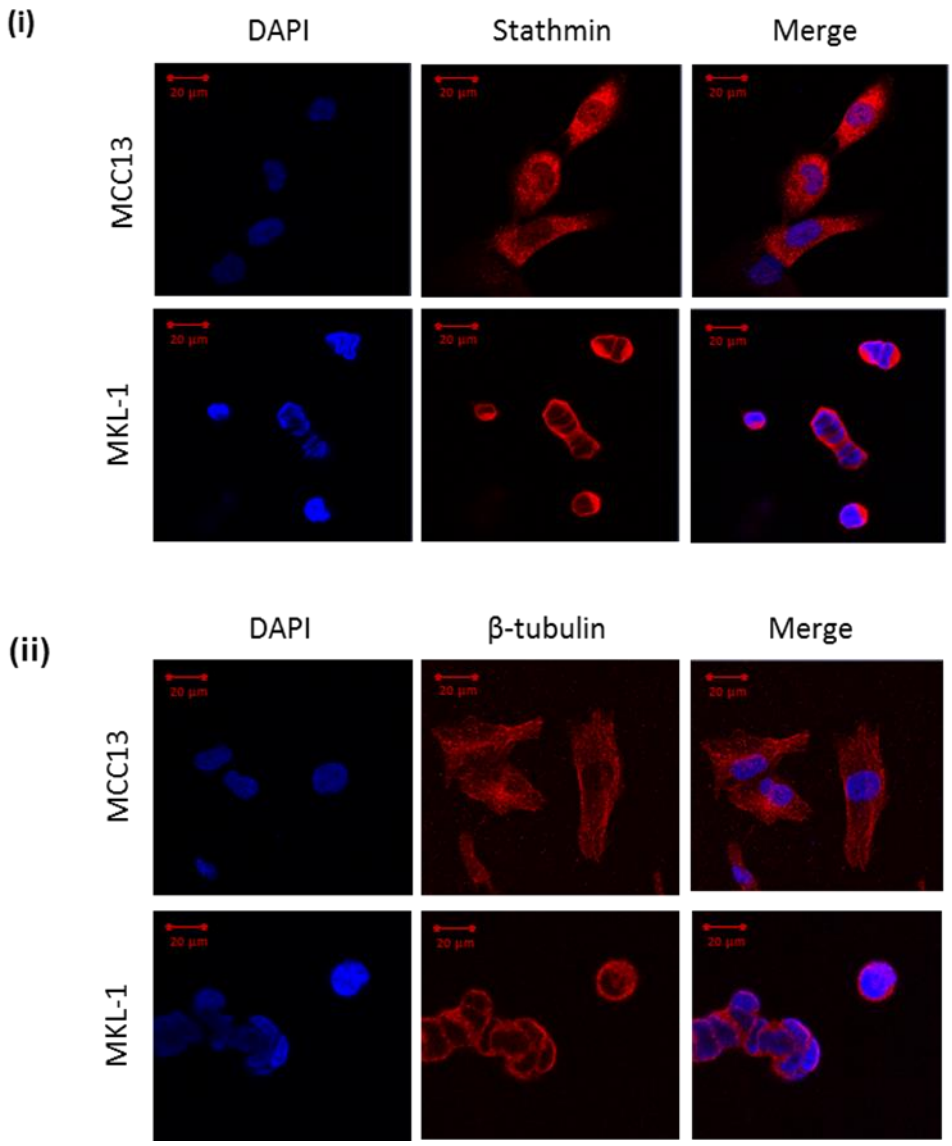

Figure 3.11. MCPyV-positive MCC cells (MKL-1) demonstrate microtubule destabilisation and stathmin redistribution. MCC13 and MKL-1 cells were analysed by immunofluorescence using stathmin- (i) and β-tubulin-specific antibodies (ii). The nucleus was stained with DAPI-containing mounting medium.

3.7 MCPyV ST affects stathmin phosphorylation levels and microtubule stability

As previous immunofluorescence analysis indicated the rearrangement of the microtubules was indicative of destabilisation, the inherent stability of the microtubules was assessed by immunoblotting using a marker for stable microtubules, namely an acetylated tubulin-specific antibody[376]. i293-ST cell lysates were analysed at 0, 24 and 48 hours post induction with Doxycyline hylate. Figure

3.12 (i) and (ii) demonstrates that upon increased expression of MCPyV ST over time, there is a statistically significant decrease in acetylated tubulin levels. This demonstrates that MCPyV ST expression promotes a decrease in stable microtubule structures.

As previously discussed, there is a tight association between stathmin and microtubule dynamics, whereby stathmin phosphorylation promotes microtubule assembly and its subsequent depshosphorylation promotes microtubule disassembly and catastrophe. MCPyV ST promotes the upregulation of stathmin, therefore the phosphorylation status of stathmin in MCPyV ST expressing cells was investigated. Using i293-ST cells, uninduced and induced lysates were analysed by immunoblotting with a phospho-stathmin-specific antibody (Serine 16). The results in Figure 3.12 (iii) and (iv) indicate that upon MCPyV ST expression there is a statistically significant decrease in stathmin phosphorylation.

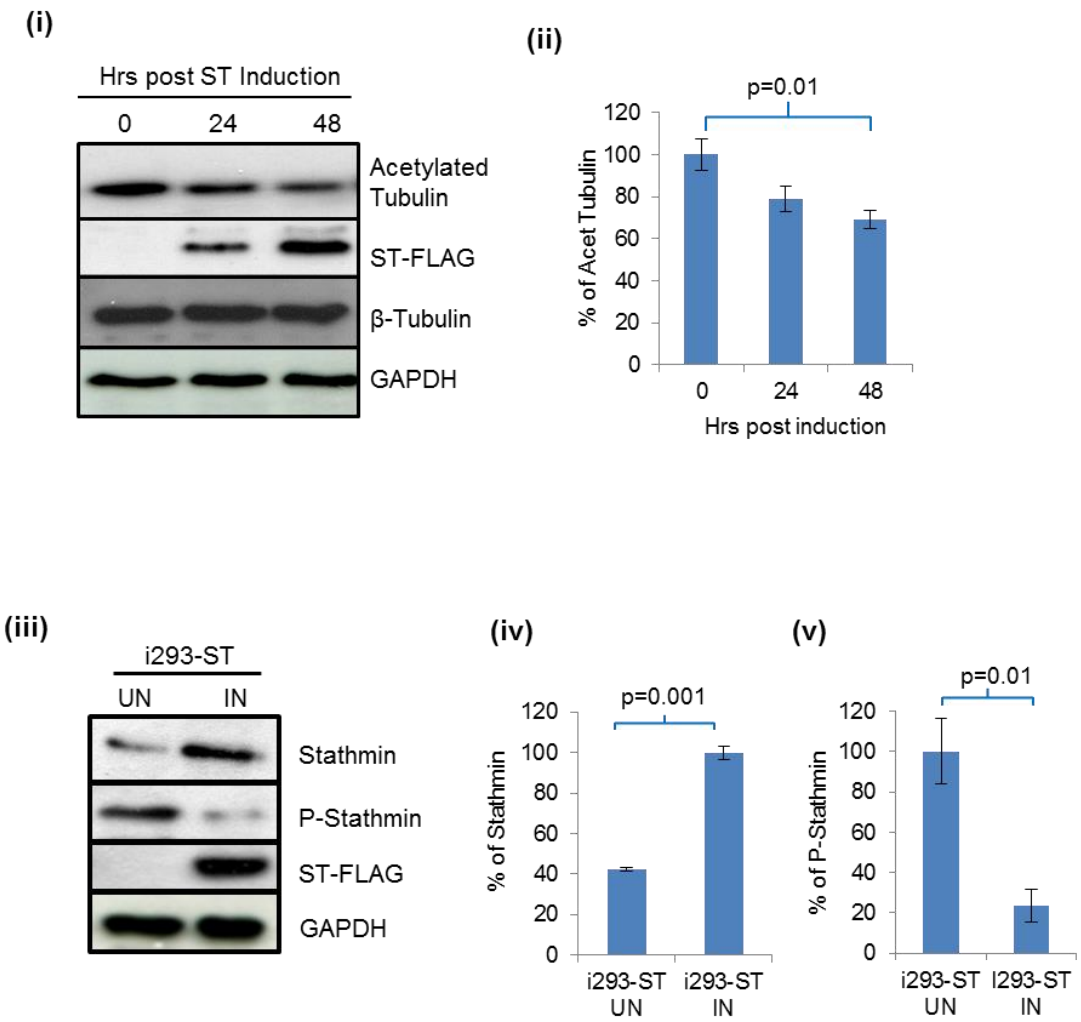

Figure 3.12. MCPyV ST expression affects the cellular levels of phosphorylated stathmin and acetylated tubulin. (i) i293-ST cells were left uninduced or induced and cell lysates harvested at 0, 24 and 48 hours post-induction. Lysates were analysed by western blot using acetylated tubulin-, FLAG-, β-tubulin- and GAPDH-specific antibodies. (iii) i293-ST cells were left uninduced or induced for 48 hours after which cellular lysates were analysed by western blot using stathmin-, phosphorylated (Ser16) stathmin-, FLAG- and GAPDH-specific antibodies. (ii) and (iv) GAPDH was used as a measure of equal loading and densitometry analysis using Image J software enabled calculation of the percentage of relative densitometry of either acetylated tubulin or phosphorylated stathmin, normalised to the loading control. Data analysed using three biological replicates per experiment, n=3. Statistical analysis employed was a two-tailed T-test with unequal variance.

To verify that the observed differences in acetylated tubulin and phosphorylated stathmin were not a result of chemical induction, western blot analysis was performed, as seen in Figure 3.13. HEK 293 FlpIn™ were treated in the presence or absence of Doxycyline hyclate for 48 hours and the cellular lysates analysed. The results demonstrate that chemical induction does not affect the post translational modifications of either protein. Serine 16 (Ser16) was chosen as a marker for phosphorylated stathmin, as it it one of the dominant phosphorylated residues, as

mentioned previously. Dephosphorylation of stathmin at Ser16, has been shown to induce significantly greater activation of stathmin, thus an increase in MT depolymerisation. As such, Ser16 is an appropriate measure of stathmin dephosphorylation and function in terms of these experiements.

.

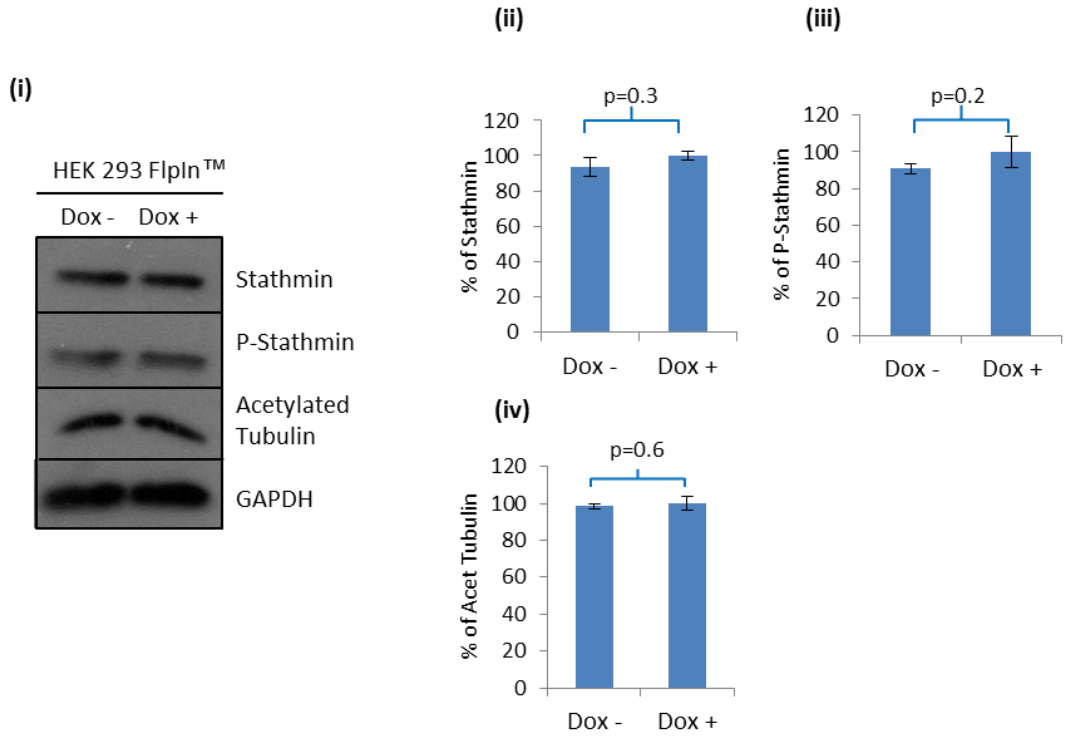

Figure 3.13. Doxycyline hylcate induction does not affect protein levels. (i) HEK 293 FlpIn™ cells were incubated for 48 hours in the presence or absence of doxycycline hyclate. Lysates were isolated and immunoblot analysis performed using stathmin-, phosphorylated stathmin- and acetylated tubulin-specific antibodies. GAPDH was used as a measure of equal loading and allowed the relative densitometry of stathmin (ii), phosphorylated stathmin (iii) and acetylated tubulin (iv) to be calculated using Image J software. Data analysed using three biological replicates per experiment, n=3. Statistical analysis employed was a two-tailed T-test with unequal variance.

To confirm these results, experiments were repeated comparing MCC13 and MKL-1 cells. Lysates were collected and immunoblotting performed using stathmin-, phosphorylated stathmin- and acetylated tubulin-specific antibodies. Figure 3.14 highlights that in cells expressing MCPyV ST a statistically significant increase in stathmin and a reduction in both acetylated tubulin and phosphorylated stathmin was seen, compared to control cells. This demonstrates that a MCPyV-positive cell

line, coincident with MCPyV ST expression, shows both microtubule destabilisation and a reduction in stathmin phosphorylation.

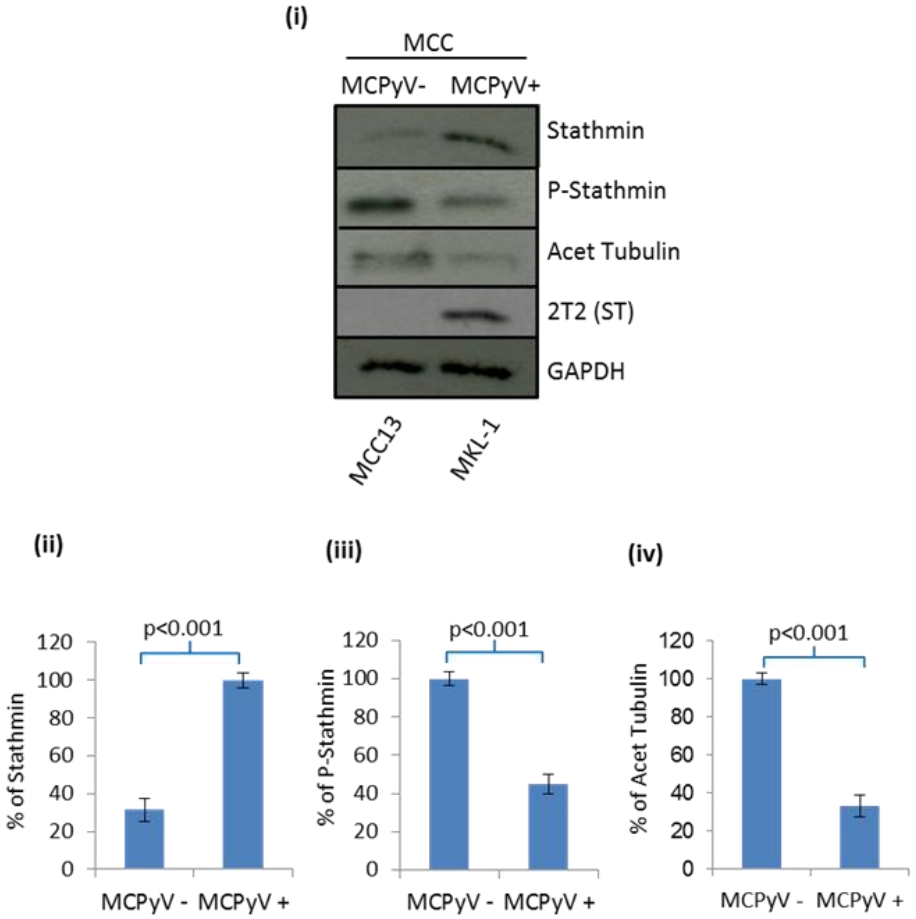

Figure 3.14. MCPyV-positive MKL-1 MCC cells shows microtubule destabilisation and altered phosphorylated stathmin levels. MKL-1 cells and MCC13 cells were isolated and the lysates analysed by western blotting using stathmin-, phosphorylated stathmin-, acetylated tubulin-, 2T2-, GFP- and GAPDH-specific antibodies. The 2T2 antibody recognises MCPyV T antigens and is used to detect the presence of MCPyV ST. GAPDH was used as a measure of equal loading and densitometry analysis using Image J software enabled calculation of the percentage of relative densitometry of stathmin (ii), phosphorylated stathmin (iii) and acetylated tubulin (iv), all normalised to the loading control. Data analysed using three biological replicates per experiment, n=3. Statistical analysis employed was a two-tailed T-test with unequal variance.

To verify that the observed results were due to MCPyV ST expression, MCC13 cells were transfected with either EGFP or EGFP-ST and the cell lysates analysed by immunoblotting with acetylated tubulin- and phosphorylated stathmin-specific antibodies. Figure 3.15 demonstrates that upon MCPyV ST expression there is a significant increase in stathmin expression and a decrease in both acetylated tubulin and phosphorylated stathmin levels. Clearly indicating that MCPyV ST expression is responsible for this phenotype.

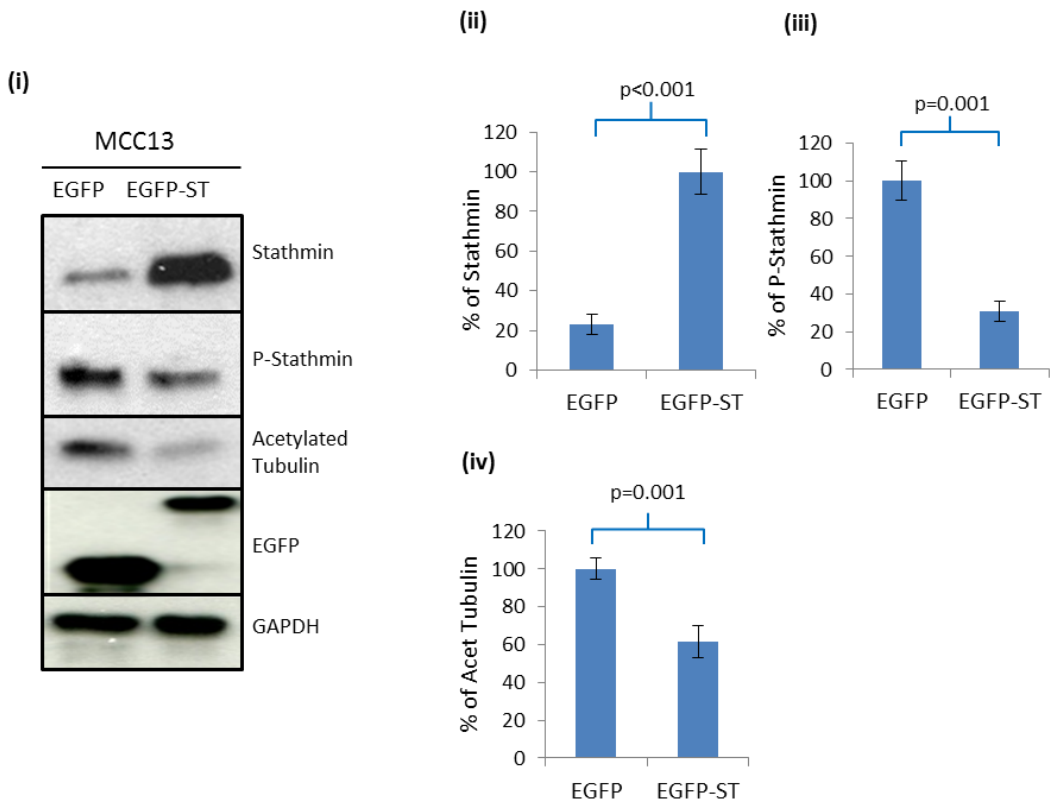

Figure 3.15. MCPyV ST expression promotes microtubule destabilisation in MCC13 cells. (i) MCC13 cells were transfected with either EGFP or EGFP-ST. After 24 hours lysates were analysed by immunoblotting using a stathmin-, phosphorylated stathmin-, and acetylated tubulin-specific antibody. GAPDH was used as a measure of equal loading and allowed the relative densitometry of stathmin (ii), phosphorylated stathmin (iii) and acetylated tubulin (iv) to be calculated using Image J software. Data analysed using three biological replicates per experiment, n=3. Statistical analysis employed was a two-tailed T-test with unequal variance.

Furthermore to ensure that these results were not due to the presence of an EGFP fusion tag, this experiment was repeated with MCC13 cells transfected with either EGFP or an untagged-ST expression construct. Figure 3.16 verifies that the observed increase in stathmin and decrease in acetylated tubulin and phosphorylated stathmin is a result of MCPyV ST expression and not the presence of a tagged epitope. Moreover, this data confirms that the conclusions drawn with regard to MCPyV ST expression in i293-ST cells is physiologically relevant with regards to the MCC tumour cell lines.

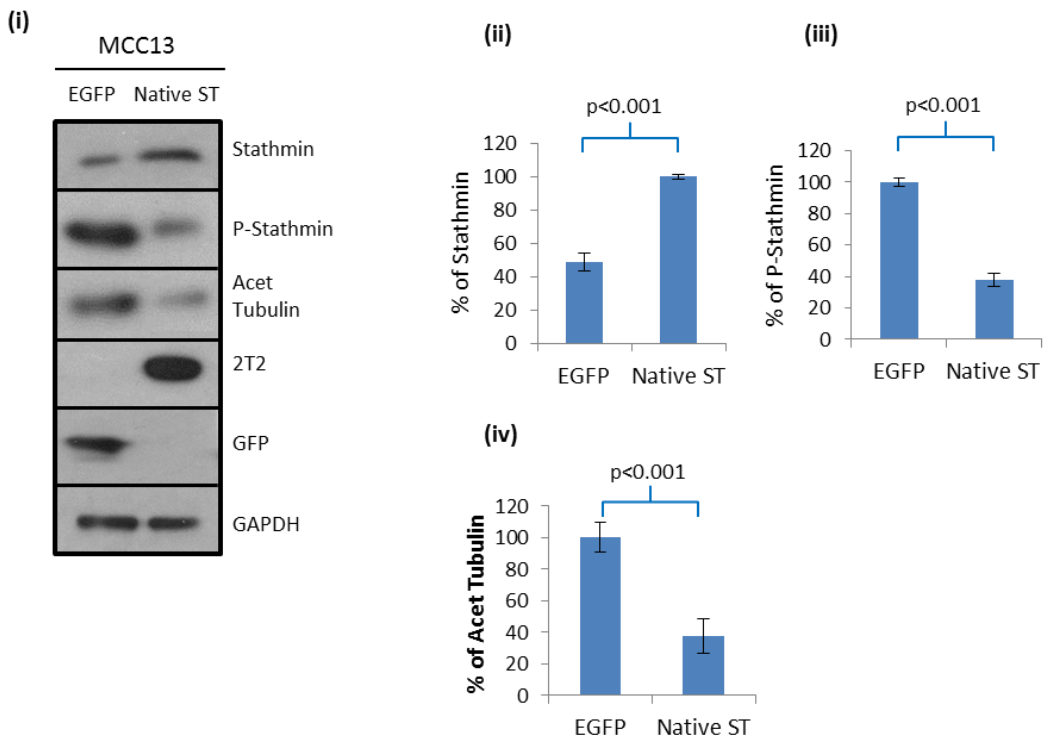

Figure 3.16. An EGFP tag does not affect MCPyV ST function. (i) MCC13 cells were transfected with either EGFP or native-ST (untagged) and 24 hours later the cell lysates isolated. Lysates were analysed by immunoblotting using stathmin-, phosphorylated stathmin-, and acetylated tubulin-specific antibodies. GAPDH was used as a measure of equal loading and allowed the relative densitometry of stathmin (ii), phosphorylated stathmin (iii) and acetylated tubulin (iv) to be calculated using Image J software. Data analysed using three biological replicates per experiment, n=3. Statistical analysis employed was a two-tailed T-test with unequal variance.

3.8 MCPyV ST affects the distribution of the actin cytoskeletal network

Quantitative proteomic analysis also revealed that the gene ontology grouping 'cytoskeletal regulation, organisation and dynamics' consisted of a number of actin cytoskeletal proteins that were also upregulated upon MCPyV ST expression. Therefore to investigate if MCPyV ST promotes alterations within the actin cytoskeletal network, immunofluorescence analysis was performed. HEK 293 FlpIn™ cells were transfected with either EGFP or EGFP-ST for 24 hours. The actin cytoskeletal network was analysed using the actin stain, Phallodin. HEK 293 FlpIn™ cells, rather than MCC13 cells, were used for this analysis as untransfected MCC13 cells show significant actin cytoskeletal protrusions. This is likely due to gain of function mutations in MCPyV-negative MCC cells. Thus HEK 293 FlpIn™ cells were

used to analyse the effect of MCPyV ST on the actin network, as untransfected HEK 293 FlpIn™ demonstrate few, if any, actin cytoskeletal protrusions and form ordered and stable actin networks.

Figure 3.17 demonstrates that EGFP expressing cells contain an ordered and stable actin cytoskeletal network. In contrast, EGFP-ST expressing cells show the actin network is altered in a manner characteristic of protrusion formation e.g. filopodia and invadepodia. Two distinct distributions of the actin cytoskeletal network were observed upon MCPyV ST expression. Firstly, a diffused nature with multiple protrusions on all sides of the cell surface membrane and secondly, a more polarised distribution of protrusions concentrated on one side of the cell. The difference seen in the architecture of the actin network in MCPyV ST expressing cells may be a result of cells becoming polarised in order to facilitate cell motility. However, what is clear is that MCPyV ST expression promotes the formation of cell protrusions, likely filopodia or invadepodia which may be involved in cell motility and migration.

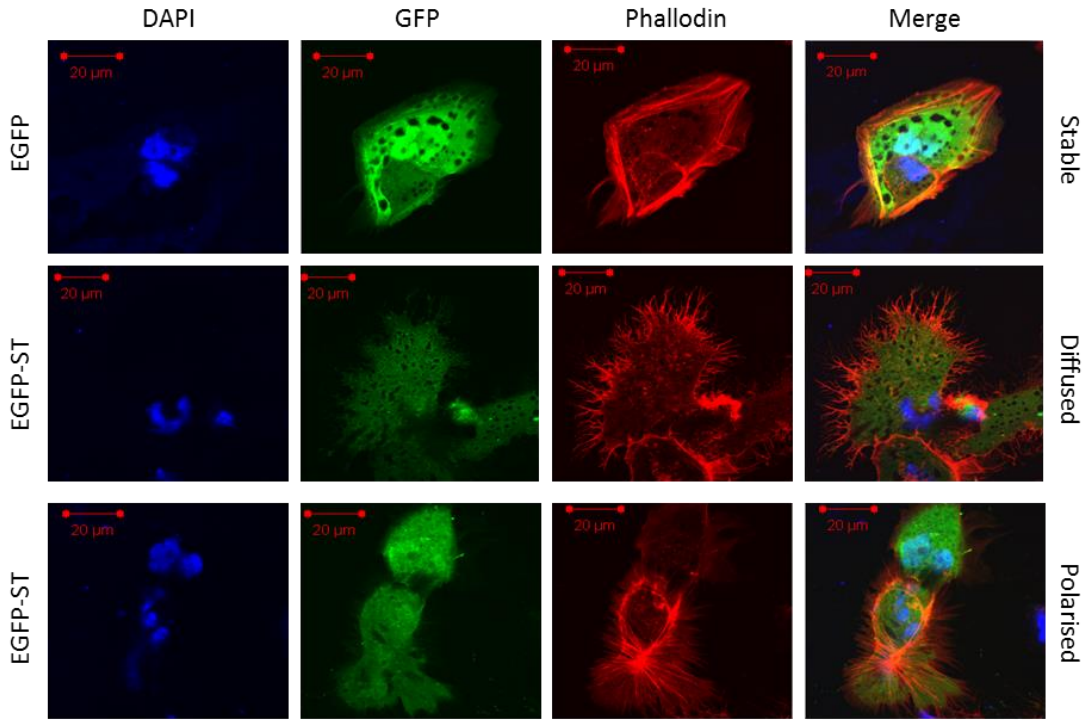

Figure 3.17. MCPyV ST promotes a rearrangement of the actin cytoskeletal network. HEK 293 FlpIn™ cells were transfected with either EGFP or EGFP-ST mammalian expression vectors. Cells were fixed and permeabilised and incubated for 30 minutes with an actin stain, Phallodin. DAPI-containing mounting medium was used to visualise the nucleus.

3.9 Discussion

The oncogenic MCPyV ST protein has been shown to be sufficient to promote anchorage independent growth of rodent cells and facilitate transformation[247]. However, no studies have addressed the mechanism by which MCC tumour cells readily metastase, and the possible role the MCPyV T antigens may play in this phenotype. Herein, quantitative proteomic analysis has demonstrated an upregulation of a large proportion of cytoskeletal proteins upon MCPyV ST expression. SILAC-based analysis, coupled with LC-MS/MS and bioinformatical analysis is an effective way of studying the host cell proteome, and has recently been applied in increasing areas of microbiology research[377]. Furthermore, reducing sample complexity allows analysis of subcellular trafficking between various cellular compartments, to understand in greater detail the virus-host interactions.

Data presented here, demonstrates that MCPyV ST promotes the upregulation of specific cytoskeletal and actin proteins, crucial to their regulation, organisation and dynamics. Bearing in mind the highly aggressive nature of MCC and the well-established links between cell motility and cytoskeletal dynamics, this suggested a possible link between this phenotype and MCPyV ST expression. Moreover, MCC distant metastases results in poor patient survival rates, therefore addressing the mechanism by which this occurs may present novel targets for chemotherapy regimens.

MCC tumour formation is effectively an indirect result of the monoclonal integration of the MCPyV genome into the host chromosome, which results in defective viral replication and leaves the MCPyV unable to generate infectious virions. Interestingly, this indirect promotion of metastases is not without precedent in the viral world. Other tumour-associated viruses, such as HPV 16, EBV, HBV and SV40 have all demonstrated the capacity to promote metastasis, through expression of viral oncoproteins. These mechanisms vary but include alteration of cellular adhesion complexes, manipulation of matrix

metalloproteinases, gene expression modulation and cytoskeletal reorganisation[299,378,379].

Furthermore, results demonstrate that MCPyV ST expression correlates with an upregulation of stathmin. This has been shown in both i293-ST cells and formalin-fixed paraffin-embedded sections of primary MCC tumours. Interestingly, stathmin overexpression is a feature of multiple cancer types and has been shown to correlate with tumour growth, poor patient prognosis and a high metastatic potential[340,354]. This has been confirmed by RNA interference studies that demonstrate that stathmin levels can drastically reduce the motility of various tumour cells[340,356-358]. As such, the data presented here, suggests that MCPyV ST may contribute to the metastatic phenotype of MCC tumour cells through alterations in crucial cytoskeletal regulatory proteins, specifically by promoting the overexpression of stathmin.

Due to the known association between stathmin and microtubule dynamics, and the importance of the microtubule network in facilitating cell motility, the structure of the microtubules in MCPyV ST expressing cells was investigated. Data presented herein, demonstrates that MCPyV ST expression promotes a rearrangement of the microtubule network, in a peri-nuclear halo-like ring, indicative of microtubule destabilisation[341,375]. MCPyV-positive MCC cells, coincident with MCPyV ST expression, also show a destabilised microtubule network compared to MCPyV-negative MCC cells, further confirming that microtubule destabilisation is a result of MCPyV ST expression. Moreover, through the use of a marker of stable microtubule, namely acetylated tubulin, results demonstrated there was a significant decrease in stable microtubule structures upon MCPyV ST expression.

Moreover, the activity of stathmin is regulated by phosphorylation at multiple serine residues, whereby dephosphorylation promotes stathmins' tubulin binding ability, thereby promoting microtubule destabilisation[346,364,365]. Therefore in order to account for the ability of MCPyV ST to promote microtubule destabilisation, the phosphorylation status of stathmin was investigated. Findings here demonstrate that upon MCPyV ST expression there is an increase in the pool of

unphosphorylated stathmin. This suggests that MCPyV ST expression promotes stathmin dephosphorylation, thereby resulting in MCPyV ST-induced microtubule destabilisation.

This data represents the first quantitative proteomics study into MCPyV and MCC biology and provides a novel line of enquiry into cytoskeletal biology which may be an underlying mechanism in MCC metastasis.

Chapter 4

MCPyV ST promotes cell motility, migration and invasion by facilitating microtubule destabilisation

4. MCPyV ST promotes cell motility, migration and invasion by facilitating microtubule destabilisation

4.1 Introduction

The spread of malignant cells from the primary solid tumour to remote sites within the body is one of the biggest problems facing cancer treatment, and results in more than 90% of cancer associated-deaths[286]. Despite the clinical important of metastasis, the molecular mechanisms by which this phenotype is acquired have yet to be fully elucidated[285]. This poses a significant problem in real terms for cancer prognosis and treatment of patients and is an area of cancer biology that needs much research.

As previously discussed, MCC is regarded as the most aggressive form of skin cancer and is associated with poor patient prognosis and quick progression to distant metastases[201]. Thus it is important to address the underlying molecular mechanisms by which this phenotype arises in MCC tumour cells.

It is clear that cell motility, migration and invasion are key aspects that facilitate dissemination of cancer cells from the primary tumour. It has long since been established that the actin cytoskeletal network is crucial in the process of cell motility and migration[321], however recent evidence also highlights the emerging role of the microtubule network in both regulating and facility cell motility[322]. While the microtubule (MT) cytoskeletal network is pivotal for intracellular vesicle transport, organelle positing and mitotic spindle formation[324-327], it is also important for the control of cell shape and polarised cell motility[322,328].

Microtubules form a dense cytoplasmic network and are composed of hollow tubes of αβ-tubulin heterodimers. These tubulin heterodimers can self-assemble and disassemble, a process known as dynamic instability[329]. This process is tightly regulated and is controlled by two classes of MT-associated proteins (MAPs), known as MT stabilising and MT destabilising proteins[324,329].

One such MT destabilising protein is stathmin, also known as oncoprotein-18, and is a key regulator of MT dynamics[340-342]. Stathmin has demonstrated both indirect sequestration of tubulin dimers and direct binding of protofilaments present at growing MT tips[346], both of which facilitate MT destabilisation.

Quantitative proteomic analysis highlighted that a large proportion of differentially expressed proteins upon MCPyV ST expression were involved in microtubule organisation, regulation and dynamics. Bearing in mind the link between microtubules and cell motility and combined with the fact that MCC is highly metastatic, investigations were conducted into the ability of MCPyV ST to promote cell motility, migration and invasion. Various methods of cell motility assays were performed using a range of cell lines, including the physiologically relevant MCPyV-negative (MCC13) and MCPyV-positive (MKL-1) MCC cell lines. This chapter focusses on MCPyV ST ability to promote microtubule destabilisation, possibly through stathmin activity, which in turn promotes a more motile and migratory phenotype.

4.2 MCPyV ST promotes cell motility, migration and invasion in i293-ST cells

To assess if expression of MCPyV ST affects cell motility and migration, a variety of motility and invasion assays were performed. Initially, HEK 293 FlpIn™ cell movement was assessed using live cell imaging and tracking through the use of an IncuCyte kinetic live cell imaging system. Cells were transfected with either EGFP or EGFP-ST, and cells imaged over the course of 24 hours, at 30 minute intervals to determine cell movement. It has previously been demonstrated within the Whitehouse Laboratory that the EGFP fusion does not affect MCPyV ST function[226]. Using Image J analysis software, transfected cells were tracked and the distance moved calculated, as can be seen in Figure 4.1.

Separate line traces (blue, red, yellow, cyan and green) were used to demonstrate the path of movement of individual cells over a 24 hour period. The results

demonstrate that HEK 293 FlpIn™ cells transfected with EGFP-ST show a statistically significant increase in cell motility in comparison to cells expressing EGFP. Moreover, live cell imaging also demonstrated that HEK 293 FlpIn™ cells grow in a colony, however upon MCPyV ST expression cells rapidly dissociate from the rest of the colony, unlike EGFP expressing cells (depicted in supplementary movies on the attached CD-ROM) This once again suggests that MCPyV ST expression promotes a more motile and migratory phenotype.

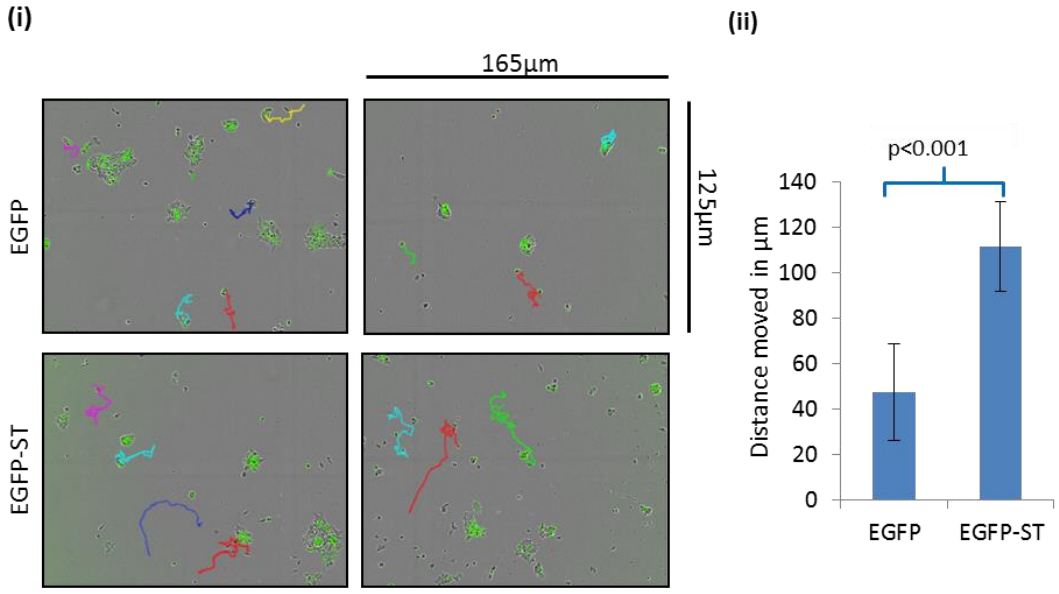

Figure 4.1. MCPyV ST expression promotes cell motility in HEK 293 FlpIn™ cells. (i) Cells were transiently transfected with either EGFP or EGFP-ST and 12 hours after transfection cell motility was analysed using an IncuCyte kinetic live cell imaging system. Images were taken over the course of 24 hours every 30 minutes and cell movement tracked using Image J software. Red, blue, cyan, yellow and green line tracks depict the path of cell movement over the time course. (ii) The average distance moved by transfected cells was measured in µM (n=50). Data analysed using three biological replicates per experiment, n=3. Statistical analysis employed was a two-tailed T-test with unequal variance.

To verify this finding, a scratch-wound healing assay was performed using i293-ST cells to compare wound healing capabilities as a result of MCPyV ST expression. i293-ST cells were left uninduced or induced for 48 hours, the confluent cell monolayer was then subjected to a scratch wound. The cellular growth back into the wound was then recorded every 24 hours for a course of 3 days as demonstrated in Figure 4.2. The results clearly indicate that cells expressing MCPyV ST migrate more quickly into the wound, compared to uninduced cells, and fully

occlude the wound after 72 hours. Once again confirming that MCPyV ST expression significantly increases the motility and migration of cells.

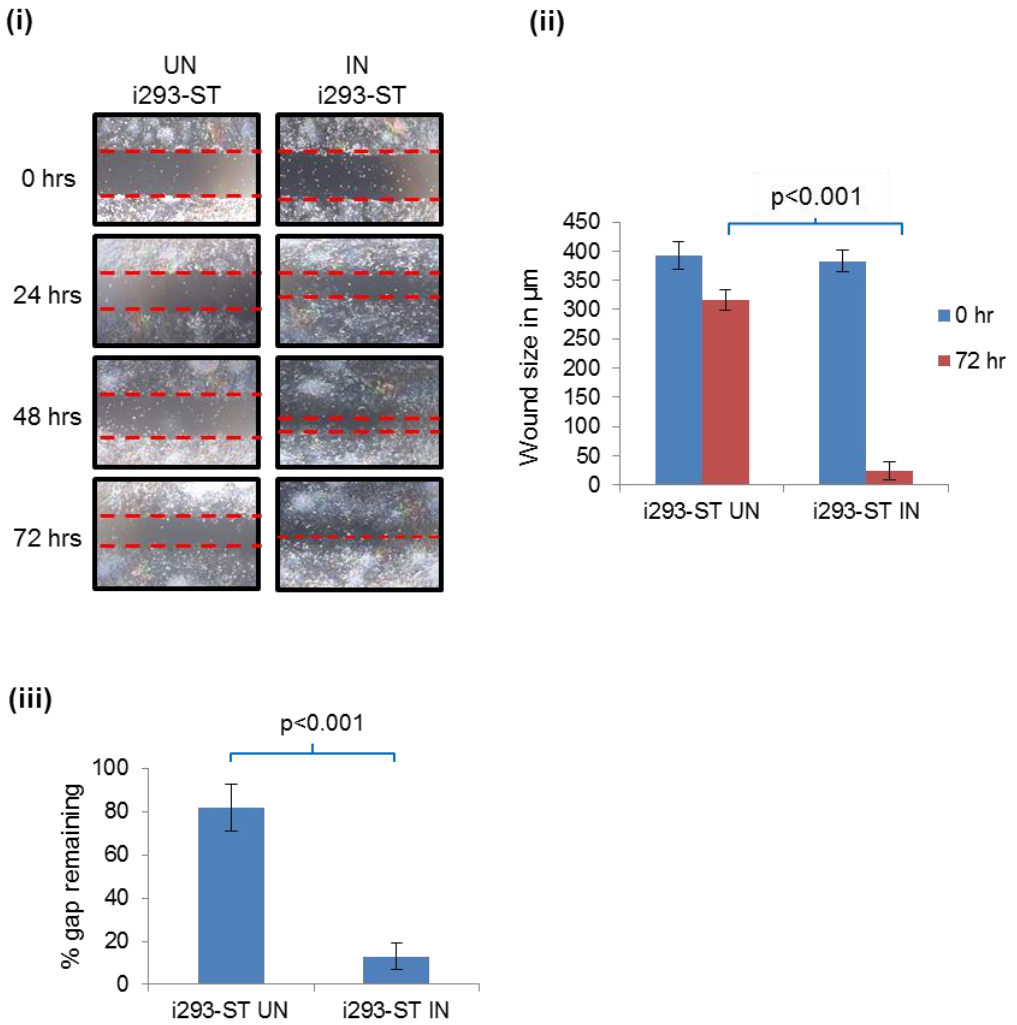

Figure 4.2. Scratch-wound healing analysis indicates that MCPyV ST expression promotes cell motility and migration in i293-ST. Cells were seeded onto poly-L-lysine coated 6 well plates and left uninduced or induced for 24 hours, followed by generation of a scratch-wound across the cell monolayer. Cells were imaged every 24 hours over the course of 3 days, using a Zeiss light microscope at 4x magnification. (ii) The size of the wound was measured at 0 and 72 hours post-scratch. (iii) Image J analysis was conducted to determine the area remaining at 72 hrs post scratch. The area is expressed as a percentage of the original area of the sratch-wound at 0 hrs. All scratch assays were performed in triplicate. Data analysed using three biological replicates per experiment, n=3. Statistical analysis employed was a two-tailed T-test with unequal variance.

To further investigate the role MCPyV ST plays in promoting cell motility and migration, the growth characteristics were analysed using matrigel- and fibronectin-based transwell migration and invasion assays. The invasive human fibrosarcoma cell line, HT-1080, was used a positive control for cell migration and invasion. The effect of MCPyV ST expression was observed in both the i293-ST

inducible cell line and HEK 293 FlpIn™ transfected with either EGFP or EGFP-ST. After 24 hours cells were seeded at the same cell density onto the matrigel or fibronectin coated transwells, along with an uncoated control plate and incubated for 22 hours. Cells were then incubated with a Calcein AM dye and the percentage of cells which moved through the transwell, compared to the uncoated control plate was calculated and is displayed in Figure 4.3.

Figure 4.3 demonstrates that cells expressing MCPyV ST, whether by induction with Dox or transfection show significantly increased migratory and invasive properties, in comparison to uninduced or EGFP expressing cells, respectively.

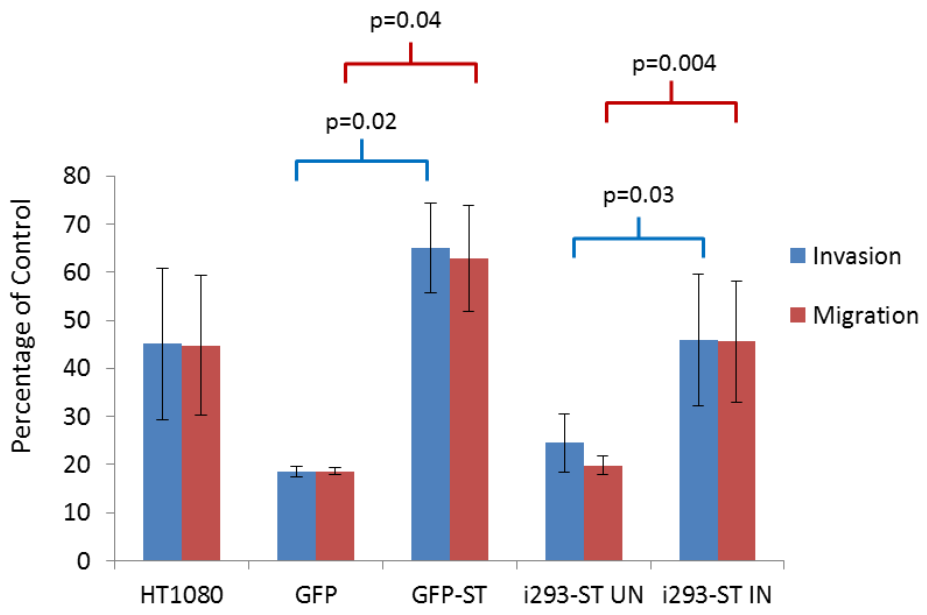

Figure 4.3. MCPyV ST expression promotes cell motility, migration and invasion. i293-ST cells were left uninduced or induced for 24 hours, while HEK 293 FlpIn™ cells were transfected with either EGFP or EGFP-ST. Cells were seeded onto precoated matrigel- or fibronectin-based transwell migration and invasion tissue culture wells. Cells were incubated at 37 ^{o}C for 22 hours and subsequently labelled with Calcein AM fluorescent dye for 90 minutes. The fluorescence was measured between 494-517 nM and the relative percentage of cells moved through the transwell was calculated as a percentage of the uncoated control plate (set at 100%). Data analysed using three biological replicates per experiment, n=3. Statistical analysis employed was a two-tailed T-test with unequal variance.

In addition, to confirm that the observed increase in cell motility, migration and invasion was not a result of increased cell proliferation, the growth characteristics of MCPyV ST expressing cells was analysed. Cell proliferation assays were

performed, comparing the growth of MCPyV ST expressing cells in both i293-ST cells and HEK 293 FlpIn™ cells transfected with either EGFP or EGFP-ST expressing cells. Cells were grown in 10% serum, as per the motility assays, and the proliferative rate assessed over a 3 day period using a dye exclusion protocol using Trypan Blue solution. Figure 4.4 demonstrates that there is no statistically significant difference in the growth rate of cells expressing MCPyV ST, in comparison to the respective negative counterparts. This confirms that MCPyV ST is capable of promoting cells to adopt a more motile, migratory and invasive phenotype without increasing cell proliferation.

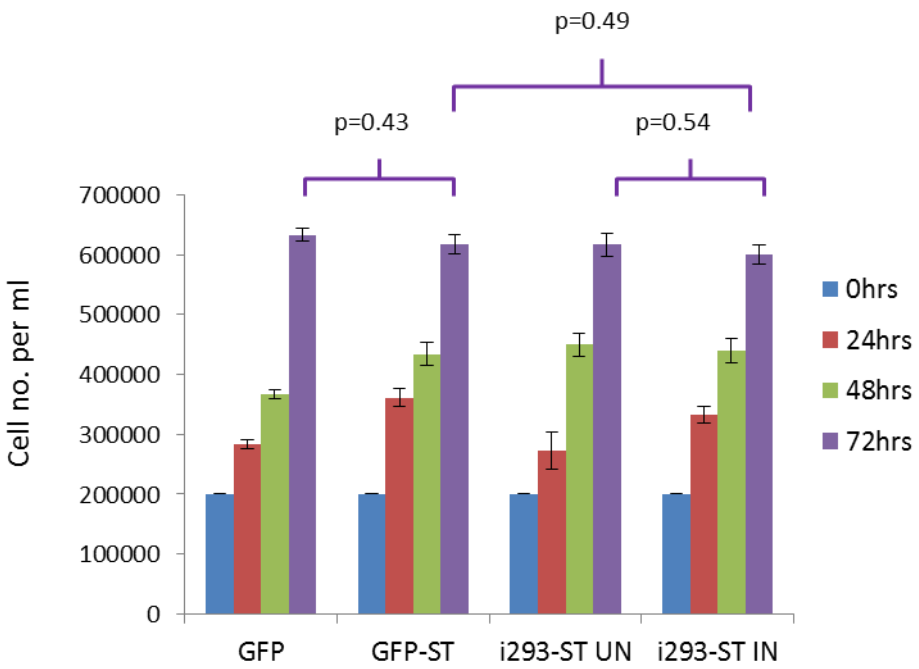

Figure 4.4. MCPyV ST expression does not promote cell proliferation in i293-ST and HEK 293 FlpIn™ cells. i293-ST cells were uninduced or induced for 24 hours, while HEK 293 FlpIn™ cells were transfected with either EGFP or EGFP-ST expression constructs. $2x10^5$ cells were seeded into 6 well plates in DMEM containing 10% FCS (same as all motility experiments) and the cell number counted every 24 hours for a period of 3 days (n=3).

4.3 MCPyV ST promotes cell motility, migration and invasion in MCC13 cells

The i293-ST cell line is a useful and robust tool in order to conduct initial investigations and analysis into the role of MCPyV ST in tumourigenesis and

metastasis. However, in order to demonstrate that MCPyV ST expression promotes cell motility, migration and invasion in a physiologically relevant tumour setting, it was necessary to repeat these experiments using MCC13 and MKL-1 cell lines.

To confirm the accuracy of the previous findings live cell imaging was performed using the MCPyV-negative cell line, MCC13. MCC13 cells were transfected with either EGFP or EGFP-ST expression vectors and imaged every 30 minutes over the course of 24 hours. Figure 4.5 demonstrates that MCC13 cells expressing MCPyV ST show a statistically significant increase in the distance moved by cells. One point to note is that the average distance moved between EGFP and EGFP-ST in MCC13 cells is less than between EGFP and EGFP-ST expressing HEK 293 FlpIn™ cells. This is likely due to the MCC13 cell line being derived from a primary MCC tumour, and as mentioned previously MCC tumours are highly metastatic, suggesting gain of function mutations within MCPyV-negative MCC cells that result in increased cell motility. Despite this it is clear that in a physiologically relevant cell line such as MCC13, MCPyV ST can promote a significant increase in cell motility.

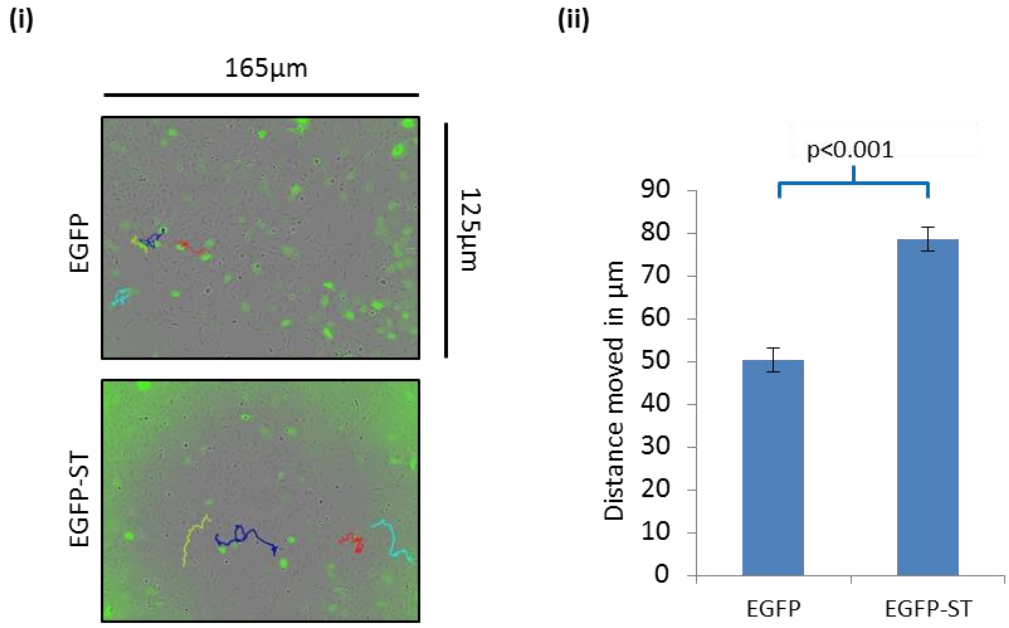

Figure 4.5. MCPyV ST expression promotes cell motility in MCC13 cells. (i) Cells were transfected with either EGFP or EGFP-ST and 12 hours after cell motility was analysed using an Incucyte kinetic live cell imaging system. Images were taken over the course of 24 hours every 30 minutes and cell movement tracked using Image J software. Red, blue, cyan and green line tracks depict the path of cell movement over the time course. (ii) The average distance moved by transfected cells was

measured in µM (n=50). Data analysed using three biological replicates per experiment, n=3. Statistical analysis employed was a two-tailed T-test with unequal variance.

Furthermore, matrigel-based migration assays were repeated using MCC13 cells transfected with either EGFP or EGFP-ST. Following the same procedure as previously described, transfected MCC13 cells were seeded onto the transwells and allowed to migrate over the course of 22 hours. This was followed by cell staining and the number of cells that migrated was calculated as a percentage of the uncoated control plate. Figure 4.6 demonstrates MCPyV-ST expression results in a statistically significant increase in the percentage of cells migrating in comparison to MCC13 cells expressing EGFP. This once again confirms that MCPyV ST expression promotes a more migratory phenotype in both HEK 293 FlpIn™ and MCC13 cells.

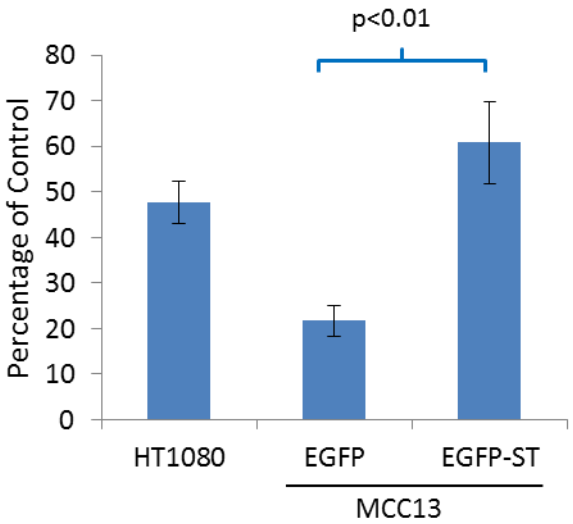

Figure 4.6. MCPyV ST expression promotes cell motility, migration and invasion in MCC13 cells. Cells were transfected with either EGFP or EGFP-ST and seeded onto precoated matrigel- or fibronectin-based transwell migration and invasion tissue culture wells. HT-1080 fibrosarcoma cells were used as a positive control for migration. Cells were incubated at 37 °C for 22 hours and subsequently labelled with Calcein AM fluorescent dye for 90 minutes. The fluorescence was measured between 494-517 nM and the relative percentage of cells moved through the transwell was calculated as a percentage of the uncoated control plate (set at 100%). Data analysed using three biological replicates per experiment, n=3. Statistical analysis employed was a two-tailed T-test with unequal variance.

4.4 Taxane compounds inhibit MCPyV ST-mediated microtubule destabilisation

Microtubule reorganisation plays an important role in cell motility, migration and invasion[324,328]. Therefore, to assess if MCPyV ST-mediated microtubule destabilisation could be inhibited, immunofluorescence was conducted in the presence of Paclitaxel. MCC13 cells were transfected with either EGFP and EGFP-ST, then 4 hours prior to cell fixation cells were incubated with Paclitaxel (Figure 4.7 (ii)). Microtubule structures were then analysed using a β-tubulin-specific antibody. Figure 4.7 shows that MCPyV ST expressing cells exposed to Paclitaxel, show rigid, stable bundles of microtubules, in contrast to MCPyV ST expressing cells without Paclitaxel (Figure 4.7 (i) and Figure 3.9). Paclitaxel treatment has no effect on the stable microtubule structures in EGFP expressing cells, and is consistent with EGFP expressing cells alone (previously shown in Figure 3.9). Another taxane compound termed Docetaxel (a derivative of Pacliatxel) was also used, to similar effect (results not shown). This data highlights that exposure to the chemotherapeutic drug, Paclitaxel, is able to inhibit MCPyV ST-mediated microtubule destabilisation.

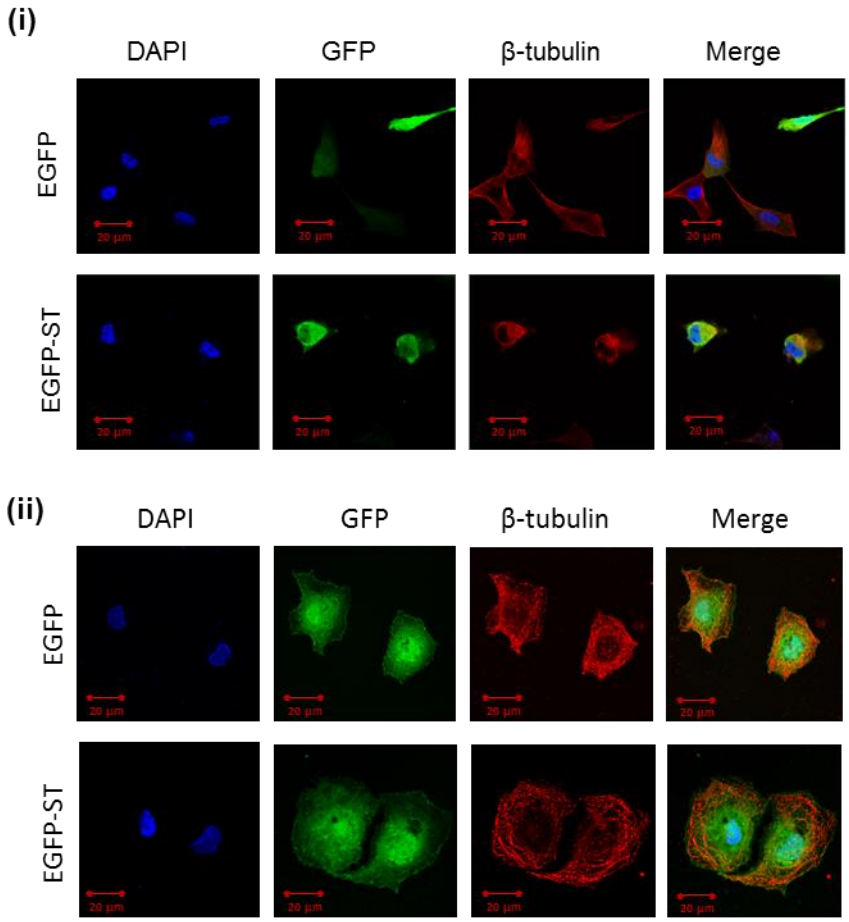

Figure 4.7. Paclitaxel treatment inhibits MCPyV ST-mediated microtubule destabilisation. MCC13 cells were transfected with either EGFP or EGFP-ST. 20 hours after transfection cells were incubated without Paclitaxel (i) or with Paclitaxel (ii) for 4 hours, followed by fixation and permeabilisation. Immunofluorescence was conducted using a β-tubulin-specific antibody. The nucleus was stained with DAPI-containing mounting medium and GFP fluorescence was analysed by direct visualisation. Paclitaxel was used at a concentration of 10 µM.

4.5 Microtubule destabilisation is crucial for MCPyV ST-mediated cell motility and migration

Paclitaxel treatment proved successful in the inhibition of MCPyV ST-mediated microtubule destabilisation, therefore in order to establish if microtubule destabilisation was a prerequisite for MCPyV-ST cell motility, scratch-wound healing assays were performed. i293-ST cells were left uninduced or induced for 24 hours and incubated with or without Paclitaxel for 4 hours prior to scratch-wound generation and the wound imaged every 24 hours for 3 days. In parallel, MCC13 cells were transfected with either EGFP or EGFP-ST and incubated for 4 hours prior

to scratch-wound generation, with or without Paclitaxel. The results in Figure 4.8, clearly demonstrate that cells expressing MCPyV ST in the absence of Paclitaxel show enhance cell motility and migration, which is statistically significant. However, in the presence of Paclitaxel MCPyV ST expressing cells no longer show enhanced motility, instead migrate at a similar rate as uninduced i293-ST or EGFP transfected MCC13 cells. This data confirms that the ability of MCPyV ST to destabilise the microtubule network is crucial for MCPyV ST-mediated cell motility and migration and that this cell motility phenotype can be inhibited by the use of taxane-based drugs.

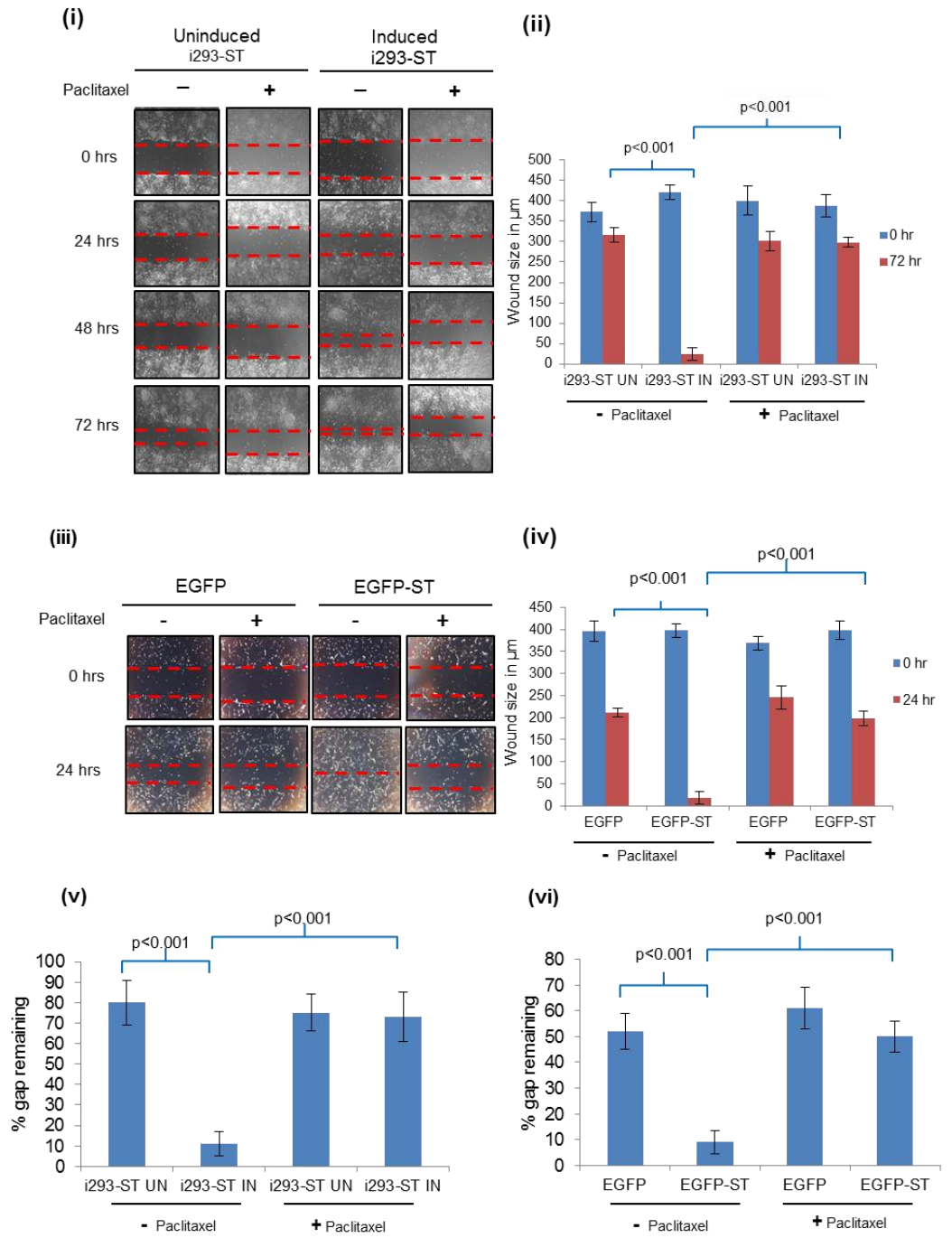

Figure 4.8. Paclitaxel treatment inhibits MCPyV ST-mediated cell motility and migration. (i) i293-ST cells were left uninduced or induced for 24 hours, upon which cells were incubated with or without Paclitaxel for 4 hours. Cells were then subjected to a scratch-wound and analysed every 24 hours over the course of 3 days. (iii) MCC13 cells were transfected with either EGFP or EGFP-ST for 24 hours, followed by incubation with Paclitaxel for 4 hours. The cell monolayer was then subjected to a scratch-wound and analysed over the course of 24 hours. The size of the wound was measured at 0 and 72 hours for i293-ST cells (ii) and 0 and 24 hours for MCC13 cells (iv) post scratch. (v) and (vi) Image J analysis was conducted to determine the area remaining at either 72 hrs or 24 hrs post scratch, repectively. The area is expressed as a percentage of the original area of the sratch-wound at 0 hrs. All scratch assays were performed in triplicate. Data analysed using three biological replicates per experiment, n=3. Statistical analysis employed was a two-tailed T-test with unequal variance.

To verify this data, and to analyse the levels of stathmin, phosphorylated stathmin and acetylated tubulin, western blot analysis was conducted using these samples. Figure 4.9 demonstrates that Paclitaxel treatment did not affect the ability of MCPyV ST to promote upregulation of stathmin or affect the levels of phosphorylated stathmin. However, Paclitaxel treatment did significantly increase the levels of acetylated tubulin in MCPyV ST-expressing cells, a marker of stabilised microtubules.

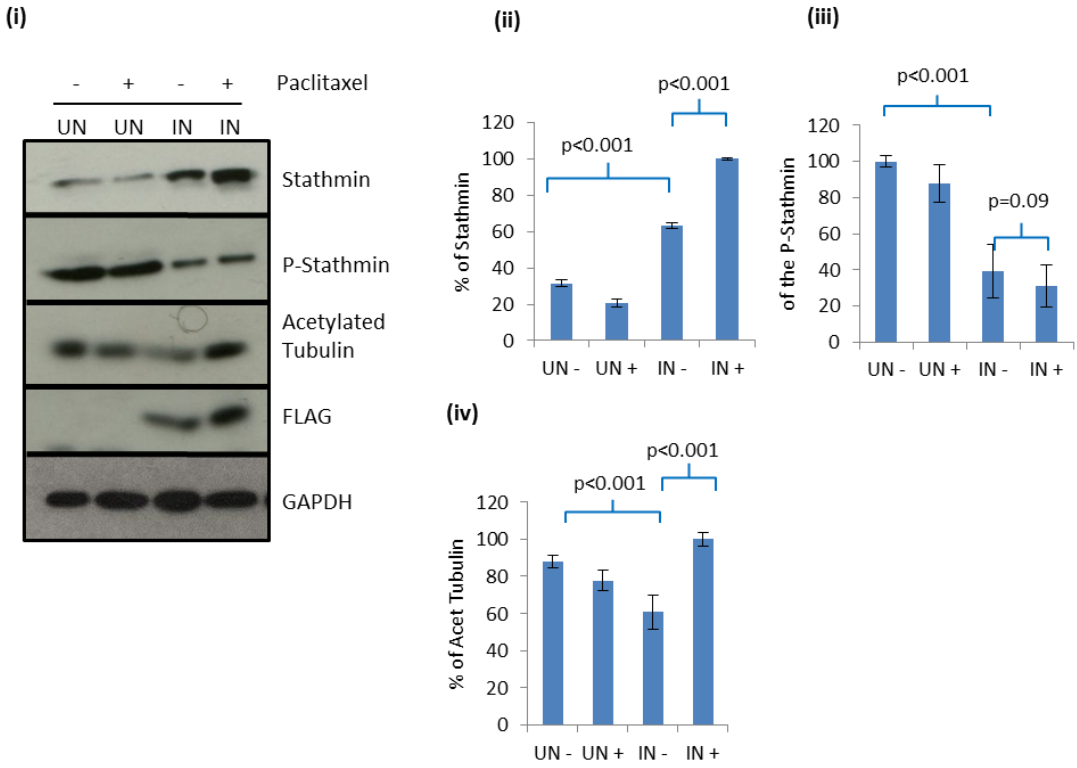

Figure 4.9. Paclitaxel inhibits MCPyV ST ability to promote microtubule destabilisation and stathmin dephosphorylation. (i) i293-ST cells were left uninduced or induced for 24 hours followed by incubation with or without Paclitaxel. Lysates were analysed by immunoblotting using a stathmin-, phosphorylated stathmin-, and acetylated tubulin-specific antibody. GAPDH was used as a measure of equal loading and allowed the relative densitometry of stathmin (ii), phosphorylated stathmin (iii) and acetylated tubulin (iv) to be calculated using Image J software. Data analysed using three biological replicates per experiment, n=3. Statistical analysis employed was a two-tailed T-test with unequal variance. Data analysed using three biological replicates per experiment, n=3. Statistical analysis employed was a two-tailed T-test with unequal variance.

To further confirm MCPyV ST-induced microtubule destabilisation is required for increased cell motility and migration in MCC tumour cells, MCPyV ST was depleted using a lentiviral-based knockdown system. The MCPyV-positive MKL-1 cell line was transduced with either lentivirus-based vectors expressing either shRNAs targeting

either ST alone, both LT and ST (PanT) or a scrambled negative control[247,371]. Figure 4.10 shows that MCPyV ST knockdown leads to a reduction in stathmin levels and increased levels of phosphorylated stathmin and acetylated tubulin. This indicates that upon MCPyV ST knockdown microtubules are stabilised.

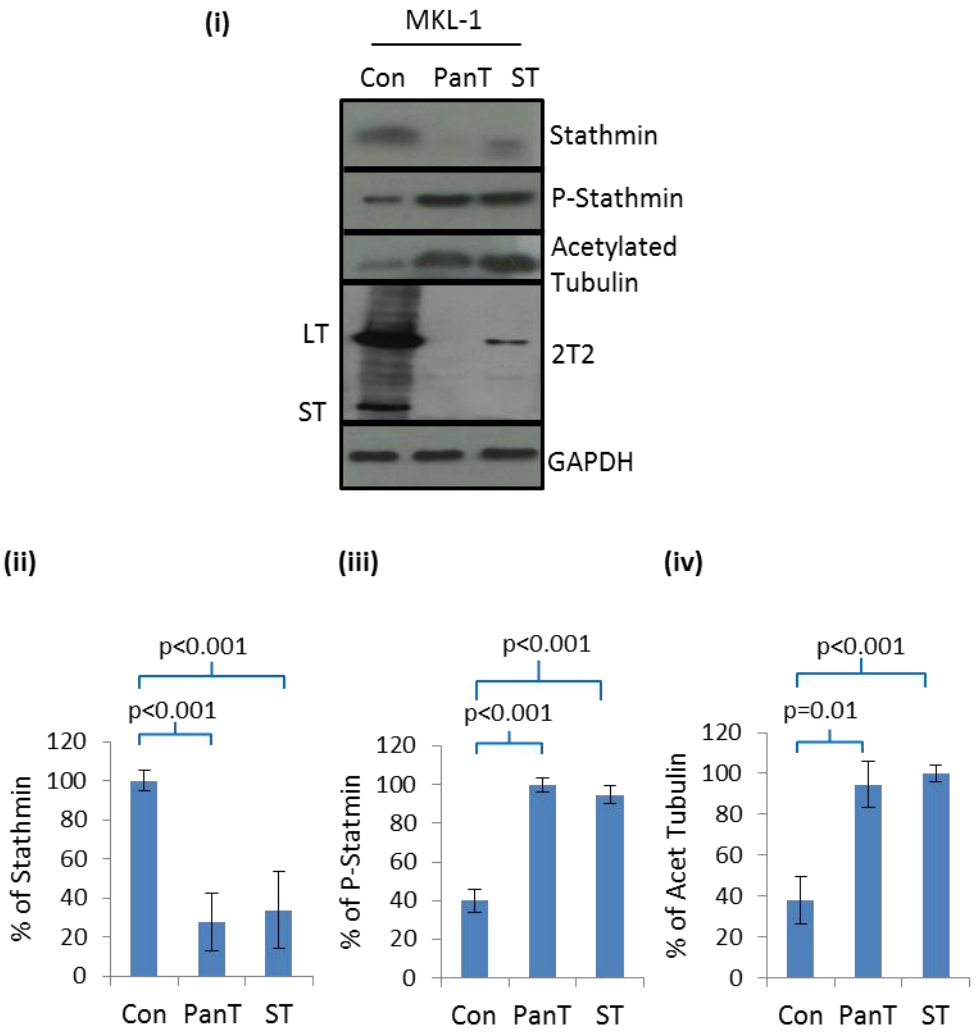

Figure 4.10. MCPyV ST is required for microtubule destabilisation in MKL-1 cells. MKL-1 cells were transduced with lentivirus-based vectors expressing shRNAs targeting ST alone, both LT and ST (Pan T) and a scrambled negative control. Cells lysates were isolated and analysed by western blot using stathmin-, phosphorylated stathmin-, acetylated tubulin- and 2T2-specific antibodies. GAPDH was used as a measure of equal loading and densitometry analysis using Image J software enabled calculation of the percentage of relative densitometry of stathmin (ii), phosphorylated stathmin (iii) and acetylated tubulin (iv), all normalised to the loading control. Data analysed using three biological replicates per experiment, n=3. Statistical analysis employed was a two-tailed T-test with unequal variance.

Furthermore, the effect of MKL-1 lentiviral knockdown of ST and PanT was assessed in matrigel-based transwell assays, specific for non-adherent cells as demonstrated in Figure 4.11. The results show that MCPyV ST depletion results in a statistically

significant decrease in cell migration, with cells migrating at a much reduced rate in comparison to scrambled-control cells. This once again confirms that MCPyV ST expression is crucial for microtubule destabilisation, which in turn promotes are more motile and migratory phenotype.

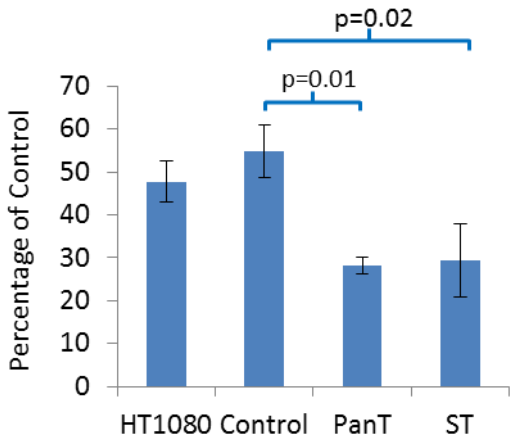

Figure 4.11. MCPyV ST is required cell motility and migration in MKL-1 cells. MKL-1 cells were transduced with lentivirus-based vectors expressing shRNAs targeting ST alone, both LT and ST (Pan T) and a scrambled negative control. HT-1080 fibrosarcoma cells were used as a positive control for migration. Cells were seeded onto transwells and incubated for 22 hours, followed by labelling with Calcein AM fluorescent dye for a further 90 minutes. Fluorescence was measured between 494-517 nM and the relative percentage of cells moved through the transwell was calculated as a percentage of the uncoated control plate (set at 100%). Data analysed using three biological replicates per experiment, n=3. Statistical analysis employed was a two-tailed T-test with unequal variance.

4.6 Stathmin depletion inhibits MCPyV ST-mediated cell motility, migration and invasion

Paclitaxel is widely used in chemotherapy regimes and can inhibit MCPyV ST-mediated microtubule destabilisation and motility as discussed previously. However, a caveat in using Paclitaxel for scratch motility assays is that taxane-based compounds may affect cell division and therefore could prevent the growth of cells into the scratch-wound. To overcome this issue and to more closely study the role of stathmin within this phenotype, scratch-wound assays were performed using i293-ST depleted of stathmin. i293-ST cells were left uninduced or induced for 24 hours and then transfected with either a scrambled control or stathmin-specific siRNA. Upon transfection a scratch-wound was generated, 24 hours after the initial transfection cells were transfected again for a further 6 hours. Cells were imaged

every 24 hours for the course of 3 days. Western blots analysis of the same samples confirmed that stathmin was successfully depleted in cells with a significant decrease in stathmin levels at 72 hours post transfection, as seen in Figure 4.12 (i) and (ii). Similar rates of cell motility were observed in i293-ST induced cells transfected with a scrambled-control compared to i293-ST induced cells, as seen in Figure 4.12 (iii) and (iv). This clearly demonstrates that the scrambled control as no effect on cell motility and upregulation of stathmin upon MCPyV ST expression (Figure 4.12 (i)). However, cells induced for MCPyV ST expression and depleted of stathmin, show a statistically significant decrease in cell motility and migration in scratch-wound analysis (Figure 4.12 (iii) and (iv)). Importantly, these results indicate for the first time that the microtubule-associated protein, stathmin, is required for MCPyV ST-mediated cell motility.

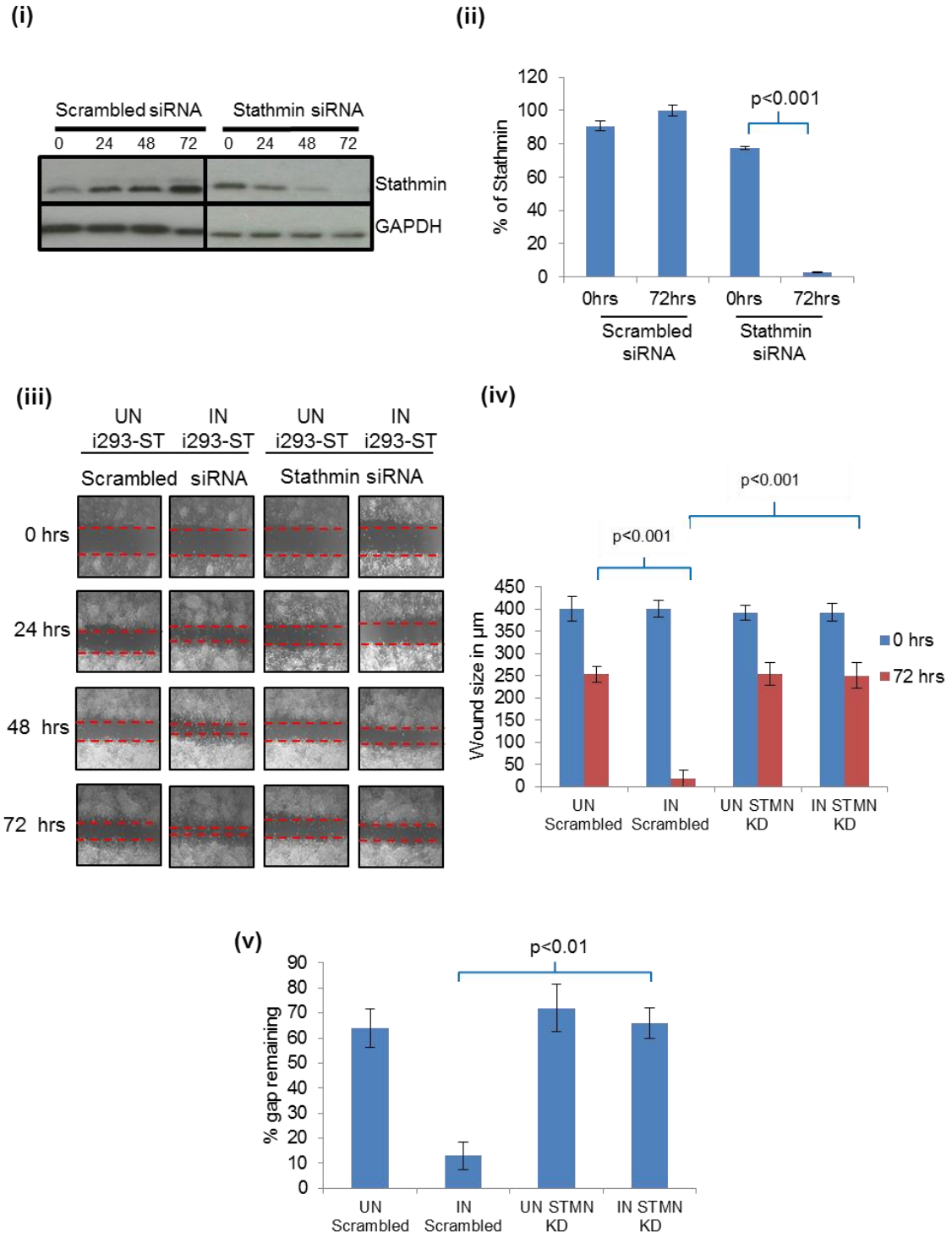

Figure 4.12. Stathmin is required for MCPyV ST-mediated cell motility and migration. (i) i293-ST cells were transfected with either stathmin-specific siRNA or a scrambled control siRNA, and after 24 hours left uninduced or induced. Cell lysates were isolated at 0, 24, 48 and 72 hours and analysed by western blot using stathmin- and GAPDH-specific antibodies. (ii) GAPDH was used as a measure of equal loading and densitometry analysis using Image J software enabled calculation of the percentage of relative densitometry of stathmin, normalised to the loading control. (iii) i293-ST cells were seeded onto poly-L-lysine coated 6 wells and transfected with either stathmin-specific siRNA or a scrambled control siRNA and left uninduced or induced. 24 hours later cells were subjected to a scratch-wound and analysed every 24 hours for 3 days. (iv) The size of the wound was measured at

0 and 72 hours. All scratch assays were performed in triplicate, n=3. (v) Scratch wound analysis using Image j software to calculate the area of the gap remaining at 72 hrs. All numbers expressed as a percentage of the area remaining. Statistical analysis employed was a two-tailed T-test with unequal variance.

Furthermore, subsequent analysis of stathmin depletion in the context of matrigel-based migration assays was conducted, in order to determine the potential of stathmin upregulation on MCPyV ST-enhanced cell motility and migration. MKL-1 cells were transfected with either a scrambled-control or stathmin-specific siRNA on two consecutive days and seeded onto matrigel-coated transwells or uncoated control wells. Figure 4.13 clearly demonstrates that stathmin depletion in cells positive for MCPyV show a statistically significant decrease in motility and migration through the transwells. This confirms that stathmin is a crucial component for MCPyV ST-mediated cell motility and migration.

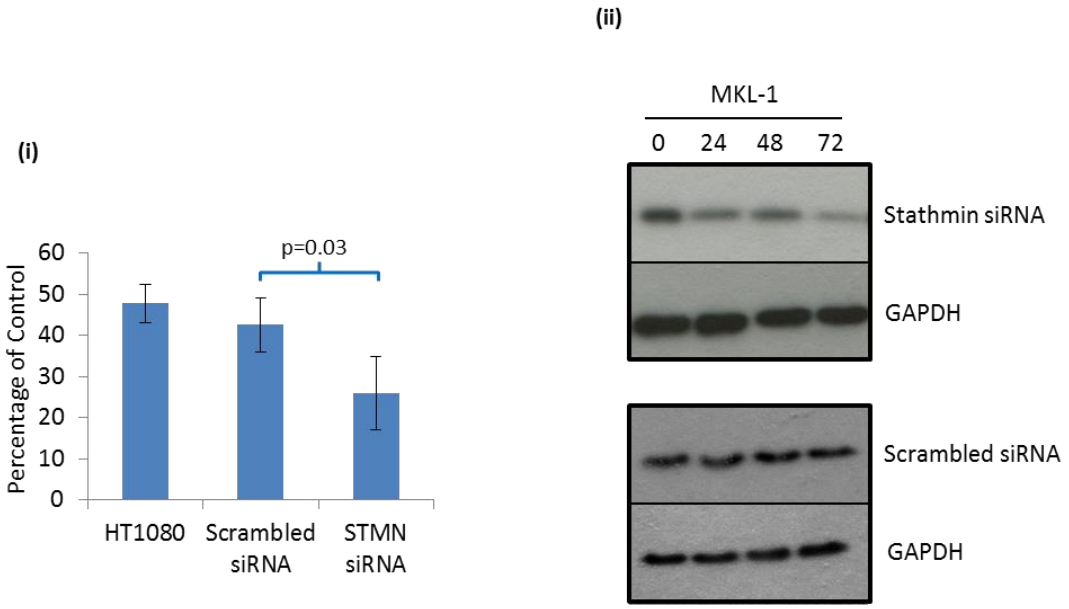

Figure 4.13. Stathmin is required for MCPyV ST-mediated cell migration in transwell assays. MKL-1 cells were transfected with either stathmin-specific siRNA or a scrambled control siRNA. (i) 24 hours later cells were seeded onto precoated matrigel-based transwell migration culture tissue wells. Cells were incubated for 22 hours and then labelled for 90 minutes with Calcein AM fluorescent dye. The fluorescence was measured between 494-517 nM and the relative percentage of cells moved through the transwell was calculated as a percentage of the uncoated control plate (set at 100%). (ii) MKL-1 cells transfection with stathmin-specific or scrambled siRNA and the cellular lysates isolated at 0, 24, 48 and 72 hours after transfection. Lysates were analysed by immunoblotting using a stathmin- and GAPDH specific antibodies. Data analysed using three biological replicates per experiment, n=3. Statistical analysis employed was a two-tailed T-test with unequal variance.

4.7 Discussion

There is a strong association between stathmin overexpression and enhanced metastasis in numerous cancer types[340,354], hence the role of MCPyV ST in promoting cell motility was investigated. Data herein, demonstrates that MCPyV ST expression promotes cell motility, migration and invasion and this was confirmed using a range of cell lines, such as i293-ST cells and MCC13 and MKL-1 MCC cell lines. For accuracy, a range of motility assays and techniques were employed, from live cell imaging and tracking to 2D scratch-wound healing assays and 3D migration and invasion transwell assays. All motility assays used demonstrated that MCPyV ST expression promoted a statistically significant increase in cell motility. This suggests a possible role of the MCPyV ST oncoprotein in facilitating MCC metastasis and provides evidence for further investigation into the underlying mechanisms. Indeed, other tumour-associated viruses have been shown to promote metastasis, such as HPV 16, EBV, HBV and SV40[299,378,379].

Therefore, in order to establish the requirement of MCPyV ST in promotion of microtubule destabilisation and cell motility a group of chemotherapeutic drugs were employed, known as taxanes. Taxanes such as Paclitaxel and Docetaxel bind directly to the microtubule structures and prevent tubulin heterodimer dissociation from the filament, hence stabilising the micortubules[380]. Treatment of cells with Paclitaxel was able to inhibit MCPyV ST-mediated microtubule destabilisation and cell motility. This is significant as it demonstrates that MCPyV ST is required for microtubule destabilisation and that microtubule destabilisation is fundamental in facilitating enhanced cell motility and migration.

Furthermore, lentiviral-based siRNA knockdown of MCPyV ST demonstrated that MCPyV ST is absolutely required for microtubule destabilisation, as depletion resulted in restoration of wild type levels of acetylated tubulin and phosphorylated stathmin. Moreover, stathmin depletion in MKL-1 cells, significantly reduced the potential of cells to migrate in transwell assays. Once again clearly demonstrating

the fundamental role MCPyV ST plays in promoting microtubule destabilisation and in turn cell motility, migration and invasion.

Quantitative proteomic analysis suggested that MCPyV ST affects the expression of multiple proteins involved in microtubule organisation and dynamics. Interestingly, microtubule dynamics has now been shown to play a role in cell shape and polarised cell motility[324,328]. Chapter 3 highlighted that MCPyV ST expression promotes the upregulation of stathmin and also facilitates a decrease in the pool of unphosphorylated stathmin. Unphosphorylated stathmin promotes the microtubule destabilising activity of this protein and subsequent analysis confirmed that MCPyV ST expression resulted in destabilisation of the microtubule network. This data strongly implicated stathmin in MCPyV ST induced microtubule destabilisation.

In an effort to circumvent the caveats associated with Paclitaxel treatment and subsequently analyse the role of stathmin in the context of MCPyV ST-induced cell motility, stathmin depletion studies were conducted. Findings herein, demonstrates that siRNA depletion of stathmin in scratch-wound healing and matrigel based assays and demonstrated that stathmin expression is required for the ability of MCPyV ST to promote cell motility and migration. This data is supported by RNA interference studies that demonstrate that stathmin levels can drastically reduce the motility of tumour cells[355-358]. Moreover, this is the first time that stathmin has been shown to be required for viral-enhanced cell motility and demonstrates the novel mechanisms by which tumour virus can manipulate the host cell.

Chapter 5

Cellular phosphatases are required for MCPyV ST-enhanced cell motility and migration

5. Cellular phosphatases are required for MCPyV ST-enhanced cell motility and migration

5.1 Introduction

Microtubule dynamics is an important aspect of cell motility and polarisation, and is a process that is heavily regulated by the action of microtubule-associated proteins (MAPs)[324,329]. A master regulator of microtubule destabilisation is the MAP protein, stathmin. Stathmin regulates microtubule destabilisation through two mechanisms, termed indirect and direct. Stathmin possess two binding sites of equal size and affinity for tubulin heterodimers, and forms the T_2S complex, thus sequestering tubulin heterodimers and reducing the substrate for growing MT structures[346]. Stathmin can also act in a direct manner, through binding protofilament structures present at the growing MT tips, thereby inhibiting the interactions required to maintain its structure and function[346].

Importantly, stathmin overexpression is a feature of multiple cancer types and has been shown to correlate with tumour growth, poor patient prognosis and a high metastatic potential[340,354]. Furthermore, RNA interference studies have demonstrated that reducing stathmin levels can drastically reduce the motility of various tumours[355-358]. Stathmin is regulated by phosphorylation, whereby phosphorylation at one or more serine residues (Ser16, Ser25, Ser38, and Ser63) weakens stathmin's tubulin binding ability and leads to an increase in free tubulin within the cells, required for MT growth[346]. Conversely, dephosphorylation by cellular phosphatases, promotes stathmin MT destabilising ability and can contribute to transformation[346,359]. As such it has been suggested that the phosphorylation status of stathmin can directly impact on cell motility, migration and invasion.

Similar to SV40, MCPyV ST has been shown to interact with multiple cellular phosphatases, including PP2A Aα, PP2A Aβ and PP4C[226,247]. Therefore in order to

assess the role of these cellular phosphatases in MCPyV ST-mediated microtubule destabilisation and stathmin phosphorylation status, experiments were performed using cellular phosphatase transdominant mutants and MCPyV ST mutants, incapable of interacting with specific cellular phosphatases. This chapter assesses the role of MCPyV ST binding to specific cellular phosphatases, particularly PP4C, in relation to microtubule destabilisation. Further studies were also conducted to address the mechanism by which MCPyV ST promotes the upregulation of stathmin, either by transcriptional or translation enhancement or by increasing stathmin protein stability. Moreover the interactions of MCPyV ST, stathmin and PP4C were addressed in order to establish a novel mechanism of action of MCPyV ST-induced cell motility.

5.2 ST binding mutants identify specific cellular phosphatases required for MCPyV ST-mediated microtubule destabilisation

The function of stathmin is regulated by phosphorylation which in turn regulates microtubule stability[346,381]. Previous findings demonstrate that MCPyV ST expression increases the levels of unphosphorylated stathmin, which increases microtubule destabilisation. Findings from the Whitehouse laboratory and other research groups have shown that MCPyV ST interacts with multiple cellular phosphatase subunits including PP2A Aα, PP2A Aβ and PP4C[226,247].

To determine if these cellular phosphatases were important in MCPyV ST-mediated microtubule destabilisation, two previously generated MCPyV ST mutants were employed. The R7A mutant fails to interact with PP2A Aα, while the Δ95-111 fails to interact with both PP4C and PP2A Aβ. Significantly, it has previously been shown that both mutants retain the inherent functions associated with MCPyV ST, as both stimulate the expression of the MCPyV early promoter, to similar levels as those seen with wild-type MCPyV ST[226]. Initially, MCC13 cells were transfected with either EGFP, EGFP-ST, EGFP-R7A or EGFP-Δ95-111, followed by fixation and permeabilisation. Cells were then incubated with a β-tubulin-specific antibody to analyse the microtubule structure (Figure 5.1). The R7A binding mutant, which fails

to interact with PP2A Aα, retains the ability to promote microtubule destabilisation, similar to EGFP-ST, suggesting that the MCPyV ST-PP2A Aα is not required for microtubule destabilisation. However, the Δ95-111 mutant shows a stable microtubule network, similar to EGFP. Indicating that abolishing MCPyV ST interaction with PP4C and or PP2A Aβ prevents MCPyV ST-mediated microtubule destabilisation.

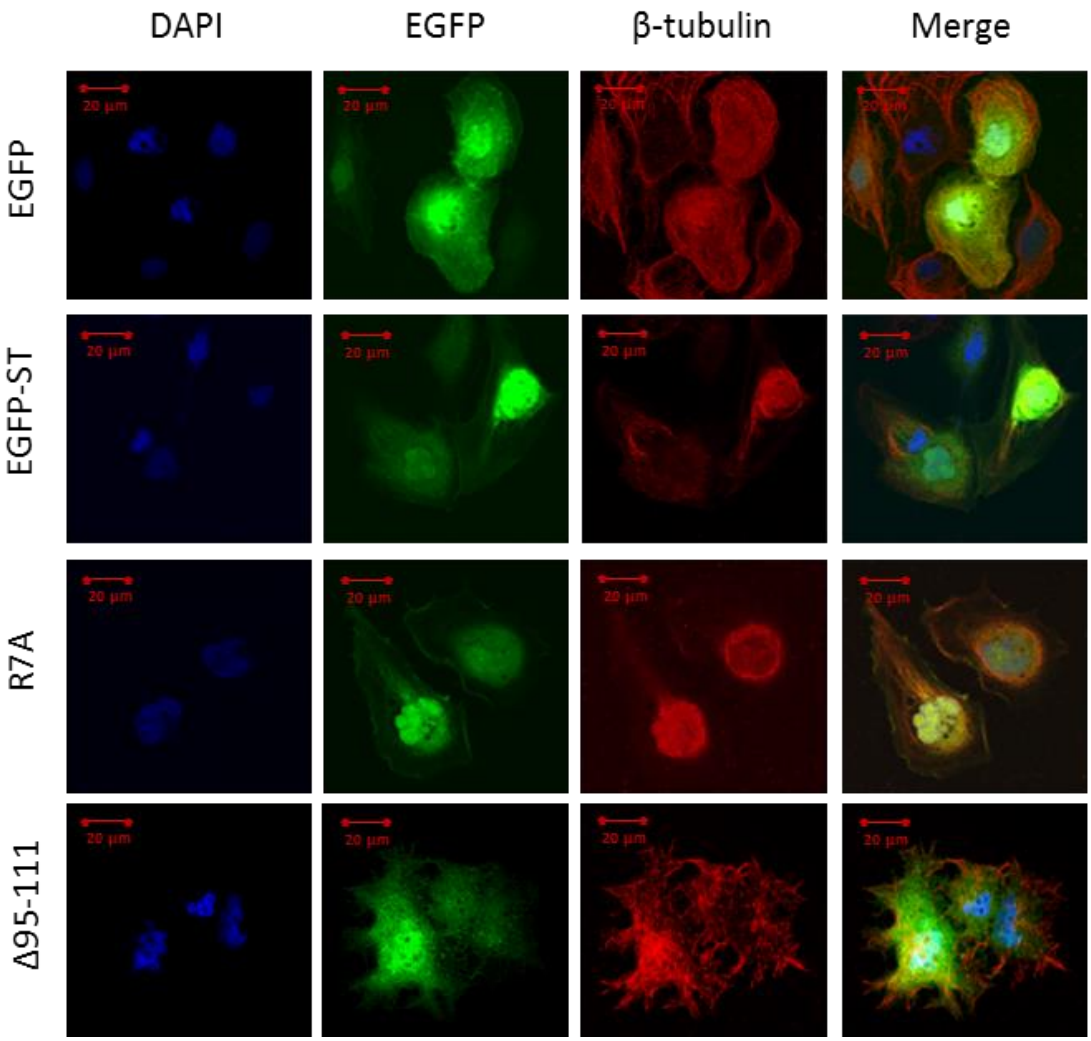

Figure 5.1. Cellular phosphatases are required for MCPyV ST-mediated microtubule destabilisation in MCC13 cells. Cells were transfected with either EGFP, EGFP-ST, EGFP-R7A or EGFP-Δ95-111 mammalian expression constructs. 24 hours after transfection cells were fixed and permeablised, followed by analysis using an endogenous β-tubulin-specific antibody to visualise the microtubule network. GFP fluorescence was visualised by direct visualisation and the nucleus was stained with DAPI-containing mounting medium.

To verify these results, western blot analysis was conducted using MCC13 cell lysates transfected with EGFP, EGFP-ST, EGFP-R7A and EGFP-Δ95-11 and the levels

of phosphorylated stathmin, stathmin and acetylated tubulin analysed. Figure 5.2 demonstrates that EGFP-R7A and EGFP-ST show statistically similar increases in stathmin and a decrease in acetylated tubulin and phosphorylated stathmin, indicative of microtubule destabilisation. However, EGFP-Δ95-111 demonstrates a phenotype similar to EGFP, whereby an increase in acetylated tubulin and phosphorylated stathmin levels is observed. Importantly, this suggests that the association of MCPyV ST with PP2A Aα is not required for microtubule destabilisation. Conversely, these results indicate a possible mechanism by which MCPyV ST may act through binding to either PP4C and/or PP2A Aβ which facilitates MCPyV ST-mediated microtubule destabilisation.

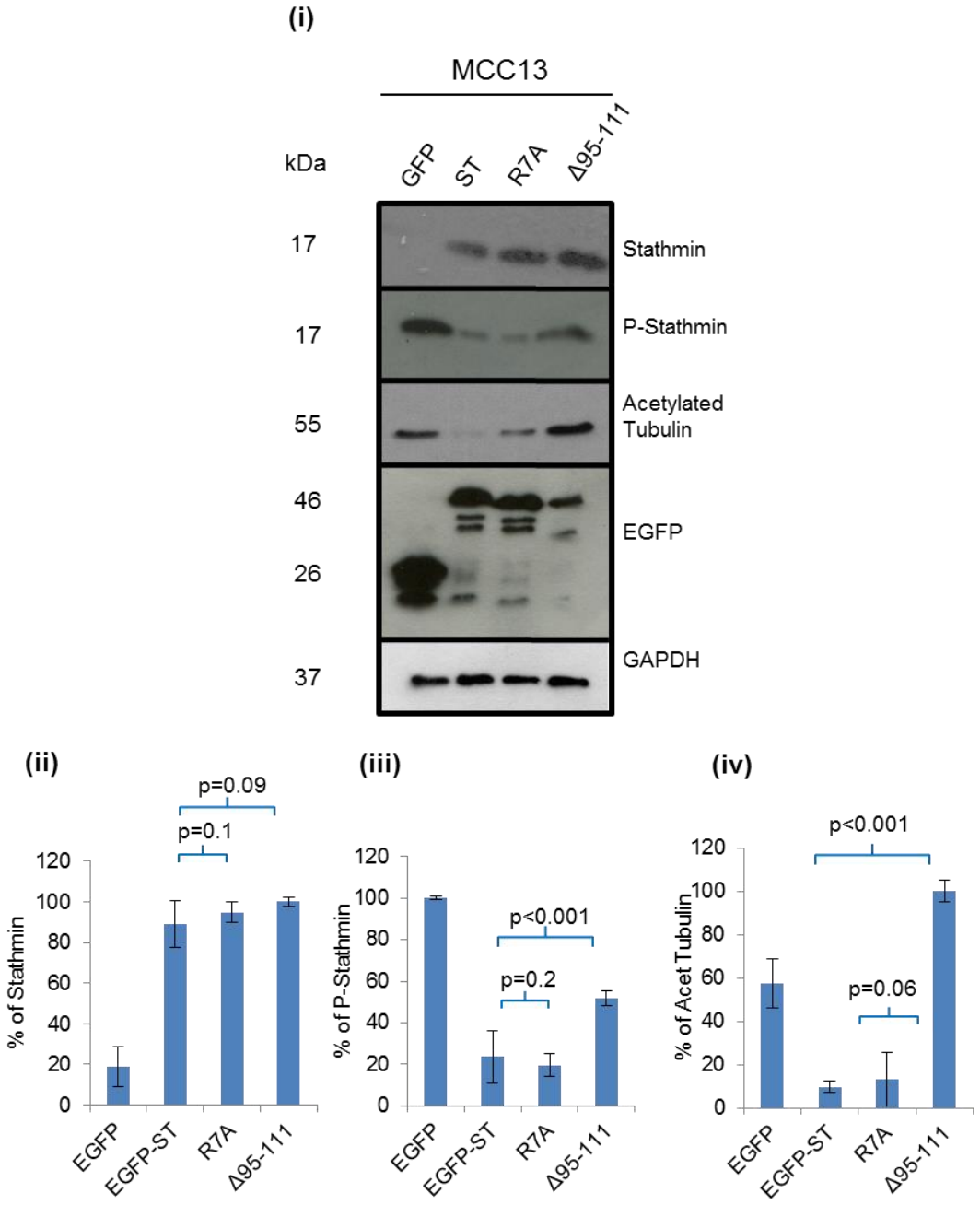

Figure 5.2. Cellular phosphatases are required for MCPyV ST-mediated microtubule destabilisation and affect microtubule stability. Cells were transfected with either EGFP, EGFP-ST, EGFP-R7A or EGFP-Δ95-111 mammalian expression constructs. (i) 24 hours after transfection cell lysates were harvested and analysed by immunoblotting using stathmin-, phosphorylated stathmin-, acetylated tubulin-, EGFP- and GAPDH-specific antibodies. GAPDH was used as a measure of equal loading and densitometry analysis using Image J software enabled calculation of the percentage of relative densitometry of stathmin (ii), phosphorylated stathmin (iii) and acetylated tubulin (iv), all normalised to the loading control. Data analysed using three biological replicates per experiment, n=3. Statistical analysis employed was a two-tailed T-test with unequal variance.

5.3 ST binding mutants identify specific cellular phosphatases required for MCPyV ST-enhanced cell motility

From previous results the binding of MCPyV ST to the cellular phosphatases PP4C and/or PP2A Aβ is required for microtubule destabilisation. As such scratch-wound healing assays were performed to determine if these cellular phosphatases are required for MCPyV ST-enhanced cell motility. Wound healing analysis was conducted in HEK 293 FlpIn™ cells, transfected with either EGFP, EGFP-ST, EGFP-R7A or EGFP-Δ95-111. After transfection a scratch wound was generated and cells imaged every 24 hours for 3 days. The results in Figure 5.3 clearly demonstrate that cells expressing R7A migrate at a similar rate as EGFP-ST expressing cells. However, EGFP-Δ95-111 expressing cells show a statistically significant reduction in cellular growth back into the wound (similar to EGFP).

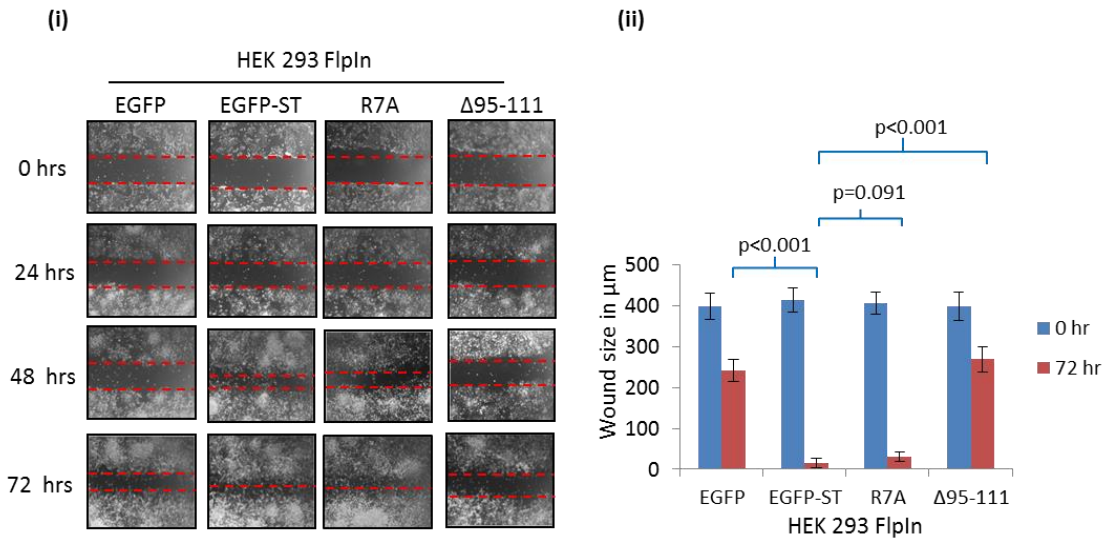

Figure 5.3. Cellular phosphatases are required for MCPyV ST-mediated cell motility in HEK 293 FlpIn™ cells. Cells were seeded onto poly-L-lysine coated 6 well plates and transfected with either EGFP, EGFP-ST, EGFP-R7A or EGFP-Δ95-111 mammalian expression constructs. (i) 24 hours after transfection a scratch wound was generated and cells imaged every 24 hours over the course of 3 days, using a Zeiss light microscope at 4x magnification. (ii) The size of the wound was measured at 0 and 72 hours post-scratch. All scratch assays were performed in triplicate. Data analysed using three biological replicates per experiment, n=3. Statistical analysis employed was a two-tailed T-test with unequal variance.

To verify this result, scratch wound analysis was performed using MCC13 cells transfected with either EGFP, EGFP-ST, EGFP-R7A or EGFP-Δ95-111. Cellular

growth back into the wound was analysed over the course of 24 hours. Figure 5.4 shows similar results as observed in the HEK 293 FlpIn™ cell line analysis, whereby EGFP-Δ95-111 expression does not enhance cellular growth back into the wound. This data indicates that PP4C and/or PP2A Aβ are required for MCPyV ST-induced cell motility and migration, possibly through dephosphorylation of stathmin.

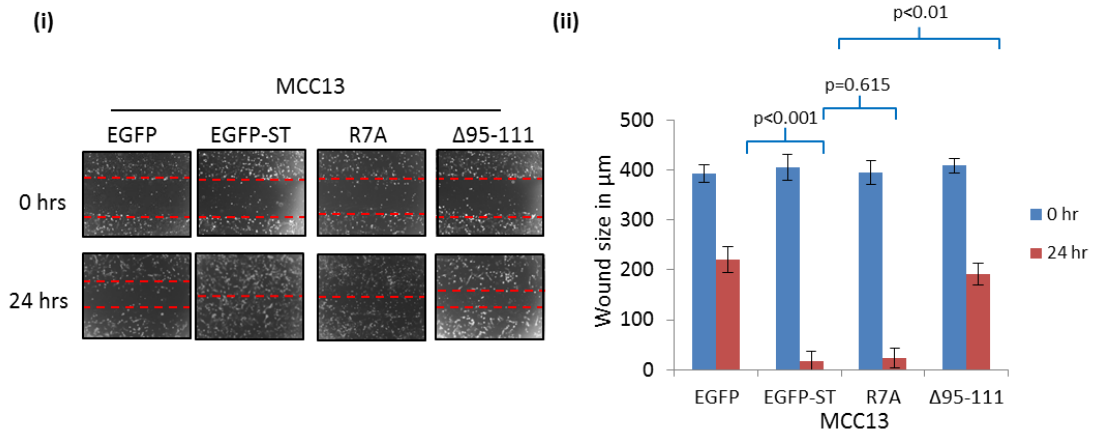

Figure 5.4. Cellular phosphatases are required for MCPyV ST-mediated cell motility in MCC13 cells. Cells were seeded onto poly-L-lysine coated 6 well plates and transfected with either EGFP, EGFP-ST, EGFP-R7A or EGFP-Δ95-111 mammalian expression constructs. (i) 24 hours after transfection a scratch wound was generated and cells imaged every 24 hours over the course of 3 days, using a Zeiss light microscope at 4x magnification. (ii) The size of the wound was measured at 0 and 72 hours post-scratch. Data analysed using three biological replicates per experiment, n=3. Statistical analysis employed was a two-tailed T-test with unequal variance.

In addition, these results were confirmed by live cell tracking of MCC13 cells transfected with either EGFP, EGFP-ST, EGFP-R7A or EGFP-Δ95-111. Cells were imaged over the course of 24 hours every 30 minutes and the path of movement by each cell marked in blue, cyan, green and red. Figure 5.5 demonstrates that MCC13 cells transfected with Δ95-111 show a statistically significant decrease in cell motility in comparison to EGFP-ST or EGFP-R7A expression cells. Taken together, this data indicates that PP4C and/or PP2A Aβ are required for MCPyV ST-induced cell motility and migration, possible through dephosphorylation of stathmin which would promote microtubule destabilisation.

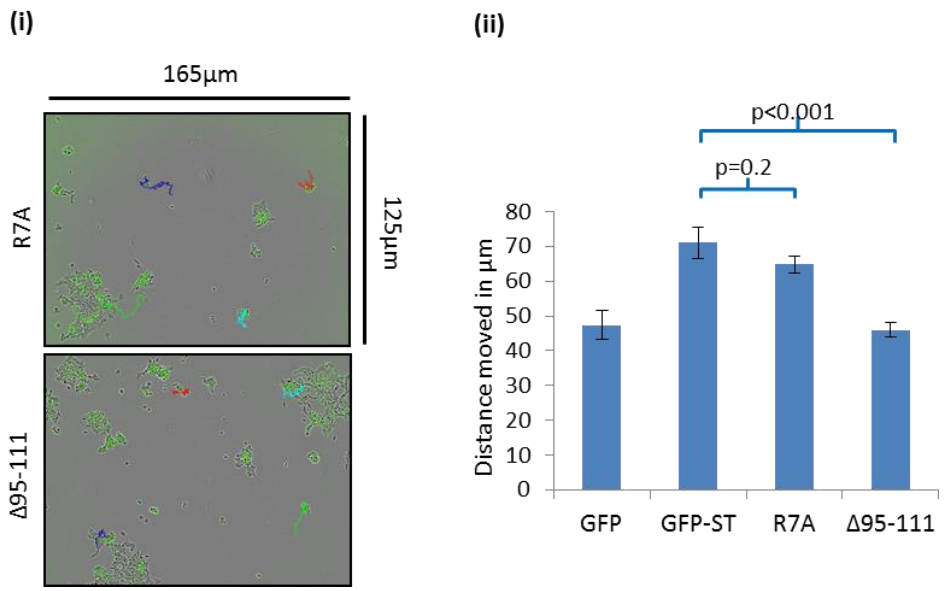

Figure 5.5. Live cell tracking shows that cellular phosphatases are required for MCPyV ST-mediated cell motility in MCC13 cells. Cells were transiently transfected with either EGFP, EGFP-ST, EGFP-R7A or EGFP-Δ95-111. (i) 12 hours after transfection cell motility was analysed using an IncuCyte kinetic live cell imaging system. Images were taken over the course of 24 hours every 30 minutes and cell movement tracked using Image J software. Red, blue, cyan and green line tracks depict the path of cell movement over the time course. (ii) The average distance moved by transfected cells was measured in µM (n=50). Data analysed using three biological replicates per experiment, n=3. Statistical analysis employed was a two-tailed T-test with unequal variance.

5.4 PP4C is important for microtubule organisation and dynamics

It is clear that the ability of MCPyV ST to bind specific cellular phosphatases is important for microtubule dynamics and stability, therefore to further define the role of these phosphatases in MCPyV ST-mediated cell motility, transdominant mutants of PP2A and PP4 were employed. The PP4-RL is a phosphatase dead mutant of PP4, whereby arginine 236 has been replaced with a leucine[169]. The PP2AcH118N, is a catalytically inactive dominant negative mutant of the PP2A catalytic subunit, with a mutation within the active site incorporating a His[118] residue[382].

Immunofluorescence analysis was performed using MCC13 cells co-transfected with either EGFP or EGFP-ST and in the presence of either the wild-type or the transdomiant PP2A. Cells were stained with a β-tubulin-specific antibody and the microtubule network analysed. Figure 5.6 demonstrates that transfection with

wild-type PP2A has little effect on the microtubule structures in either EGFP or EGFP-ST expressing cells, with MCPyV ST showing distinct microtubule destabilisation. However, co-expression of the control EGFP with the catalytically inactive PPAcH118N mutant, results in distinct destabilisation of the microtubule structures. This suggests that PP2A transdomiant overexpression is important for microtubule dynamics and that its inhibition can result in microtubule destabilisation. As previously dicussed MCPyV ST binds PP2A, thus expression of an inactive PP2A isoform may prevent MCPyV ST interacting with or facilitating the dephosphorylation of downstream substrates, thereby resulting in subsequent MT destablilation. As such, no further conclusions regarding the role of PP2A in MCPyV ST-mediated microtubule destabilisation could be drawn.

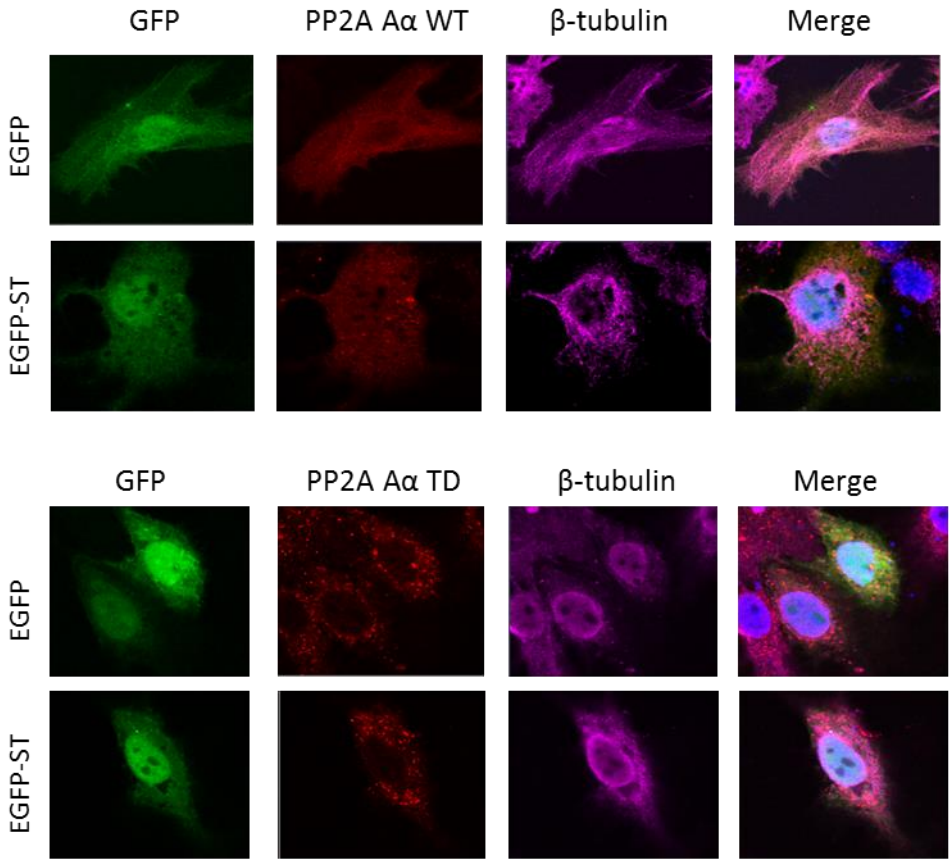

Figure 5.6. PP2A Aα is important for microtubule stability in control cells. MCC13 cells were transfected with either EGFP or EGFP-ST in the presence of either wild type or inactive PP2A. Cells were fixed, permeablised and analysed by immunofluorescence using a β-tubulin-specific antibody. GFP fluorescence was analysed by direct visualisation and the nucleus identified using DAPI-containing mounting medium. WT (wild type), TD (transdomiant). To detect the expression of both PP2A Aα WT and PP2A Aα TD, a glu-glu-specific and a HA-specific antibody were used for analysis, respectively.

Therefore, in order to further investigate the role of the MCPyV ST-PP4C interaction, these experiments were repeated using MCC13 cells transfected with either EGFP or EGFP-ST in the presence of either wild-type or transdomiant PP4. Figure 5.7 demonstrates that co-expression of wild-type PP4 with EGFP results in stable microtubule structures, however co-expression with MCPyV ST once again demonstrates microtubule destabilisation. Furthermore, co-expression of a transdomiant PP4 with EGFP results in stable microtubules structures, in comparison to transfection with a transdominant PP2A. This demonstrates that PP4 is not crucial for microtubule dynamics in healthy cells. Importantly though, co-expression of EGFP-ST and the catalytically transdominant PP4-RL mutant does not result in microtubule destabilisation, indicative of MCPyV ST expression alone. This is a crucial point and indicates that PP4C is pivotal for MCPyV ST-mediated microtubule destabilisation and that subsequent inhibition of PP4C can inhibit this MCPyV ST-induced phenotype. Importantly, this demonstrates a novel molecular mechanism by which the MCPyV ST-PP4C interaction, perhaps by facilitating the dephosphorylation of stathmin, leads to microtubule destabilisation and enhanced cell motility.

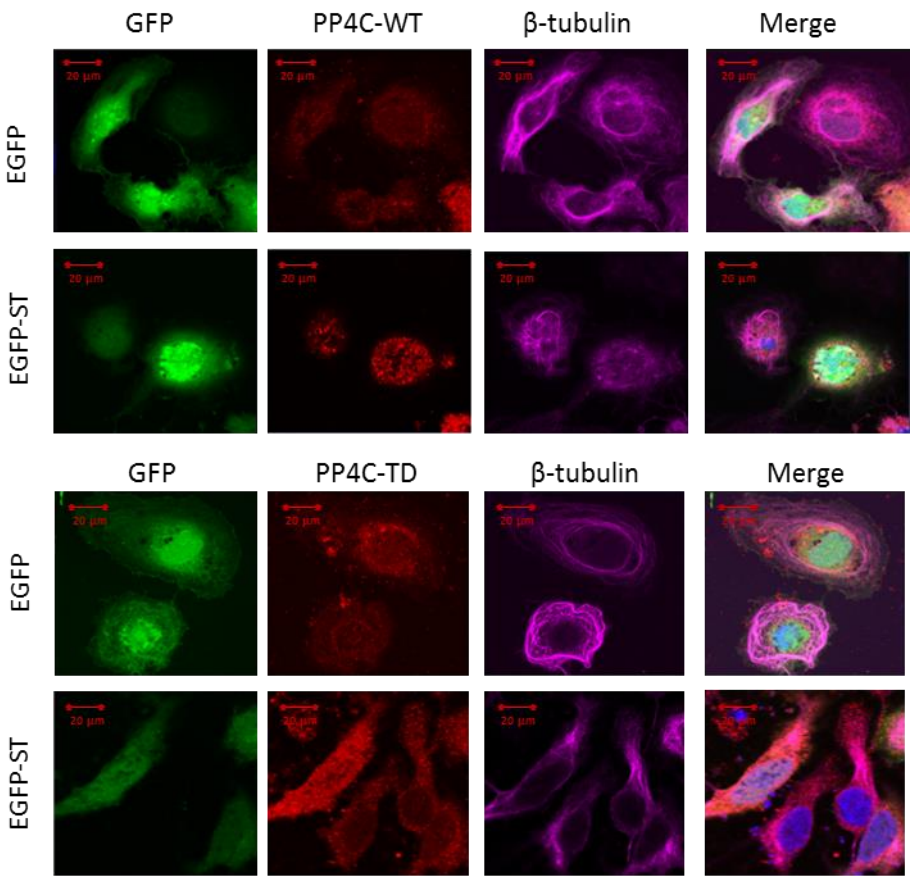

Figure 5.7. Expression of a transdominant PP4C mutant inhibits MCPyV ST-mediated microtubule destabilisation. MCC13 cells were transfected with either EGFP or EGFP-ST in the presence of wild type or inactive PP4C mammalian expression constructs. 24 hours after transfection cells were fixed, permeablised and stained with an endogenous β-tubulin-specific antibody. GFP fluorescence was analysed by direct visualisation and the nucleus stained using DAPI-containing mounting medium.

To verify these results, immunoblotting was performed using MCC13 cell lysates transfected with either EGFP or EGFP-ST in the presence of wild type or transdominant PP4. Cell lysates were analysed using stathmin-, phosphorylated stathmin- and acetylated tubulin-specific antibodies (Figure 5.8). In EGFP-ST expressing cells, co-expression of PP4-RL resulted in a notable increase in phosphorylated stathmin and acetylated tubulin levels, in comparison to EGFP-ST expressing cells cotransfected with wild type PP4. These results are similar to those seen with EGFP-Δ95-111, suggesting that PP4C may be important of MCPyV ST-mediated microtubule destabilisation.

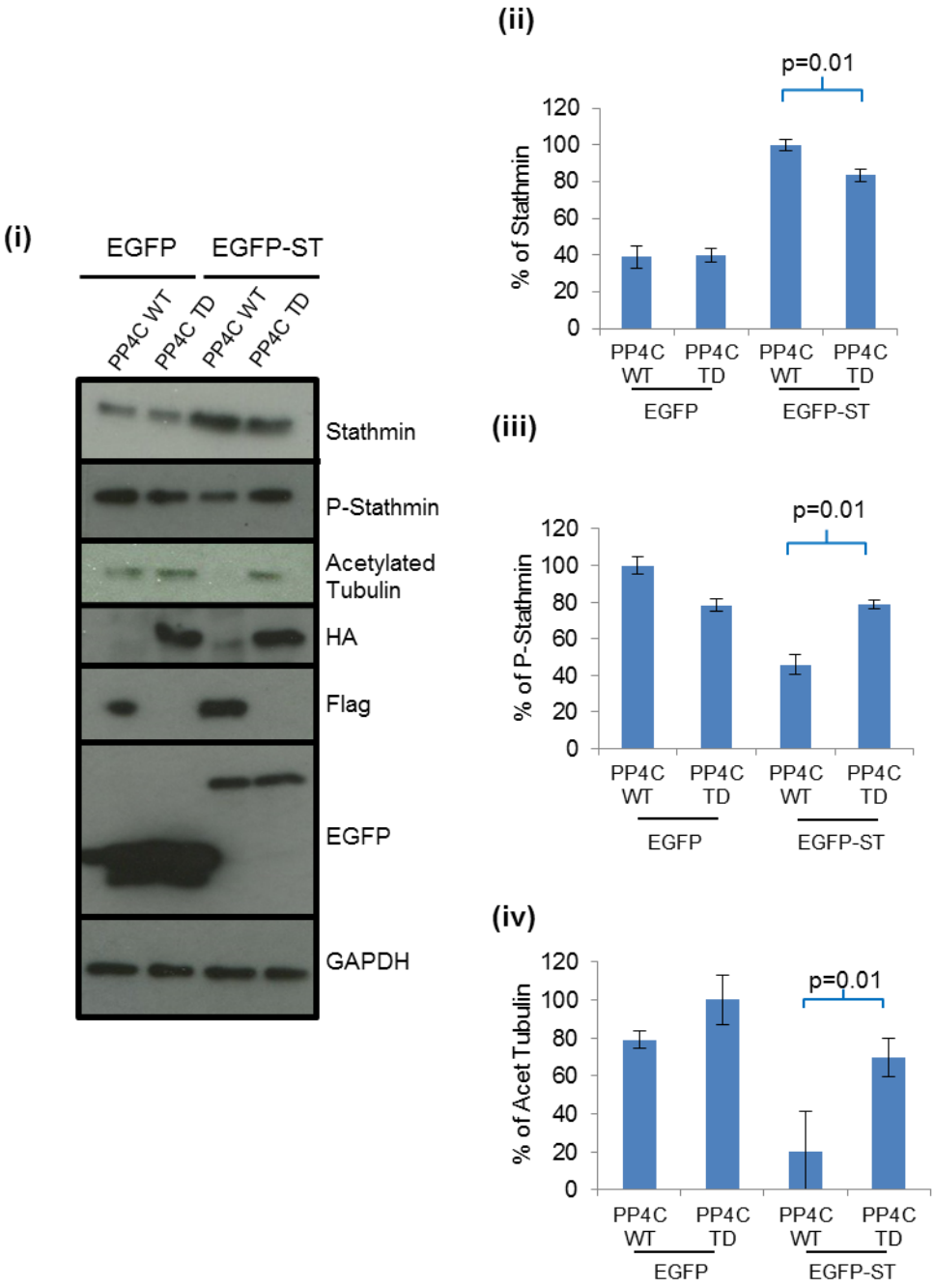

Figure 5.8. Expression of a transdominant PP4C mutant promotes microtubule destabilisation. MCC13 cells were transfected with either EGFP or EGFP-ST in the presence of wild type or inactive PP4C mammalian expression constructs. (i) 24 hours after transfection cell lysates were harvested and immunoblotting performed using stathmin-, phosphorylated stathmin-, acetylated tubulin-, EGFP- and GAPDH-specific antibodies. GAPDH was used as a measure of equal loading and densitometry analysis using Image J software enabled calculation of the percentage of relative densitometry of stathmin (ii), phosphorylated stathmin (iii) and acetylated tubulin (iv), all normalised to the loading control. Data analysed using three biological replicates per experiment, n=3. Statistical analysis employed was a two-tailed T-test with unequal variance.

To further investigate the role of PP4C in MCPyV ST-mediated cell motility, scratch-wound healing assays were performed using uninduced and induced

i293-ST cells transfected with either wild type or inactive PP4. Figure 5.9 demonstrates that expression of the catalytically inactive PP4 inhibits cellular growth back into the wound in MCPyV ST expressing cells, in comparison to expression of the wild type construct which shows typical MCPyV ST-induced cell motility and migration.

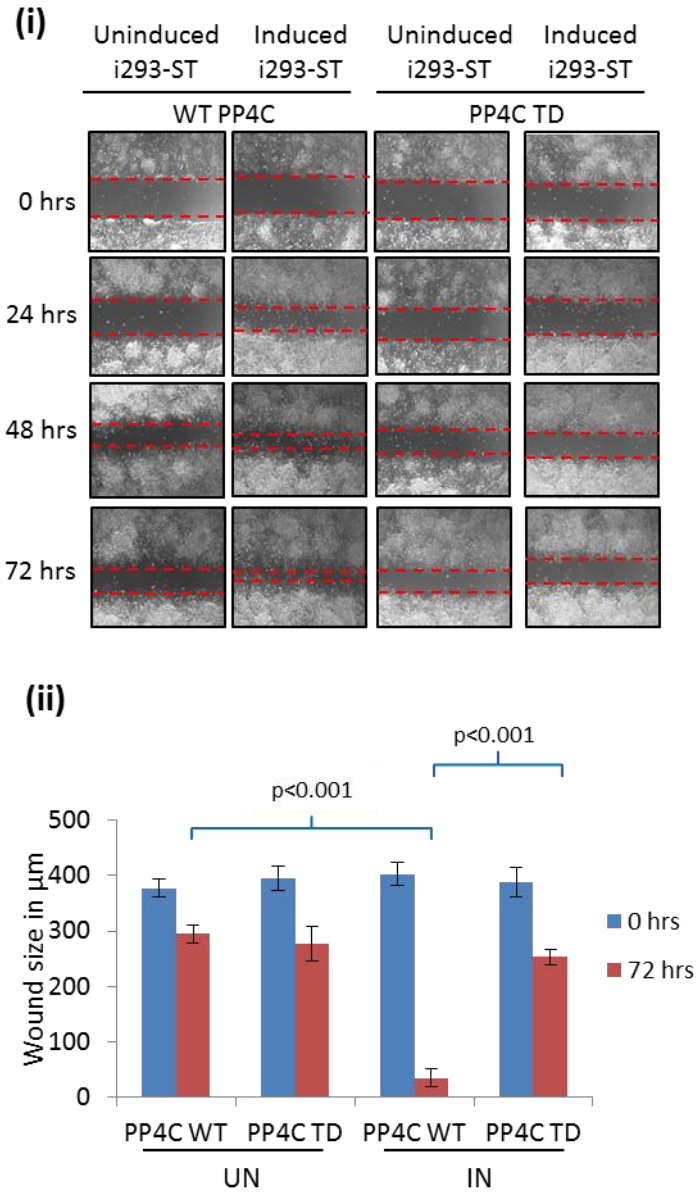

Figure 5.9. Expression of a transdominant PP4C mutant inhibits MCPyV ST-mediated cell motility in i293-ST cells. (i) Cells were seeded onto poly-L-lysine coated 6 well plates and transfected with either wild type or the catalytically inactive PP4-RL expression constructs. 24 hours after transfection a scratch wound was generated and cells imaged every 24 hours over the course of 3 days, using a Zeiss light microscope at 4x magnification. (ii) The size of the wound was measured at 0 and 72 hours post-scratch. Data analysed using three biological replicates per experiment, n=3. Statistical analysis employed was a two-tailed T-test with unequal variance.

These results were then confirmed using MCC13 cells transfected with either EGFP or EGFP-ST in the presence of either wild type or inactive PP4 (Figure 5.10). Once again these results demonstrate that expression of the inactive PP4-RL in EGFP-ST expressing cells inhibits cellular growth. Taken together, these results suggest that PP4C is important for MCPyV ST-mediated microtubule destabilisation and in turn increases cell motility.

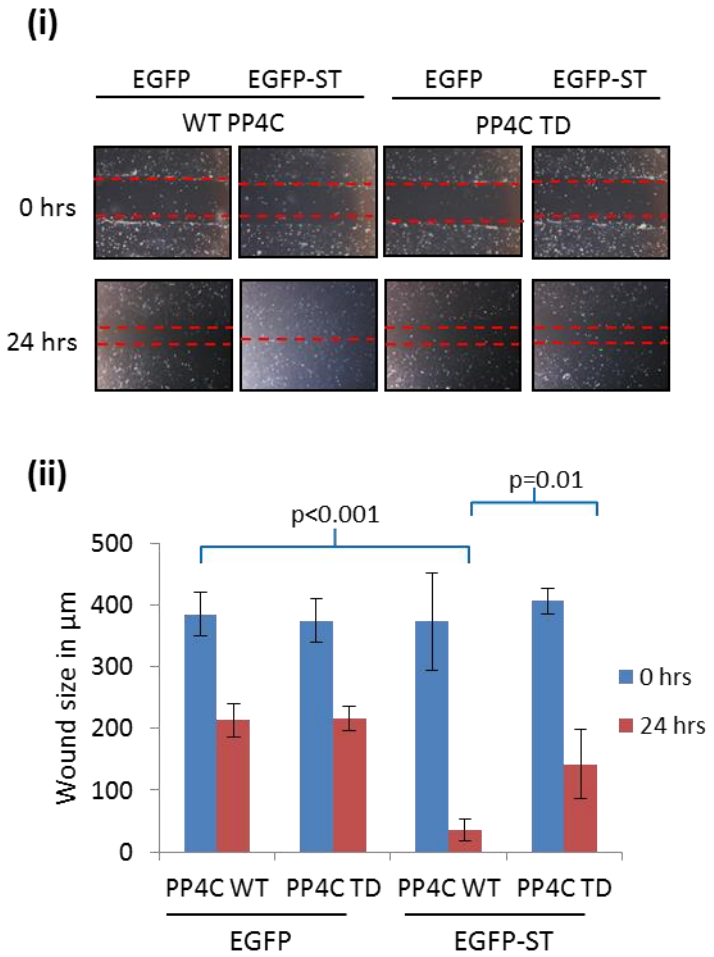

Figure 5.10. Expression of a transdominant PP4C mutant inhibits MCPyV ST-mediated cell motility in MCC13 cells. (i) Cells were seeded onto poly-L-lysine coated 6 well plates and transfected with either EGFP or EGFP-ST in the presence of either wild type or the catalytically inactive PP4-RL expression constructs. 24 hours after transfection a scratch wound was generated and cells imaged over the course of 24 hours, using a Zeiss light microscope at 4x magnification. (ii) The size of the wound was measured at 0 and 24 hours post-scratch. All scratch assays were performed in triplicate. Data analysed using three biological replicates per experiment, n=3. Statistical analysis employed was a two-tailed T-test with unequal variance.

5.5 MCPyV ST interacts with stathmin

Previous results have demonstrated that PP4C is required for MCPyV ST-induced microtubule destabilisation and cell motility. This may also be due to the interaction between MCPyV ST and PP4C, and through this interaction MCPyV ST may increase the levels of unphosphorylated stathmin. As previously mentioned the Whitehouse laboratory have shown that MCPyV ST binds the cellular phosphatase catalytic subunit PP4C[226]. Therefore, results herein examined whether MCPyV ST interacts with stathmin and also whether stathmin binds PP4C. Dr Andrew Macdonald and Hussein Abdul-Sada performed co-immunoprecipitation assays in HEK 293 FlpIn™ cells, transfected with either EGFP, EGFP-ST, empty-FLAG, or FLAG-PP4C mammalian expression constructs. MCPyV ST immunoprecipitations were then performed using GFP-TRAP beads, while PP4C cell lysates were immunoprecipitated using FLAG-affinity agarose beads. The subsequent precipitated proteins were identified using a stathmin-specific antibody and Figure 5.11 demonstrates that stathmin binds both PP4C and MCPyV ST. Importantly, this indicates that these interactions may facilitate an increase in unphosphorylated stathmin, resulting in microtubule destabilisation and in turn enhancement of cell motility, migration and invasion.

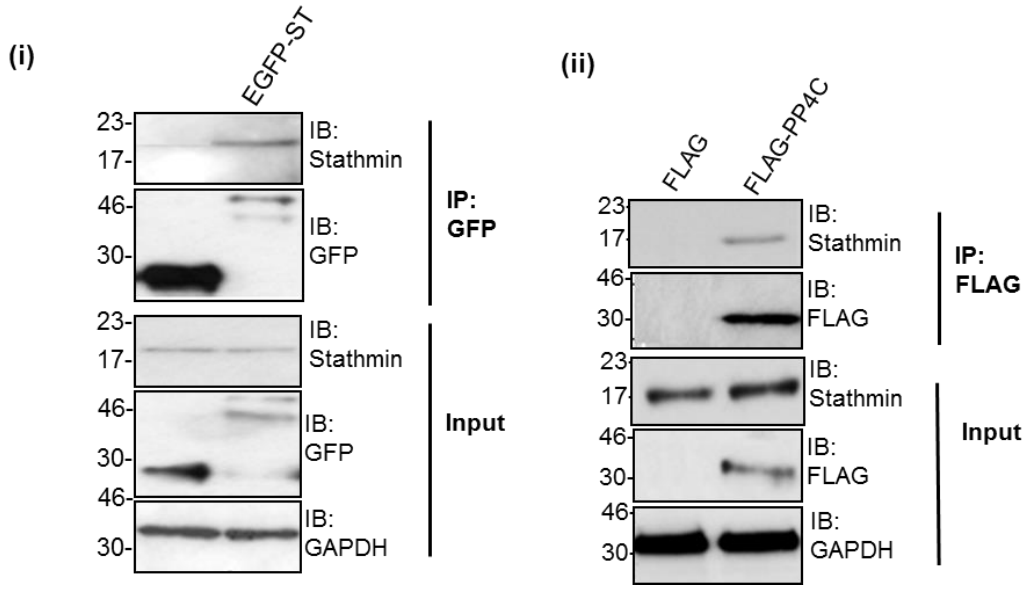

Figure 5.11. Stathmin interacts with both MCPyV and PP4C. (i) HEK 293 FlpIn™ cells were co-transfected with EGFP or EGFP-ST mammalian expression constructs. Cell lysates were incubated with GFP-TRAP affinity beads and immunblotting performed on precipitates using a control GFP-, stathmin and GAPDH-specific antibodies. (ii) HEK 293 FlpIn™ cells were co-transfected with empty-FLAG or FLAG-PP4C mammalian expression constructs. Cell lysates were incubated with FLAG affinity agarose beads and the precipitate analysed by western blot using a control FLAG-, stathmin- and GAPDH-specific antibodies. (These experiments were performed by Hussein Abdul-Sada).

5.6 MCPyV ST may enhance stathmin translation

The previous findings indicate that MCPyV ST expression promotes the upregulation of stathmin and through an interaction of MCPyV ST with cellular phosphatases (particularly PP4C) stathmin is dephosphorylated. This leads to an increase in the pool of unphosphorylated stathmin and promotes microtubule destabilisation, enhancing cell motility and migration. However, the level at which stathmin protein levels are regulated needs to be addressed. Initially, qRT-PCR analysis was conducted using uninduced and induced i293-ST cells, in order to establish if MCPyV ST enhances stathmin at the transcriptional level. Figure 5.12 clearly shows that despite there being a slight increase in stathmin mRNA levels in MCPyV ST cells, this is insignificant, and suggests that MCPyV ST does not increase stathmin transcript levels.

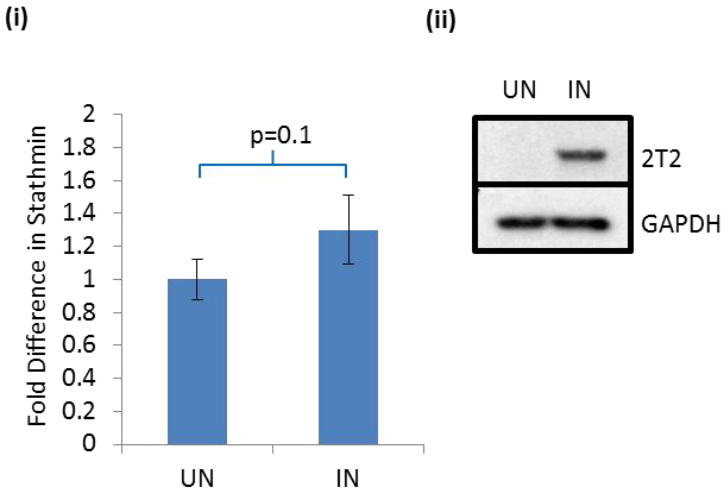

Figure 5.12. MCPyV ST does not promote enhanced transcription of stathmin. (i) Using uninduced and induced i293-ST cells, total RNA was extracted after 24 hours and reversed transcribed to produce a cDNA library. The relative stathmin levels were analysed by qRT-PCR using GAPDH as a reference. The relative fold increase was calculated using ΔΔcT values and statistical analysis by a non-paired *t*-test. The data from 3 independent studies is presented as a fold change against the uninduced control. (ii) MCPyV ST expression was confirmed by western blot using the same samples and analysed using the 2T2-specific antibody that detects MCPyV T antigen expression. Data analysed using three biological replicates per experiment, n=3. Statistical analysis employed was a two-tailed T-test with unequal variance.

This result suggests that MCPyV ST promotes an increase in stathmin levels at a post-transcriptional level. Therefore to assess if stathmin protein stability is affected by MCPyV ST expression, immunoblotting was performed on induced i293-ST cell lysates in the absence or presence of cyclohexamide. Figure 5.13 demonstrates that there is a slight, but insignificant increase in the half-life of stathmin in cells incubated with cyclohexamide. As a positive control, p53 showed reduced protein levels in the presence of cyclohexamide over time. Therefore, these results suggest that MCPyV ST does not actively increase the protein stability of stathmin.

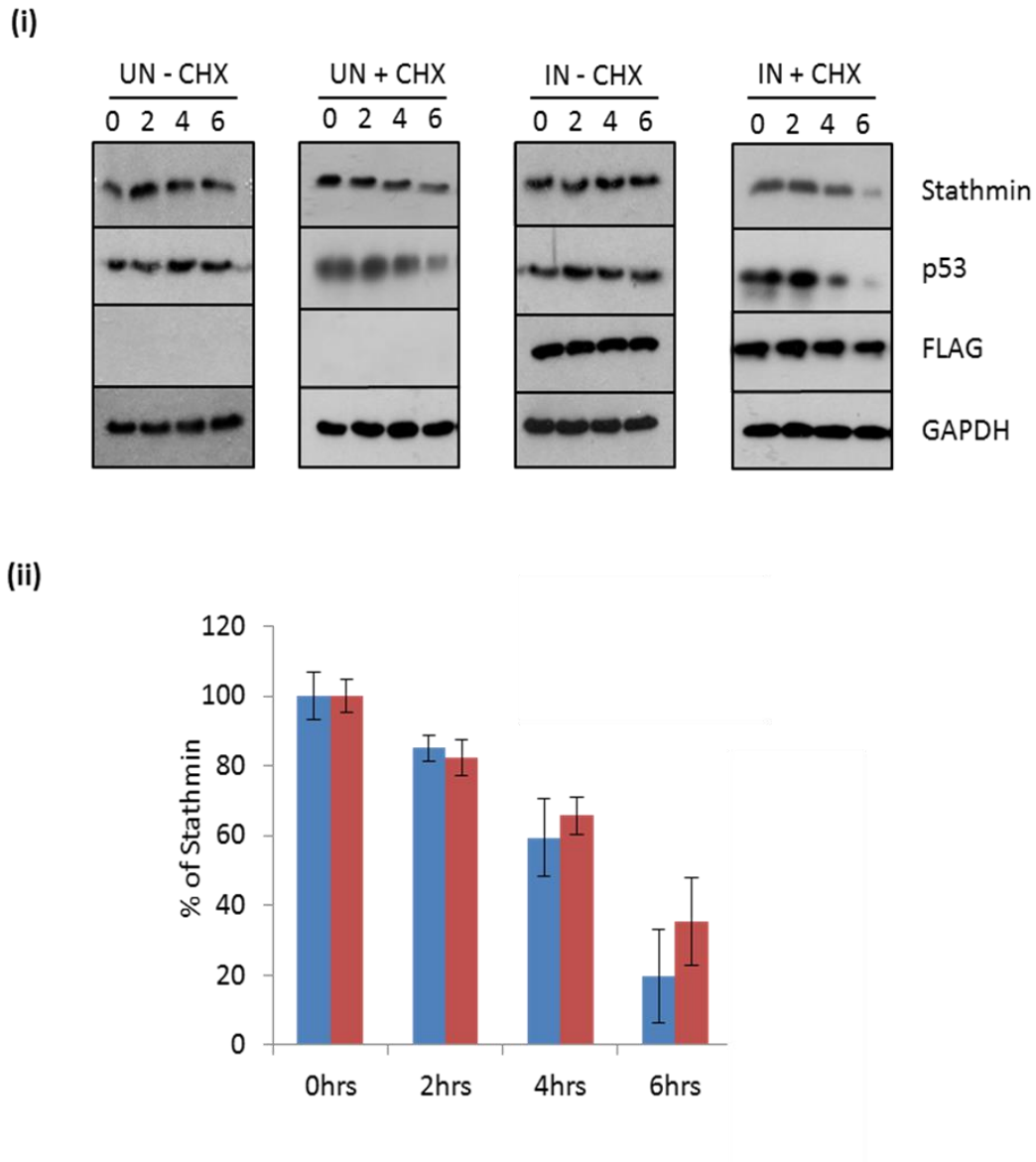

Figure 5.13. MCPyV ST does not enhance stathmin protein stability. i293-ST cells were left uninduced or induced in the presence or absence of cyclohexamide and samples harvest at 0, 2, 4 and 6 hours post cyclohexamide treatment. (i) Cell lysates were analysed by western blot using stathmin-, FLAG- and GAPDH-specific antibodies. (ii) Relative stathmin protein levels were quantified using Image J software, between unindued and induced cells in the presence of CHXl, and is shown as a percentage of relative densitometry compared to the loading control, GAPDH. Data analysed using three biological replicates per experiment, n=3. Statistical analysis employed was a two-tailed T-test with unequal variance.

Previous findings have indicated that MCPyV ST acts downstream in the mammalian target of rapamycin (mTOR) signaling pathway, deregulating cap-dependent translation by maintaining the hyperphosphorylated state of the translation initiation factor, 4E-BP1[247]. Therefore, to establish if MCPyV ST enhances stathmin expression through this mechanism, immunoblotting was performed comparing

uninduced and induced i239-ST cells in the absence or presence of rapamycin. Rapamycin specifically binds FK-binding protein 12 (FKBP12) and through this complex is able to inhibit mTOR signaling. mTOR activation results in the phosphorylation of 4E-BP1 and subsequently prevents 4E-BP1 binding to eIF4E, thereby allowing eIF4E to form at the cap of mRNA molecules, resulting in ribosome recruitment and translation. As mentioned MCPyV ST expression preserves the hyperphosphorylated state of 4E-BP1, even under rapamycin treatment, to stimulate cap-dependent translation.

The results in Figure 5.14 demonstrate that in the absence or presence of rapamycin the induced levels of stathmin remain the same, suggesting that even though rapamycin treatment inhibits mTOR activation and subsequent translation, this does not affect the translation of stathmin. This indicates that induced stathmin levels are unaffected by rapamycin, due to the ability of MCPyV ST to maintain the hyperphosphorylated state of 4E-BP1. Moreover, this suggests that MCPyV ST may enhance stathmin expression levels through an enhancement of cap-dependent translation.

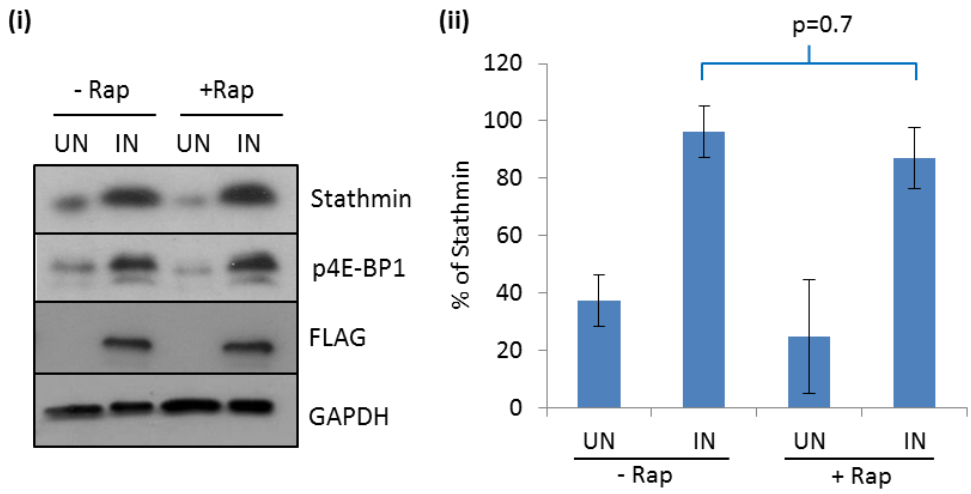

Figure 5.14. MCPyV ST dysregulation of cap-dependent translation is required for enhanced stathmin expression. (i) i293-ST cells were left uninduced or induced for 24 hours, followed by incubation with rapamycin for 4 hours. Cells lysates were harvested and analysed by western blot using stathmin-, phosphorylated 4E-BP1, and GAPDH-specific antibodies. (ii) Relative stathmin levels were quantified using Image J software, and is shown as a percentage of relative densitometry compared to the loading control, GAPDH.

5.7 Discussion

In terms of MCC treatment and metastasis prevention, understanding the mechanism by which MCPyV ST promotes microtubule destabilisation and cell motility is a key factor for possible therapeutic regimes. This Chapter discusses the role MCPyV ST has in promoting the upregulation of stathmin and its subsequent dephosphorylation. To date few studies have directly implicated any specific cellular phosphatases in stathmin dephosphorylation. However studies have indicated that okadaic acid treatment inhibits protein phosphatases type 1, type 2A and type 2B, and drastically elevated the levels of phosphorylated stathmin, thereby implicating these phosphatases in stathmin regulation[383]. Interestingly, MCPyV has been shown to interact with a number of cellular phosphatases such as PP2A Aα, PP2A Aβ and PP4C[226,247].

Data herein demonstrates a likely role for PP4C in MCPyV ST-mediated microtubule destabilisation and enhancement of cell motility. Cell motility assays conducted using either a MCPyV ST mutant incapable of binding PP4C or an inactive PP4C mutant showed a significant reduction in cell motility upon MCPyV ST expression in both i293-ST cells and MCC13 cells. Immunoblotting and immunofluorescence analysis further confirmed that inhibition of the PP4C-MCPyV ST interaction resulted in a significant increase in microtubule stability. Interestingly, PP4C has previously been shown to affect microtubule organisation at the centrosome through recruitment of katanin p60 and regulation of NEDL1[384].

Moreover, further analysis herein demonstrates a novel interaction of MCPyV ST and stathmin and a further novel interaction between stathmin and PP4C. Work is now ongoing to determine is a tertiary complex involving stathmin, PP4C and MCPyV ST is formed and to assess whether the interaction between stathmin and PP4C is enhanced by the presence of MCPyV ST.

Data presented herein, allows a model of MCPyV ST-mediated cell motility to be established. Whereby, the interaction between MCPyV and stathmin may facilitate

an interaction between PP4C and stathmin. This may direct PP4C dephosphatase activity towards stathmin, subsequently increasing the pool of unphosphorylated stathmin. High unphosphorylated stathmin levels therefore promote microtubule destabilisation which in turn promotes enhanced cell motility of MCPyV ST expressing cells.

In summary, while the role of MCPyV ST in the proliferation of MCC tumour cells is controversial within the field, findings here highlight the pivotal role PP4C plays in MCPyV ST-induced microtubule destabilisation and cell motility. Importantly, two novel interactions have been characterised which allow a model of MCPyV ST-induced cell motility to be established. This data suggests novel virus-host interactions which may allow for therapeutic intervention and chemotherapy regimes to be established.

Chapter 6

Final discussion and future perspectives

6. Final discussion and future perspectives

MCC is a skin cancer of neuroendocrine origin and arises from Merkel cell situated within the basal layer of the epidermis. Merkel cells are mechanoreceptor cells, stimulated by light touch and form the Merkel-cell neurite complex, one of the four main mammalian sensory receptors[179]. MCC is a highly aggressive skin cancer with a propensity to spread through the dermal lymphatic system and is associated with a poor 5 year survival rate and early establishment of distant metastases[186,187]. It has now been established that MCPyV is the causative agent in the MCC tumour development and is monoclonally integrated in 80-90% of both primary and metastatic tumour forms[71]. Furthermore, all MCPyV LT sequences derived from MCPyV-positive tumour cells demonstrate tumour specific mutations that render the virus replication defective[71]. Due to the monoclonal integration pattern and acquisition of tumour specific mutations, the notion that MCPyV may be a passenger virus has been dismissed.

MCC tumour formation is effectively an indirect result of monoclonal integration of the MCPyV genome within the host chromosome, resulting in impaired viral replication. Interestingly, indirect promotion of metastasis is not without precedence, as several tumour-associated viruses, such as HPV, EBV and SV40 have all demonstrated the capacity to promote metastasis. The mechanisms vary, but include alteration of cellular adhesion complexes, matrix metalloproteinase production, gene expression modulation and cytoskeletal reorganisation[299,378,379].

Since the discovery of MCPyV, several studies have highlighted a role for the MCPyV T antigens, in viral replication and tumour formation[227,247,281]. It has also been demonstrated that expression of MCPyV ST is sufficient to promote anchorage independent growth of rodent cells and facilitate transformation[247]. However, to date, no studies have addressed the underlying molecular mechanisms that promote MCC metastasis nor the potential role of the MCPyV T antigens in this phenotype.

Therefore, using a cell line capable of inducible expression of MCPyV ST, high throughput quantitative SILAC-based proteomic analysis was conducted to enable

differentially expressed proteins to be identified upon MCPyV ST expression. SILAC-based analysis coupled with LC-MS/MS and bioinformatical analysis is an effective way in which to study the host cell proteome, and has recently been established as a highly informative tool for studying virus-host interactions[377]. Furthermore, this technique is capable of reducing the sample complexity and allows analysis of subcellular trafficking between various cellular compartments.

Through this approach, the bioinformatical analysis highlighted that MCPyV ST promotes the differential expression of numerous proteins involved in cytoskeletal processes, particularly those associated with microtubule regulation, organisation and dynamics. While it has been established that the microtubule network is pivotal for intracellular vesicle transport, organelle positioning and mitotic spindle formation[324,326,327], there is also an emerging role of the microtubule network in the control of cell shape and polarised cell motility[322,328].

Following identification of crucial pathways altered upon MCPyV ST expression, it was necessary to determine if any key proteins involved in microtubule dynamics were upregulated. Importantly, the bioinformatical analysis highlighted that one of the most upregulated proteins, was the microtubule-associated protein, stathmin. To confirm this result, stathmin protein levels were examined and MCPyV ST expression was shown to correlate with upregulation of stathmin in both i293-ST and MCPyV-positive MCC cells, in addition to formalin-fixed, paraffin embedded sections of primary MCC tumours.

Previous studies have demonstrated that stathmin overexpression is a feature of multiple cancer types and has been shown to correlate with tumour growth, poor patient prognosis and a high metastatic potential[340,354]. Furthermore, this has been confirmed by RNA interference studies that demonstrate that decreased stathmin levels can drastically reduce the motility of various tumour cells[355,358]. As such, the data presented here, suggests that MCPyV ST may contribute to the metastatic phenotype of MCC tumour cells through alterations in crucial cytoskeletal regulatory proteins, specifically by promoting the overexpression of stathmin.

Despite this, the mechanism by which stathmin promotes metastasis and tumour development is still poorly understood, however it is known that stathmin is a key regulator of the microtubule network and has inherent microtubule destabilising abilities. Furthermore, recent findings have been able to distinguish the indirect and direct manner in which stathmin can promote both microtubule destabilisation and promote catastrophe, through the use of distinct stathmin mutants[340,385]. Using mutation studies it has been shown that overexpression of wild type stathmin and a mutant containing only the tubulin sequestering activity resulted in a significant decrease in stable acetylated microtubules and an enhancement of cell motility[355]. This suggests that there is a strong link between stathmin dephosphorylation, microtubule destabilisation and enhanced cell motility.

Findings presented here, demonstrate that MCPyV ST expression promotes cell motility, migration and invasion and this was confirmed using a range of cell types, such as i293-ST, MCC13 and MKL-1 cells. For accuracy a range of motility assays and techniques were employed, from live cell imaging and tracking, to 2D scratch-wound healing assays and 3D migration and invasion transwell assays. All motility assays used demonstrated that MCPyV ST expression, coincident with stathmin upregulation, promoted a statistically significant increase in cell motility, and further highlighted the important role of MCPyV ST in metastasis.

In contrast, recent data has suggested that certain cell types with stathmin overexpression and altered microtubule dynamics has been shown to be insufficient to promote cell motility in 2D would closure assays[355,385,386]. However, the underlying molecular mechanisms have yet to be identified and it has been speculated that there may be a link with specific molecular mechanisms that regulate cell shape and morphology[387,388]. This is interesting as previous studies have demonstrated that a less phosphorylated stathmin mutant can promote alterations in cell morphology and promote a rounded cell shape with amoeboid-like protrusions, thus allowing enhanced cell motility through bleb-like propulsion mechanisms[340]. These findings suggest that stathmin overexpression may result in a more dynamic and flexible microtubule network. Moreover, as the microtubule network forms a crucial regulatory component of healthy cells, any alterations may

induce changes in other arms of the cytoskeletal network which may contribute to additional morphological changes and enhance cell motility. In particular, depletion of stathmin has been shown to affect the activation of the Rho-Rho associated coiled-coil forming serine/threonine kinase signalling pathway, an important regulator of actin cytoskeletal remodelling, though phosphorylation of cofilin and myosin light chains, and the microtubule network[358].

Interestingly, herein bioinformatical analysis highlighted that other gene ontology groupings consisting of more general cytoskeletal changes were altered upon MCPyV ST expression. Importantly, initial findings demonstrated that there were significant alterations in the actin cytoskeletal network structure upon MCPyV ST expression, consistent with filopodia or lamelipodia formation. The actin cytoskeletal network has long since been established as crucial mediator of cell motility[321], and is an important aspect of MCPyV ST biology that is currently under investigation.

Furthermore, findings here demonstrate that upon expression of MCPyV ST the pool of unphosphorylated stathmin is significantly increased. Unphosphorylated stathmin activity has been shown to promote microtubule destabilisation and catastrophe, along with enhanced cell motility[340,354,364,365]. Herein, it has been demonstrated that MCPyV ST expression promotes destabilisation of the microtubule network and a decrease in stable acetylated tubulin levels, further confirming the importance of stathmin in regulating microtubule dynamics. The role of stathmin as a microtubule destabilising protein has long since been established, however to date, few cellular phosphatases have been directly implicated in regulating stathmin phosphorylation. It has been demonstrated that treatment with okadaic acid results in inhibition of cellular phosphatases, leading to a significant increase in phosphorylated stathmin[389]. This indicates a role for protein phosphatases type 1, type 2A and type 2B in stathmin dephosphorylation. Furthermore, it has been suggested through the use of *in vitro* dephosphorylation assays, that stathmin dephosphorylation occurs through the sequential activity of multiple cellular phosphatases[389].

It has been demonstrated that MCPyV ST has specific binding sites which facilitate interactions with multiple cellular phosphatases, including PP2A Aα, PP2A Aβ and PP4C[226,247]. Interestingly, these cellular phosphatases have been previously implicated in microtubule regulation and dynamics[375,383,390], thereby suggesting a possible link between these phosphatases and MCPyV ST-mediated microtubule destabilisation. Moreover, PP4C has previously been shown to affect the correct at timely organisation of the microtubules at the centromsome, through the regulation of NDEL1 and the recruitment of katanin p60[384]. Data presented here, indicates the likely role of the cellular phosphatase PP4C in MCPyV ST-induced microtubule destabilisation and in the promotion of cell motility, whereby expression of an inactive PP4C mutant is capable of inhibiting MCPyV ST-mediated microtubule destabilisation.

Furthermore, these findings highlight a novel interaction between PP4C and stathmin and for the first time an interaction between MCPyV ST and stathmin. This allows a model of MCPyV ST-mediated cell motility to be established. Whereby expression of MCPyV ST promotes the upregulation of stathmin, in a post-transcriptional manner, believed to be a result of MCPyV ST deregulation of cap-dependent translation, through preservation of the hyperphosphorylated state of the translation initiation factor, 4E-BP1. Evidence here suggests that the ability to MCPyV ST to interact with stathmin, may facilitate an interaction between stathmin and PP4C, and the subsequent dephosphorylation of stathmin. This in turn results in an increase in the cellular pool of unphosphorylated stathmin, thereby promoting stathmins' microtubule destabilising properties and enhanced cell motility and migration.

Historically, identification of MCC tumours was particularly difficult and often mistaken for small-cell carcinoma of the lung, which presents as a visibly similar tumour[190]. However, recently, a robust MCC detection system has been developed, and requires positive CK20 staining along with neuroendocrine biomarkers such as chromatogranin and somatostatin[194]. Despite this improved detection system, the management and treatment of MCC is a concerning issue and there is no specific therapeutic regime available. Current regimes used to treat MCC are those used for

small-cell carcinoma of the lung, however none have shown to increase the survival of MCC patients[203]. Therefore, it essential to understand the molecular biology of this disease in order to enable optimal treatment and care for patients.

The discovery of a novel polyomavirus associated with MCC, provides an important aspect in understanding MCC tumour formation and development and may provide potential therapeutic targets and novel virus-targeted chemotherapy regimes. The recent study into MCPyV has highlighted the important role of MCPyV LT in the upregulation of survivin, which is essential for the survival of MCPyV-positive MCC cells[281]. Furthermore, this study demonstrated that treatment with a small molecule inhibitor of the survivin promoter, YM155, activates cell death pathways, specifically in MCPyV-positive cell lines and delayed formation of MCC xenografts in mice models.

Herein, results demonstrate that MCPyV ST-mediated cell motility, a result of microtubule destabilisation, may be a possible therapeutic target for the treatment of MCC. The group of chemotherapeutic drugs known as taxanes, have been widely used for a number of years, in combination with other therapeutics, in order to treat a variety of different cancers types. Taxanes are microtubule inhibitors which directly bind to the microtubule structures and stabilise them, thus may be of benefit in the treatment of MCC. Findings presented here demonstrate that treatment with taxane compounds inhibits both MCPyV ST-mediated microtubule destabilisation and MCPyV ST-induced cell motility. Moreover, these drugs are already in use in the clinic, thus could potentially be used to treat MCC patients within a few years, in an endeavour to prevent metastasis of MCC tumour cells from the primary carcinoma. However, there are significant side effects associated with Paclitaxel treatment and it is usually reserved as an end-stage drug. Furthermore its use is restricted on a patient by patient basis, due to the acquisition of multi-drug resistance (MDR) to one or more of these compounds.

However, in the last few years newly developed Paclitaxel derivatives have entered clinical trials, such as the nanoparticle paclitaxel (FDA approved Abraxane®), which has proved its efficacy in both breast and non-small cell lung cancer clinical trials.

Furthermore, three new taxanes have been isolated from the Japanese Yew, and may provide treatment for early diagnosed cancer patients[391]. Thus it would be encouraging to determine if these newly developed taxanes are able to prevent MCPyV ST-mediated microtubule destabilisation. .

Furthermore, in order to overcome taxane MDR, novel microtubule-targeting compounds have since been developed. The class of compounds referred to as, epothilones, isolated from myxobacterium *Sorangium cellulosum*, can be used to treat taxane resistant cell lines and xenograft tumours[391,392]. Once again, it would be useful to determine if these class of compounds have the same inhibitory effects on MCPyV ST-induced cell motility compared to taxanes.

The upregulation of stathmin, is key to the ability of MCPyV ST to promote cell motility and may provide novel therapeutic targets for the treatment of MCC patients. Interestingly, gene profiling of melanoma cells identified that the microRNA, miR-193b, specifically targets stathmin and that ectopic expression of miR-193b decreases stathmin protein levels and reduces the ability of melanoma cells to migrate[356]. This demonstrates that the use of RNAi-based therapies may be a viable solution to decreases stathmin levels upon MCPyV T antigen expression. More specifically, findings herein demonstrate that siRNA depletion of stathmin inhibits MCPyV ST-induced cell motility and migration in MCPyV-positive cells lines. This indicates that RNAi-based therapies, delivering stathmin-specific siRNAs through the use of virus-based delivery systems or biodegradable nanoparticles, may be a successful new chemotherapeutic regime in order to prevent cell motility and metastasis associated with MCC. Furthermore, the development of small molecule inhibitors that prevent MCPyV ST interacting with PP4C and/or stathmin, may prevent stathmin dephosphorylation and MCPyV ST-induced cell motility.

While the role of MCPyV ST in the promotion of cell proliferation is controversial, data herein highlights the fundamental role of MCPyV ST in enhancement of cell motility and migration. This is the first study to demonstrate that MCPyV ST promotes the differential expression of cytoskeletal proteins, with specific regard to the upregulation of stathmin. Furthermore, these findings highlight the essential

role of MCPyV ST and stathmin in MCPyV ST-mediated microtubule destabilisation and cell motility. Importantly, the interaction between MCPyV ST and the cellular phosphatase catalytic subunit PP4C has been implicated and provides a novel molecular mechanism for MCPyV ST-mediated cell motility. Moreover, this provides an explanation for the highly metastatic nature of MCC and demonstrates that stathmin may be a useful biomarker for MCC prognosis and in the future a viable therapeutic target for MCC treatment.

Moreover, a fundamental aspect of cancer development and metastasis involves specific alterations within the host cell metabolism, and is now regarded as a 'Hallmark of Cancer'. Cancer cell metabolism is the broad category, used to described specific adaptations within metabolic pathways that allows cancer cell to consume more glucose and produce a large quantity of lactose, a process known as aerobic glycolysis[393]. While this process may generate less ATP than conventional mitochondrial respiration, the process is much more rapid[394,395]. Thus providing the necessary energy required by cancer cells for increased cell proliferation, adaptation to the environment and provides energy for processes such as metastasis.

Although not a focus of this thesis, the quantitative proteomic approach used herein highlighted that MCPyV ST expression also promotes alterations in the host cell metabolism, including pathways such as, glucose, serine, lactate and lipid synthesis. Importantly, key proteins in these pathways were upregulated upon MCPyV ST expression, such as pyruvate kinase, lactate dehydrogenase and serine synthesis enzymes. Previous studies have demonstrated that overexpression of these proteins has been shown to facilitate aerobic glycolysis and promote the accumulation of upstream metabolic intermediates. Thereby contributing to a shift in metabolism toward amino acid, nucleotide and lipid synthesis, all required in increasing amounts for maintenance and growth of cancer cells[394,396].

While the study of virus-host interactions in terms of the host cell metabolism has not been widely explored, there is precedence for metabolic alterations during viral infection. Dramatic intermediary metabolic alterations have been demonstrated

during infection of human cell lines with human cytomegalovirus (HCMV), in a similar manner as those seen in tumour cells[397]. Such changes could be attributed to pathogenesis and potentially implicate HMCV as a subtle cofactor in human malignancy. Furthermore, the human tumour-associated virus hepatitis C virus (HCV), has been implicated in the upregulation of host cell lipid metabolism through inhibition of AMP-activated protein kinase[398,399].

Despite the controversy within the MCPyV field regarding the role of MCPyV ST in cell proliferation, data herein suggests that MCPyV ST expression alone does not enhance cell proliferation or alterations in the cell cycle. However, findings do suggest that MCPyV ST expression may promote alterations of specific metabolic processes that allow survival of cells in low nutrient conditions. Conditions that are experienced by cancer cells in an expanding primary tumour environment[286].

However, this in itself represents a dichotomy as a switch to a cancer cell metabolism phenotype is generally consistent with an increase in cell proliferation. Interestingly, while data here indicates that MCPyV ST alone does not facilitate increased cell proliferation, the expression of both MCPyV LT and ST results in a significant increase in cell growth. Importantly, research in the Whitehouse laboratory using a quantitative proteomic approach to investigate the role of MCPyV LT in the cellular proteome revealed that MCPyV LT expression promotes the differential expression of proteins involved in cell cycle control at G_1-S phase. This suggests that MCPyV LT may directly promote increased cell proliferation through facilitating a switch from G_1 to S phase and is consistent with the polyomavirus literature, whereby LT promotes progression to S phase to stimulate viral DNA replication[227]. Alternatively, it may also be a result of the combined expression of both MCPyV T antigens that provide the necessary cellular pathway alterations in order to facilitate enhanced cell proliferation. This notion of cooperative T antigen activity is supported by evidence indicating that MCPyV ST expression promotes the stability of LT, and facilitates enhanced viral replicative functions[227].

As previously mentioned, quantitative proteomic analysis highlighted the upregulation of pyruvate kinase (PK), a crucial candidate enzyme in facilitating the switch from normal host cell metabolism to aerobic glycolysis. PK catalyses the last reaction in glycolysis and is essentially irreversible, thus lowering the activity of PK results in decreased pyruvate synthesis and accumulation of upstream metabolic intermediates[396].

The principle form of PK expressed in healthy non-cancerous cells is PKM1, however it has been demonstrated that cancer cell predominantly express an alternatively spliced isoform of PK, referred to as PKM2[396]. PKM2 is a master regulator of glycolysis and is less activate thereby promoting aerobic glycolysis and accumulation of upstream metabolites. To ensure the preferential splicing of PKM2, cancer cells have evolved a number of mechanisms involving enhanced expression of heterogenous nuclear ribonucleoproteins and polypyrimidine-tract-binding protein. Interestingly, analysis highlighted the upregulation of both of these protein subsets, suggesting that MCPyV ST expression may promote the preferentially splicing of PKM2.

Importantly, other tumour-associated viruses have been shown to enhance PKM2 expression, such as human papillomavirus-16 (HPV)[400]. This suggests that upregulation of PKM2 by specific viral proteins may be a widely used mechanism by which to facilitate enhanced aerobic glycolysis thus enhancing cell proliferation and metastasis.

As PMK2 is a master regulator of aerobic glycolysis and facilitates macromolecular synthesis, it also presents an attractive target for therapeutic intervention in cancer patients. However, to date, this enzyme has not been targeted for virus-induced cancers. In 2007, a seven amino acid peptide inhibitor of PKM2, referred to as TLN-232/CAP-232, underwent Phase II clinical trials in metastatic renal carcinoma[401]. The results were encouraging and the treatment well tolerated. More recently, in 2012, a large library of synthetic compounds were screened and two small water-soluble molecule inhibitors, with specific PKM2 selectivity were identified[401]. Furthermore, the compounds shikonin and alkannin also inhibit PKM2,

resulting in a 50% reduction in PKM2 levels, without affecting expression of PKM1[401]. Consequently, these compounds could be used to inhibit glucose consumption, promote anaerobic glycolysis and exhibit the potential to be used as novel anti-cancer drugs.

Furthermore, a range of PKM2 activators have been developed including, DASA-58 and TEPP-46, both of which promote the tetramerisation of PKM2. Thus shifting metabolism towards anaerobic glycolysis and respiration thought the TCA cycle, and consequently have been shown to inhibit tumour growth[400]. Further characterisation of the MCC metabolic phenotype, may provide novel anti-viral and chemotherapeutic targets, such as PKM2, which may aid in the treatment of MCC and improve overall patient prognosis.

Chapter 7

Appendix

7. Appendices

7.1 Quantitative proteomics highlights that MCPyV ST promotes alterations in multiple cellular processes

Additional Cytoskeletal Regulation, Organisation and Dynamics, Cell Morphology, Establishment of Localisation and directed movement

Uniprot Number	Protein	Fold Increase	Number of Peptide Hits
P33176	KIF5B	2.6	40
O75369	FLNB	2.6	105
P07355	ANXA2	3.5	20
P46939	UTRN	2.0	49
Q9ULV4	CORO1C	4.0	13
Q14247	CTTN	3.7	17
P61160	ARP2	3.3	11
P61158	ARP3	2.1	13
P61586	RHOA	3.7	9
P07737	PFN1	6.7	10
P60981	DSTN	5.0	6
P23528	CFL1	5.0	16
P18206	VCL	5.3	42
P13797	PLS3	5.6	28
P29966	MARCKS	6.2	7

DNA Replication, recombination and repair, Cell cycle regulation, proliferation and growth

Uniprot Number	Protein	Fold Increase	Number of Peptide Hits
P60953	CDC42	7.00	5
P04114	APOB	41.0	4
Q9NVV4	MTPAP	2.0	5
P28340	POLD1	2.0	5
P00441	SOD1	8.6	8
Q9NRR5	UBQLN4	3.0	7
P20248	CCNA2	1.9	2
P24941	CDK2	2.0	7
Q9Y5K6	CD2AP	2.7	9
P62826	RAN	7.0	7
Q96GD4	AURKB	1.6	6
P28482	MAPK1	2.9	12
Q9Y3F4	STRAP	3.6	17

Post-translational modification, protein turnover, chaperones, Intracellular trafficking and secretion

Uniprot Number	Protein	Fold Increase	Number of Peptide Hits
O43301	HSPA12A	2.1	3
O14773	TPP1	2	2
O95487	SEC24B	2	2
D4A2D7	Ipo4	2	24
O00505	KPNA3	2	10
Q15833	STXBP2	2.6	3
Q5THJ4	VPS13D	2	6
Q9BTE6	AARSD1	2.1	2
Q5T160	RARS2	2	2
P41250	GARS	2.1	24
O00303	EIF3F	4.6	8

Table 7.1. Bioinformatical analysis highlighting gene ontology groupings differentially expression upon MCPyV ST expression. Proteins differential expressed upon MCPyV ST are highlighted under each gene ontology heading. The uniprot accession number, protein name, fold increase in induced cells and peptides hits are referred to.

References

1 Mathers, C. D. & Loncar, D. Projections of global mortality and burden of disease from 2002 to 2030. *Plos Medicine* **3**, doi:10.1371/journal.pmed.0030442 (2006).

2 Maddams, J., Utley, M. & Moller, H. Projections of cancer prevalence in the United Kingdom, 2010-2040. *British Journal of Cancer* **107**, 1195-1202, doi:10.1038/bjc.2012.366 (2012).

3 Javier, R. T. & Butel, J. S. The history of tumor virology. *Cancer Research* **68**, 7693-7706, doi:10.1158/0008-5472.can-08-3301 (2008).

4 Moore, P. S. & Chang, Y. Why do viruses cause cancer? Highlights of the first century of human tumour virology. *Nature Reviews Cancer* **10**, 878-889, doi:10.1038/nrc2961 (2010).

5 Stewart, S. E., Eddy, B. E. & Borgese, N. Neoplasms in mice inoculated with a tumor agent carried in tissue culture. *Journal of the National Cancer Institute* **20**, 1223-& (1958).

6 Sweet, B. H. & Hilleman, M. R. The vacuolating virus, SV40. *Proceedings of the Society for Experimental Biology and Medicine* **105**, 420-427 (1960).

7 Parkin, D. M. The global health burden of infection -associated cancers in the year 2002. *International Journal of Cancer* **118**, 3030-3044, doi:10.1002/ijc.21731 (2006).

8 de Martel, C. *et al.* Global burden of cancers attributable to infections in 2008: a review and synthetic analysis. *Lancet Oncology* **13**, doi:10.1016/s1470-2045(12)70137-7 (2012).

9 Dimmock, N. J. & Primrose, S. B. Basic Microbiology Series Vol 2. Introduction to modern virology. *Dimmock, N. J. and S. B. Primrose. Basic Microbiology Series, Vol. 2. Introduction to Modern Virology, Third Edition. Ix+349p. Blackwell Scientific Publications, Inc.: Palo Alto, California, USA; Oxford, England, Uk (Dist. in Australia by Blackwell Scientific Publications (Australia) Pty. Ltd.: Carlton, Victoria). Illus. Paper*, IX+349P-IX+349P (1987).

10 Cole, C. N. Polyomavirinae: The viruses and their replication. *Fundamental virology, Third edition*, 917-945 (1996).

11 Imperiale, M. J. Oncogenic transformation by the human polyomaviruses. *Oncogene* **20**, 7917-7923, doi:10.1038/sj.onc.1204916 (2001).

12 White, M. K. & Khalili, K. Polyomaviruses and human cancer: molecular mechanisms underlying patterns of tumorigenesis. *Virology* **324**, 1-16, doi:10.1016/j.virol.2004.03.025 (2004).

13 Arrington, A. S., Lednicky, J. A. & Butel, J. S. Molecular characterization of SV40 DNA in multiple samples from a human mesothelioma. *Anticancer Research* **20**, 879-884 (2000).

14 Vilchez, R. A., Kozinetz, C. A., Arrington, A. S., Madden, C. R. & Butel, J. S. The molecular evidence of polyomavirus SV40 in human cancers: Meta-analysis of controlled studies. *Proceedings of the American Association for Cancer Research Annual Meeting* **43**, 777-777 (2002).

15 Padgett, B. L., Walker, D. L., Zurhein, G. M., Eckroade, R. J. & Dessel, B. H. Cultivation of papova-like virus from human brain with progressive multifocal leucoencephalopathy. *Lancet* **1**, 1257-& (1971).

16 Padgett, B. L. & Walker, D. L. Prevalence of antibodies in human sera against virus, an isolate from a case of progressive multifocal leukoencephalopathy. *Journal of Infectious Diseases* **127**, 467-470 (1973).

17 Shackelton, L. A., Rambaut, A., Pybus, O. G. & Holmes, E. C. JC virus evolution and its association with human populations. *Journal of Virology* **80**, 9928-9933, doi:10.1128/jvi.00441-06 (2006).
18 Bofill-Mas, S., Formiga-Cruz, M., Clemente-Casares, P., Calafell, F. & Girones, R. Potential transmission of human polyomaviruses through the gastrointestinal tract after exposure to virions or viral DNA (vol 75, pg 10290, 2001). *Journal of Virology* **82**, 8244-8244, doi:10.1128/jvi.01216-08 (2008).
19 Monao, M. C. G., Jensen, P. N., Hou, J., Durham, L. C. & Major, E. O. Detection of JC virus DNA in human tonsil tissue: Evidence for site of initial viral infection. *Journal of Virology* **72**, 9918-9923 (1998).
20 Ricciardiello, L. *et al.* JC virus DNA sequences are frequently present in the human upper and lower gastrointestinal tract. *Gastroenterology* **119**, 1228-1235, doi:10.1053/gast.2000.19269 (2000).
21 Chesters, P. M., Heritage, J. & McCance, D. J. Persistence of DNA-sequences of BK virus and JC virus in normal tissue-tissues and in diseased tissues. *Journal of Infectious Diseases* **147**, 676-684 (1983).
22 Safak, M. & Khalili, K. An overview: Human polyomavirus JC virus and its associated disorders. *Journal of Neurovirology* **9**, 3-9, doi:10.1080/13550280390195360 (2003).
23 Khalili, K., Safak, M., Del Valle, L. & White, M. K. JC virus molecular biology and the human demyelinating disease, progressive multifocal leukoencephalopathy. *Neurotropic Viral Infections*, 190-211, doi:10.1017/cbo9780511541728.014 (2008).
24 Krynska, B. *et al.* Detection of human neurotropic JC virus DNA sequence and expression of the viral oncogenic protein in pediatric medulloblastomas. *Proceedings of the National Academy of Sciences of the United States of America* **96**, 11519-11524, doi:10.1073/pnas.96.20.11519 (1999).
25 Gardner, S. D., Field, A. M., Coleman, D. V. & Hulme, B. New human papovavirus (BK) isolated from urine after renal transplantation. *Lancet* **1**, 1253-& (1971).
26 Egli, A. *et al.* Prevalence of Polyomavirus BK and JC Infection and Replication in 400 Healthy Blood Donors. *Journal of Infectious Diseases* **199**, 837-846, doi:10.1086/597126 (2009).
27 Hirsch, H. H. & Steiger, J. Polyomavirus BK. *Lancet Infectious Diseases* **3**, 611-623, doi:10.1016/s1473-3099(03)00770-9 (2003).
28 Tognon, M., Corallini, A., Martini, F., Negrini, M. & Barbanti-Brodano, G. Oncogenic transformation by BK virus and association with human tumors. *Oncogene* **22**, 5192-5200, doi:10.1038/sj.onc.1206550 (2003).
29 **zur Hausen, H.** *Infections causing human cancer*. (Weinheim Wiley-VCH, 2006).
30 Allander, T. *et al.* Identification of a third human polyomavirus. *Journal of Virology* **81**, 4130-4136, doi:10.1128/jvi.00028-07 (2007).
31 Gaynor, A. M. *et al.* Identification of a novel polyomavirus from patients with acute respiratory tract infections. *Plos Pathogens* **3**, 595-604, doi:10.1371/journal.ppat.0030064 (2007).
32 Csoma, E., Meszaros, B., Asztalos, L., Konya, J. & Gergely, L. Prevalence of WU and KI Polyomaviruses in Plasma, Urine, and Respiratory Samples From Renal Transplant Patients. *Journal of Medical Virology* **83**, 1275-1278, doi:10.1002/jmv.22083 (2011).
33 Rao, S., Garcea, R. L., Robinson, C. C. & Simoes, E. A. F. WU and KI polyomavirus infections in pediatric hematology/oncology patients with acute respiratory tract illness. *Journal of Clinical Virology* **52**, 28-32, doi:10.1016/j.jcv.2011.05.024 (2011).
34 Schowalter, R. M., Pastrana, D. V., Pumphrey, K. A., Moyer, A. L. & Buck, C. B. Merkel Cell Polyomavirus and Two Previously Unknown Polyomaviruses Are

Chronically Shed from Human Skin. *Cell Host & Microbe* **7**, 509-515, doi:10.1016/j.chom.2010.05.006 (2010).
35 van der Meijden, E. *et al.* Discovery of a New Human Polyomavirus Associated with Trichodysplasia Spinulosa in an Immunocompromized Patient. *Plos Pathogens* **6**, doi:10.1371/journal.ppat.1001024 (2010).
36 Scuda, N. *et al.* A Novel Human Polyomavirus Closely Related to the African Green Monkey-Derived Lymphotropic Polyomavirus. *Journal of Virology* **85**, 4586-4590, doi:10.1128/jvi.02602-10 (2011).
37 Siebrasse, E. A. *et al.* Identification of MW Polyomavirus, a Novel Polyomavirus in Human Stool. *Journal of Virology* **86**, 10321-10326, doi:10.1128/jvi.01210-12 (2012).
38 Buck, C. B. *et al.* Complete Genome Sequence of a Tenth Human Polyomavirus. *Journal of Virology* **86**, 10887-10887, doi:10.1128/jvi.01690-12 (2012).
39 Yu, G. *et al.* Discovery of a Novel Polyomavirus in Acute Diarrheal Samples from Children. *Plos One* **7**, doi:10.1371/journal.pone.0049449 (2012).
40 Korup, S. *et al.* Identification of a Novel Human Polyomavirus in Organs of the Gastrointestinal Tract. *Plos One* **8**, doi:10.1371/journal.pone.0058021 (2013).
41 Lim, E. S. *et al.* Discovery of STL polyomavirus, a polyomavirus of ancestral recombinant origin that encodes a unique T antigen by alternative splicing. *Virology* **436**, 295-303, doi:10.1016/j.virol.2012.12.005 (2013).
42 Axthelm, M. K. *et al.* Meningoencephalitis and demyelination are pathologic manifestations of primary polyomavirus infection in immunosuppressed rhesus monkeys. *Journal of Neuropathology and Experimental Neurology* **63**, 750-758 (2004).
43 Dang, X., Wuthrich, C., Axthelm, M. K. & Koralnik, I. J. Productive simian virus 40 infection of neurons in immunosuppressed rhesus monkeys. *Journal of Neuropathology and Experimental Neurology* **67**, 784-792 (2008).
44 Horvath, C. J. *et al.* Simian-virus 40-induced disease in rhesus-monkeys with simian acquired-immunodeficiency-syndrome. *American Journal of Pathology* **140**, 1431-1440 (1992).
45 Murakami, Y., Wobbe, C. R., Weissbach, L., Dean, F. B. & Hurwitz, J. Role of DNA polymerase-alpha and DNA primase in simian virus-40 DNA-replication in vitro. *Proceedings of the National Academy of Sciences of the United States of America* **83**, 2869-2873, doi:10.1073/pnas.83.9.2869 (1986).
46 Arroyo, J. D. & Hahn, W. C. Involvement of PP2A in viral and cellular transformation. *Oncogene* **24**, 7746-7755, doi:10.1038/sj.onc.1209038 (2005).
47 Todaro, G. J. & Green, H. High frequency of SV40 transformation of mouse cell line 3T3. *Virology* **28**, 756-&, doi:10.1016/0042-6822(66)90261-3 (1966).
48 Ahuja, D., Saenz-Robles, M. T. & Pipas, J. M. SV40 large T antigen targets multiple cellular pathways to elicit cellular transformation. *Oncogene* **24**, 7729-7745, doi:10.1038/sj.onc.1209046 (2005).
49 Qi, F., Carbonen, M., Yang, H. & Gaudino, G. Simian virus 40 transformation, malignant mesothelioma and brain tumors. *Expert Review of Respiratory Medicine* **5**, 683-697, doi:10.1586/ers.11.51 (2011).
50 Gee, G. V. *et al.* SV40 associated miRNAs are not detectable in mesotheliomas. *British Journal of Cancer* **103**, 885-888, doi:10.1038/sj.bjc.6605848 (2010).
51 Kjaerheim, K. *et al.* Absence of SV40 antibodies or DNA fragments in prediagnostic mesothelioma serum samples. *International Journal of Cancer* **120**, 2459-2465, doi:10.1002/ijc.22592 (2007).

52 Moens, U., Van Ghelue, M. & Johannessen, M. Oncogenic potentials of the human polyomavirus regulatory proteins. *Cellular and Molecular Life Sciences* **64**, 1656-1678, doi:10.1007/s00018-007-7020-3 (2007).
53 Suzuki, T. *et al.* The Human Polyoma JC Virus Agnoprotein Acts as a Viroporin. *Plos Pathogens* **6**, doi:10.1371/journal.ppat.1000801 (2010).
54 Raghava, S., Giorda, K. M., Romano, F. B., Heuck, A. P. & Hebert, D. N. The SV40 Late Protein VP4 Is a Viroporin that Forms Pores to Disrupt Membranes for Viral Release. *Plos Pathogens* **7**, doi:10.1371/journal.ppat.1002116 (2011).
55 Neu, U., Woellner, K., Gauglitz, G. & Stehle, T. Structural basis of GM1 ganglioside recognition by simian virus 40. *Proceedings of the National Academy of Sciences of the United States of America* **105**, 5219-5224, doi:10.1073/pnas.0710301105 (2008).
56 Campanero-Rhodes, M. A. *et al.* N-glycolyl GM1 ganglioside as a receptor for simian virus 40. *Journal of Virology* **81**, 12846-12858, doi:10.1128/jvi.01311-07 (2007).
57 Norkin, L. C. Simian virus 40 infection via MHC class I molecules and caveolae. *Immunological Reviews* **168**, 13-22, doi:10.1111/j.1600-065X.1999.tb01279.x (1999).
58 Komagome, R. *et al.* Oligosaccharides as receptors for JC virus. *Journal of Virology* **76**, 12992-13000, doi:10.1128/jvi.76.24.12992-13000.2002 (2002).
59 Smith, A. E., Lilie, H. & Helenius, A. Ganglioside-dependent cell attachment and endocytosis of murine polyomavirus-like particles. *Febs Letters* **555**, 199-203, doi:10.1016/s0014-5793(03)01220-1 (2003).
60 Tsai, B. *et al.* Gangliosides are receptors for murine polyoma virus and SV40. *Embo Journal* **22**, 4346-4355, doi:10.1093/emboj/cdg439 (2003).
61 Low, J. A., Magnuson, B., Tsai, B. & Imperiale, M. J. Identification of gangliosides GD1b and GT1b as receptors for BK virus. *Journal of Virology* **80**, 1361-1366, doi:10.1128/jvi.80.3.1361-1366.2006 (2006).
62 Anderson, H. A., Chen, Y. Z. & Norkin, L. C. Bound simian virus 40 translocates to caveolin-enriched membrane domains, and its entry is inhibited by drugs that selectively disrupt caveolae. *Molecular Biology of the Cell* **7**, 1825-1834 (1996).
63 Querbes, W., Benmerah, A., Tosoni, D., Di Fiore, P. P. & Atwood, W. J. A JC virus-induced signal is required for infection of glial cells by a clathrin- and eps15-dependent pathway. *Journal of Virology* **78**, 250-256, doi:10.1128/jvi.78.1.250-256.2004 (2004).
64 Qu, Q. M. *et al.* Nuclear entry mechanism of the human polyomavirus JC virus-like particle - Role of importins and the nuclear pore complex. *Journal of Biological Chemistry* **279**, 27735-27742, doi:10.1074/jbc.M310827200 (2004).
65 Bikel, I. & Loeken, M. R. Involvement of simian virus-40 (SV40) small T-antigen in transactivation of SV40 early and late promoters. *Journal of Virology* **66**, 1489-1494 (1992).
66 Jat, P. S., Cepko, C. L., Mulligan, R. C. & Sharp, P. A. Recombinant retroviruses encoding simia-virus 40 large T-antigen and polyomavirus large and middle T-antigen. *Molecular and Cellular Biology* **6**, 1204-1217 (1986).
67 Chowdhury, M. *et al.* Regulation of the human neurotropic virus promoter by JCV-T antigen and HIV-1 TAT protein. *Oncogene* **5**, 1737-1742 (1990).
68 Chenciner, N. *et al.* Integrated and free viral-DNA in hamster tumors induced by BK virus. *Proceedings of the National Academy of Sciences of the United States of America-Biological Sciences* **77**, 975-979, doi:10.1073/pnas.77.2.975 (1980).
69 Mandl, C. W. & Frisque, R. J. Characterization of cells transformed by the human polyomavirus JC virus. *Journal of General Virology* **67**, 1733-1739, doi:10.1099/0022-1317-67-8-1733 (1986).

70 Hirai, K., Lehman, J. & Defendi, V. Integration of simian virus 40 deoxyribonucleic acid into deoxyribonucleic acid of primary infected Chinese hamster cells. *Journal of Virology* **8**, 708-& (1971).
71 Feng, H. C., Shuda, M., Chang, Y. & Moore, P. S. Clonal integration of a polyomavirus in human Merkel cell carcinoma. *Science* **319**, 1096-1100, doi:10.1126/science.1152586 (2008).
72 Martel-Jantin, C. *et al.* Genetic variability and integration of Merkel cell polyomavirus in Merkel cell carcinoma. *Virology* **426**, 134-142, doi:10.1016/j.virol.2012.01.018 (2012).
73 DeCaprio, J. A. & Garcea, R. L. A cornucopia of human polyomaviruses. *Nature Reviews Microbiology* **11**, 264-276, doi:10.1038/nrmicro2992 (2013).
74 Shuda, M. *et al.* T antigen mutations are a human tumor-specific signature for Merkel cell polyomavirus. *Proceedings of the National Academy of Sciences of the United States of America* **105**, 16272-16277, doi:10.1073/pnas.0806526105 (2008).
75 Houben, R. *et al.* Merkel Cell Polyomavirus-Infected Merkel Cell Carcinoma Cells Require Expression of Viral T Antigens. *Journal of Virology* **84**, 7064-7072, doi:10.1128/jvi.02400-09 (2010).
76 Wallenburg, J. C., Nepveu, A. & Chartrand, P. Random and nonrandom integration of a polyomavirus DNA molecule containing highly repetitive cellular sequences. *Journal of Virology* **50**, 678-683 (1984).
77 Chang, L. S., Pan, S., Pater, M. M. & Dimayorca, G. Differential requirement for SV40 early genes in immortalization and transformation of primary rat and human-embryonic cells. *Virology* **146**, 246-261, doi:10.1016/0042-6822(85)90008-x (1985).
78 Hahn, W. C. *et al.* Enumeration of the simian virus 40 early region elements necessary for human cell transformation. *Molecular and Cellular Biology* **22**, 2111-2123, doi:10.1128/mcb.22.7.2111-2123.2002 (2002).
79 Crandall, K. A., Perez-Losada, M., Christensen, R. G., McClellan, D. A. & Viscidi, R. P. Phylogenomics and molecular evolution of polyomaviruses. *Polyomaviruses and Human Diseases* **577**, 46-59 (2006).
80 Horton, R. M., Hunt, H. D., Ho, S. N., Pullen, J. K. & Pease, L. R. Engineering hybrid genes without the use of restriction enzymes - gene-splicing by overlap extension. *Gene* **77**, 61-68, doi:10.1016/0378-1119(89)90359-4 (1989).
81 Janssens, V. & Goris, J. Protein phosphatase 2A: a highly regulated family of serine/threonine phosphatases implicated in cell growth and signalling. *Biochemical Journal* **353**, 417-439, doi:10.1042/0264-6021:3530417 (2001).
82 Rodriguez-Viciana, P., Collins, C. & Fried, M. Polyoma and SV40 proteins differentially regulate PP2A to activate distinct cellular signaling pathways involved in growth control. *Proceedings of the National Academy of Sciences of the United States of America* **103**, 19290-19295, doi:10.1073/pnas.0609343103 (2006).
83 Usui, H. *et al.* 3 distinct forms of type-2A protein phosphatase i human-erythrocyte cytosol3 DISTINCT FORMS OF TYPE-2A PROTEIN PHOSPHATASE IN HUMAN-ERYTHROCYTE CYTOSOL. *Journal of Biological Chemistry* **263**, 3752-3761 (1988).
84 Ogris, E., Gibson, D. M. & Pallas, D. C. Protein phosphatase 2A subunit assembly: the catalytic subunit carboxy terminus is important for binding cellular B subunit but not polyomavirus middle tumor antigen. *Oncogene* **15**, 911-917, doi:10.1038/sj.onc.1201259 (1997).
85 Silverstein, A. M., Barrow, C. A., Davis, A. J. & Mumby, M. C. Actions of PP2A on the MAP kinase pathway and apoptosis are mediated by distinct regulatory subunits. *Proceedings of the National Academy of Sciences of the United States of America* **99**, 4221-4226, doi:10.1073/pnas.072071699 (2002).

86 Mumby, M. PP2A: Unveiling a reluctant tumor suppressor. *Cell* **130**, 21-24, doi:10.1016/j.cell.2007.06.034 (2007).
87 Zhou, J., Pham, H. T., Ruediger, R. & Walter, G. Characterization of the A alpha and A beta subunit isoforms of protein phosphatase 2A: differences in expression, subunit interaction, and evolution. *Biochemical Journal* **369**, 387-398, doi:10.1042/bj20021244 (2003).
88 Yang, S. I. *et al.* Control of protein phosphatase-2A by simian virus-40 small-T antigen. *Molecular and Cellular Biology* **11**, 1988-1995 (1991).
89 Peden, K. W. C. *et al.* A DNA replication-positive mutant of simian virus-40 that is defective for transformation and the production of infectious virions. *Journal of Virology* **64**, 2912-2921 (1990).
90 Yeh, E. *et al.* A signalling pathway controlling c-Myc degradation that impacts oncogenic transformation of human cells. *Nature Cell Biology* **6**, 308-318, doi:10.1038/ncb1110 (2004).
91 Ruediger, R., Hentz, M., Fait, J., Mumby, M. & Walter, G. Molecular-model of the A-subunit of protein phosphatase 2A - interaction with other subunits and tumor-antigens. *Journal of Virology* **68**, 123-129 (1994).
92 Yu, J., Boyapati, A. & Rundell, K. Critical role for SV40 small-t antigen in human cell transformation. *Virology* **290**, 192-198, doi:10.1006/viro.2001.1204 (2001).
93 Loeken, M., Bikel, I., Livingston, D. M. & Brady, J. Trans-activation of RNA polymerase-II and polymerase-III promoters by SV40 small T-antigen. *Cell* **55**, 1171-1177, doi:10.1016/0092-8674(88)90261-9 (1988).
94 Cavender, J. F., Mummert, C. & Tevethia, M. J. Transactivation of a ribosomal gene by simian virus 40 large-T antigen requires at least three activities of the protein. *Journal of Virology* **73**, 214-224 (1999).
95 Sugano, S., Yamaguchi, N. & Shimojo, H. Small T-protein of simian virus-40 is required for dense focus formation in a rat-cell line. *Journal of Virology* **41**, 1073-1075 (1982).
96 Bikel, I. *et al.* SV40 small T-antigen enhances the transformation activity of limiting concentrations of SV40 large T-antigen. *Cell* **48**, 321-330, doi:10.1016/0092-8674(87)90435-1 (1987).
97 Huang, K., Flanagan, J. M. & Prestegard, J. H. The influence of C-terminal extension on the structure of the "J-domain" in E-coli DnaJ. *Protein Science* **8**, 203-214 (1999).
98 Campbell, K. S. *et al.* DnaJ/hsp40 chaperone domain of SV40 large T antigen promotes efficient viral DNA replication. *Genes & Development* **11**, 1098-1110, doi:10.1101/gad.11.9.1098 (1997).
99 Sontag, E. *et al.* The interaction of SV40 Small tumor-antigen with protein phosphatase-2A stimulates the MAP kinase pathways and induces cell-proliferation. *Cell* **75**, 887-897, doi:10.1016/0092-8674(93)90533-v (1993).
100 Winston, J., Dong, F. & Pledger, W. J. Differential modulation of G(1) cyclins and the Cdk inhibitor p27(kip1) by platelet-derived growth factor and plasma factors in density-arrested fibroblasts. *Journal of Biological Chemistry* **271**, 11253-11260 (1996).
101 Polyak, K. *et al.* p27(kip1), a cyclin-cdk inhibitor, links transforming growth-factor-beta and contact inhibition to cell-cycle arrest. *Genes & Development* **8**, 9-22, doi:10.1101/gad.8.1.9 (1994).
102 Moreno, C. S. *et al.* Signaling and transcriptional changes critical for transformation of human cells by simian virus 40 small tumor antigen or protein phosphatase 2A B56 gamma knockdown. *Cancer Research* **64**, 6978-6988, doi:10.1158/0008-5472.can-04-1150 (2004).

103 Pipas, J. M. Common and unique features of T-antigens encoded by the polyomavirus group. *Journal of Virology* **66**, 3979-3985 (1992).
104 Yaciuk, P., Carter, M. C., Pipas, J. M. & Moran, E. Simian virus-40 large-T antigen expresses a biological-activity complementary to the p300-associated transforming function of the adenovirus E1A gene-products. *Molecular and Cellular Biology* **11**, 2116-2124 (1991).
105 Martinato, F., Cesaroni, M., Amati, B. & Guccione, E. Analysis of Myc-Induced Histone Modifications on Target Chromatin. *Plos One* **3**, doi:10.1371/journal.pone.0003650 (2008).
106 Tiemann, F., Zerrahn, J. & Deppert, W. Cooperation of simian-virus-40 large-T and small-T antigens in metabolic stabilization of tumor-suppressor p53 during cellular-transformation. *Journal of Virology* **69**, 6115-6121 (1995).
107 Conkright, M. D. & Montminy, M. CREB: the unindicted cancer co-conspirator. *Trends in Cell Biology* **15**, 457-459, doi:10.1016/j.tcb.2005.07.007 (2005).
108 Piva, R., Belardo, G. & Santoro, M. G. NF-kappa B: A stress-regulated switch for cell survival. *Antioxidants & Redox Signaling* **8**, 478-486, doi:10.1089/ars.2006.8.478 (2006).
109 Ozanne, B. W., Spence, H. J., McGarry, L. C. & Hennigan, R. F. Transcription factors control invasion: AP-1 the first among equals. *Oncogene* **26**, 1-10, doi:10.1038/sj.onc.1209759 (2007).
110 Yuan, T. L. & Cantley, L. C. PI3K pathway alterations in cancer: variations on a theme. *Oncogene* **27**, 5497-5510, doi:10.1038/onc.2008.245 (2008).
111 Hiyama, E. & Hiyama, K. Telomerase detection in the diagnosis and prognosis of cancer. *Cytotechnology* **45**, 61-74, doi:10.1007/s10616-004-5126-0 (2004).
112 Yuan, H., Veldman, T., Rundell, K. & Schlegel, R. Simian virus 40 small tumor antigen activates AKT and telomerase and induces anchorage-independent growth of human epithelial cells. *Journal of Virology* **76**, 10685-10691, doi:10.1128/jvi.76.21.10685-10691.2002 (2002).
113 Kang, S. S., Kwon, T., Kwon, D. Y. & Do, S. I. Akt protein kinase enhances human telomerase activity through phosphorylation of telomerase reverse transcriptase subunit. *Journal of Biological Chemistry* **274**, 13085-13090, doi:10.1074/jbc.274.19.13085 (1999).
114 Poulsen, M. Merkel-cell carcinoma of the skin. *Lancet Oncology* **5**, 593-599, doi:10.1016/s1470-2045(04)01593-1 (2004).
115 Guo, C. *et al.* Bub1 up-regulation and hyperphosphorylation promote malignant transformation in SV40 tag-induced transgenic mouse models. *Molecular Cancer Research* **4**, 957-969, doi:10.1158/1541-7786.mcr-06-0168 (2006).
116 Decaprio, J. A. *et al.* SV40 large tumor-antigen forms a specific complex with the product of the retinoblastoma susceptibility gene. *Cell* **54**, 275-283, doi:10.1016/0092-8674(88)90559-4 (1988).
117 Kierstead, T. D. & Tevethia, M. J. Association of p53 binding ad immortalization of primary C57BL/6 mouse embryo fibroblasts by using simian-virus 40 T-antigen mutants bearing internal overlapping deletion mutations. *Journal of Virology* **67**, 1817-1829 (1993).
118 Peden, K. W. C., Srinivasan, A., Farber, J. M. & Pipas, J. M. Mutants with changes within or near a hydrophobic region of simian virus-40 large tumor-antigen are defective for binding cellular protein-p53. *Virology* **168**, 13-21, doi:10.1016/0042-6822(89)90398-x (1989).
119 Liu, X. *et al.* Merkel Cell Polyomavirus Large T Antigen Disrupts Lysosome Clustering by Translocating Human Vam6p from the Cytoplasm to the Nucleus. *Journal of Biological Chemistry* **286**, 17079-17090, doi:10.1074/jbc.M110.192856 (2011).

120 Ali, S. H. & DeCaprio, J. A. Cellular transformation by SV40 large T antigen: interaction with host proteins. *Seminars in Cancer Biology* **11**, 15-22, doi:10.1006/scbi.2000.0342 (2001).
121 Stahl, H., Droge, P. & Knippers, R. DNA helicase activity of SV40 large tumor-antigen. *Embo Journal* **5**, 1939-1944 (1986).
122 Dean, F. B. *et al.* Simian-virus 40 (SV40) DNA-replication - SV40 large T-antigen unwinds DNA containing the SV40 origin of replicaiton. *Proceedings of the National Academy of Sciences of the United States of America* **84**, 16-20, doi:10.1073/pnas.84.1.16 (1987).
123 Brady, J., Bolen, J. B., Radonovich, M., Salzman, N. & Khoury, G. Stimulation of simian virus-40 late gene-expression by simian virus-40 tumor-antigen. *Proceedings of the National Academy of Sciences of the United States of America-Biological Sciences* **81**, 2040-2044, doi:10.1073/pnas.81.7.2040 (1984).
124 Zhu, J. Y., Rice, P. W., Chamberlain, M. & Cole, C. N. Mapping the transcriptional transactivation function of simian virus-40 large T-antigen. *Journal of Virology* **65**, 2778-2790 (1991).
125 Dornreiter, I., Hoss, A., Arthur, A. K. & Fanning, E. SV40 T-antigen binds directly to the large subunit of purified DNA polymerase-alpha. *Embo Journal* **9**, 3329-3336 (1990).
126 Melendy, T. & Stillman, B. An interaction between replication protein-A and SV40 T-antigen appears essential for primosome assembly during SV40 DNA-replication. *Journal of Biological Chemistry* **268**, 3389-3395 (1993).
127 Seinsoth, S., Uhlmann-Schiffler, H. & Stahl, H. Bidirectional DNA unwinding by a ternary complex of T antigen, nucleolin and topoisomerase I. *Embo Reports* **4**, 263-268, doi:10.1038/sj.embor.embor770 (2003).
128 Saenz-Robles, M. T., Sullivan, C. S. & Pipas, J. M. Transforming functions of Simian Virus 40. *Oncogene* **20**, 7899-7907, doi:10.1038/sj.onc.1204936 (2001).
129 Sullivan, C. S. & Pipas, J. M. T antigens of Simian virus 40: Molecular chaperones for viral replication and turnorigenesis. *Microbiology and Molecular Biology Reviews* **66**, 179-+, doi:10.1128/mmbr.66.2.179-202.2002 (2002).
130 Sachsenmeier, K. F. & Pipas, J. M. Inhibition of Rb and p53 is insufficient for SV40 T-antigen transformation. *Virology* **283**, 40-48, doi:10.1006/viro.2001.0866 (2001).
131 Harris, K. F., Christensen, J. B., Radany, E. H. & Imperiale, M. J. Novel mechanisms of E2F induction by BK virus large-T antigen: Requirement of both the pRb-binding and the J domains. *Molecular and Cellular Biology* **18**, 1746-1756 (1998).
132 Bollag, B., Prins, C., Snyder, E. L. & Frisque, R. J. Purified JC virus T and T ' proteins differentially interact with the retinoblastoma family of tumor suppressor proteins. *Virology* **274**, 165-178, doi:10.1006/viro.2000.0451 (2000).
133 Chen, S. & Paucha, E. Identification of a region of simain virus-40 large T-antigen required for cell transformation. *Journal of Virology* **64**, 3350-3357 (1990).
134 Liu, X. & Marmorstein, R. Structure of the retinoblastoma protein bound to adenovirus E1A reveals the molecular basis for viral oncoprotein inactivation of a tumor suppressor. *Genes & Development* **21**, 2711-2716, doi:10.1101/gad.1590607 (2007).
135 Rowland, B. D. & Bernards, R. Re-evaluating cell-cycle regulation by E2Fs. *Cell* **127**, 871-874, doi:10.1016/j.cell.2006.11.019 (2006).
136 Weinberg, R. A. The retinoblastoma protein and cell-cycle control. *Cell* **81**, 323-330, doi:10.1016/0092-8674(95)90385-2 (1995).
137 Felsani, A., Mileo, A. M. & Paggi, M. G. Retinoblastoma family proteins as key targets of the small DNA virus oncoproteins. *Oncogene* **25**, 5277-5285, doi:10.1038/sj.onc.1209621 (2006).

138 Harris, K. F., Christensen, J. B. & Imperiale, M. J. BK virus large T antigen: Interactions with the retinoblastoma family of tumor suppressor proteins and on cellular growth control. *Journal of Virology* **70**, 2378-2386 (1996).
139 Srinivasan, A., Peden, K. W. C. & Pipas, J. M. The Large Tumor-Antigen Of Simian-Virus-40 Encodes At Least 2 Distinct Transforming Functions. *Journal Of Virology* **63**, 5459-5463 (1989).
140 Hollstein, M., Sidransky, D., Vogelstein, B. & Harris, C. C. p53 mutations in human cancers. *Science* **253**, 49-53, doi:10.1126/science.1905840 (1991).
141 Quelle, D. E., Zindy, F., Ashmun, R. A. & Sherr, C. J. Alternative reading frames of the INK4A tumor-suppressor gene encode 2 unrelated proteins capable of inducing cell-cycle arrest. *Cell* **83**, 993-1000 (1995).
142 Segawa, K., Minowa, A., Sugasawa, K., Takano, T. & Hanaoka, F. Abrogation of p53-mediated transactivation by SV40 large T-antigen. *Oncogene* **8**, 543-548 (1993).
143 Jiang, D., Srinivasan, A., Lozano, G. & Robbins, P. D. SV40 T-antigen abrogates p53-mediated transcriptional activity. *Oncogene* **8**, 2805-2812 (1993).
144 Mietz, J. A., Unger, T., Huibregtse, J. M. & Howley, P. M. The transcriptional transactivation function of wild-type-p53 is inhibited by SV40 large T-antigen and by HPV-16 E6-oncoprotein. *Embo Journal* **11**, 5013-5020 (1992).
145 Dias, D. C., Dolios, G., Wang, R. & Pan, Z. Q. CUL7: A DOC domain-containing cullin selectively binds Skp1 center dot Fbx29 to form an SCF-like complex. *Proceedings of the National Academy of Sciences of the United States of America* **99**, 16601-16606, doi:10.1073/pnas.252646399 (2002).
146 Ali, S. H., Kasper, J. S., Arai, T. & DeCaprio, J. A. Cu17/p185/p193 binding to simian virus 40 large T antigen has a role in cellular transformation. *Journal of Virology* **78**, 2749-2757, doi:10.1128/jvi.78.6.2749-2757.2004 (2004).
147 Trojanek, J. *et al.* T-Antigen of the human polyomavirus JC attenuates faithful DNA repair by forcing nuclear interaction between IRS-1 and Rad51. *Journal of Cellular Physiology* **206**, 35-46, doi:10.1002/jcp.20425 (2006).
148 Prisco, M. *et al.* Nuclear translocation of insulin receptor substrate-1 by the simian virus 40 T antigen and the activated type 1 insulin-like growth factor receptor. *Journal of Biological Chemistry* **277**, 32078-32085, doi:10.1074/jbc.M204658200 (2002).
149 Lassak, A. *et al.* Insulin receptor substrate 1 translocation to the nucleus by the human JC virus T-antigen. *Journal of Biological Chemistry* **277**, 17231-17238, doi:10.1074/jbc.M110885200 (2002).
150 Urbanska, K. *et al.* Estrogen Receptor beta-Mediated Nuclear Interaction Between IRS-1 and Rad51 Inhibits Homologous Recombination Directed DNA Repair in Medulloblastoma. *Journal of Cellular Physiology* **219**, 392-401, doi:10.1002/jcp.21683 (2009).
151 Enam, S. *et al.* Association of human polyomavirus JCV with colon cancer: Evidence for interaction of viral T-antigen and beta-catenin. *Cancer Research* **62**, 7093-7101 (2002).
152 Gan, D. D. *et al.* Involvement of Wnt signaling pathway in murine medulloblastoma induced by human neurotropic JC virus. *Oncogene* **20**, 4864-4870, doi:10.1038/sj.onc.1204670 (2001).
153 Reya, T. & Clevers, H. Wnt signalling in stem cells and cancer. *Nature* **434**, 843-850, doi:10.1038/nature03319 (2005).
154 Berger, L. C. *et al.* Interaction between T antigen and TEA domain of the factor TEF-1 derepresses simian virus 40 late promoter in vitro: Identification of T-antigen domains important for transcription control. *Journal of Virology* **70**, 1203-1212 (1996).

155 Zuzarte, P. C., Farrance, I. K. G., Simpson, P. C. & Wildeman, A. G. Tumor cell splice variants of the transcription factor TEF-1 induced by SV40 T-antigen transformation. *Biochimica Et Biophysica Acta-Gene Structure and Expression* **1517**, 82-90, doi:10.1016/s0167-4781(00)00261-x (2000).
156 Ito, Y., Brocklehurst, J. R. & Dulbecco, R. Virus-specific proteins in plasma-membrane of cells lytically infected or transformed by poloma-virus. *Proceedings of the National Academy of Sciences of the United States of America* **74**, 4666-4670, doi:10.1073/pnas.74.10.4666 (1977).
157 Dilworth, S. M. *et al.* Subcellular-localization of the middle and large T-antigens of polyoma-virus. *Embo Journal* **5**, 491-499 (1986).
158 Fluck, M. M. & Schaffhausen, B. S. Lessons in Signaling and Tumorigenesis from Polyomavirus Middle T Antigen. *Microbiology and Molecular Biology Reviews* **73**, 542-+, doi:10.1128/mmbr.00009-09 (2009).
159 Mueller, C. R., Muller, W. J. & Hassell, J. A. The polyomavirus enhancers comprises multiple functional elements. *Journal of Virology* **62**, 1667-1678 (1988).
160 Freund, R., Sotnikov, A., Bronson, R. T. & Benjamin, T. L. Polyoma-virus middle T-antigen is essential for virus-replication and persistence as well as for tumor-induction in mice. *Virology* **191**, 716-723, doi:10.1016/0042-6822(92)90247-m (1992).
161 Schonthal, A., Srinivas, S. & Eckhart, W. Induction of C-jun protooncogene expression and transcription factor AP-1 activity by the polyoma-virus middle-sized tumor-antigen. *Proceedings of the National Academy of Sciences of the United States of America* **89**, 4972-4976, doi:10.1073/pnas.89.11.4972 (1992).
162 Urich, M., Elshemerly, M. Y. M., Besser, D., Nagamine, Y. & Ballmerhofer, K. Activation and nuclear translocation of mitogen-activated protein-kinases by polyomavirus middle-T or serum depend on phosphatidylinositol 3-kinase. *Journal of Biological Chemistry* **270**, 29286-29292 (1995).
163 Srinivas, S., Schonthal, A. & Eckhart, W. Polyomavirus middle-sized tumor-antigen modulates C-Jun phosphorylation and transcriptional activity. *Proceedings of the National Academy of Sciences of the United States of America* **91**, 10064-10068, doi:10.1073/pnas.91.21.10064 (1994).
164 Garcea, R. L. & Benjamin, T. L. Host range transforming gene of polyoma-virus plays a role in virus assembly. *Proceedings of the National Academy of Sciences of the United States of America-Biological Sciences* **80**, 3613-3617, doi:10.1073/pnas.80.12.3613 (1983).
165 Li, M. L. & Garcea, R. L. Identification of the threonine phosphorylation sites on the polyomavirus major capsid protein VP1 - realtionship of middle T-antigen. *Journal of Virology* **68**, 320-327 (1994).
166 Elliott, J., Jones, M. D., Griffin, B. E. & Krauzewicz, N. Regulation of cytoskeletal association by a basic amino acid motif in polyoma virus middle T antigen. *Oncogene* **17**, 1797-1806, doi:10.1038/sj.onc.1202083 (1998).
167 Templeton, D. & Eckhart, W. N-TERMINAL AMINO-ACID-SEQUENCES OF THE POLYOMA MIDDLE-SIZE T-ANTIGEN ARE IMPORTANT FOR PROTEIN-KINASE ACTIVITY AND CELL-TRANSFORMATION. *Molecular and Cellular Biology* **4**, 817-821 (1984).
168 Zhu, W. J., Eicher, A., Leber, B. & Andrews, D. W. At the onset of transformation polyomavirus middle-T recruits shc and src to a perinuclear compartment coincident with condensation of endosomes. *Oncogene* **17**, 565-576, doi:10.1038/sj.onc.1201979 (1998).

169 Zhou, G. S. *et al.* Protein phosphatase 4 is involved in tumor necrosis factor-alpha-induced activation of c-Jun N-terminal kinase. *Journal of Biological Chemistry* **277**, 6391-6398, doi:10.1074/jbc.M107014200 (2002).
170 Pallas, D. C. *et al.* Polyoma small and middle T-antigens and SV40 small T-antigen form stable complexes with protein phosphatase 2A. *Cell* **60**, 167-176, doi:10.1016/0092-8674(90)90726-u (1990).
171 Mullane, K. P., Ratnofsky, M., Cullere, X. & Schaffhausen, B. Signaling from polyomavirus middle T and small T defines different roles for protein phosphatase 2A. *Molecular and Cellular Biology* **18**, 7556-7564 (1998).
172 Glover, H. R., Brewster, C. E. P. & Dilworth, S. M. Association between src-kinases and the polyoma virus oncogene middle T-antigen requires PP2A and a specific sequence motif. *Oncogene* **18**, 4364-4370, doi:10.1038/sj.onc.1202816 (1999).
173 Templeton, D. & Eckhart, W. N-terminal amino-acid-sequences of the polyomavirus middle-size T-antigen are important for protein-kinase activity and cell-transformation. *Molecular and Cellular Biology* **4**, 817-821 (1984).
174 Harvey, R., Oostra, B. A., Belsham, G. J., Gillett, P. & Smith, A. E. An antibody to a synthetic peptide recognizes polyomavirus middle-T antigen and reveals multiple in vitro tyrosine phosphorylation sites. *Molecular and Cellular Biology* **4**, 1334-1342 (1984).
175 Hunter, T., Hutchinson, M. A. & Eckhart, W. Polyoma middle-sized T-antigen can be phosphorylated on tyrosine at multiple sites in vitro. *Embo Journal* **3**, 73-79 (1984).
176 Zerrahn, J., Knippschild, U., Winkler, T. & Deppert, W. Independent expression of the transforming amino-terminal domain of SV40 large T-antigen from an alternatively spliced 3rd early messenger-RNA. *Embo Journal* **12**, 4739-4746 (1993).
177 Bollag, B., Kilpatrick, L. H., Tyagarajan, S. K., Tevethia, M. J. & Frisque, R. J. JC virus T '(135), T '(136) and T '(165) proteins interact with cellular p107 and p130 in vivo and influence viral transformation potential. *Journal of Neurovirology* **12**, 428-442, doi:10.1080/13550280601009553 (2006).
178 Frisque, R. J., Hofstetter, C. & Tyagarajan, S. K. Transforming activities of JC virus early proteins. *Polyomaviruses and Human Diseases* **577**, 288-309 (2006).
179 Morrison, K. M., Miesegaes, G. R., Lumpkin, E. A. & Maricich, S. M. Mammalian Merkel cells are descended from the epidermal lineage. *Developmental Biology* **336**, 76-83, doi:10.1016/j.ydbio.2009.09.032 (2009).
180 Merkel, F. Vol. 11 636-652 (Arch. Mikr. Anat., 1875).
181 Szeder, V., Grim, M., Halata, Z. & Sieber-Blum, M. Neural crest origin of mammalian Merkel cells. *Developmental Biology* **253**, 258-263, doi:10.1016/s0012-1606(02)00015-5 (2003).
182 Moll, I., Paus, R. & Moll, R. Merkel cells in mouse skin: Intermediate filament pattern, localization, and hair cycle-dependent density. *Journal of Investigative Dermatology* **106**, 281-286, doi:10.1111/1523-1747.ep12340714 (1996).
183 May, C. A. & Osterland, I. Merkel cell distribution in the human eyelid. *European Journal of Histochemistry* **57**, 224-226, doi:10.4081/ejh.2013.e33 (2013).
184 Grim, M. & Halata, Z. Developmental origin of avian Merkel cells. *Anatomy and Embryology* **202**, 401-410, doi:10.1007/s004290000121 (2000).
185 Compton, C. C., Regauer, S., Seiler, G. R. & Landry, D. B. Human Merkel cell regeneration in skin derived from cultured keratinocyte grafts. *Laboratory Investigation* **63**, 233-241 (1990).
186 Kuwamoto, S. Recent advances in the biology of Merkel cell carcinoma. *Human Pathology* **42**, 1063-1077, doi:10.1016/j.humpath.2011.01.020 (2011).

187 Fernandez-Figueras, M.-T. *et al.* Expression profiles associated with aggressive behavior in Merkel cell carcinoma. *Modern Pathology* **20**, 90-101, doi:10.1038/modpathol.3800717 (2007).
188 Heath, M. *et al.* Clinical characteristics of Merkel cell carcinoma at diagnosis in 195 patients: the AEIOU features. *Journal of the American Academy of Dermatology* **58**, 375-381, doi:10.1016/j.jaad.2007.11.020 (2008).
189 Gueler-Nizam, E. *et al.* Clinical course and prognostic factors of Merkel cell carcinoma of the skin. *British Journal of Dermatology* **161**, 90-94, doi:10.1111/j.1365-2133.2009.09155.x (2009).
190 Goedert, J. J. & Rockville Merkel Cell Carcinoma, G. Merkel Cell Carcinoma: Recent Progress and Current Priorities on Etiology, Pathogenesis, and Clinical Management. *Journal of Clinical Oncology* **27**, 4021-4026, doi:10.1200/jco.2009.22.6605 (2009).
191 Bobos, M., Hytiroglou, P., Kostopoulos, I., Karkavelas, G. & Papadimitriou, C. S. Immunohistochemical distinction between Merkel cell carcinoma and small cell carcinoma of the lung. *American Journal of Dermatopathology* **28**, 99-104, doi:10.1097/01.dad.0000183701.67366.c7 (2006).
192 Wong, H. H. & Wang, J. Vol. 134(11) 1711-1716 (Archives of Pathology & Laboratory Medicine, 2009).
193 Donepudi, S., DeConti, R. C. & Samlowski, W. E. Recent Advances in the Understanding of the Genetics, Etiology, and Treatment of Merkel Cell Carcinoma. *Seminars in Oncology* **39**, 163-172, doi:10.1053/j.seminoncol.2012.01.003 (2012).
194 Calder, K. B., Coplowitz, S., Schlauder, S. & Morgan, M. B. A case series and immunophenotypic analysis of CK20-/CK7+primary neuroendocrine carcinoma of the skin. *Journal of Cutaneous Pathology* **34**, 918-923, doi:10.1111/j.1600-0560.2007.00759.x (2007).
195 Ferringer, T., Rogers, H. C. & Metcalf, J. S. Merkel cell carcinoma in situ. *Journal of Cutaneous Pathology* **32**, 162-165, doi:10.1111/j.0303-6987.2005.00270.x (2005).
196 Network, N.-N. C. I. *Rare skin cancer in England*, 2008).
197 Agelli, M. & Clegg, L. X. Epidemiology of primary Merkel cell carcinoma in the United States. *Journal of the American Academy of Dermatology* **49**, 832-841, doi:10.1067/s0190-9622(03)02108-x (2003).
198 Miller, R. W. & Rabkin, C. S. Merkel cell carcinoma and melanoma: Etiological similarities and differences. *Cancer Epidemiology Biomarkers & Prevention* **8**, 153-158 (1999).
199 Lemos, B. D. *et al.* Pathologic nodal evaluation improves prognostic accuracy in Merkel cell carcinoma: Analysis of 5823 cases as the basis of the first consensus staging system. *Journal of the American Academy of Dermatology* **63**, 751-761, doi:10.1016/j.jaad.2010.02.056 (2010).
200 Sarnaik, A. A., Lien, M. H., Nghiem, P. & Bichakjian, C. K. Clinical Recognition, Diagnosis, and Staging of Merkel Cell Carcinoma, and the Role of the Multidisciplinary Management Team. *Current Problems in Cancer* **34**, 38-46, doi:10.1016/j.currproblcancer.2010.01.002 (2010).
201 Lemos, B. & Nghiem, P. Merkel cell carcinoma: More deaths but still no pathway to blame. *Journal of Investigative Dermatology* **127**, 2100-2103, doi:10.1038/sj.jid.5700925 (2007).
202 Mogha, A. *et al.* Merkel Cell Polyomavirus Small T Antigen mRNA Level Is Increased following In Vivo UV-Radiation. *Plos One* **5**, doi:10.1371/journal.pone.0011423 (2010).

203 Nathu, R. M., Mendenhall, W. M. & Parsons, J. T. Radiotherapy for Merkel cell carcinoma of the skin. *International Journal of Radiation Oncology Biology Physics* **39**, 310-310, doi:10.1016/s0360-3016(97)80907-8 (1997).
204 Gupta, S. G. *et al.* Sentinel lymph node biopsy for evaluation and treatment of patients with Merkel cell carcinoma - The Dana-Farber experience and meta-analysis of the literature. *Archives of Dermatology* **142**, 685-690, doi:10.1001/archderm.142.6.685 (2006).
205 Tai, P. T. H. *et al.* Chemotherapy in neuroendocrine/Merkel cell carcinoma of the skin: Case series and review of 204 cases. *Journal of Clinical Oncology* **18**, 2493-2499 (2000).
206 Boshoff, C. & Chang, Y. Kaposi's sarcoma - Associated herpesvirus: A new DNA tumor virus. *Annual Review of Medicine* **52**, 453-470, doi:10.1146/annurev.med.52.1.453 (2001).
207 Becker, J. C. Merkel cell carcinoma. *Annals of Oncology* **21**, 81-85, doi:10.1093/annonc/mdq366 (2010).
208 Sastre-Garau, X. *et al.* Merkel cell carcinoma of the skin: pathological and molecular evidence for a causative role of MCV in oncogenesis. *Journal of Pathology* **218**, 48-56, doi:10.1002/path.2532 (2009).
209 Kean, J. M., Rao, S., Wang, M. & Garcea, R. L. Seroepidemiology of Human Polyomaviruses. *Plos Pathogens* **5**, doi:10.1371/journal.ppat.1000363 (2009).
210 Katano, H. *et al.* Detection of Merkel Cell Polyomavirus in Merkel Cell Carcinoma and Kaposi's Sarcoma. *Journal of Medical Virology* **81**, 1951-1958, doi:10.1002/jmv.21608 (2009).
211 Andres, C., Ihrler, S., Puchta, U. & Flaig, M. J. Merkel cell polyomavirus is prevalent in a subset of small cell lung cancer: a study of 31 patients. *Thorax* **64**, 1007-1008, doi:10.1136/thx.2009.117911 (2009).
212 Kassem, A. *et al.* Merkel cell polyomavirus sequences are frequently detected in nonmelanoma skin cancer of immunosuppressed patients. *International Journal of Cancer* **125**, 356-361, doi:10.1002/ijc.24323 (2009).
213 Koljonen, V. *et al.* Chronic lymphocytic leukaemia patients have a high risk of Merkel-cell polyomavirus DNA-positive Merkel-cell carcinoma. *British Journal of Cancer* **101**, 1444-1447, doi:10.1038/sj.bjc.6605306 (2009).
214 Teman, C. J., Tripp, S. R., Perkins, S. L. & Duncavage, E. J. Merkel cell polyomavirus (MCPyV) in chronic lymphocytic leukemia/small lymphocytic lymphoma. *Leukemia Research* **35**, 689-692, doi:10.1016/j.leukres.2011.01.032 (2011).
215 Reisinger, D. M., Shiffer, J. D., Cognetta, A. B., Jr., Chang, Y. & Moore, P. S. Lack of evidence for basal or squamous cell carcinoma infection with Merkel cell polyomavirus in immunocompetent patients with Merkel cell carcinoma. *Journal of the American Academy of Dermatology* **63**, 400-403, doi:10.1016/j.jaad.2009.08.064 (2010).
216 Rollison, D. E. *et al.* Case-control Study of Merkel Cell Polyomavirus Infection and Cutaneous Squamous Cell Carcinoma. *Cancer Epidemiology Biomarkers & Prevention* **21**, 74-81, doi:10.1158/1055-9965.epi-11-0764 (2012).
217 Dalianis, T., Ramqvist, T., Andreasson, K., Kean, J. M. & Garcea, R. L. KI, WU and Merkel cell polyomaviruses: A new era for human polyomavirus research. *Seminars in Cancer Biology* **19**, 270-275, doi:10.1016/j.semcancer.2009.04.001 (2009).
218 Johne, R. *et al.* Taxonomical developments in the family Polyomaviridae. *Archives of Virology* **156**, 1627-1634, doi:10.1007/s00705-011-1008-x (2011).
219 Matsushita, M. *et al.* Merkel cell polyomavirus (MCPyV) strains in Japanese merkel cell carcinomas (MCC) are distinct from Caucasian type MCPyVs: genetic variability

and phylogeny of MCPyV genomes obtained from Japanese MCPyV-infected MCCs. *Virus Genes* **48**, 233-242, doi:10.1007/s11262-013-1023-y (2014).

220 De Gascun, C. F. & Carr, M. J. Human Polyomavirus Reactivation: Disease Pathogenesis and Treatment Approaches. *Clinical & Developmental Immunology*, doi:10.1155/2013/373579 (2013).

221 Stakaityte, G. *et al.* Merkel cell polyomavirus: molecular insights into the most recently discovered human tumour virus. *Cancers* **6**, 1267-1297, doi:10.3390/cancers6031267 (2014).

222 Kwun, H. J. *et al.* The Minimum Replication Origin of Merkel Cell Polyomavirus Has a Unique Large T-Antigen Loading Architecture and Requires Small T-Antigen Expression for Optimal Replication. *Journal of Virology* **83**, 12118-12128, doi:10.1128/jvi.01336-09 (2009).

223 Li, J. *et al.* Merkel Cell Polyomavirus Large T Antigen Disrupts Host Genomic Integrity and Inhibits Cellular Proliferation. *Journal of Virology* **87**, 9173-9188, doi:10.1128/jvi.01216-13 (2013).

224 Topalis, D., Andrei, G. & Snoeck, R. The large tumor antigen: A "Swiss Army knife" protein possessing the functions required for the polyomavirus life cycle. *Antiviral Research* **97**, 122-136, doi:10.1016/j.antiviral.2012.11.007 (2013).

225 Seo, G. J., Chen, C. J. & Sullivan, C. S. Merkel cell polyomavirus encodes a microRNA with the ability to autoregulate viral gene expression. *Virology* **383**, 183-187, doi:10.1016/j.virol.2008.11.001 (2009).

226 Griffiths, D. A. *et al.* Merkel Cell Polyomavirus Small T Antigen Targets the NEMO Adaptor Protein To Disrupt Inflammatory Signaling. *Journal of Virology* **87**, 13853-13867, doi:10.1128/jvi.02159-13 (2013).

227 Kwun, H. J. *et al.* Merkel cell polyomavirus small T antigen controls viral replication and oncoprotein expression by targeting the cellular ubiquitin ligase SCFFbw7. *Cell host & microbe* **14**, 125-135, doi:10.1016/j.chom.2013.06.008 (2013).

228 Comerford, S. A., Schultz, N., Hinnant, E. A., Klapproth, S. & Hammer, R. E. Comparative analysis of SV40 17kT and LT function in vivo demonstrates that LT's C-terminus re-programs hepatic gene expression and is necessary for tumorigenesis in the liver. *Oncogenesis* **1**, e28-e28, doi:10.1038/oncsis.2012.27 (2012).

229 Carter, J. J. *et al.* Identification of an overprinting gene in Merkel cell polyomavirus provides evolutionary insight into the birth of viral genes. *Proceedings of the National Academy of Sciences of the United States of America* **110**, 12744-12749, doi:10.1073/pnas.1303526110 (2013).

230 Sabath, N., Wagner, A. & Karlin, D. Evolution of Viral Proteins Originated De Novo by Overprinting. *Molecular Biology and Evolution* **29**, 3767-3780, doi:10.1093/molbev/mss179 (2012).

231 Tolstov, Y. L. *et al.* Human Merkel cell polyomavirus infection II. MCV is a common human infection that can be detected by conformational capsid epitope immunoassays. *International Journal of Cancer* **125**, 1250-1256, doi:10.1002/ijc.24509 (2009).

232 Touze, A. *et al.* Generation of Merkel Cell Polyomavirus (MCV)-Like Particles and Their Application to Detection of MCV Antibodies. *Journal of Clinical Microbiology* **48**, 1767-1770, doi:10.1128/jcm.01691-09 (2010).

233 Schowalter, R. M. & Buck, C. B. The Merkel Cell Polyomavirus Minor Capsid Protein. *Plos Pathogens* **9**, doi:10.1371/journal.ppat.1003558 (2013).

234 Neu, U. *et al.* Structures of Merkel Cell Polyomavirus VP1 Complexes Define a Sialic Acid Binding Site Required for Infection. *Plos Pathogens* **8**, doi:10.1371/journal.ppat.1002738 (2012).

235 Sullivan, C. S., Grundhoff, A. T., Tevethia, S., Pipas, J. M. & Ganem, D. SV40-encoded microRNAs regulate viral gene expression and reduce susceptibility to cytotoxic T cells. *Nature* **435**, 682-686, doi:10.1038/nature03576 (2005).
236 Seo, G. J., Fink, L. H. L., O'Hara, B., Atwood, W. J. & Sullivan, C. S. Evolutionarily Conserved Function of a Viral MicroRNA. *Journal of Virology* **82**, 9823-9828, doi:10.1128/jvi.01144-08 (2008).
237 Schowalter, R. M., Reinhold, W. C. & Buck, C. B. Entry Tropism of BK and Merkel Cell Polyomaviruses in Cell Culture. *Plos One* **7**, doi:10.1371/journal.pone.0042181 (2012).
238 Neumann, F. *et al.* Replication, Gene Expression and Particle Production by a Consensus Merkel Cell Polyomavirus (MCPyV) Genome. *Plos One* **6**, doi:10.1371/journal.pone.0029112 (2011).
239 Schowalter, R. M., Pastrana, D. V. & Buck, C. B. Glycosaminoglycans and Sialylated Glycans Sequentially Facilitate Merkel Cell Polyomavirus Infectious Entry. *Plos Pathogens* **7**, doi:10.1371/journal.ppat.1002161 (2011).
240 Bauer, P. H. *et al.* Discrimination between sialic acid-containing receptors and pseudoreceptors regulates polyomavirus spread in the mouse. *Journal of Virology* **73**, 5826-5832 (1999).
241 Sapp, M. & Day, P. M. Structure, attachment and entry of polyoma- and papillomaviruses. *Virology* **384**, 400-409, doi:10.1016/j.virol.2008.12.022 (2009).
242 Erickson, K. D., Garcea, R. L. & Tsai, B. Ganglioside GT1b Is a Putative Host Cell Receptor for the Merkel Cell Polyomavirus. *Journal of Virology* **83**, 10275-10279, doi:10.1128/jvi.00949-09 (2009).
243 Feng, H. *et al.* Cellular and Viral Factors Regulating Merkel Cell Polyomavirus Replication. *Plos One* **6**, doi:10.1371/journal.pone.0022468 (2011).
244 Wang, X. *et al.* Bromodomain Protein Brd4 Plays a Key Role in Merkel Cell Polyomavirus DNA Replication. *Plos Pathogens* **8**, doi:10.1371/journal.ppat.1003021 (2012).
245 Tsang, S. H., Wang, X., Li, J., Buck, C. B. & You, J. Host DNA Damage Response Factors Localize to Merkel Cell Polyomavirus DNA Replication Sites To Support Efficient Viral DNA Replication. *Journal of Virology* **88**, 3285-3297, doi:10.1128/jvi.03656-13 (2014).
246 Wang, X., Helfer, C. M., Pancholi, N., Bradner, J. E. & You, J. Recruitment of Brd4 to the Human Papillomavirus Type 16 DNA Replication Complex Is Essential for Replication of Viral DNA. *Journal of Virology* **87**, 3871-3884, doi:10.1128/jvi.03068-12 (2013).
247 Shuda, M., Kwun, H. J., Feng, H. C., Chang, Y. & Moore, P. S. Human Merkel cell polyomavirus small T antigen is an oncoprotein targeting the 4E-BP1 translation regulator. *Journal of Clinical Investigation* **121**, 3623-3634, doi:10.1172/jci46323 (2011).
248 Welcker, M. & Clurman, B. E. FBW7 ubiquitin ligase: a tumour suppressor at the crossroads of cell division, growth and differentiation. *Nature Reviews Cancer* **8**, 83-93, doi:10.1038/nrc2290 (2008).
249 Maser, R. S. *et al.* Chromosomally unstable mouse tumours have genomic alterations similar to diverse human cancers. *Nature* **447**, 966-U963, doi:10.1038/nature05886 (2007).
250 Wood, L. D. *et al.* The genomic landscapes of human breast and colorectal cancers. *Science* **318**, 1108-1113, doi:10.1126/science.1145720 (2007).
251 Mao, J. H. *et al.* Fbxw7/Cdc4 is a p53-dependent, haploinsufficient tumour suppressor gene. *Nature* **432**, 775-779, doi:10.1038/nature03155 (2004).

252 Mao, J.-H. *et al.* FBXW7 targets mTOR for degradation and cooperates with PTEN in tumor suppression. *Science* **321**, 1499-1502, doi:10.1126/science.1162981 (2008).
253 Gupta-Rossi, N. *et al.* Functional interaction between SEL-10, an F-box protein, and the nuclear form of activated Notch1 receptor. *Journal of Biological Chemistry* **276**, 34371-34378, doi:10.1074/jbc.M101343200 (2001).
254 Khalili, K., White, M. K., Sawa, H., Nagashima, K. & Safak, M. The agnoprotein of polyomaviruses: A multifunctional auxiliary protein. *Journal of Cellular Physiology* **204**, 1-7, doi:10.1002/jcp.20266 (2005).
255 Daniels, R., Sadowicz, D. & Hebert, D. N. A very late viral protein triggers the lytic release of SV40. *Plos Pathogens* **3**, 928-938, doi:10.1371/journal.ppat.0030098 (2007).
256 Clayson, E. T., Brando, L. V. J. & Compans, R. W. Release of simian virus-40 virions from epithelial-cells is polarized and occurs without cell-lysis. *Journal of Virology* **63**, 2278-2288 (1989).
257 Takeda, K. & Akira, S. Toll-like receptors in innate immunity. *International Immunology* **17**, 1-14, doi:10.1093/intimm/dxh186 (2005).
258 Hayden, M. S. & Ghosh, S. Signaling to NF-kappa B. *Genes & Development* **18**, 2195-2224, doi:10.1101/gad.1228704 (2004).
259 Le Negrate, G. Viral interference with innate immunity by preventing NF-kappa B activity. *Cellular Microbiology* **14**, 168-181, doi:10.1111/j.1462-5822.2011.01720.x (2012).
260 Joo, M. S. *et al.* Hepatitis C virus core protein suppresses NF-kappa B activation and cyclooxygenase-2 expression by direct interaction with I kappa B kinase beta. *Journal of Virology* **79**, 7648-7657, doi:10.1128/jvi.79.12.7648-7657.2005 (2005).
261 Spitkovsky, D., Hehner, S. P., Hofmann, T. G., Moller, A. & Schmitz, M. L. The human papillomavirus oncoprotein E7 attenuates NF-kappa B activation by targeting the I kappa B kinase complex. *Journal of Biological Chemistry* **277**, 25576-25582, doi:10.1074/jbc.M201884200 (2002).
262 Randall, C. M. H., Jokela, J. A. & Shisler, J. L. The MC159 Protein from the Molluscum Contagiosum Poxvirus Inhibits NF-kappa B Activation by Interacting with the I kappa B Kinase Complex. *Journal of Immunology* **188**, 2371-2379, doi:10.4049/jimmunol.1100136 (2012).
263 Fliss, P. M. *et al.* Viral Mediated Redirection of NEMO/IKK gamma to Autophagosomes Curtails the Inflammatory Cascade. *Plos Pathogens* **8**, doi:10.1371/journal.ppat.1002517 (2012).
264 Shahzad, N. *et al.* The T Antigen Locus of Merkel Cell Polyomavirus Downregulates Human Toll-Like Receptor 9 Expression. *Journal of Virology* **87**, 13009-13019, doi:10.1128/jvi.01786-13 (2013).
265 Tsujimura, H. *et al.* Toll-like receptor 9 signaling activates NF-kappa B through IFN regulatory Factor-8/IFN consensus sequence binding protein in dendritic cells. *Journal of Immunology* **172**, 6820-6827 (2004).
266 Hasan, U. A. *et al.* TLR9 expression and function is abolished by the cervical cancer-associated human papillomavirus type 16. *Journal of Immunology* **178**, 3186-3197 (2007).
267 Fathallah, I. *et al.* EBV Latent Membrane Protein 1 Is a Negative Regulator of TLR9. *Journal of Immunology* **185**, 6439-6447, doi:10.4049/jimmunol.0903459 (2010).
268 Lauttia, S. *et al.* Prokineticins and Merkel cell polyomavirus infection in Merkel cell carcinoma. *British Journal of Cancer* **110**, 1446-1455, doi:10.1038/bjc.2014.20 (2014).

269 Zhao, J. J. *et al.* Human mammary epithelial cell transformation through the activation of phosphatidylinositol 3-kinase. *Cancer Cell* **3**, 483-495, doi:10.1016/s1535-6108(03)00088-6 (2003).
270 Buchkovich, N. J., Yu, Y., Zampieri, C. A. & Alwine, J. C. The TORrid affairs of viruses: effects of mammalian DNA viruses on the PI3K-Akt-mTOR signalling pathway. *Nature reviews. Microbiology* **6**, 266-275, doi:10.1038/nrmicro1855 (2008).
271 Dowling, R. J. O. *et al.* mTORC1-Mediated Cell Proliferation, But Not Cell Growth, Controlled by the 4E-BPs. *Science* **328**, 1172-1176, doi:10.1126/science.1187532 (2010).
272 Richter, J. D. & Sonenberg, N. Regulation of cap-dependent translation by eIF4E inhibitory proteins. *Nature* **433**, 477-480, doi:10.1038/nature03205 (2005).
273 Pause, A. *et al.* Insulin-dependent stimulation of protein-synthesis by phosphorylation of regulator of 5'-cap function. *Nature* **371**, 762-767, doi:10.1038/371762a0 (1994).
274 Lazariskaratzas, A., Montine, K. S. & Sonenberg, N. Malignant transformation by a eukaryotic initiation-factor subunit that binds to messenger-RNA 5' cap. *Nature* **345**, 544-547, doi:10.1038/345544a0 (1990).
275 Avdulov, S. *et al.* Activation of translation complex eIF4F is essential for the genesis and maintenance of the malignant phenotype in human mammary epithelial cells. *Cancer Cell* **5**, 553-563, doi:10.1016/j.ccr.2004.05.024 (2004).
276 Beretta, L., Gingras, A. C., Svitkin, Y. V., Hall, M. N. & Sonenberg, N. Rapamycin blocks the phosphorylation of 4E-BP1 and inhibits cap-dependent initiation of translation. *Embo Journal* **15**, 658-664 (1996).
277 Angermeyer, S., Hesbacher, S., Becker, J. C., Schrama, D. & Houben, R. Merkel Cell Polyomavirus-Positive Merkel Cell Carcinoma Cells Do Not Require Expression of the Viral Small T Antigen. *Journal of Investigative Dermatology* **133**, 2059-2064, doi:10.1038/jid.2013.82 (2013).
278 Shuda, M. *et al.* Human Merkel cell polyomavirus infection I. MCV T antigen expression in Merkel cell carcinoma, lymphoid tissues and lymphoid tumors. *International Journal of Cancer* **125**, 1243-1249, doi:10.1002/ijc.24510 (2009).
279 Cheng, J., Rozenblatt-Rosen, O., Paulson, K. G., Nghiem, P. & DeCaprio, J. A. Merkel Cell Polyomavirus Large T Antigen Has Growth-Promoting and Inhibitory Activities. *Journal of Virology* **87**, 6118-6126, doi:10.1128/jvi.00385-13 (2013).
280 Shi, Y. L., Dodson, G. E., Rundell, K. & Tibbetts, R. S. Ataxia-telangiectasia-mutated (ATM) is a T-antigen kinase that controls SV40 viral replication in vivo. *Journal of Biological Chemistry* **280**, 40195-40200, doi:10.1074/jbc.C500400200 (2005).
281 Arora, R. *et al.* Survivin Is a Therapeutic Target in Merkel Cell Carcinoma. *Science Translational Medicine* **4**, doi:10.1126/scitranslmed.3003713 (2012).
282 Ambrosini, G., Adida, C. & Altieri, D. C. A novel anti-apoptosis gene, survivin, expressed in cancer and lymphoma. *Nature Medicine* **3**, 917-921, doi:10.1038/nm0897-917 (1997).
283 Pina-Oviedo, S. *et al.* Effects of JC virus infection on anti-apoptotic protein survivin in progressive multifocal leukoencephalopathy. *American Journal of Pathology* **170**, 1291-1304, doi:10.2353/ajpath.2007.060689 (2007).
284 Miller, N. J., Bhatia, S., Parvathaneni, U., Iyer, J. G. & Nghiem, P. Emerging and Mechanism-Based Therapies for Recurrent or Metastatic Merkel Cell Carcinoma. *Current Treatment Options in Oncology* **14**, 249-263, doi:10.1007/s11864-013-0225-9 (2013).
285 Gueron, G., De Siervi, A. & Vazquez, E. Key Questions in Metastasis: New Insights in Molecular Pathways and Therapeutic Implications. *Current Pharmaceutical Biotechnology* **12**, 1867-1880 (2011).

286 Chambers, A. F., Groom, A. C. & MacDonald, I. C. Dissemination and growth of cancer cells in metastatic sites. *Nat Rev Cancer* **2**, 563-572, doi:10.1038/nrc865 (2002).
287 Gatenby, R. A. & Gillies, R. J. Hypoxia and metabolism - Opinion - A microenvironmental model of carcinogenesis. *Nature Reviews Cancer* **8**, 56-61, doi:10.1038/nrc2255 (2008).
288 Cavallaro, U. & Christofori, G. Cell adhesion and signalling by cadherins and Ig-CAMs in cancer. *Nature Reviews Cancer* **4**, 118-132, doi:10.1038/nrc1276 (2004).
289 Beavon, I. R. G. The E-cadherin-catenin complex in tumour metastasis: structure, function and regulation. *European Journal of Cancer* **36**, 1607-1620, doi:10.1016/s0959-8049(00)00158-1 (2000).
290 Lebivic, A., Sambuy, Y., Mostov, K. & Rodriguezboulan, E. Vectorial targeting of an endogenous apical membrane sialoglycoprotein and uvomorulin in MDCK cells. *Journal of Cell Biology* **110**, 1533-1539, doi:10.1083/jcb.110.5.1533 (1990).
291 Lewis, J. E., Jensen, P. J., Johnson, K. R. & Wheelock, M. J. E-cadherin mediates adherens junction organization through protein-kinase-C. *Journal of Cell Science* **107**, 3615-3621 (1994).
292 Geiger, T. R. & Peeper, D. S. Metastasis mechanisms. *Biochimica Et Biophysica Acta-Reviews on Cancer* **1796**, 293-308, doi:10.1016/j.bbcan.2009.07.006 (2009).
293 Yilmaz, M. & Christofori, G. Mechanisms of Motility in Metastasizing Cells. *Molecular Cancer Research* **8**, 629-642, doi:10.1158/1541-7786.mcr-10-0139 (2010).
294 Talis, A. L., Huibregtse, J. M. & Howley, P. M. The role of E6AP in the regulation of p53 protein levels in human papillomavirus (HPV)-positive and HPV-negative cells. *Journal of Biological Chemistry* **273**, 6439-6445, doi:10.1074/jbc.273.11.6439 (1998).
295 Watson, R. A., Thomas, M., Banks, L. & Roberts, S. Activity of the human papillomavirus E6 PDZ-binding motif correlates with an enhanced morphological transformation of immortalized human keratinocytes. *Journal of Cell Science* **116**, 4925-4934, doi:10.1242/jcs.00809 (2003).
296 Kanai, Y. *et al.* The E-cadherin gene is silenced by CpG methylation in human hepatocellular carcinomas. *International Journal of Cancer* **71**, 355-359 (1997).
297 Yoshiura, K. *et al.* Silencing of the E-cadherin invasion-suppressor gene by CPG methylation in human carcinomas. *Proceedings of the National Academy of Sciences of the United States of America* **92**, 7416-7419, doi:10.1073/pnas.92.16.7416 (1995).
298 Lee, J. O. *et al.* Hepatitis B virus X protein represses E-cadherin expression via activation of DNA methyltransferase 1. *Oncogene* **24**, 6617-6625, doi:10.1038/sj.onc.1208827 (2005).
299 Nunbhakdi-Craig, V., Craig, L., Machleidt, T. & Sontag, E. Simian virus 40 small tumor antigen induces deregulation of the actin cytoskeleton and tight junctions in kidney epithelial cells. *Journal of Virology* **77**, 2807-2818, doi:10.1128/jvi.77.5.2807-2818.2003 (2003).
300 Han, A. C., Soler, A. P., Tang, C. K., Knudsen, K. A. & Salazar, H. Nuclear localization of E-cadherin expression in Merkel cell carcinoma. *Archives of Pathology & Laboratory Medicine* **124**, 1147-1151 (2000).
301 Mehlen, P. & Puisieux, A. Metastasis: a question of life or death. *Nature Reviews Cancer* **6**, 449-458, doi:10.1038/nrc1886 (2006).
302 Sahai, E. Mechanisms of cancer cell invasion. *Current Opinion in Genetics & Development* **15**, 87-96, doi:10.1016/j.gde.2004.12.002 (2005).

303 Nabeshima, K., Inoue, T., Shimao, Y. & Sameshima, T. Matrix metalloproteinases in tumor invasion: Role for cell migration. *Pathology International* **52**, 255-264, doi:10.1046/j.1440-1827.2002.01343.x (2002).
304 Friedl, P. Prespecification and plasticity: shifting mechanisms of cell migration. *Current Opinion in Cell Biology* **16**, 14-23, doi:10.1016/j.ceb.2003.11.001 (2004).
305 Gupta, G. P. & Massague, J. Cancer metastasis: Building a framework. *Cell* **127**, 679-695, doi:10.1016/j.cell.2006.11.001 (2006).
306 Wolfsberg, T. G., Primakoff, P., Myles, D. G. & White, J. M. ADAM, a novel family of membrane-proteins containing a disintegrin and metalloprotease domain - multipotential functions in cell-cell and cell-matrix interactions. *Journal of Cell Biology* **131**, 275-278, doi:10.1083/jcb.131.2.275 (1995).
307 Edwards, D. R., Handsley, M. M. & Pennington, C. J. The ADAM metalloproteinases. *Molecular Aspects of Medicine* **29**, 258-289, doi:10.1016/j.mam.2008.08.001 (2008).
308 Blobel, C. P. Adams: Key components in EGFR signalling and development. *Nature Reviews Molecular Cell Biology* **6**, 32-43, doi:10.1038/nrm1548 (2005).
309 Moss, M. L. & Lambert, M. H. Shedding of membrane proteins by ADAM family proteases. *Proteases in Biology and Medicine* **38**, 141-153 (2002).
310 Rocks, N. *et al.* Emerging roles of ADAM and ADAMTS metalloproteinases in cancer. *Biochimie* **90**, 369-379, doi:10.1016/j.biochi.2007.08.008 (2008).
311 Arai, I. *et al.* Overexpression of MT3-MMP in hepatocellular carcinoma correlates with capsular invasion. *Hepato-Gastroenterology* **54**, 167-171 (2007).
312 Zhai, Y. L. *et al.* Expression of membrane type 1 matrix metalloproteinase is associated with cervical carcinoma progression and invasion. *Cancer Research* **65**, 6543-6550, doi:10.1158/0008-5472.can-05-0231 (2005).
313 Morris, M. A., Young, L. S. & Dawson, C. W. DNA tumour viruses promote tumour cell invasion and metastasis by deregulating the normal processes of cell adhesion and motility. *European Journal of Cell Biology* **87**, 677-697, doi:10.1016/j.ejcb.2008.03.005 (2008).
314 Truong, H. & Danen, E. H. J. Integrin switching modulates adhesion dynamics and cell migration. *Cell Adhesion & Migration* **3**, 179-181, doi:10.4161/cam.3.2.8036 (2009).
315 Huttenlocher, A. & Horwitz, A. R. Integrins in Cell Migration. *Cold Spring Harbor Perspectives in Biology* **3**, doi:10.1101/cshperspect.a005074 (2011).
316 Albelda, S. M. *et al.* Integrin distribution in malignant-melanoma - association of the beta-3-subunit with tumor progression. *Cancer Research* **50**, 6757-6764 (1990).
317 Filardo, E. J., Brooks, P. C., Deming, S. L., Damsky, C. & Cheresh, D. A. Requirement of the NPXY motif in the integrin beta-3 subunit cytoplasmic tail for melanoma cell-migration in-vitro and in-vivo. *Journal of Cell Biology* **130**, 441-450, doi:10.1083/jcb.130.2.441 (1995).
318 Huang, S., Stupack, D., Liu, A. H., Cheresh, D. & Nemerow, G. R. Cell growth and matrix invasion of EBV-immortalized human B lymphocytes is regulated by expression of alpha(v) integrins. *Oncogene* **19**, 1915-1923, doi:10.1038/sj.onc.1203509 (2000).
319 Paget, S. The distribution of secondary growths in cancer of the breast Paget, Stephen paper reproduced from the Lancet, 1989. *Cancer and Metastasis Reviews* **8**, 98-101 (1989).
320 Kaplan, R. N. *et al.* VEGFR1-positive haematopoietic bone marrow progenitors initiate the pre-metastatic niche. *Nature* **438**, 820-827, doi:10.1038/nature04186 (2005).

321 Olson, M. F. & Sahai, E. The actin cytoskeleton in cancer cell motility. *Clinical & Experimental Metastasis* **26**, 273-287, doi:10.1007/s10585-008-9174-2 (2009).
322 Kaverina, I. & Straube, A. Regulation of cell migration by dynamic microtubules. *Seminars in Cell & Developmental Biology* **22**, 968-974, doi:10.1016/j.semcdb.2011.09.017 (2011).
323 Yamaguchi, H., Wyckoff, J. & Condeelis, J. Cell migration in tumors. *Current Opinion in Cell Biology* **17**, 559-564, doi:10.1016/j.ceb.2005.08.002 (2005).
324 de Forges, H., Bouissou, A. & Perez, F. Interplay between microtubule dynamics and intracellular organization. *International Journal of Biochemistry & Cell Biology* **44**, 266-274, doi:10.1016/j.biocel.2011.11.009 (2012).
325 Stehbens, S. & Wittmann, T. Targeting and transport: How microtubules control focal adhesion dynamics. *Journal of Cell Biology* **198**, 481-489, doi:10.1083/jcb.201206050 (2012).
326 Ross, J. L., Ali, M. Y. & Warshaw, D. M. Cargo transport: molecular motors navigate a complex cytoskeleton. *Current Opinion in Cell Biology* **20**, 41-47, doi:10.1016/j.ceb.2007.11.006 (2008).
327 Gatlin, J. C. & Bloom, K. Microtubule motors in eukaryotic spindle assembly and maintenance. *Seminars in Cell & Developmental Biology* **21**, 248-254, doi:10.1016/j.semcdb.2010.01.015 (2010).
328 Etienne-Manneville, S. Microtubules in Cell Migration. *Annual Review of Cell and Developmental Biology, Vol 29* **29**, 471-499, doi:10.1146/annurev-cellbio-101011-155711 (2013).
329 Valiron, O., Caudron, N. & Job, D. Microtubule dynamics. *Cellular and Molecular Life Sciences* **58**, 2069-2084, doi:10.1007/pl00000837 (2001).
330 Gardner, M. K., Zanic, M. & Howard, J. Microtubule catastrophe and rescue. *Current Opinion in Cell Biology* **25**, 14-22, doi:10.1016/j.ceb.2012.09.006 (2013).
331 Wiese, C. & Zheng, Y. Microtubule nucleation: gamma-tubulin and beyond. *Journal of Cell Science* **119**, 4143-4153, doi:10.1242/jcs.03226 (2006).
332 Dehmelt, L. & Halpain, S. The MAP2/Tau family of microtubule-associated proteins. *Genome Biology* **6** (2005).
333 Moores, C. A. *et al.* Distinct roles of doublecortin modulating the microtubule cytoskeleton. *Embo Journal* **25**, 4448-4457, doi:10.1038/sj.emboj.7601335 (2006).
334 Drechsel, D. N., Hyman, A. A., Cobb, M. H. & Kirschner, M. W. Modulation of the dynamic instability of tubulin assembly in the microtubule-associated protein Tau. *Molecular Biology of the Cell* **3**, 1141-1154 (1992).
335 Komarova, Y. *et al.* Mammalian end binding proteins control persistent microtubule growth. *Journal of Cell Biology* **184**, 691-706, doi:10.1083/jcb.200807179 (2009).
336 Mimori-Kiyosue, Y. *et al.* CLASP1 and CLASP2 bind to EB1 and regulate microtubule plus-end dynamics at the cell cortex. *Journal of Cell Biology* **168**, 141-153, doi:10.1083/jcb.200405094 (2005).
337 Kita, K., Wittmann, T., Nathke, I. S. & Waterman-Storer, C. M. Adenomatous polyposis coli in cell extensions can promote with or without EB1. *Molecular Biology of the Cell* **17**, 2331-2345, doi:10.1091/mbc.E05-06-0498 (2006).
338 Kodama, A., Karakesisoglou, L., Wong, E., Vaezi, A. & Fuchs, E. ACF7: An essential integrator of microtubule dynamics. *Cell* **115**, 343-354, doi:10.1016/s0092-8674(03)00813-4 (2003).
339 Newton, C. N., Wagenbach, M., Ovechkina, Y., Wordeman, L. & Wilson, L. MCAK, a Kin I kinesin, increases the catastrophe frequency of steady-state HeLa cell microtubules in an ATP-dependent manner in vitro. *Febs Letters* **572**, 80-84, doi:10.1016/j.febslet.2004.06.093 (2004).

340 Belletti, B. *et al.* Stathmin activity influences sarcoma cell shape, motility, and metastatic potential. *Molecular Biology of the Cell* **19**, 2003-2013, doi:10.1091/mbc.E07-09-0894 (2008).
341 Gavet, O. *et al.* The stathmin phosphoprotein family: intracellular localization and effects on the microtubule network. *Journal of Cell Science* **111**, 3333-3346 (1998).
342 Belmont, L. D. & Mitchison, T. J. Identification of a protein that interacts with tubulin dimers and increases the catastrophe rate of microtubules. *Cell* **84**, 623-631, doi:10.1016/s0092-8674(00)81037-5 (1996).
343 Dyson, H. J. & Wright, P. E. Intrinsically unstructured proteins and their functions. *Nature Reviews Molecular Cell Biology* **6**, 197-208, doi:10.1038/nrm1589 (2005).
344 Gigant, B. *et al.* The 4 angstrom X-ray structure of a tubulin : stathmin-like domain complex. *Cell* **102**, 809-816, doi:10.1016/s0092-8674(00)00069-6 (2000).
345 Amayed, P., Carlier, M. F. & Pantaloni, D. Stathmin slows down guanosine diphosphate dissociation from tubulin in a phosphorylation-controlled fashion. *Biochemistry* **39**, 12295-12302, doi:10.1021/bi000279w (2000).
346 Steinmetz, M. O. Structure and thermodynamics of the tubulin-stathmin interaction. *Journal of Structural Biology* **158**, 137-147, doi:10.1016/j.jsb.2006.07.018 (2007).
347 Manna, T., Thrower, D., Miller, H. P., Curmi, P. & Wilson, L. Stathmin strongly increases the minus end catastrophe frequency and induces rapid treadmilling of bovine brain microtubules at steady state in vitro. *Journal of Biological Chemistry* **281**, 2071-2078, doi:10.1074/jbc.M510661200 (2006).
348 Larsson, N., Marklund, U., Gradin, H. M., Brattsand, G. & Gullberg, M. Control of microtubule dynamics by oncoprotein 18: Dissection of the regulatory role of multisite phosphorylation during mitosis. *Molecular and Cellular Biology* **17**, 5530-5539 (1997).
349 Tholey, A., Lindemann, A., Kinzel, V. & Reed, J. Direct effects of phosphorylation on the preferred backbone conformation of peptides: A nuclear magnetic resonance study. *Biophysical Journal* **76**, 76-87 (1999).
350 Luo, X. N., Mookerjee, B., Ferrari, A., Mistry, S. & Atweh, G. F. REGULATION OF PHOSPHOPROTEIN P18 IN LEUKEMIC-CELLS - CELL-CYCLE-REGULATED PHOSPHORYLATION BY P34(CDC2) KINASE. *Journal of Biological Chemistry* **269**, 10312-10318 (1994).
351 Brattsand, G., Marklund, U., Nylander, K., Roos, G. & Gullberg, M. CELL-CYCLE-REGULATED PHOSPHORYLATION OF ONCOPROTEIN-18 ON SER16, SER25 AND SER38. *European Journal of Biochemistry* **220**, 359-368, doi:10.1111/j.1432-1033.1994.tb18632.x (1994).
352 Rubin, C. I. & Atweh, G. F. The role of stathmin in the regulation of the cell cycle. *Journal of Cellular Biochemistry* **93**, 242-250, doi:10.1002/jcb.20187 (2004).
353 Marklund, U., Brattsand, G., Shingler, V. & Gullberg, M. SERINE-25 OF ONCOPROTEIN-18 IS A MAJOR CYTOSOLIC TARGET FOR THE MITOGEN-ACTIVATED PROTEIN-KINASE. *Journal of Biological Chemistry* **268**, 15039-15049 (1993).
354 Baldassarre, G. *et al.* p27(Kip1)-stathmin interaction influences sarcoma cell migration and invasion. *Cancer Cell* **7**, 51-63, doi:10.1016/j.ccr.2004.11.025 (2005).
355 Rana, S., Maples, P. B., Senzer, N. & Nemunaitis, J. Stathmin 1: a novel therapeutic target for anticancer activity. *Expert Review of Anticancer Therapy* **8**, 1461-1470, doi:10.1586/14737140.8.9.1461 (2008).
356 Chen, J. *et al.* Stathmin 1 is a potential novel oncogene in melanoma. *Oncogene* **32**, 1330-1337, doi:10.1038/onc.2012.141 (2013).

357 Tan, H. T. *et al.* Proteomic Analysis of Colorectal Cancer Metastasis: Stathmin-1 Revealed as a Player in Cancer Cell Migration and Prognostic Marker. *Journal of Proteome Research* **11**, 1433-1445, doi:10.1021/pr2010956 (2012).
358 Byrne, F. L. *et al.* RNAi-mediated stathmin suppression reduces lung metastasis in an orthotopic neuroblastoma mouse model. *Oncogene* **33**, 882-890, doi:10.1038/onc.2013.11 (2014).
359 Li, N. *et al.* Siva1 suppresses epithelial-mesenchymal transition and metastasis of tumor cells by inhibiting stathmin and stabilizing microtubules. *Proc Natl Acad Sci U S A* **108**, 12851-12856, doi:10.1073/pnas.1017372108 (2011).
360 Grossmann, C., Podgrabinska, S., Skobe, M. & Ganem, D. Activation of NF-kappa B by the latent vFLIP gene of Kaposi's sarcoma-associated herpesvirus is required for the spindle shape of virus-infected endothelial cells and contributes to their proinflammatory phenotype. *Journal of Virology* **80**, 7179-7185, doi:10.1128/jvi.01603-05 (2006).
361 Romashko, A. A. & Young, M. R. I. Protein phosphatase-2A maintains focal adhesion complexes in keratinocytes and the loss of this regulation in squamous cell carcinomas. *Clinical & Experimental Metastasis* **21**, 371-379, doi:10.1023/B:CLIN.0000046178.08043.f8 (2004).
362 Miceli, C., Tejada, A., Castaneda, A. & Mistry, S. J. Cell cycle inhibition therapy that targets stathmin in in vitro and in vivo models of breast cancer. *Cancer Gene Therapy* **20**, 298-307, doi:10.1038/cgt.2013.21 (2013).
363 Lee, S. H. *et al.* Transgenic Expression of Polyomavirus Middle T Antigen in the Mouse Prostate Gives Rise to Carcinoma. *Journal of Virology* **85**, 5581-5592, doi:10.1128/jvi.02609-10 (2011).
364 Howell, B., Deacon, H. & Cassimeris, L. Decreasing oncoprotein 18/stathmin levels reduces microtubule catastrophes and increases microtubule polymer in vivo. *Journal of Cell Science* **112**, 3713-3722 (1999).
365 Cassimeris, L. The oncoprotein 18/stathmin family of microtubule destabilizers. *Current Opinion in Cell Biology* **14**, 18-24, doi:10.1016/s0955-0674(01)00289-7 (2002).
366 Cox, J. & Mann, M. MaxQuant enables high peptide identification rates, individualized p.p.b.-range mass accuracies and proteome-wide protein quantification. *Nature Biotechnology* **26**, 1367-1372, doi:10.1038/nbt.1511 (2008).
367 Huang, D. W., Sherman, B. T. & Lempicki, R. A. Systematic and integrative analysis of large gene lists using DAVID bioinformatics resources. *Nature Protocols* **4**, 44-57, doi:10.1038/nprot.2008.211 (2009).
368 Jackson, B. R., Noerenberg, M. & Whitehouse, A. A Novel Mechanism Inducing Genome Instability in Kaposi's Sarcoma-Associated Herpesvirus Infected Cells. *Plos Pathogens* **10**, doi:10.1371/journal.ppat.1004098 (2014).
369 Boyne, J. R. & Whitehouse, A. Nucleolar trafficking is essential for nuclear export of intronless herpesvirus mRNA. *Proceedings of the National Academy of Sciences of the United States of America* **103**, 15190-15195, doi:10.1073/pnas.0604890103 (2006).
370 Hall, K. T. *et al.* The activation domain of herpesvirus saimiri R protein interacts with the TATA-binding protein. *Journal of Virology* **73**, 9756-9763 (1999).
371 Shuda, M., Chang, Y. & Moore, P. S. Merkel Cell Polyomavirus-Positive Merkel Cell Carcinoma Requires Viral Small T-Antigen for Cell Proliferation. *Journal of Investigative Dermatology* **134**, 1479-1481, doi:10.1038/jid.2013.483 (2014).
372 Crowe, J. S. *et al.* Improved cloning efficiency of polymerase chain-reaction (PCR) products after proteinase-K digestion. *Nucleic Acids Research* **19**, 184-184, doi:10.1093/nar/19.1.184 (1991).

373 Spencer, V. A. Nuclear actin: A key player in extracellular matrix-nucleus communication. *Communicative & integrative biology* **4**, 511-512, doi:10.4161/cib.4.5.16256 (2011).
374 Sobel, A. Stathmin - a relay phosphoprotein for multiple signal transduction. *Trends in Biochemical Sciences* **16**, 301-305, doi:10.1016/0968-0004(91)90123-d (1991).
375 Gurland, G. & Gundersen, G. G. Protein phosphatase inhibitors induced the selective breakdown of stable microtubules in fibroblasts and epithelial-cell. *Proceedings of the National Academy of Sciences of the United States of America* **90**, 8827-8831, doi:10.1073/pnas.90.19.8827 (1993).
376 Piperno, G., Ledizet, M. & Chang, X. J. Microtubules containing acetylated alpha-tubulin in mammalian-cell in culture. *Journal of Cell Biology* **104**, 289-302, doi:10.1083/jcb.104.2.289 (1987).
377 Munday, D. C. *et al.* Using SILAC and quantitative proteomics to investigate the interactions between viral and host proteomes. *Proteomics* **12**, 666-672, doi:10.1002/pmic.201100488 (2012).
378 Yasmeen, A. *et al.* E6/E7 of HPV type 16 promotes cell invasion and metastasis of human breast cancer cells. *Cell Cycle* **6**, 2038-2042 (2007).
379 Kaul, R., Murakami, M., Choudhuri, T. & Robertson, E. S. Epstein-Barr virus latent nuclear antigens can induce metastasis in a nude mouse model. *Journal of Virology* **81**, 10352-10361, doi:10.1128/jvi.00886-07 (2007).
380 Fitzpatrick, F. A. & Wheeler, R. The immunophannacology of paclitaxel (Taxol (R)) docetaxel (Taxotere (R)), and related agents. *International Immunopharmacology* **3**, 1699-1714, doi:10.1016/j.intimp.2003.08.007 (2003).
381 Manna, T., Thrower, D. A., Honnappa, S., Steinmetz, M. O. & Wilson, L. Regulation of Microtubule Dynamic Instability in Vitro by Differentially Phosphorylated Stathmin. *Journal of Biological Chemistry* **284**, 15640-15649, doi:10.1074/jbc.M900343200 (2009).
382 Myles, T., Schmidt, K., Evans, D. R. H., Cron, P. & Hemmings, B. A. Active-site mutations impairing the catalytic function of the catalytic subunit of human protein phosphatase 2A permit baculovirus-mediated overexpression in insect cells. *Biochemical Journal* **357**, 225-232, doi:10.1042/0264-6021:3570225 (2001).
383 Merrick, S. E., Trojanowski, J. Q. & Lee, V. M. Y. Selective destruction of stable microtubules and axons by inhibitors of protein serine/threonine phosphatases in cultured human neurons (NT2N cells). *Journal of Neuroscience* **17**, 5726-5737 (1997).
384 Toyo-oka, K. *et al.* Protein phosphatase 4 catalytic subunit regulates Cdk1 activity and microtubule organization via NDEL1 dephosphorylation. *Journal of Cell Biology* **180**, 1133-1147 (2008).
385 Nemunaitis, J. Stathmin 1: a protein with many tasks. New biomarker and potential target in cancer. *Expert Opinion on Therapeutic Targets* **16**, 631-634, doi:10.1517/14728222.2012.696101 (2012).
386 Wittmann, T., Bokoch, G. M. & Waterman-Storer, C. M. Regulation of microtubule destabilizing activity of Op18/stathmin downstream of Rac1. *Journal of Biological Chemistry* **279**, 6196-6203, doi:10.1074/jbc.M307261200 (2004).
387 Friedl, P. & Brocker, E. B. The biology of cell locomotion within three-dimensional extracellular matrix. *Cellular and Molecular Life Sciences* **57**, 41-64, doi:10.1007/s000180050498 (2000).
388 Sahai, E. & Marshall, C. J. Differing modes of tumour cell invasion have distinct requirements for Rho/ROCK signalling and extracellular proteolysis. *Nature Cell Biology* **5**, 711-719, doi:10.1038/ncb1019 (2003).

389 Mistry, S. J., Li, H. C. & Atweh, G. F. Role for protein phosphatases in the cell-cycle-regulated phosphorylation of stathmin. *Biochemical Journal* **334**, 23-29 (1998).
390 Tournebize, R. *et al.* Distinct roles of PP1 and PP2A-like phosphatases in control of microtubule dynamics during mitosis. *Embo Journal* **16**, 5537-5549, doi:10.1093/emboj/16.18.5537 (1997).
391 Cortes, J. & Vidal, M. Beyond taxanes: the next generation of microtubule-targeting agents. *Breast Cancer Research and Treatment* **133**, 821-830, doi:10.1007/s10549-011-1875-6 (2012).
392 Ferrandina, G. *et al.* Novel Drugs Targeting Microtubules: the Role of Epothilones. *Current Pharmaceutical Design* **18**, 2793-2803 (2012).
393 **Warburg, O., and Dickens, F**. *Metabolism and Tumours: Investigation form the Kaiser Wilhelm Institute for Biology*. (Constable and Co, 1930).
394 Pfeiffer, T., Schuster, S. & Bonhoeffer, S. Cooperation and competition in the evolution of ATP-producing pathways. *Science* **292**, 504-507, doi:10.1126/science.1058079 (2001).
395 Munoz, M. E. & Ponce, E. Pyruvate kinase: current status of regulatory and functional properties. *Comparative Biochemistry and Physiology B-Biochemistry & Molecular Biology* **135**, 197-218, doi:10.1016/s1096-4959(03)00081-2 (2003).
396 **Wong, N.,** De Melo, J., and Tang, D. PKM2, a central point of regulation in cancer metabolism. *Journal of Cell Biology*, 11 (Epub 2013).
397 Yu, Y., Clippinger, A. J. & Alwine, J. C. Viral effects on metabolism: changes in glucose and glutamine utilization during human cytomegalovirus infection. *Trends in Microbiology* **19**, 360-367, doi:10.1016/j.tim.2011.04.002 (2011).
398 Mankouri, J. *et al.* Enhanced hepatitis C virus genome replication and lipid accumulation mediated by inhibition of AMP-activated protein kinase. *Proceedings of the National Academy of Sciences of the United States of America* **107**, 11549-11554, doi:10.1073/pnas.0912426107 (2010).
399 Mankouri, J. & Harris, M. Viruses and the fuel sensor: the emerging link between AMPK and virus replication. *Reviews in Medical Virology* **21**, 205-212, doi:10.1002/rmv.687 (2011).
400 Mazurek, S. in *Workshop on Oncogenes Meet Metabolism - From Deregulated Genes to a Broader Understanding of Tumour Physiology.* 99-124 (2008).
401 **Porporato, P., E.**, Dhup, S., Dadhich, R, K., Copetti, T., and Sonveaux, P. Anticancer targets in the glycolytic metabolism of tumors: a comprehensice review. *Frontiers in Pharmacology* **2**, 1-18 (2011).